

Age distribution of detrital zircon grains in sandstones and stream sediments from East Greenland north of 70°N

A contribution to the project: Provenance study of possible reservoir sandstone units in East and North-East Greenland

E.F. Rehnström, K. Thrane, T.F. Kokfelt & D. Frei



Age distribution of detrital zircon grains in sandstones and stream sediments from East Greenland north of 70°N

A contribution to the project: Provenance study
of possible reservoir sandstone units in
East and North-East Greenland

E.F. Rehnström, K. Thrane, T.F. Kokfelt & D. Frei

Confidential report

Copy No.

Released 25-06-2025

Table of content

Abstract	5
Introduction	9
Zircon as a provenance tool	9
U-Th-Pb systematics and the Concordia diagram	10
Sample preparation	11
LA-SF-ICPMS analyses.....	11
Geological background	14
Crust building episodes	14
Regional geological overview	15
Major East Greenland zircon sources and their age characteristics	17
Results	23
Recent stream sediments.....	24
Southern part of the study area	25
Northern part of the study area	36
Presentation and interpretation of sandstone samples in profiles	41
Pre-Devonian sandstone sections.....	46
Post-Devonian profiles	55
South and East Jameson Land.....	55
North-East Jameson Land	63
Traill Ø	67
Geographical Society Ø.....	72
Hold with Hope	79
Wollaston Forland.....	83
NW Wollaston Forland: Niesen.....	87
E Wollaston Forland	92
Kuhn Ø.....	99
Kim Fjelde, Peary Land	103
Discussion and Summary	111
Stream sediments	111
Neoproterozoic to Palaeocene sandstones- some general comments	112
Palaeogeographic reconstructions and depositional path-ways.....	113
Southern part of the study area	114
Late Devonian	114
Late Carboniferous to Late Permian	115
Early Triassic.....	116
Triassic-Jurassic boundary	117
Middle Jurassic (Late Bajocian)	118
Middle Jurassic (Late Bathonian).....	119
Late Jurassic	120
Jurassic-Cretaceous boundary	121
Mid Cretaceous	122
Palaeocene	123
Northern part of the study area	124
Early Triassic.....	124

Jurassic-Cretaceous boundary.....	125
Acknowledgement	126
References	127

Appendix A: Sample information table **A1-A7**

**Appendix B: U-Pb analytical data plots and table of all samples
(pdf.-file only)** **B1-B892**

Abstract

Sediment transport pathways fundamentally determines the three-dimensional geometry of clastic sedimentary bodies. One way to understand these pathways is to determine the source of the sedimentary detritus. Sedimentary provenance can be investigated in many ways and in this study absolute radiometric ages of detrital zircon grains will be used to: 1) fingerprint the potential source materials and 2) investigate Post-Devonian clastic sedimentary systems on-shore East Greenland to possibly determine their source areas. The sedimentary successions in East Greenland are direct analogues to potential petroleum reservoir rocks in the North Atlantic.

In this report U-Pb analyses from detrital zircon grains from 85 stream sediments and 194 sandstone samples will be presented and interpreted. The age distribution patterns will also be discussed within a palaeogeographic framework, focusing on possible pathways.

The analysed stream sediment samples are from 70°-79° N. They yield signals mainly from Archaean and Palaeoproterozoic basement gneisses and granites, Neoproterozoic metasedimentary sequences and Caledonian and Devonian igneous rocks. This pattern may be primary, but may also be the result of reworking of older sediments with similar sources. Some signals are very influenced by the local geology, e.g. there is a strong dominance of Caledonian zircon grains in the southernmost part, there is a persistent influence of Devonian zircon grains in samples from Canning Land and there is a simple, almost bimodal distribution of ages in samples collected in the basement regions of the north. However, in large areas of East Greenland the exposed geology is dominated by Meso- to Neoproterozoic sedimentary successions (the Krummedal, Smallefjord and Eleonore Bay sequences) and they contribute with a wide range of Archaean and Proterozoic ages.

The analysed sandstones were deposited from the Neoproterozoic to the Palaeocene. The Neoproterozoic Eleonore Bay Supergroup samples are characterised by a small, but diverse Archaean population centered around 2800 Ma and Proterozoic grains with ages between 2000 and 900 Ma, with dominant peaks at 1650 and 1100 Ma. The Cambrian to Permian samples seem to have been sourced from the geological units present in East Greenland, mainly metasedimentary units and local Archaean and/or Proterozoic gneisses in the basement. A small, local Permian basin in the south of the area has a source area to the east, based on the abundance of Caledonian zircon grains. The Early to Middle Triassic samples generally have rather local sources and Liverpool Land acted as a contributor of detritus. The Jurassic Bajocian samples all display non-specific age patterns derived from mixed basement gneisses and metasediments. This is possibly in part due to the increase in basin size due to transgression and therefore a larger catchment. The Jurassic Bathonian samples are more distinctive with clearly separable source areas. The samples from the Late Jurassic constitute two groups: one with a source area to the south of 72° N and one with a source

between 74° and 75° N, both groups were probably transported towards east. The Cretaceous samples generally have detritus both from basement gneisses and metasediments. It is possible to see a difference in provenance from samples derived from south and north of 73° N, based on their basement gneiss signal. In some Cretaceous samples there are Phanerozoic age populations that cannot be explained by local Greenland sources. The Palaeocene samples also have a mixed source from Proterozoic basement and metasediments.

In Peary Land, the sediments are sourced from older sediments and it is therefore difficult to pin-point source areas with any accuracy.

Introduction

The present report is one out of three reports describing the data collected during the project: "Provenance study of possible reservoir sandstone units in East and North-East Greenland". This study is carried out under the collaboration agreement regarding 'Petroleum Geological Studies, Services and Data in East and North-East Greenland' between GEUS and Sponsoring Oil Companies. The two accompanying reports are: "Modal heavy mineral distribution and garnet composition patterns in sandstones and stream sediments from East Greenland north of 70°N" (Keulen 2010) and "Major and trace element composition of sandstones and stream sediments from East Greenland north of 70°N" (Knudsen & Steenfelt 2010).

The understanding of sediment provenance and sediment transport routes is a key element in establishing reservoir presence in clastic petroleum systems. Ultimately the three-dimensional geometry of reservoir bodies depends on the depositional environment. Two of the most fundamental concepts contributing to the specific characteristics of a basin and its infill is, i) the large-scale tectonic framework and ii) the source of the sediments themselves.

Sediment reflects its source in many ways, not least by the distribution of heavy minerals. By studying the composition of a heavy mineral assemblage, many characteristics of the source region may be discerned. However, a recurring problem with conventional heavy mineral studies is the lack of properties that can be quantified and that are truly unique.

One heavy mineral is zircon. It is a mechanically and chemically sturdy mineral that is abundant as a detritus in most sediment. Zircon is widely used for radiometric geochronology to establish absolute ages. It incorporates uranium (U) and thorium (Th) upon formation, which decays radioactively to lead (Pb) and it is possible to measure the isotopic composition of individual grains. Detrital zircon grains in sediments hence potentially reflect the age variation in the source areas. Therefore, to determine the age profile of a detrital zircon population may be a powerful tool to establish whether or not a known area is the source of a sediment.

However, there are shortcomings of this method, e.g. when the age structure of the source regions is poorly known. A robust foundation on extensive and detailed knowledge about the age distribution in the potential source areas is therefore pivotal for a successful detrital zircon provenance analysis.

The maps presented in this report are all extracted from the GIS database (except Fig. 2). The overview maps are based on Henriksen (2003), with a common legend appearing here in Fig. 3. The detailed maps with profile locations are based on Christoffersen

& Jepsen (2007); the large legend for these maps is included in the GIS database and not reproduced here.

Zircon as a provenance tool

Zircon is a physically and chemically very robust mineral. It is heavy, hard and resistant to chemical and mechanical weathering and transport processes. It can survive melting events and metamorphism, it may even resist mantle recycling. However, durability to breakdown of individual grains is dependent on a number of factors, the most important being the physical state of the zircon grain itself. In the following, issues relevant for sedimentary processes and provenance will be discussed.

The most obvious property affecting the survival of a zircon population is shape; long, slender, needle shaped crystals, typical of more mafic rocks, have lower resistance to transport than short, stubby crystals or rounded grains. Shape is to some degree dependent on the chemical composition of the magmatic source rock and hence this may skew the distribution within a population towards rocks with more favourable zircon crystal shapes. These are often granitic or high-grade metamorphic rather than mafic.

Many rocks contain zircon, from mafic to felsic, low-grade to high-grade metamorphic rocks and sedimentary rocks. Zircon grains from different rock types may have rather different properties and this may affect the abundance of a certain group in a given population. This means that a sample of zircon grains from a particular area may *not* be representative of the lithological units of that area. F. ex. ultramafic rocks are almost devoid of zircon and areas dominated by such rocks will not have a zircon population representative of the lithocomposition of the area. Orogenic areas may also pose difficulties since old rocks are reworked but may still retain their old zircon distribution, hardly altered even though the rocks themselves represent a younger event.

Further, zircon is often very abundant in felsic rocks, such as granites, but they are often uranium-rich and may suffer extensive radiation-induced lattice damages, that is, they become metamict. Metamictisation weakens the crystal lattice and hence decrease the zircon grains durability to mechanical weathering. This may cause fewer grains to survive transport and although some may survive transport, such grains cannot be analysed for age data. Moreover, even in rocks with similar composition, the concentration of zirconium may vary highly and this variable zircon fertility may also skew the apparent source rock assemblage.

Zircons from rocks of poly-metamorphic, orogenic regions are often difficult to work out. Even though rocks represent a certain event in the orogenic cycle, the zircon populations often retain the memory of the protolith in the form of cores in the zircon grains with differing age. Especially higher U-concentrations in the core may cause the grain to fracture and the younger part of it may be lost during sediment transport.

Summarising this means that zircon grains in a sediment are often of very good quality, the ugly and the bad ones were lost on the way. This is positive for analytical reasons

because the good quality zircon grains are more likely to produce good quality age data, without disturbances in the isotope systematics. But one shall interpret with caution because the age populations in a sediment based on zircon grains may produce a skewed picture of the source areas.

Another complicating factor is that many source areas contain sedimentary and meta-sedimentary rocks. These may be of different ages and may carry zircon populations of sources lost since long or they may have been redeposited several times. Because of zircon durability, scavenged zircon grains from old sediments are probably often a rich contributor to the detrital zircon population of younger sediments. In this context it is important to know the zircon age distribution in sedimentary and metasedimentary rocks from the potential source area.

U-Th-Pb systematics and the Concordia diagram

U-Pb geochronology is based on the radioactive decay of mother isotopes ^{232}Th , ^{235}U and ^{238}U to daughters ^{208}Pb , ^{207}Pb , and ^{206}Pb respectively. In addition to the radiogenic lead isotopes, there is the non-radiogenic ^{204}Pb , usually denominated “common lead”. The most utilised way to represent U-Pb data is in the so-called Concordia diagram (Fig. 1), where the ratio $^{207}\text{Pb}/^{235}\text{U}$ is plotted against the $^{206}\text{Pb}/^{238}\text{U}$ -ratio. The curve constructed in this way represent age and the curvature is due to the changing proportions of the different uranium and lead isotopes through time, which is caused by the different decay constants of the two uranium isotopes. Plotting the two U-isotopes against each other is an internal measure of whether the system has remained closed, that is if both ratios give the same age, or if the system has been open to diffusion. An analysis of an undisturbed U-Pb system in a mineral will plot on the Concordia curve and is called concordant. However, the isotopic system may become disturbed and such an analysis may plot off the curve. If it plots to the right of curve it is denoted *normally* discordant, to the left- *reverse* discordant. Depending on the method used and the aim of an investigation, discordant data may have an interest or not. In the case of provenance analyses, discordant data is usually discarded, except in very special cases. All ages will be discussed in *Mega annum* (Ma), which is millions of years.

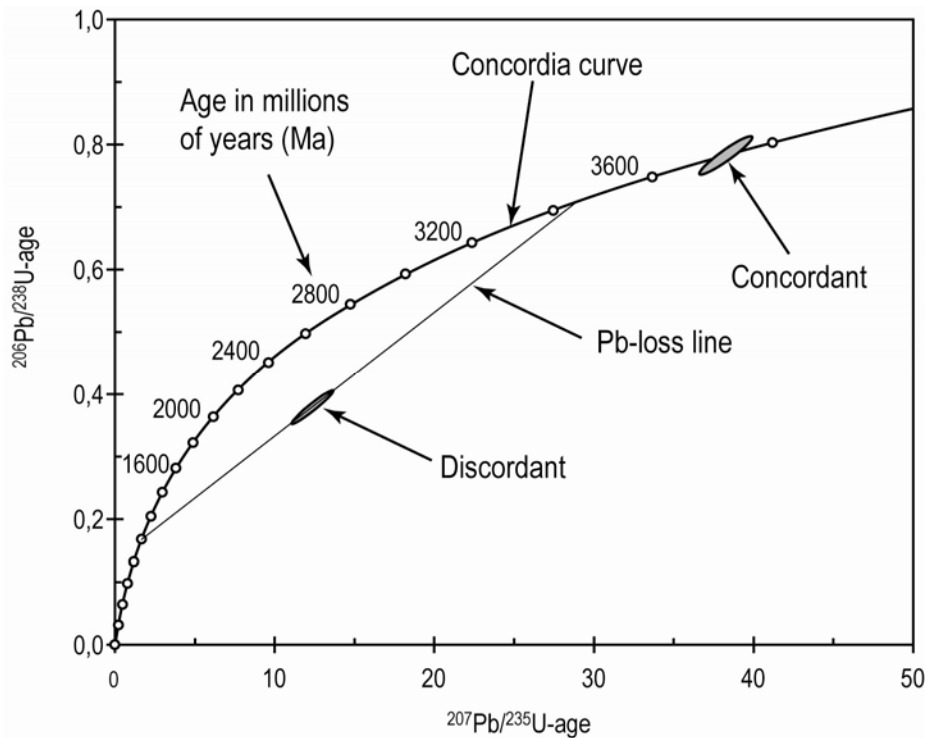


Figure 1. Wetherill Concordia diagram showing the characteristics of this plot.

Sample preparation

Rock samples were firstly crushed and milled, whilst stream sediments were sieved through a 500 μm mesh. To separate zircon and other heavy minerals the samples were then subjected to a water-shaking table and heavy liquid and magnetic separation. Zircon grains were then hand-picked under a stereo microscope and care was taken not to induce a source of error in the form of selectiveness at this stage. About 200 zircon grains from each sample were mounted on double-sided tape prior to casting into 2,5 cm \varnothing epoxy mounts. When sufficiently hardened, the mount was polished with a microgranular diamond paste and polished. Overview pictures, mapping the mounts, were taken of all samples.

LA-SF-ICPMS analyses

Constraining sediment provenance through detrital zircon U-Pb age dating is well established and highly successful (Fedó et al. 2003 and references within). An important breakthrough is the realisation of high throughput micro-beam technologies such as ion probe or laser ablation (LA) based mass spectrometry, which enables acquisition of less biased sample suites that cover a greater range (Williams & Claesson 1987; Jackson et al. 2004). **L**aser **A**blation **I**nductively **C**oupled **P**lasma **M**ass **S**pectrometry (LA-

ICP-MS) is particularly promising as it combines low cost and extraordinary speed with suitable accuracy and precision (Frei et al. 2006). A sample is assumed to reflect the different source components that fed the sediments, and if different sources have different age structures, their relative contribution can be assessed. In principle, their relative contribution should be reflected by their relative zircon occurrence in the sediment, but that assumes equal relative zircon abundances in all the source rocks, that preservation of each zircon contribution is the same and that there is no sampling bias. Such assumptions are rarely possible to comply with, and the relative zircon age distribution cannot simply be inverted to represent the relative source contributions. Nevertheless, the likelihood of identifying an age component in a sample is a function of its relative presence in the population and the size of the sample (i.e. n dated zircon grains). The more zircon grains that are analysed in any given sample, the more likely it is that all present age components are identified. This relationship can be described as

$$P = (1-f)^n \quad (1)$$

where P is the probability for finding a particular component in the population, f is the relative abundance of any given component in the population and n is the number of dated grains (Dodson et al. 1988). Thus, 117 grains have to be dated for a 95% confidence level that **all** present components, at 5% or more, are identified in a worst-case population (Vermeesch 2004). When possible we have been aiming for 200 grains, but several samples yielded considerably fewer grains.

All U-Pb age determinations reported in this study were done at GEUS in Copenhagen, Denmark. The analyses were done *in situ* using a ThermoScientific Element2 Sector Field Inductively Coupled Plasma Mass Spectrometer (SF-ICP-MS) coupled to a New Wave Research®/Merchantek® UP213 laser ablation unit that is equipped with a frequency quintupled ND-YAG laser (wavelength of 213 nm).

Samples and standards were mounted in a low-volume ablation cell specially developed for U-Pb-dating (Horstwood et al. 2003). The laser ablation microprobe uses a focused laser to ablate a small amount of a sample contained in an air-tight cell. The ablated material is transferred to the mass-spectrometer in a carrier gas (Argon mixed with Helium) via Tygon® tubing for analysis.

Most data were acquired using a 30 μm diameter single spot and an ablation time of 30 s, although a shorter ablation time were used for some samples. The result is ablation crater depths of approximately 15-20 μm , and ablated masses of approximately 65 ng. The laser was operated at a repetition rate of 10 Hz and a nominal energy output of 45 %, corresponding to a laser fluency of 3.5 J/cm². The total acquisition time for each analysis is 75 s with the first 30 s used to determine the gas blank, followed by 30 s of ablation and 15 s of washout time. The instrument is tuned to give large, stable signals for the ²⁰⁶Pb and ²³⁸U peaks, low background count rates (typically around 150 counts per second for ²⁰⁷Pb) and low oxide production rates (²³⁸U¹⁶O/²³⁸U generally below 1

%). ^{202}Hg , $^{204}(\text{Pb} + \text{Hg})$, ^{206}Pb , ^{207}Pb , ^{208}Pb , ^{232}Th , ^{235}U and ^{238}U intensities were determined through peak jumping using electrostatic scanning in low resolution mode and with the magnet resting at ^{202}Hg . All data were acquired on four peaks per sample with a sampling and settling time of 1 ms for each isotope. Mass ^{202}Hg was measured to monitor the ^{204}Hg interference on ^{204}Pb where the $^{202}\text{Hg}/^{204}\text{Hg} = 4.36$. If necessary, common Pb corrections were done using the interference and background corrected ^{204}Pb signal in combination with a model Pb composition (Stacey & Kramers 1975). The laser induced elemental fractionation was corrected by the intercept method (Sylvester & Ghaderi 1997; Kosler & Sylvester 2003) and the instrumental mass-bias on measured isotopic ratios was corrected through standard sample bracketing using the GJ-1 zircon (Jackson et al. 2004). Samples were analysed in sequences were an initial six standards are followed by ten samples, then three standards, followed by ten samples, three standards, and so on. The Plesovice zircon standard (Aftalion et al. 1989) has been used as an external reproducibility check, and yield short-term precisions (2σ RSD) of 1.5 %, 1.8 % and 1.1 % for the $^{206}\text{Pb}/^{238}\text{U}$, $^{207}\text{Pb}/^{235}\text{U}$ and $^{207}\text{Pb}/^{206}\text{Pb}$ ratios respectively (Frei & Gerdes 2009).

The raw data is corrected for instrumental mass bias and laser-induced U-Pb fractionation through normalisation to the GJ-1 zircon using our in-house software ZIRCHRON. Data evaluation and presentation is done in Excel spreadsheets and take advantage of IsoplotEx v. 3.0 (Ludwig 1999) and AgeDisplay (Sircombe 2004). All the results are stored in the zircon database accessible through the closed website <https://jupiter.geus.dk/xxx>.

Geological background

Crust building episodes

Some periods of Earth's history are characterised by extensive crustal growth (e.g. Condie 1998). Magmatic and/or metamorphic rocks of these ages can be found on almost all cratonic continents. Such ages are therefore bad indicators of provenance because they are non-conclusive. The Precambrian crust building episodes that are most important in the North Atlantic region, and on most continents in the world, are as follows; Late Archaean (2.7-2.5 Ga), Late Palaeoproterozoic (1.9-1.6 Ga) and Early Neoproterozoic (1.0-0.9 Ga). These are periods with extensive crust formation and thus formation of rock types that contain zircon.

The most important episodes of crustal reworking important in Greenland, including high-grade metamorphism and syn-orogenic magmatism, with formation of zircon, occurred during the Early Palaeoproterozoic (~2 Ga) and in the Palaeozoic (0.45-0.35 Ga) *Caledonian* orogeny (Fig. 2).

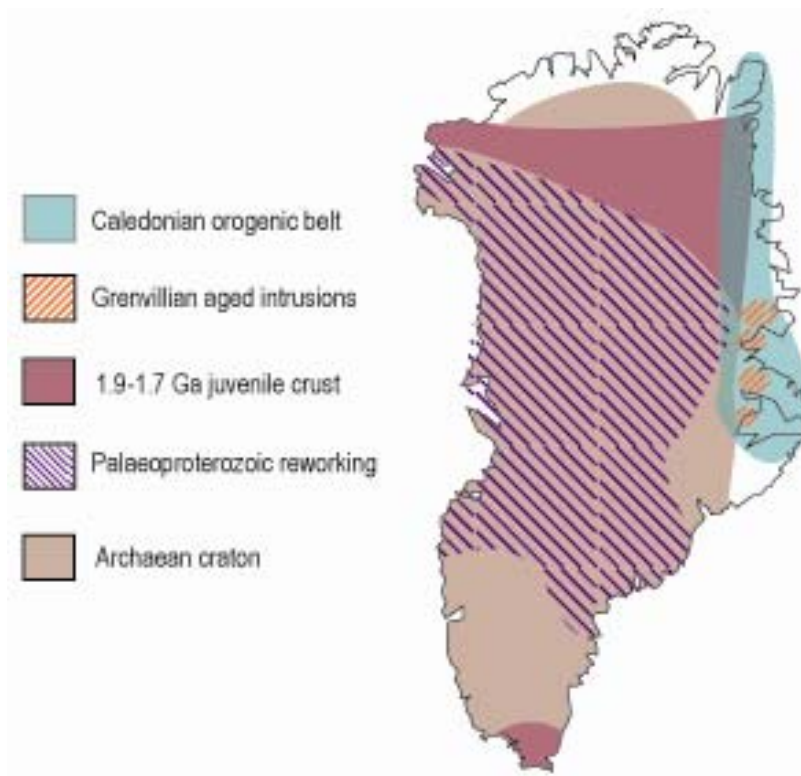


Figure 2. Very simplified overview of major crustal belts in Greenland.

Regional geological overview

East Greenland forms the western flank of the North-Atlantic rift with Scandinavia as the conjugate margin. Greenland has a large Archaean domain (Fig. 2) that stretches from the west to the east coast in the southern part of the continent (Escher & Pulvertaft 1995). Some of the oldest rocks on Earth reside in Greenland, with gneisses as old as 3.9 Ga (e.g. Whitehouse et al. 1999; Horie et al. 2010) exposed in the Nuuk area on the west coast. Some of the Archaean areas present in east Greenland is between 3.0 and 2.7 Ga (Kalsbeek et al. 1993) and is present up to 72,8° N (Thrane 2002). The Archaean domains were reworked by later tectonometamorphic events and younger parts amalgamated on their margins. In east Greenland (Fig. 3) juvenile Palaeoproterozoic rocks are found to the north of the reworked Archaean craton (Kalsbeek et al. 1993; Tucker et al. 1993). Slightly younger granites intruded subsequently. Little is known about the evolution between Palaeoproterozoic and the Palaeozoic. In the Palaeozoic, East Greenland constituted the foreland of the Caledonian orogen that formed due to the collision between Baltica and Laurentia. The northern part of East Greenland is thus geologically dominated by the 1300 km long Palaeozoic Caledonian orogenic belt. The allochthonous sheets were thrust on top the Archaean and Palaeoproterozoic foreland basement from the south-east towards north-west (Higgins et al. 2004; Higgins & Leslie 2000). The thrust-sheets contain both Palaeoproterozoic orthogneisses and Neoproterozoic metasedimentary sequences and the metamorphic conditions grade from sub-greenschist to granulite and ultra-high-pressure facies, the latter only in the gneissic basement though, the thrust-sheets contain rocks with a metamorphic grade up to eclogite and granulite facies. The orogen can be subdivided into different structural domains, from south to north, that mainly reflect different structural levels. There are four major regions that will be described in the following.

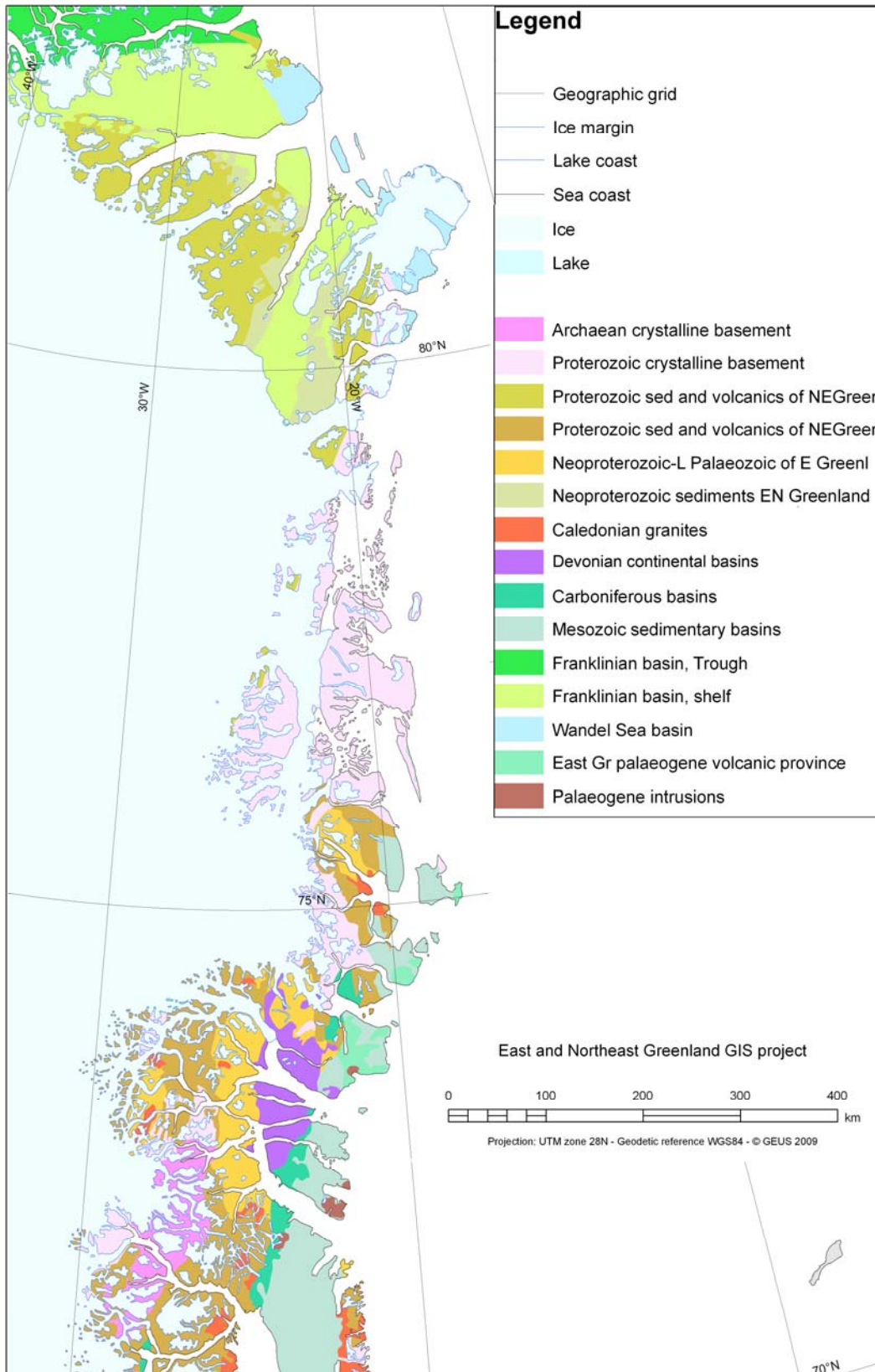


Figure 3. Regional geological map of East and eastern North Greenland.

The southernmost exposed part of the orogenic belt (Fig. 3) contains thrust-sheets with abundant migmatitic metasediments correlated with the Neoproterozoic Krummedal Supracrustal Sequence further north and Caledonian intrusives of different character (Henriksen 1986, Kalsbeek et al. 2008, Leslie & Nutman 2003, Rehnström 2010), but also a small area with eclogites (Hartz et al. 2005; Augland et al. 2010; Johnston et al. 2010). To the north of this, in the central fjord region, thrust-sheets with Archaean-Palaeoproterozoic gneisses and Neoproterozoic sedimentary cover rocks (Krummedal Supracrustal Sequence and Eleonore Bay Supergroup) are intruded by abundant Caledonian S-type leucogranites (Hartz et al. 2000; Kalsbeek et al. 2001; Strachan et al. 2001; Andresen et al. 2007). The migmatisation took place in Silurian times and the resulting leucogranite dykes and plutons have been dated to between 415 and 435 Ma (e.g. Hartz et al. 2000; 2001; White et al. 2002, Kalsbeek et al. 2001, Strachan et al. 2002; Andresen et al. 2007). Further north there are less thrust-sheets, but instead high-grade Palaeoproterozoic gneisses reworked in the Caledonian orogeny with abundant Caledonian eclogite enclaves (Gilotti 1995, Gilotti et al. 2008). The far north is dominated by exposures of a well-preserved thin-skinned fold and thrust belt (Higgins & Leslie 2008). The thrust-sheets consist of mainly Ordovician-Silurian carbonate platform rocks.

The area north-west of the Caledonian orogenic belt is covered by the Meso- to Neoproterozoic sedimentary and volcanic successions of the Independence Fjord and Hagen Fjord Groups and the Zig-Zag Dal Basalt Formation (Sønderholm et al. 2008).

Devonian basins formed syn-tectonically at high structural levels in response to extensional adjustments and the coarse sediments of the basin infill are partly deformed (Larsen & Bengaard 1991; Larsen et al. 2008). Undeformed Mesozoic sediments conformably overlie parts of the coast and Tertiary basalts totally obscure the Caledonian foldbelt south of 70° N (Henriksen 2003) (Fig. 3).

Major East Greenland zircon sources and their age characteristics

The ages that are detected in a sediment mainly represent magmatic or high-grade metamorphic ages, since these are the conditions at which zircon is formed. Therefore not all geological events in a source region will be visible in the zircon age record. The zircons may come directly from eroding basement, but older sediments are usually a substantial source for detrital zircon grains, often yielding much more complex age distribution patterns. Sediments may also record ages that are not present in the basement, either because the source is gone, tectonically or by erosion, or the sediments may not have been deposited locally. Below is a presentation of the major zircon sources in northern East Greenland and their age characteristics.

Basements gneisses

The basement south of 72,8° N consists of Archaean tonalitic gneisses associated with paragneisses, amphibolites and ultramafics. They have ages between ca. 2800 and 2700 Ma (Fig. 4) and are locally intruded by granitic rocks with an age of ~2700 Ma (Thrane 2002, Watt & Thrane 2001). North of 72,8° N, basement gneisses have Palaeoproterozoic ages, mainly from 2000 to 1800 Ma (Fig. 4), with minor granite forming at 1.75 Ga (Kalsbeek et al. 1993; Brueckner et al. 1998; Thrane 2002; Tucker et al. 1993). In the southernmost part of the study area, there is an occurrence of basement gneisses in southern Liverpool Land. They have an age of 1650 Ma (Augland et al. 2010; Johnston et al. 2010), which is very different from the rest of the basement in the area. It has been interpreted as a piece of Norwegian crust amalgamated in the Caledonian orogeny (Augland et al. 2010).

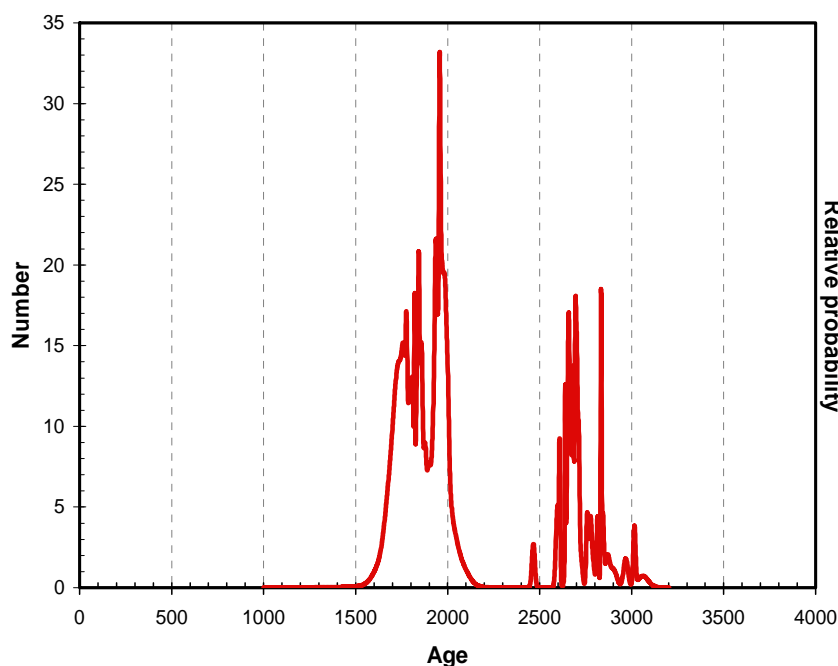


Figure 4. Probability density plot of published in-situ U-Pb zircon age determinations from Precambrian basement rocks north of 70° N. All ages are $\pm 10\%$ concordant. $N=79$. Data from Kalsbeek et al. (1993), Brueckner et al. (1998), Watt et al. (2000), Thrane (2002) and Leslie & Nutman (2003).

Neoproterozoic metasedimentary units south of 76°N

The thrust-sheets of East Greenland are dominated by the metasedimentary sequences of Krummedal, Smallefjord and Eleonore Bay Supergroup (Higgins & Leslie 2008). The Krummedal Sequence and the equivalent Smallefjord Sequence were deposited between 1000 and 930 Ma, the upper bracket defined by the youngest detrital grain and the lower bracket is the age of the oldest intrusions (Kalsbeek et al. 2000).

These two sequences contain detrital zircons with a range of ages (Fig. 5), most characteristic a more or less evenly distributed population between 1800 and 1000 Ma (Fig. 5), with prominent peaks at 1700-1600 and 1100 Ma. Notably there are very few Archaean grains. The Eleonore Bay Supergroup is younger and was deposited later in the Neoproterozoic (e.g. Dhuime et al. 2007). This sequence contains detrital zircon grains with a similar age range of ages as the Krummedal and Smallefjord Sequences (Fig. 5), but in addition, an Archaean component between 2900 and 2600 Ga.

A complicating factor is also that parts of the metasedimentary sequence have undergone high-grade metamorphic recrystallisation during the Caledonian orogeny. This has caused some zircon grains to partially re-equilibrate and yield U-Pb results with mixed age components (Dhuime et al. 2007). The resulting ages are in the Neoproterozoic age range.

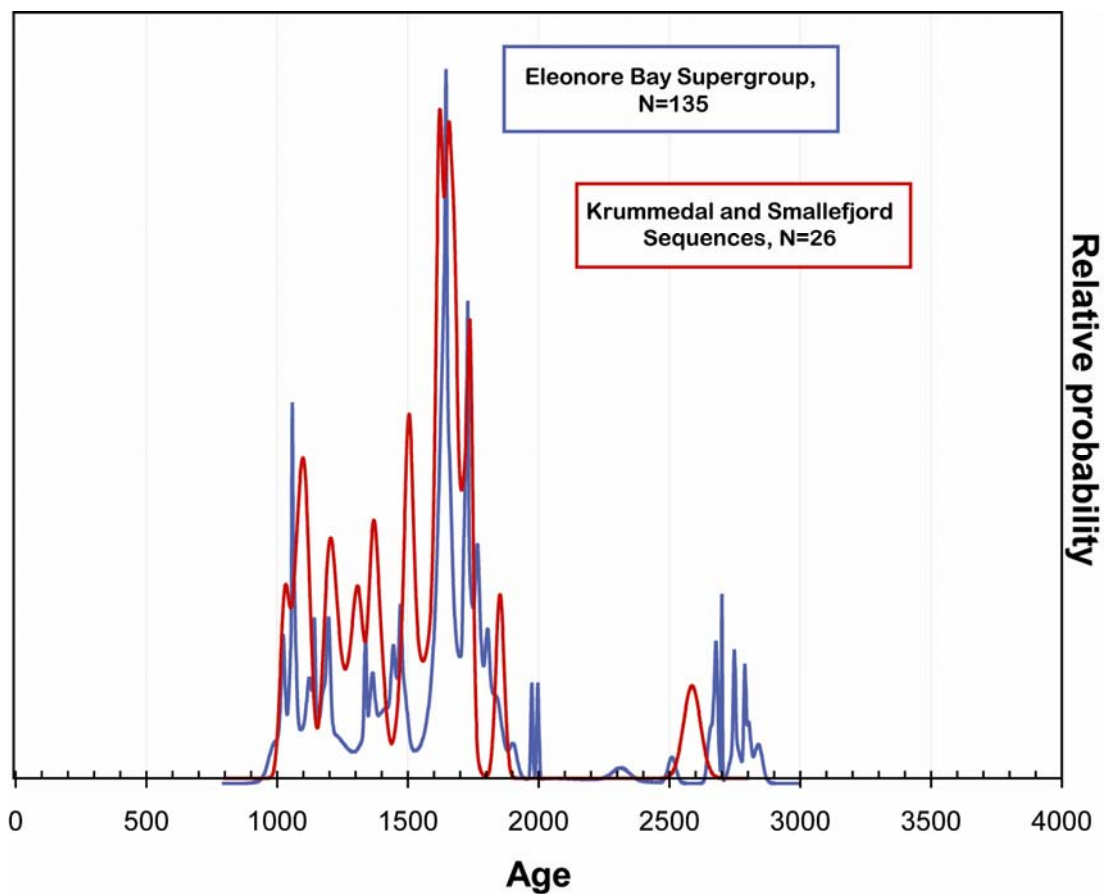


Figure 5. Probability density plot of published in situ zircon U-Pb ages from the meta-sedimentary Krummedal and Smallefjord Sequences and Eleonore Bay Supergroup. All plotted ages are $\pm 10\%$ concordant. Data from Strachan et al. (1995), Watt et al. (2000) and Dhuime et al. (2007).

Metasedimentary sequences of northernmost East Greenland

Detrital zircon analyses of Jurassic-Cretaceous sediments from northernmost east Greenland (Røhr et al. 2008) show a pattern similar (Fig. 6), but not identical, to the age pattern found in the Krummedal and Eleonore Bay Sequences. There is a multi-peak population between 3000 and 2400 Ma and another multi-peak population between 2000 and 900 Ma. This latter population contains some more abundant components that compose distinct peaks in the cumulative probability plot., namely at 1900, 1850, 1630, 1500, 1300 and 1050 Ma. The peaks at 1850, 1630 and 1050 are the most prominent. Further there are abundant zircon grains with ages between 500 and 400 Ma, but also occurrences of grains with ages between 900 and 500 Ma, a group that is completely absent in the Eleonore Bay Supergroup, as well as in younger sediments.

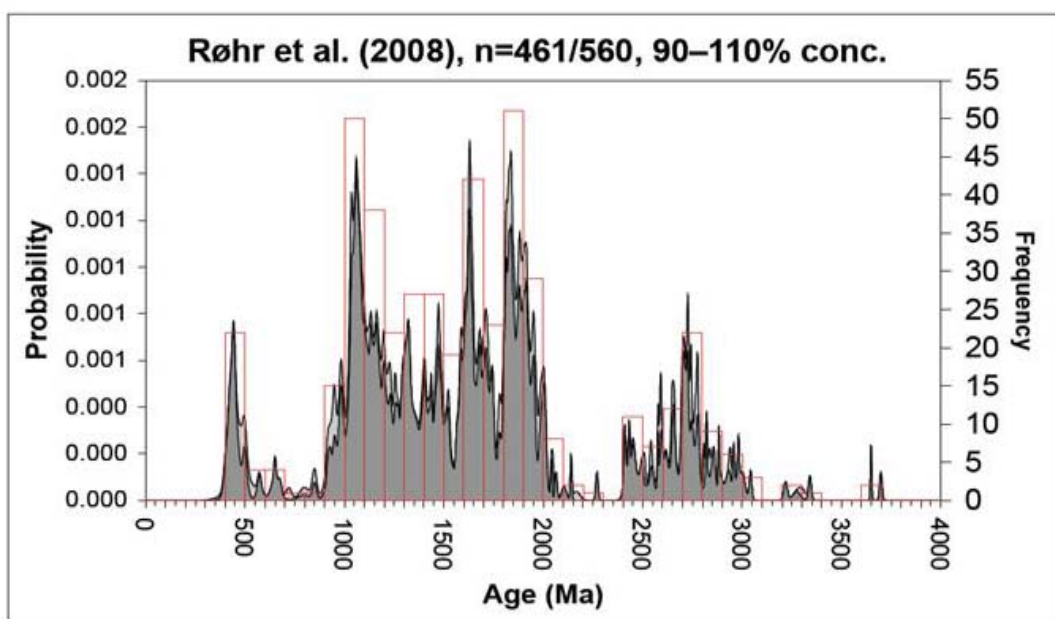


Figure 6. Probability density plot of published in situ zircon U-Pb ages from Mesozoic sediments in eastern North Greenland. Data from Røhr et al. (2008).

Neoproterozoic intrusions

The Krummedal Sequence is intruded by a number of Neoproterozoic granites (Watt & Thrane 2001, Leslie & Nutman 2003). Many of these are augengranites, but there are also numerous leucogranites. The latter are petrographically and geochemically indistinguishable from Caledonian leucogranites and only contain very minor Neoproterozoic zircon (Kalsbeek et al. 2001). This has posed some problems in determining the age of the granites and it also has the effect that only minor amounts of detrital zircon grains with Neoproterozoic age will be present from local sources in the East

Greenland depositional systems. The ages are between 950 and 930 Ma (Fig. 7) (Watt & Thrane 2001; Leslie & Nutman 2003) and they may be important as local sources.

Caledonian intrusions

In the East Greenland Caledonides, Palaeozoic syn-orogenic intrusions are common and the majority of these have a leucogranitic composition (Kalsbeek et al. 2001) and ages between 435 and 410 Ma (Fig. 7) (see Andresen et al. 2007 and references therein). These intrusions formed at low temperatures and do not contain very much zirconium, which means that only small quantities of zircon was produced during the melt crystallisation event. Practically, this means that the leucogranite intrusions have been rather difficult to date (Kalsbeek et al. 2001; Andresen et al., 2007) and that the record of Palaeozoic events have been detected from zircon overgrowths on old xenocrystic grains. As mentioned above, zircon rims can easily be lost during sedimentary transport and taken together this means that the zircon populations coming from the leucogranites contain very many ages apart from Caledonian. It also means that they are not expected to produce large amounts of Palaeozoic zircon grains when eroded. In fact, the age distribution of xenocrystic zircon grains found in the leucogranites is indistinguishable from the metasedimentary sequences discussed above and they have also been interpreted to have formed from melting of primarily the Krummedal and the Smallefjord Sequences (Kalsbeek et al. 2001). In the Scoresby Sund area, in the southernmost part of the study area, there is a concentration of calc-alkaline Caledonian intrusions (Kalsbeek et al. 2008). These are much more readily dated and some of them contain large amounts of Palaeozoic zircon grains without cores (Rehnström 2010). The ages of these intrusions have ages between 465 and 415 Ma (Leslie & Nutman 2003; Kalsbeek et al. 2008; Rehnström 2010).

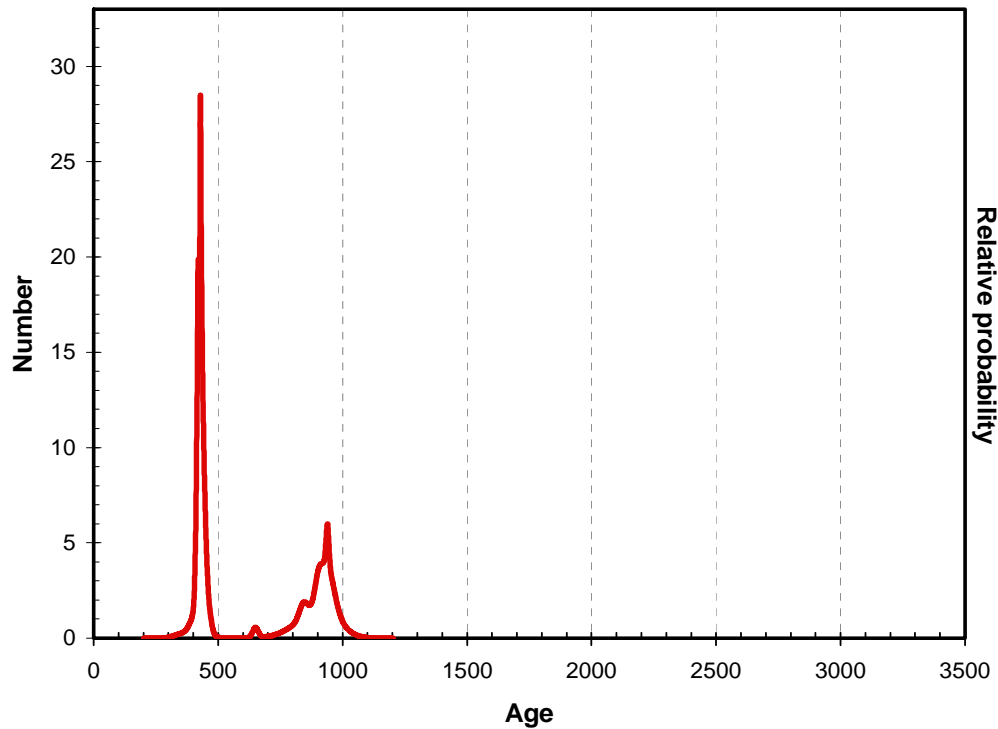


Figure 7. Probability density plot of published U-Pb zircon ages from Neoproterozoic and Palaeozoic intrusions, both in-situ and multigrain fraction data. All ages are $\pm 10\%$ concordant. Data from Kalsbeek et al. (2000; 2001; 2008), Watt et al. (2000), Strachan et al. (2001), Leslie & Nutman (2003) and Rehnström (2010).

Devonian igneous activity

There are a few minor granitic stocks intruding Lower Devonian sediments (Haller 1976). They are associated with felsic volcanic rocks of probably the same age. These rocks have not been radiometrically dated but they are around 380 Ma, based on their intrusive and extrusive relationship with Devonian sediments. These intrusions are probably no significant zircon source on a regional scale, but may be an important local contributor.

Results

This study contains analyses from 85 stream sediments and 194 sandstone samples. Some of the samples have been analysed twice for statistical reasons and in all there are 306 samples analysed. Data for all analyses of every sample is included in the data appendix. Appendix A contains a list of all samples analysed with respect to determination of the U-Pb isotope systematics of detrital zircon, with all sample information. Appendix B contains the tabled analytical data for all individual analyses and three plots, graphically displaying all data for each sample. Data is plotted in two Concordia diagrams; one Tera-Wasserburg diagram and one Wetherill Concordia diagram. There is also a probability density plot for each sample. These plots contain all data without any filtering. In this section the data in the probability density plots have been filtered so that only concordant $\pm 10\%$ analyses, with an error in the $^{206}\text{Pb}/^{238}\text{U}$ less than 10% are included. In the following the results of the U-Pb analyses will be presented and discussed as stacked probability density plots.

The first section presents the stream sediment samples. Zircon grains from a stream sediment sample give an instant picture of the age distribution pattern in present time from a given catchment area and will reflect the bedrock that is exposed today. It is important to establish the characteristics of the different lithological units present in the area, to be able to make interpretations of detrital ages from older deposits. The samples are grouped mainly on the basis of geography and to a lesser degree based on the geology of the catchment area and plotted as stacked probability plots.

The second section presents the sandstone samples. They are divided into a Pre-Devonian group and a Post-Devonian group. The rationale behind this division is purely geological and comes from the fact that the Caledonian orogen formed in the Palaeozoic. Sediments deposited prior to the Caledonian orogen are allochthonous or parautochthonous in character and they are included to give a view of the expected age distribution from these sources, which may be potentially important contributors in younger sediments. Every sample is represented by a probability density plot and these are stacked vertically, with the oldest sample at the bottom.

Recent stream sediments

The stream sediments are divided into groups that are defined in figures 8 and 18 and in tables 1 and 2. On later data analyses these groups proved not to be optimal and they are thus redefined in the integrated report (Knudsen et al. in prep.). For discussing the age characteristics in the different areas the present division is sufficient. The stacking order in the plots is broadly south to north from the bottom up, but this order is compromised in some cases. However, this does not affect the individual plots or data and to a lesser degree the stacked plots.

Southern part of the study area

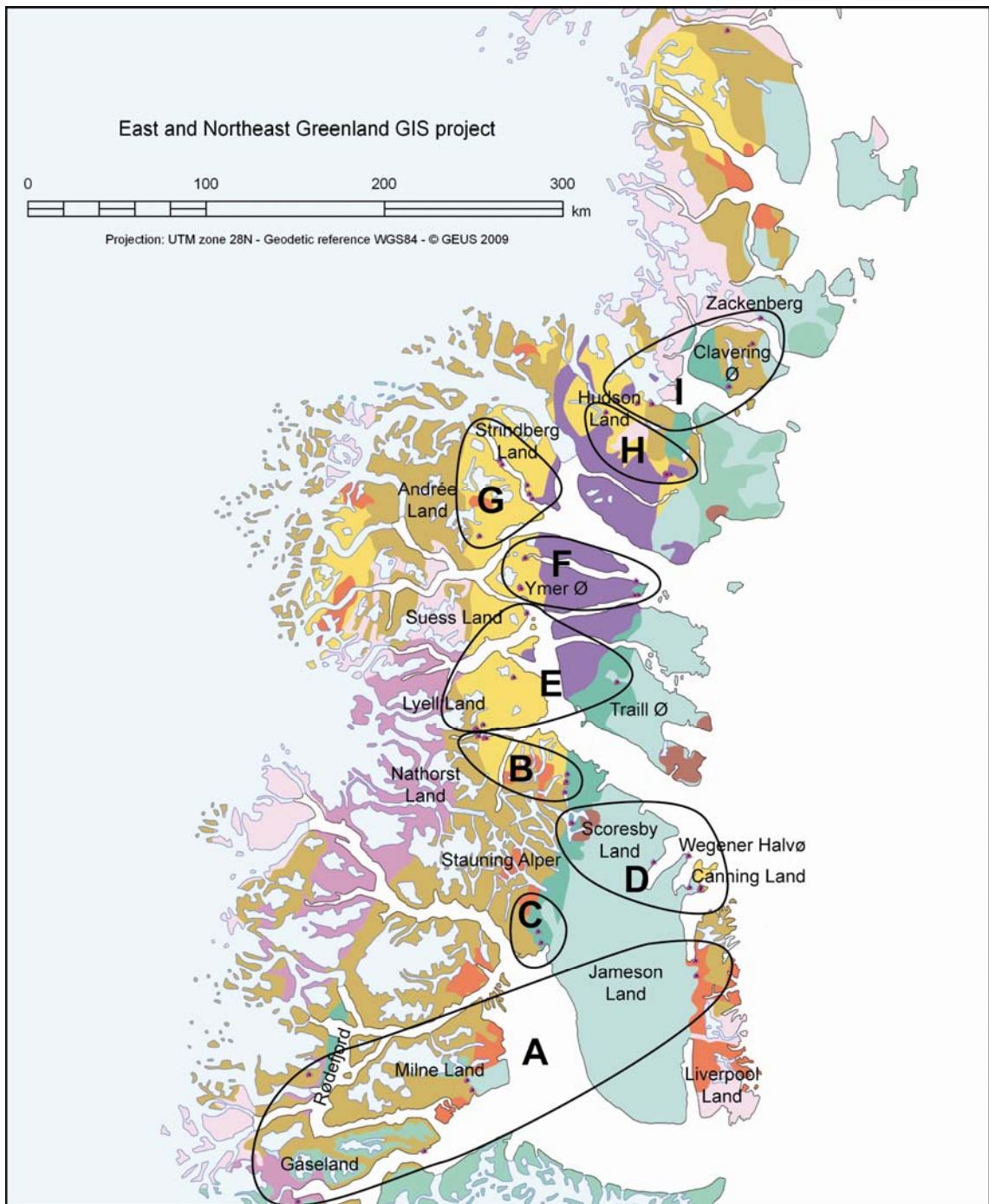


Figure 8. Location of the stream sediment samples from the southern part of the study area.

STREAM SEDIMENT SAMPLES		
Locality name	Area	Sample_nr
Gåseland, Jameson Land , Liverpool Land, Milne Land, Rødefjord	A	7203612, 7111116A, 7502851, 7502852, 7502881, 7502885, 71111109, 7111114B, 7203613
Nathorst Land N, Stauning Alper N	B	7910694-7910696, 7907651, 7907659, 7907661, 7907666
Stauning Alper S	C	8004072_08, 8004078_06
Canning Land, Scoresby Land, Wegener Halvø	D	8101189/11, 8101191/3, 8101194_1, 8101194_2, 7111129/A, 7111131/A, 8101197_1, 8101197_2
Lyell Land, Suess Land, Traill Ø	E	7910690, 7910691, 7910693, 8106242, 8106246, 8105181, 7510257_5N, 7510257_5S
Ymer Ø	F	8105161, 8105162, 8105164, 8105150, 8105153, 8105185, 8307750, 8307751
Hudson Land	G	8106248, 8106451, 8106463, 8106466, 8101198_2, 8101198_2_4, 8101198_6
Andrée Land, Strindberg Land	H	8106478, 8106498, 8106499, 8106611, 8106620, 8106621
Clavering Ø, Hudson Land, Zackenberg	I	8101199_10, 8101199_3, 8101199_4, 8101198_3, 473739

Table 1. Overview of stream sediment sample groups in the southern part of the project area.

Group A

The southernmost group of stream sediments (Fig. 8) consists of nine samples from Rødefjord, Gåseland, Milne Land, Jameson Land and Liverpool Land. They have relatively similar age distribution (Fig. 9), with an inconsistent and variably proportioned Precambrian population. The Archaean contribution is very small and there are no consistent Proterozoic peaks. The Palaeozoic peak is consistent through the group and is centred on 430 Ma. The age distribution pattern is consistent with derivation from Caledonian intrusions and possibly minor contributions from Neoproterozoic meta-sediments that are present in the sampling area.

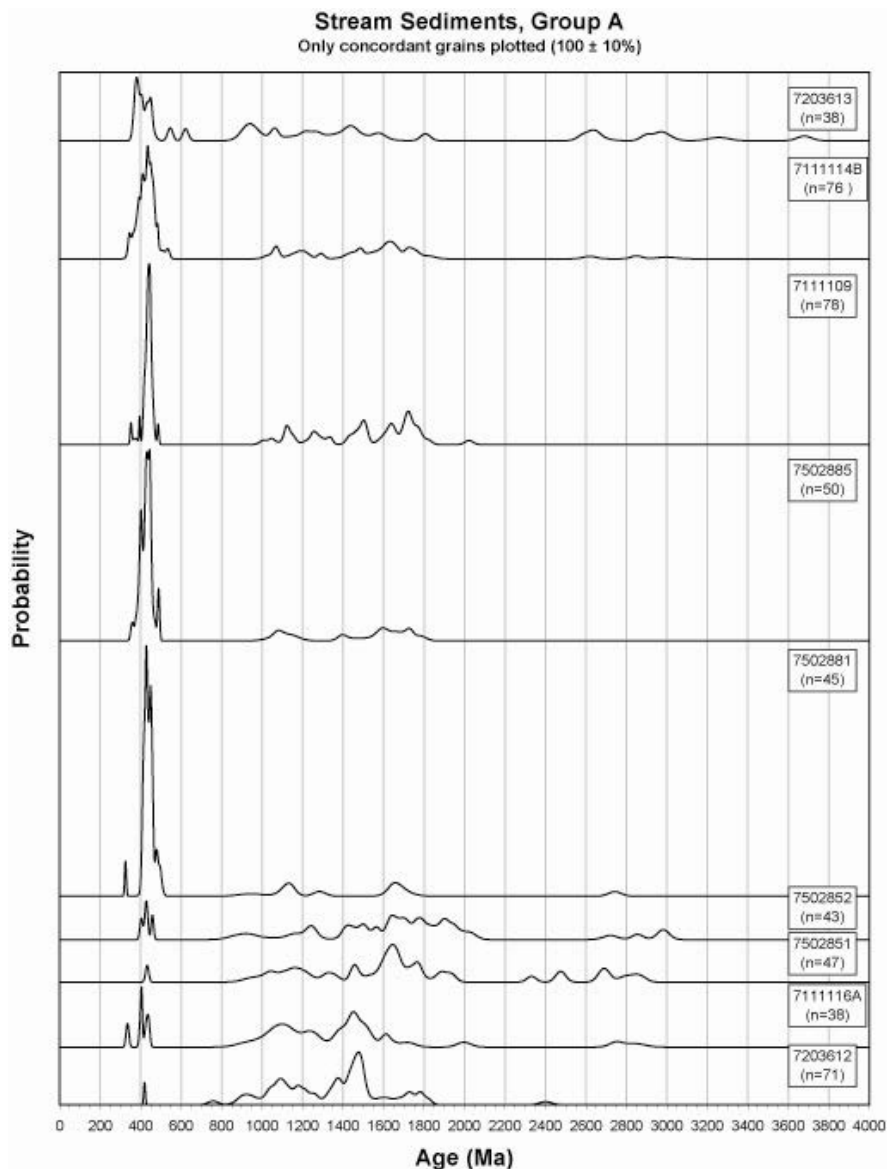


Figure 9. Detrital zircon age distribution pattern for stream sediment group A.

Group B

Group B consists of seven samples from Nathorst Land and Stauning Alper (Fig. 8) that display similar age distribution patterns (Fig. 10). Most samples have a minor, but variably aged Archaean population. All samples have diverse Proterozoic populations with a maximum peak between 1800 and 1600 Ma. An additional important Proterozoic peak is at 1100 Ma. Most samples have a Palaeozoic population consistent with the presence of Caledonian intrusions in the sampling area. The Proterozoic and Archaean contributions are consistent with a proto-source in Neoproterozoic metasedimentary rocks (see Fig. 5), but this detritus may already have been recycled and the source may thus be a younger sediment.

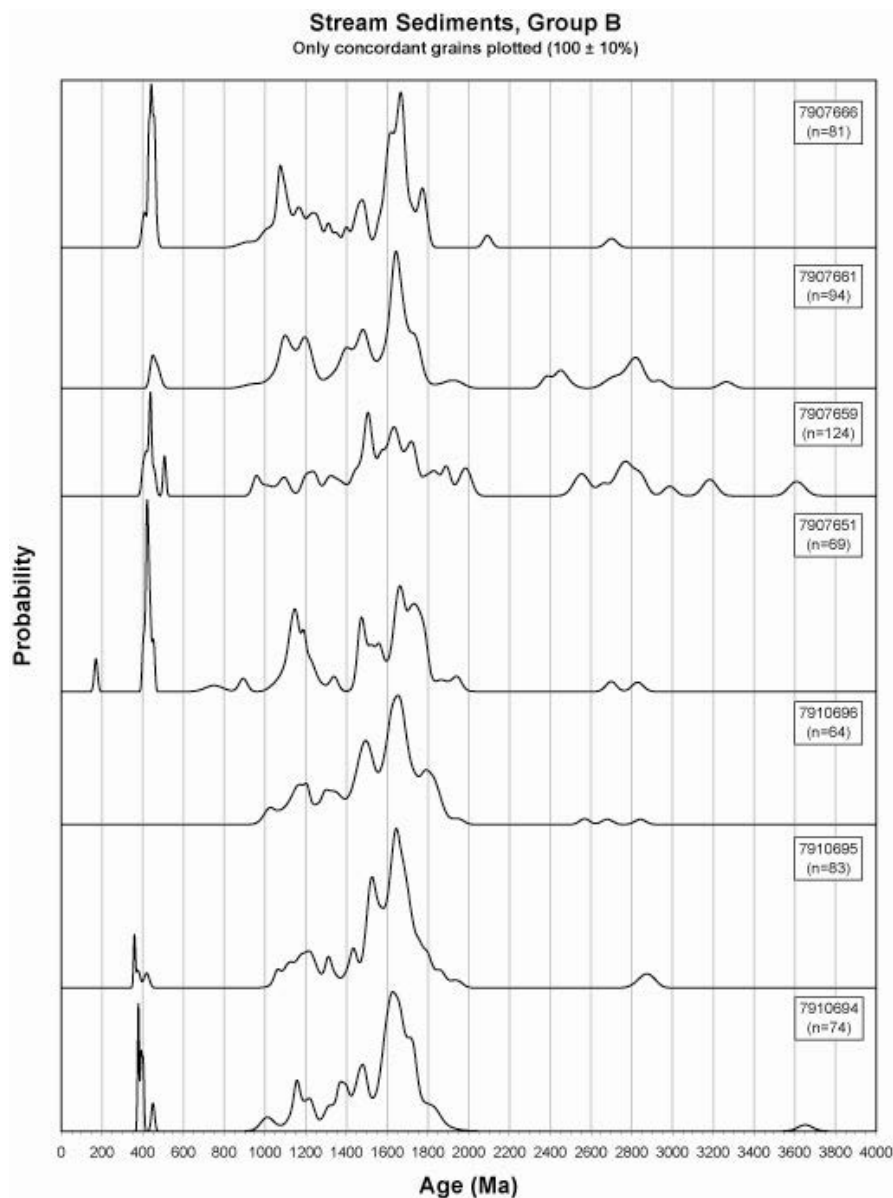


Figure 10. Detrital zircon age distribution pattern for stream sediment group B.

Group C

This group consists of two samples from the southern Stauning Alper (Fig. 8) with minor Archaean components and a large population between 1700 and 1600 Ma (Fig. 11). Other large populations that are also consistent between the two samples occur at 1450, 1150, 900, 500 and 450. The general spectra indicate some derivation from metasedimentary sources (see Fig. 5), due to the multitude of ages present. However the 900 and the 450 Ma peaks can be attributed to local igneous sources, more precisely in the Stauning Alper immediately to the west of the sample locations. The host rock to the intrusions is high-grade metasediments of the Krummedal Supracrustal Sequence. The source of the Cambrian grains is unknown.

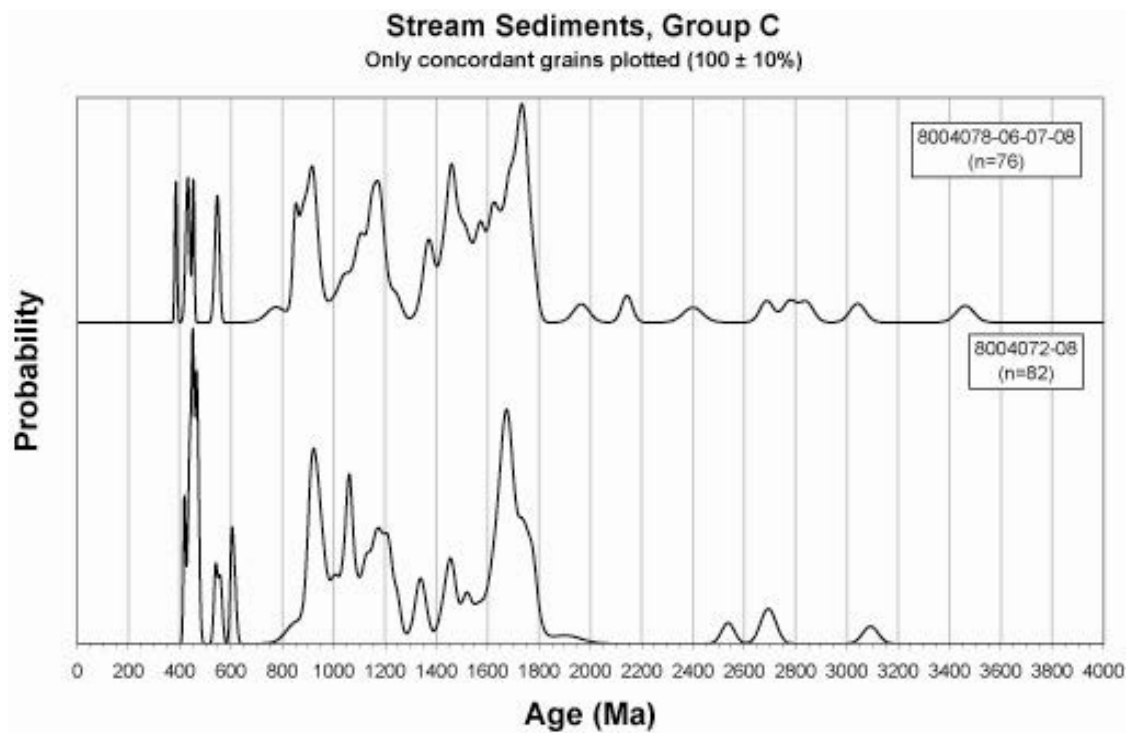


Figure 11. Detrital zircon age distribution pattern for stream sediment group C.

Group D

This group consists of ten samples from Canning Land, Scoresby Land and Wegener Halvø (Fig. 8). These samples have Archaean and Proterozoic age characteristics suggesting derivation from metasediments (Fig. 12). This detritus may also be scavenged from younger sediments that in turn received detritus from Neoproterozoic metasedimentary rocks (see Fig. 5). The 1650 Ma peak in some of the samples may be sourced in the local gneisses of southern Liverpool Land, but may as well be of meta-sedimentary origin. There are multiple peaks in the latest Neoproterozoic and Palaeozoic. The Palaeozoic peaks come from local sources in the form of both Caledonian intrusions in Liverpool Land and Devonian intrusions at Kap Wardlow in Canning Land. The Neoproterozoic ages are difficult to interpret but may represent Proterozoic zircon cores, partially recrystallised in the Palaeozoic.

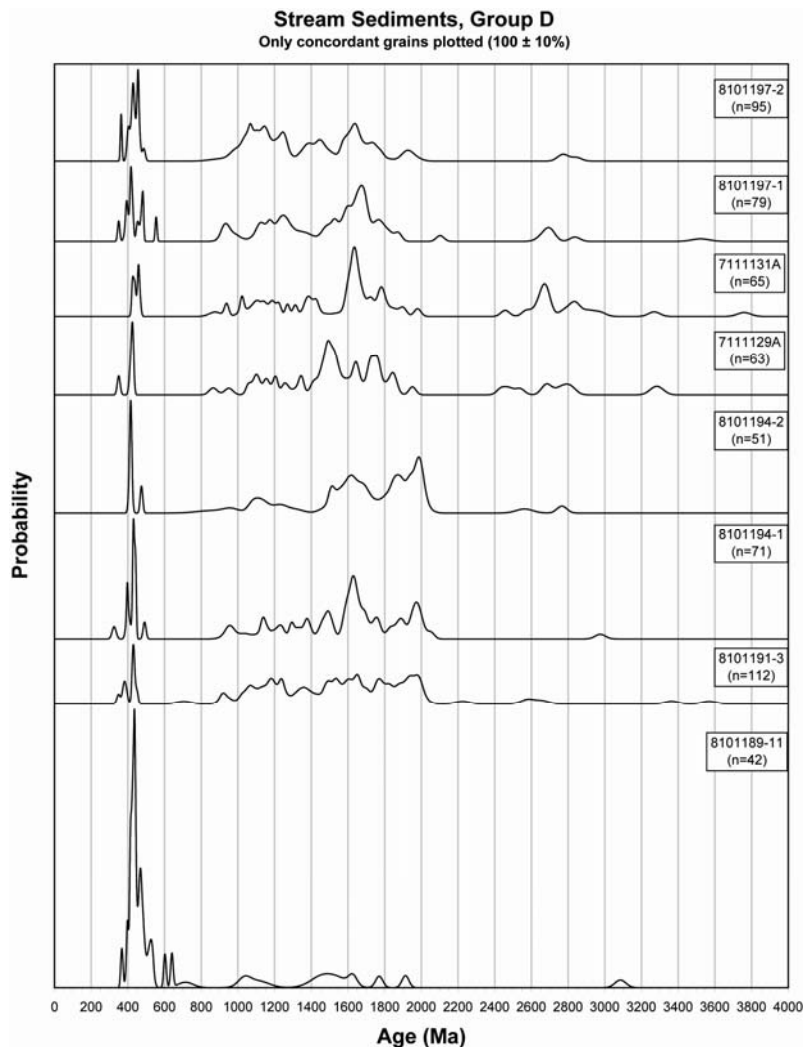


Figure 12. Detrital zircon age distribution pattern for stream sediment group D.

Group E

This group consists of seven samples from Lyell Land, Suess Land and Traill Ø (Fig. 8) with rather similar detrital ages (Fig. 13). The bottom sample (7910690) has a very simple spectrum, but this is probably due to the small number of concordant analyses obtained from this sample. All other samples have an Archaean population, centred around 2700 Ma, but with variable proportions of detritus with other Archaean ages. All samples contain a varied Proterozoic population with principal peaks at 1650 and 1200-1000 Ma. These characteristics are consistent with an initial derivation from the Neoproterozoic metasediments found in the area (see Fig. 5). Most samples contain a Palaeozoic population at ca. 420 Ma and three of the samples contain an additional Devonian peak, ca. 380 Ma. Both these population could be derived from Silurian and Devonian intrusions present in the area, but they could also come from Post-Devonian sediments.

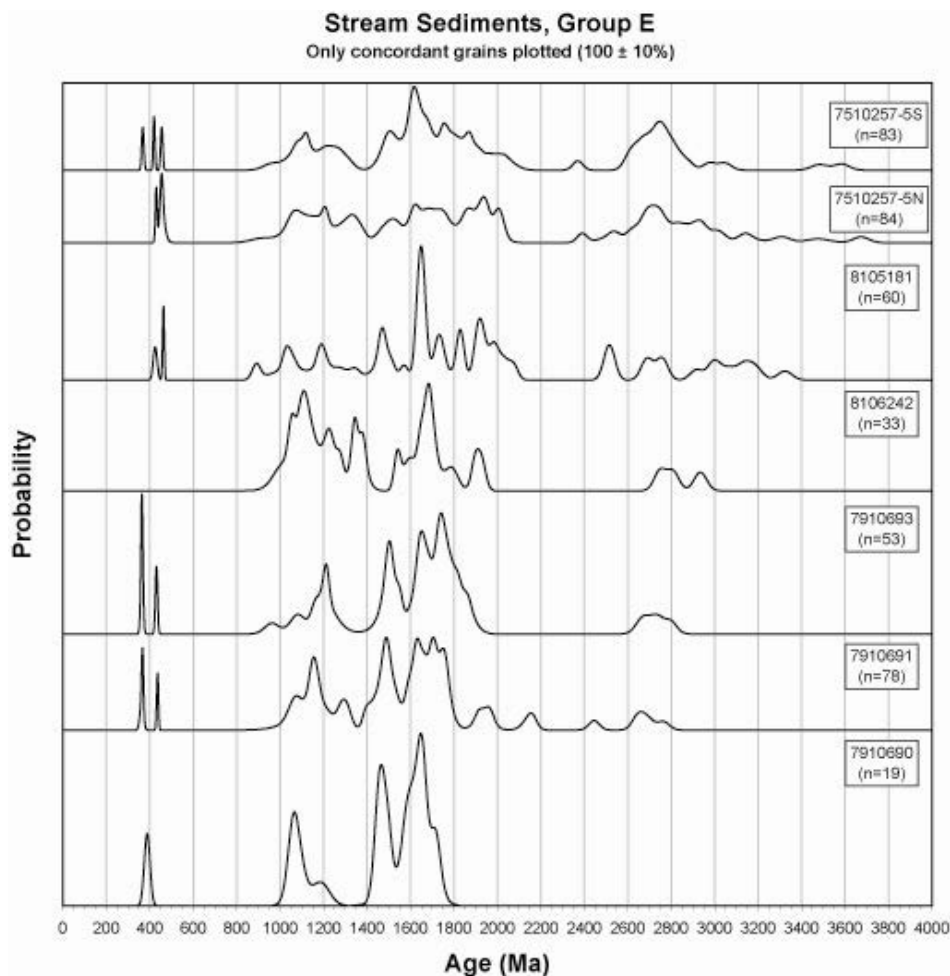


Figure 13. Detrital zircon age distribution pattern for stream sediment group E.

Group F

This group of samples consists of seven samples from Ymer Ø (fig. 8) with a similar detrital zircon age distribution (Fig. 14). All samples have minor occurrences of Archaean grains. The three samples from eastern Ymer Ø have scattered peaks between 2000 and 900 Ma and a prominent Palaeozoic population. The samples from western Ymer Ø have scattered peaks between 1900 and 1000 Ma and a prominent peak at ca. 1050 Ma. This could resemble a basement derived age population, but the peak in conjunction with the rest of the complex Proterozoic age pattern is more indicative of derivation from metasediments. The Neoproterozoic Eleonore Bay Supergroup does in some parts have a very strong signal of 1100-1000 Ma detritus (see Fig. 25). This is also the rocks exposed in the catchment areas for the streams where the samples were taken. This also explains the lack of Palaeozoic detritus. The Palaeozoic detritus in eastern Ymer Ø is probably derived from Mesozoic sediments.

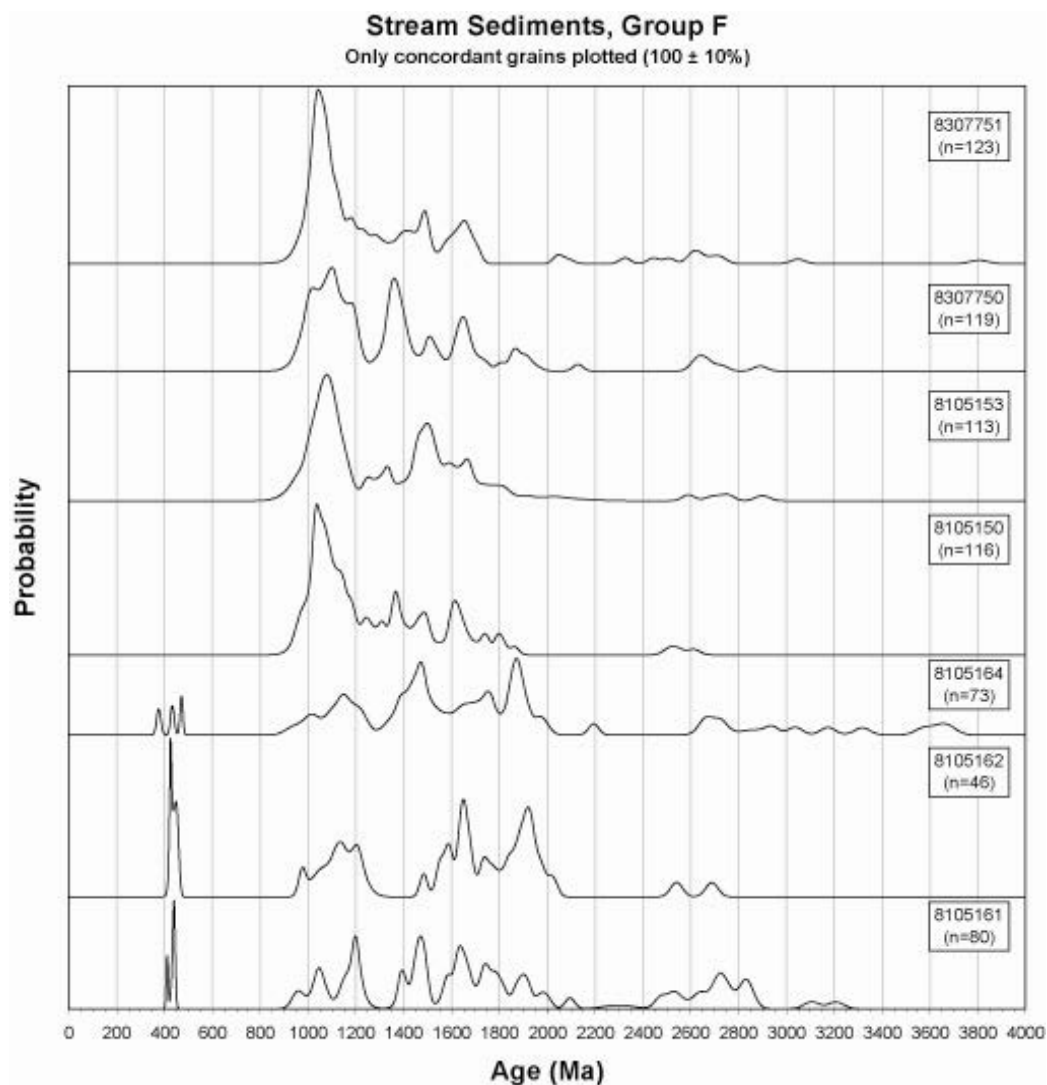


Figure 14. Detrital zircon age distribution pattern for stream sediment group F.

Group G

This group consists of seven samples from Hudson Land (Fig. 8). They have similar patterns of Archaean and Proterozoic ages that are consistent with derivation from metasedimentary units (Fig. 15). There are some large Caledonian intrusions in the area and this is reflected by voluminous Palaeozoic detritus in some samples and nothing in others.

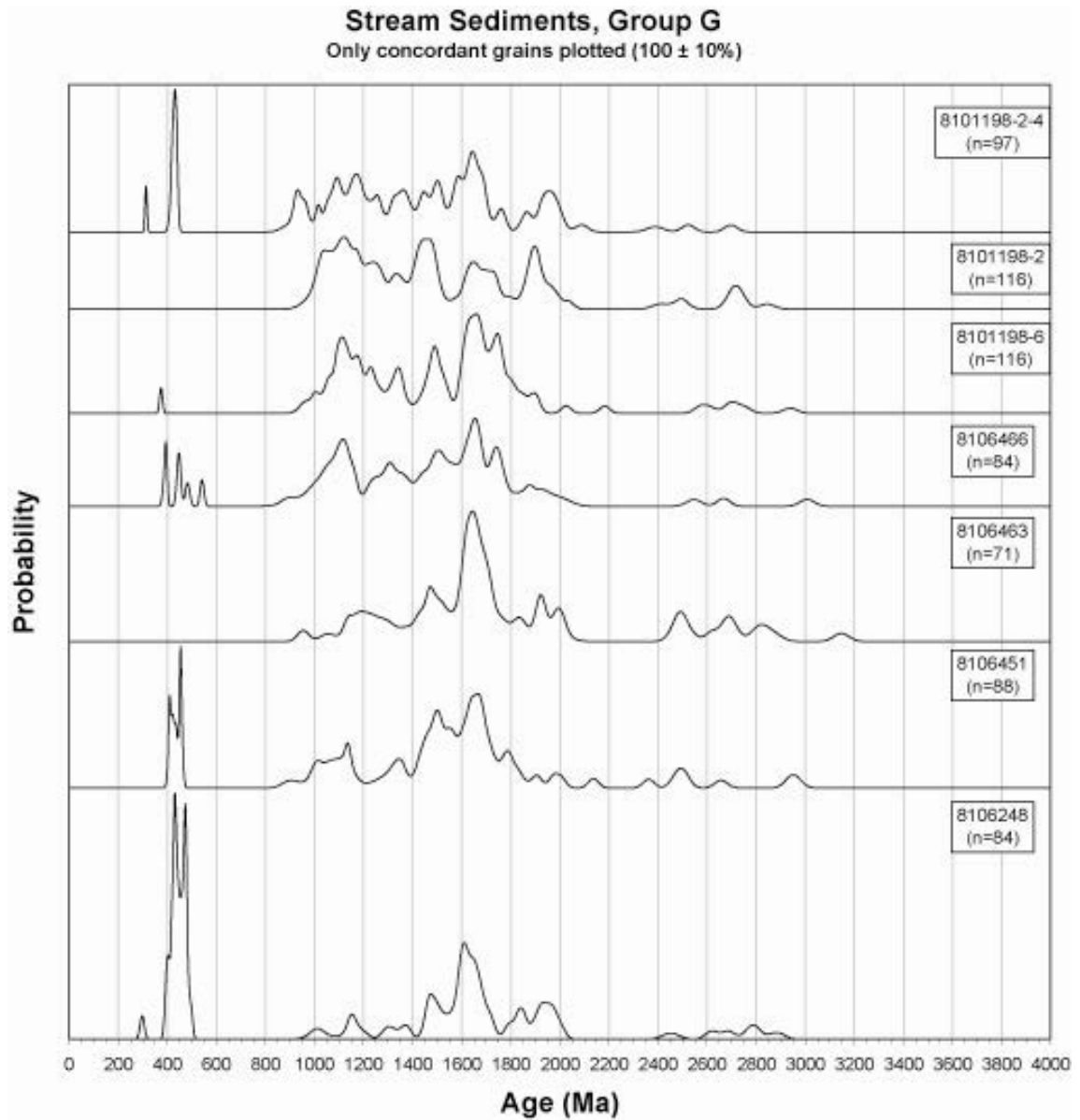


Figure 15. Detrital zircon age distribution pattern for stream sediment group G.

Group H

This group consists of six samples from Andrée Land and Strindberg Land (Fig. 8). They contain very few Archaean grains, few Palaeozoic grains and a wide selection of Proterozoic ages between 2000 and 1000 Ma (Fig. 16). The most important and consistent peak is at ~1100 Ma, which is the most common age population in some of the metasedimentary units in the area (see Fig. 5, 6 and 25). The rest of the Proterozoic pattern is also consistent with derivation from metasedimentary units. The Palaeozoic zircons come from Caledonian intrusions present in the area or from redeposited Mesozoic sediments.

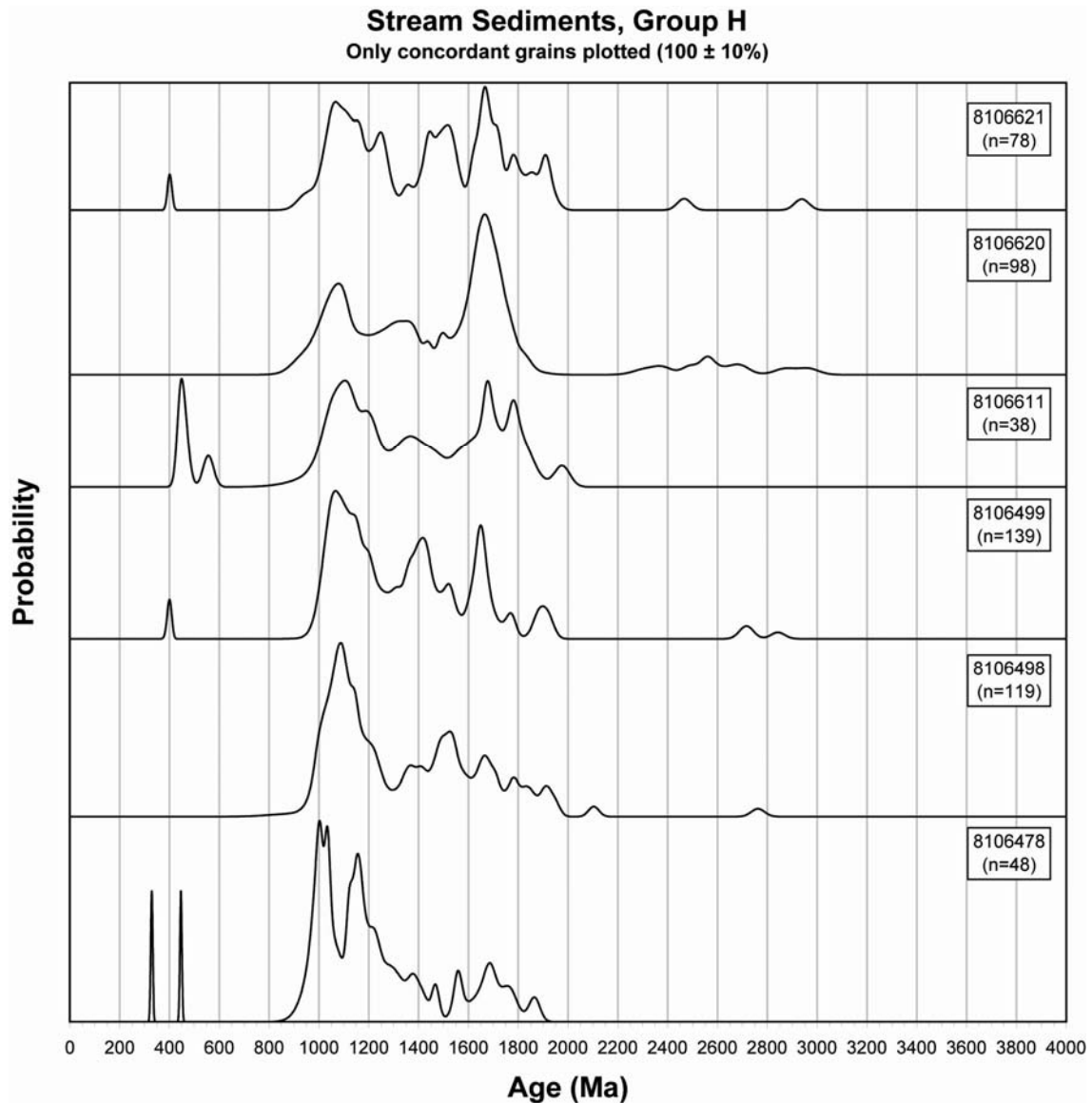


Figure 16. Detrital zircon age distribution pattern for stream sediment group H.

Group I

This group consists of five samples from Clavinging Ø, Hudson Land and Zackenberg (Fig. 8). The four lowermost samples in the plot are similar in that they have an insignificant Archaean component, a varied Proterozoic component with ages between 2000 and 900 Ma and a Palaeozoic population of varying importance (Fig. 17). Two of the samples display a proportionally important peak at 1950 Ma, which could be a sign of an increasing influence from the basement gneiss region north of 76° N. The last sample (from Zackenberg) lacks the Palaeozoic component but has an Archaean component instead. This would be consistent with a first-hand derivation from the Proterozoic Krummedal Sequence and/or Eleonore Bay Supergroup.

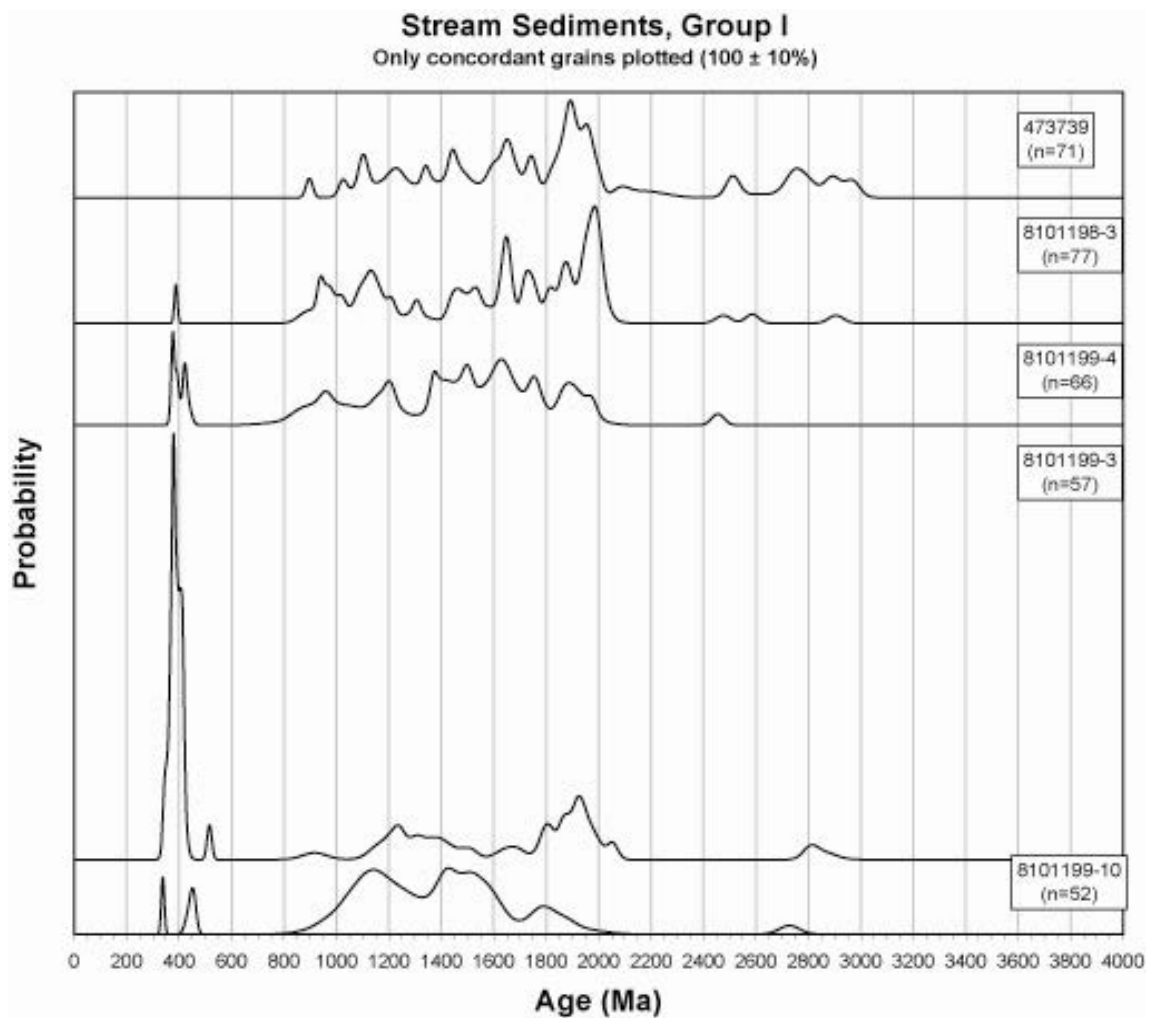


Figure 17. Detrital zircon age distribution pattern for stream sediment group I.

Northern part of the study area

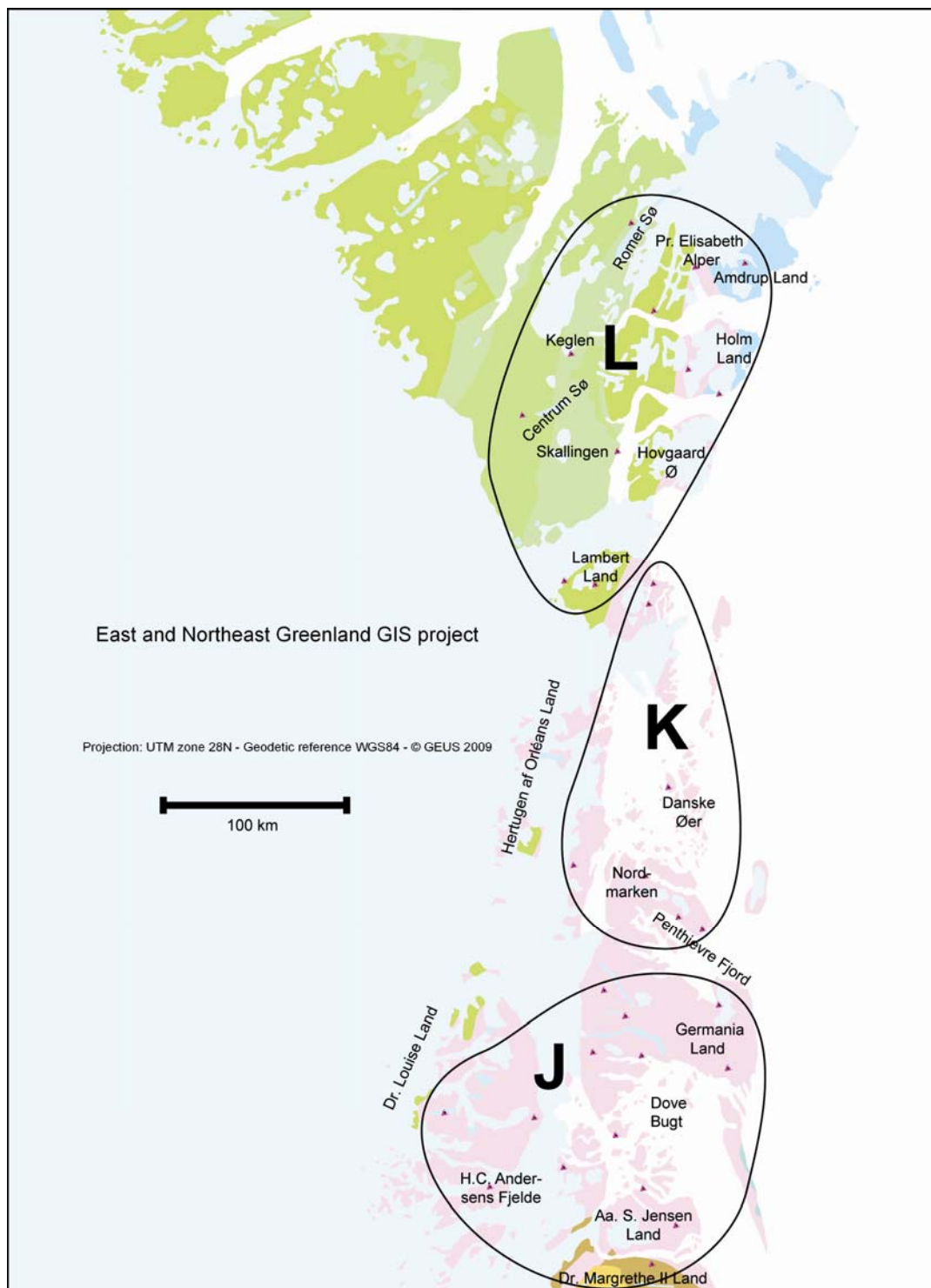


Figure 18. Locations of stream sediment samples from the northern part of the study area.

STREAM SEDIMENT SAMPLES		
Locality name	Area	Sample_nr
Dr. Margrethe II Land, Aa. S. Jensen Land, H.C. Andersen Fjelde, Dove Bugt, Dr. Louise Land, Germania Land	J	367513, 367425, 367428, 367459, 367413, 367444, 367491, 367462, 367535, 367528, 367524, 367517, 342523, 342549
Penthievre Fjord, Nordmarken, Hertugen af Orléans Land, Danske Øer, Lambert Land	K	342516, 342503, 348221, 342558, 348202, 382899, 381159
Lambert Land, Skallingen, Hovgaard Ø, Centrum Sø, Holm Land, Keglen, Pr. Elisabeth Alper, Amdrup Land, Rømer Sø	L	382931, 381356, 381276, 381236, 382722, 382715, 381241, 382682, 382696, 382708, 382946

Table 2. Overview of stream sediment sample groups in the northern part of the project area.

Group J

This group consists of 13 samples (Fig. 19) from between Dr. Margrethe II Land and Germania Land (Fig. 18). One sample (367513) has an anomalous age profile, but this is most certainly a product of very few concordant analyses from this samples (N=8). This probably also causes the relative importance of the different components to be exaggerated. Unlike the other samples this one is taken in a stream with a catchment area where metasedimentary rocks are exposed in contrast to basement gneisses. All other samples in the group have one or two principal components in the 2000-1700 Ma range, most samples have an Archaean population and some scattered Palaeo- and Mesoproterozoic ages. Ten of the samples have Palaeozoic grains. The signature picked up in these samples is indicative of derivation from basement, in this case the basement region north of 76° N. There is some contribution that most probably comes from Neoproterozoic metasediments and there are contributions from Caledonian intrusions. All known Caledonian intrusions are situated south of this area, but there is evidence of Caledonian high-grade metamorphism that also produced Palaeozoic zircon (e.g. Gilotti and McClelland 2008).

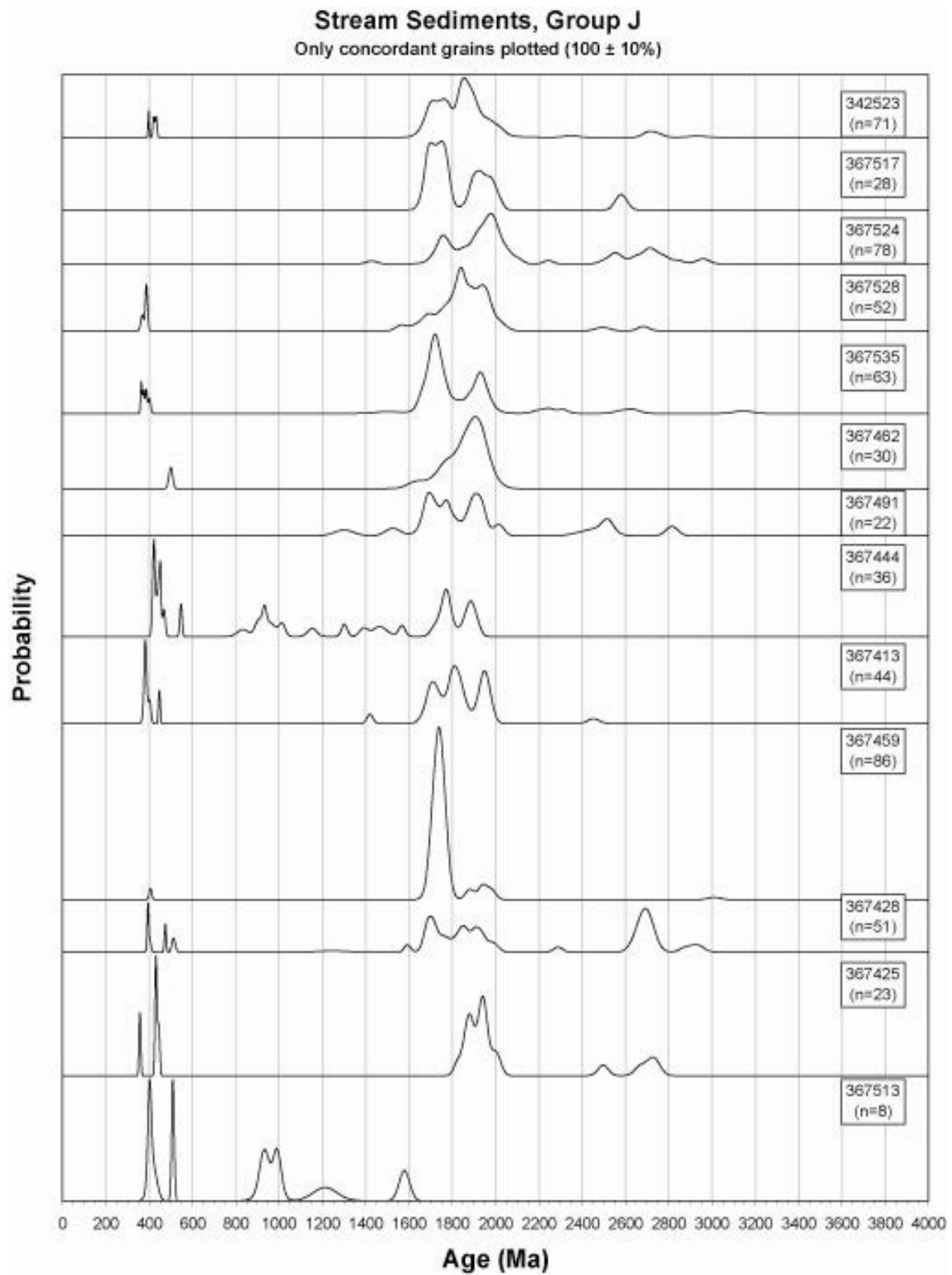


Figure 19. Detrital zircon age distribution pattern for stream sediment group J.

Group K

This group consists of seven samples from the area between Hertugen af Orléans Land and eastern Lambert Land (Fig. 18), with similar and simple age distribution patterns (Fig. 20). All samples have a varied and minor Archaean component and a prominent 1950-1900 Ma component. Some of the samples also have 1750 Ma and Palaeozoic components. The characteristics of this group are consistent with derivation from Palaeoproterozoic basement gneisses north of 76° N and from Caledonian intrusions.

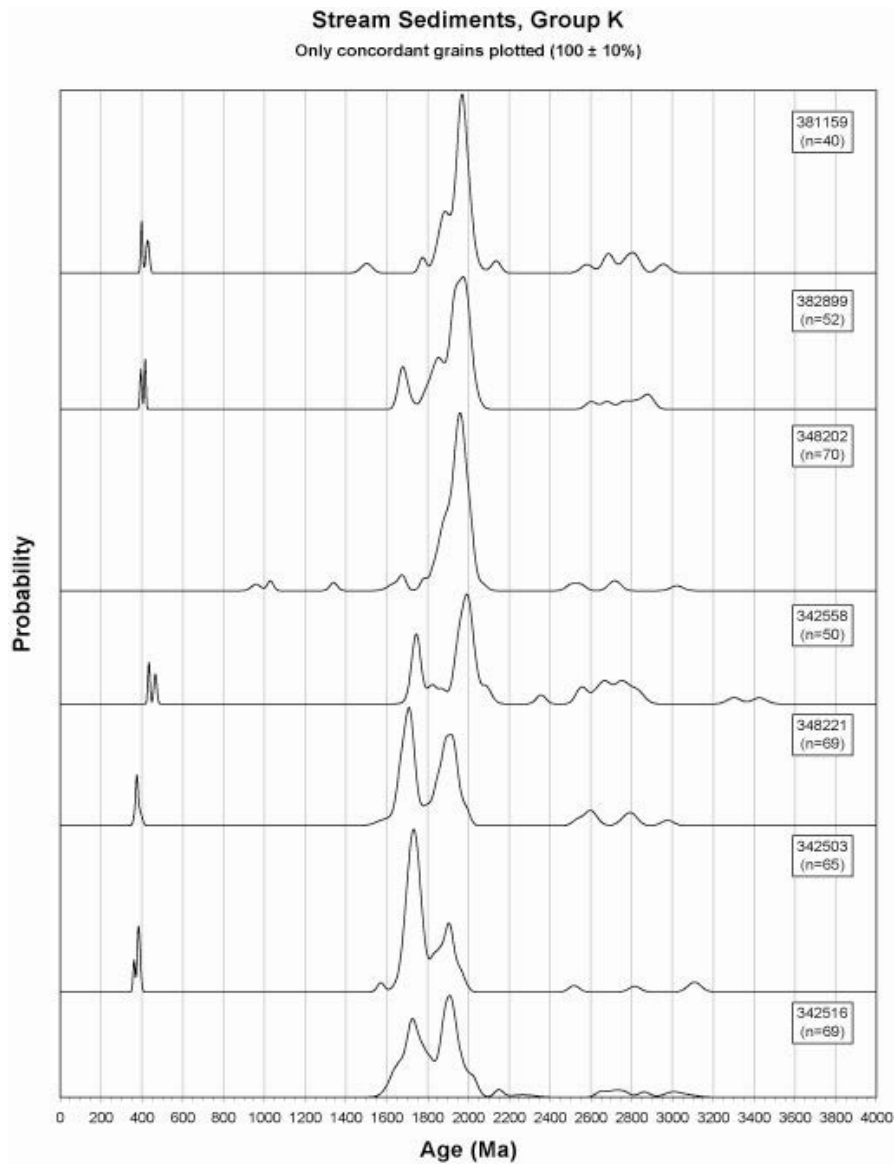


Figure 20. Detrital zircon age distribution pattern for stream sediment group K.

Group L

This group consists of eleven samples from the northernmost part of the study area (Fig. 18). Some of the samples (382931, 382722, 382715) have an extremely simple age profile (Fig. 21), but this is most certainly a product of very few concordant analyses from these samples (N=17, 22, 21). In one case (lowermost sample in plot) this probably also causes the relative importance of the Palaeozoic population to be over-exaggerated. All the samples in the group have their principal component in the 2000-1800 Ma range, most samples have an Archaean population and some scattered Palaeo- and Mesoproterozoic ages. Three of the samples have Palaeozoic grains. The signature picked up in these samples is indicative of derivation from basement, in this case the northern basement region. There is some contribution that most probably comes from Neoproterozoic sediments and from Caledonian intrusions or metamorphic rocks.

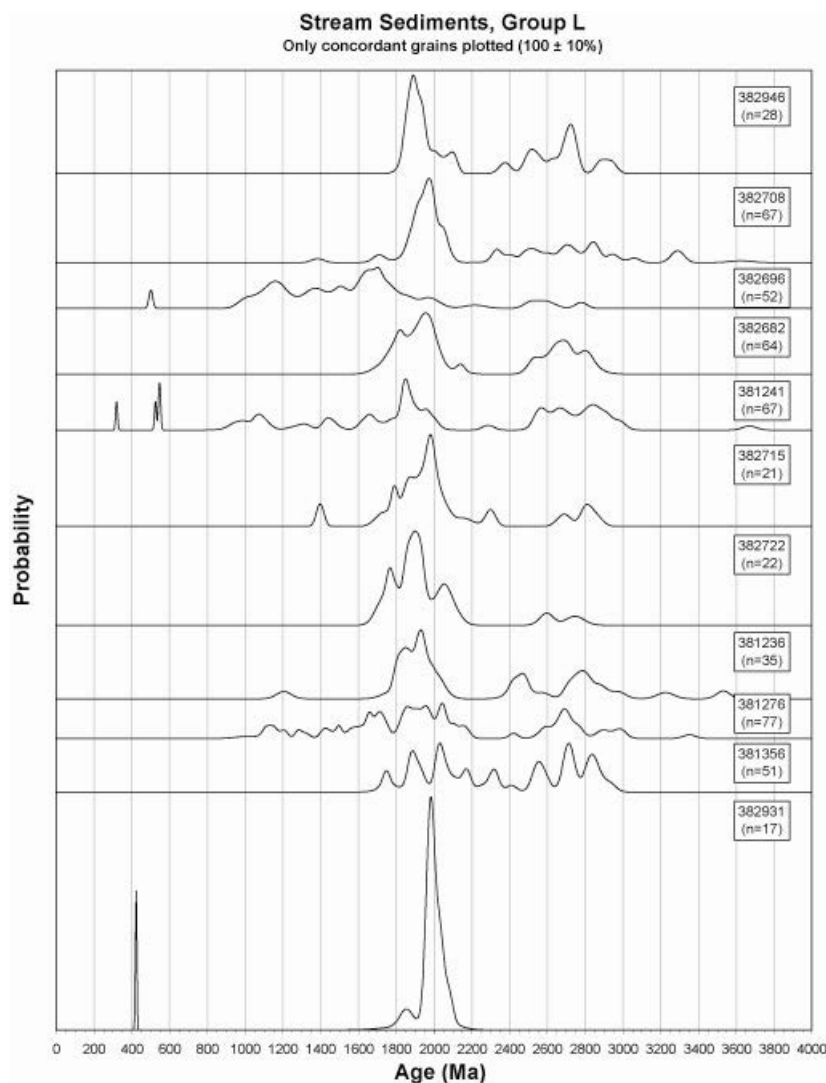


Figure 21. Detrital zircon age distribution pattern for stream sediment group L.

Presentation and interpretation of sandstone samples in profiles

This section of the results presents sandstone samples within the sections they were sampled, with the oldest sample at the bottom. Some profiles are long, some are short and yet others consist of only one sample. Some of the profiles span many stratigraphic units, whereas others are confined to within a formation or even member. Most of this information is displayed together with the stacked probability density plots, the rest can be discerned from the sample information files in Appendix A and on the NE Greenland web site. The samples are divided into Pre- and Post-Devonian samples. There is sometimes a discrepancy between the number of samples in the text and of localities on the maps. This is merely a scale problem, where samples that are collected very close to each other cannot be resolved in the map scale shown. The locations of the profiles on regional scale are shown in figures 22 and 23 an an overview of profile locations and sample numbers are presented in tables 3 and 4. The colours on the maps are referred to the geological map legend in Figure 3.

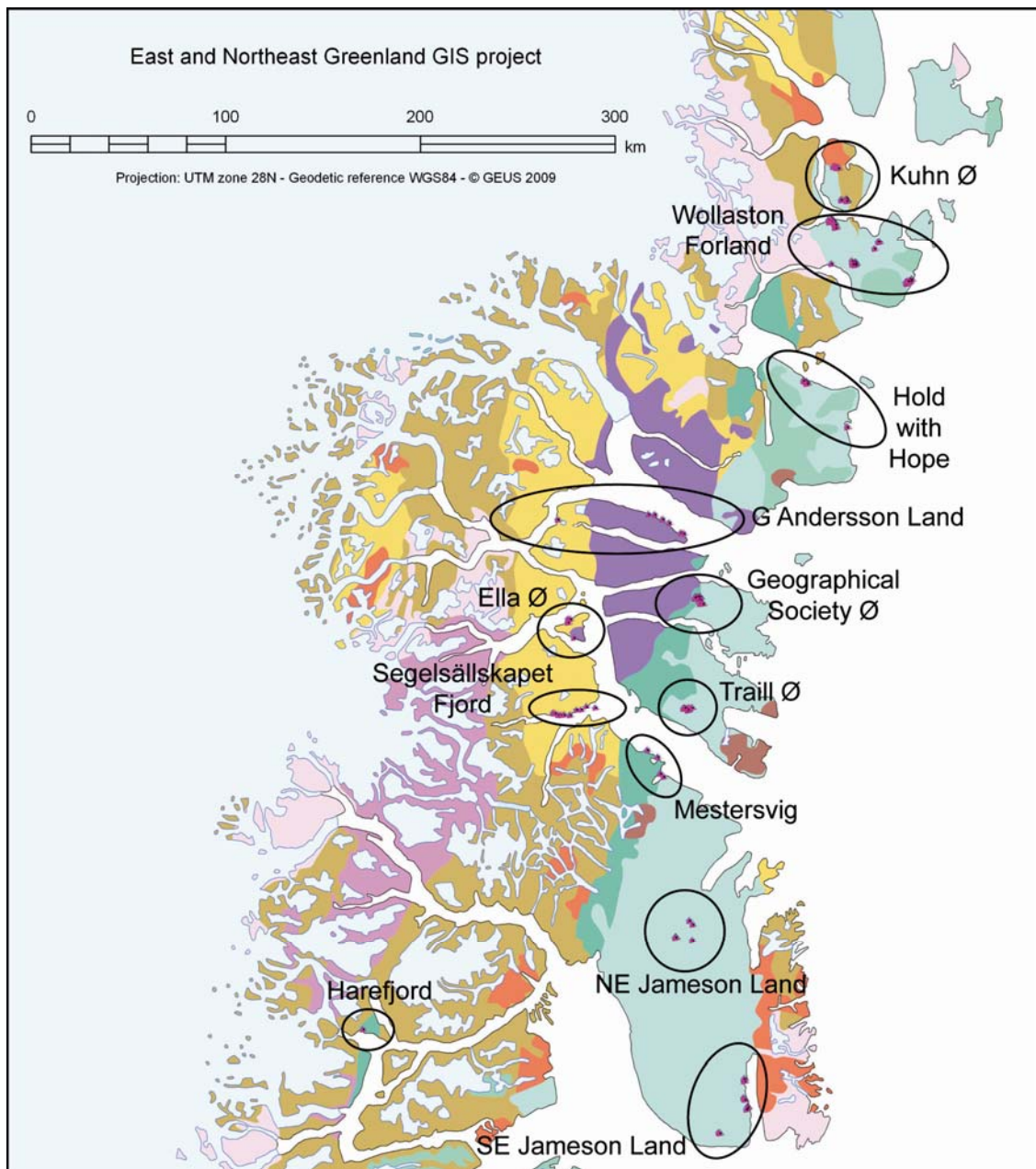


Figure 22. Location of the sandstone sample profiles in the southern part of the study area. Legend for colours in Figure 3.

SANDSTONE SAMPLES		
PRE-CARBONIFEROUS		
Locality name	Profile	Sample_nr
Harefjord	5	473702
Gunnar Andersson Land, Blomsterbugt	4	473729-473735
Mestersvig	3	473714-473718
Ella Ø	2	473707-473711
Segelsällskapet Fjord	1	473719-473728
POST-DEVONIAN		
Locality name	Profile	sample_nr
South Jameson Land	10	487716-487718
East Jameson Land	6-9	487701-487721
NE Jameson Land, Olympen Mt.	12	508789-508794 + 508798
NE Jameson Land, Pelion Mt.	11	508795-508797
Traill Ø, Svinhufvud Bjerger	18	487722-487728 + 487741
Traill Ø, Svinhufvud Bjerger	17	487729-487733
Traill Ø, Svinhufvud Bjerger	14	487734-487740
Geographical Society Ø, Tørvestakken	19	487747-487751
Geographical Society Ø, Tørvestakken	16	487742-487746
Geographical Society Ø, Tørvestakken	15	487752-487761
Geographical Society Ø, Tørvestakken	13	487762-487766
Hold with Hope East , Knudshoved	22	487777-487778
Hold with Hope North, Gulelv	21	487767-487772
Hold with Hope North, Gulelv	20	487773-487776
Haredal, E Wollaston Forland	35	508723 + 508726-508730
Haredal, E Wollaston Forland	34	508724
Haredal, E Wollaston Forland	33	508725
Haredal, E Wollaston Forland	32	508732-508734
Haredal, E Wollaston Forland	31	508731 + 508735-508738
Rødryggen, South	30	508770
Niesen 3, NW Wollaston Forland	29	508713-508717
Niesen 2, NW Wollaston Forland	28	508708-508710, 508718-508722
Niesen 1, NW Wollaston Forland	27	508705-508707
Rødryggen, East	26	508771-508773
Cardiocerasdal, W Wollaston Forland	25	508764-508767
Cardiocerasdal, W Wollaston Forland	24	508757-508763
Bastian Dal, W Kuhn Ø	38	508739-508745
Payer Dal West, Kuhn Ø	37	508780-508782
Payer Dal East, Kuhn Ø	36	508774-508779 + 508783-508784

Table 3. Overview of sandstone profiles and samples in the southern part of the project area.

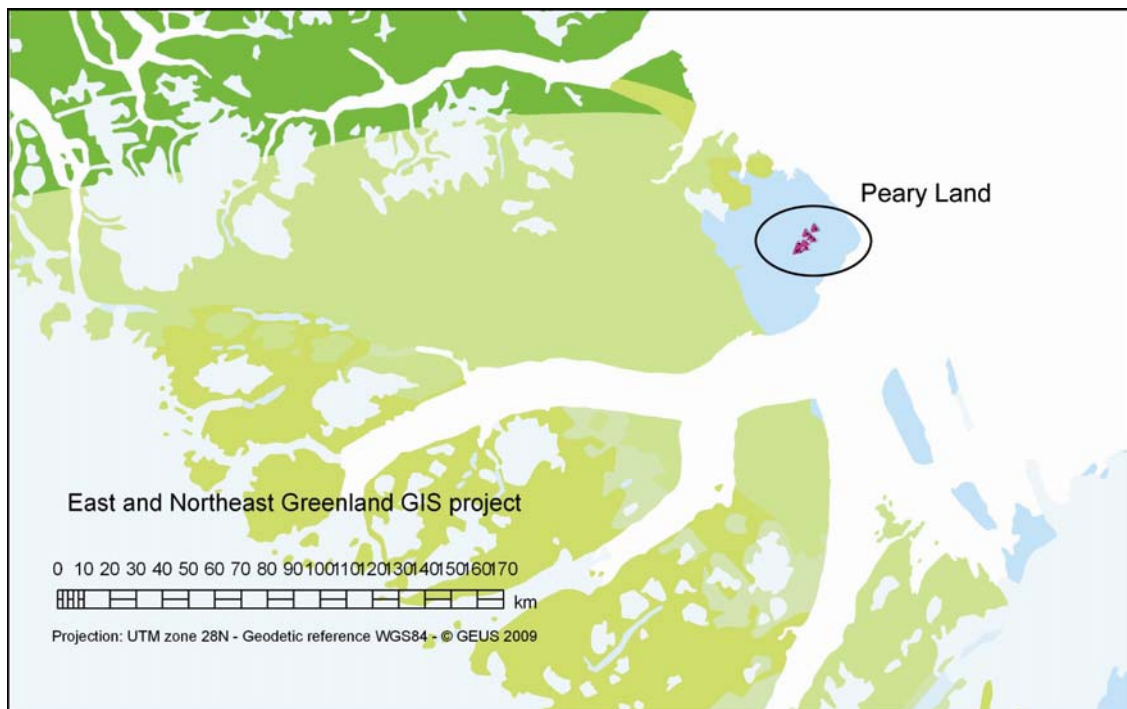


Figure 23. Location of the sandstone sample profiles in the northern part of the study area. Legend for colours in Figure 3.

POST-DEVONIAN		
Locality name	Profile	sample_nr
Dunken, Kim Fjelde	42	113464-113468
Ved Sletten, Kim Fjelde	43	113471-113474
Dunken, Kim Fjelde	42 or 44	113469
Ved Sletten, Kim Fjelde	43	113472-113474
Falkefjeld, Kim Fjelde	44	113475-113480
Falkedal Kim Fjelde	45	113470
Søjlerne, Kim Fjelde, Peary Land	46	113451-113459
Ladegårdsåen, Kim Fjelde	47	113460-113463

Table 4. Overview of sandstone profiles and samples in the northern part of the project area.

Pre-Devonian sandstone sections

Profile 1: Segelsällskapetets Fjord

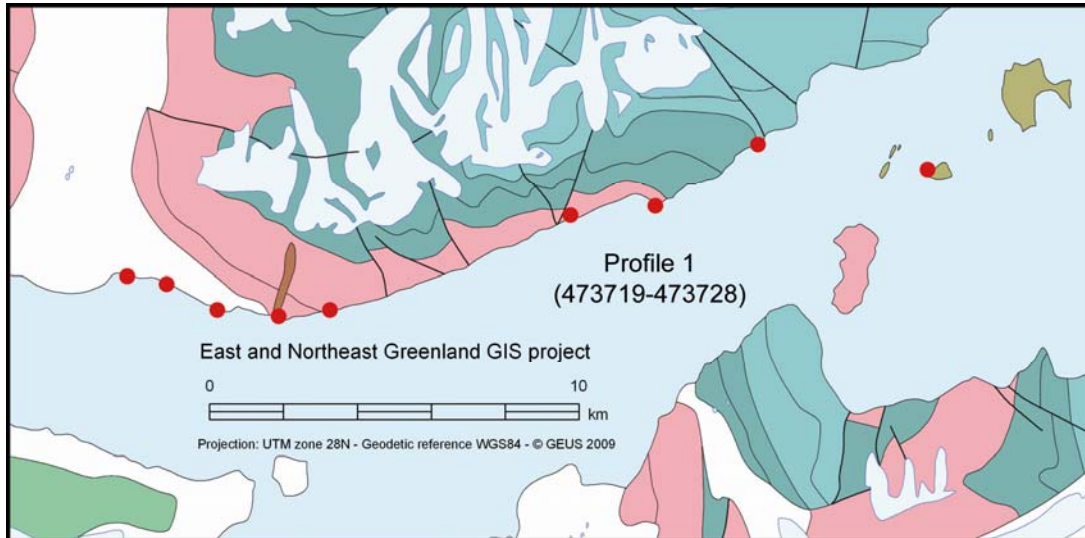


Figure 24. Locations of the sampling points of Profile 1.

This profile (Fig. 24) consists of 10 samples of the Neoproterozoic Eleonore Bay Supergroup. There is a very minor population of Archaean grains in most samples, although this population is entirely missing in some samples (Fig. 25). The main population stretches from ca. 2000 to 1000 Ma, with slight variations internally. The largest peak common to all samples is at ca. 1100 Ma, and 1650 Ma appears in many samples. The spectra seen here coincide with published data from the Eleonore Bay Supergroup (e.g. Dhuime et al. 2007) (see Fig. 5).

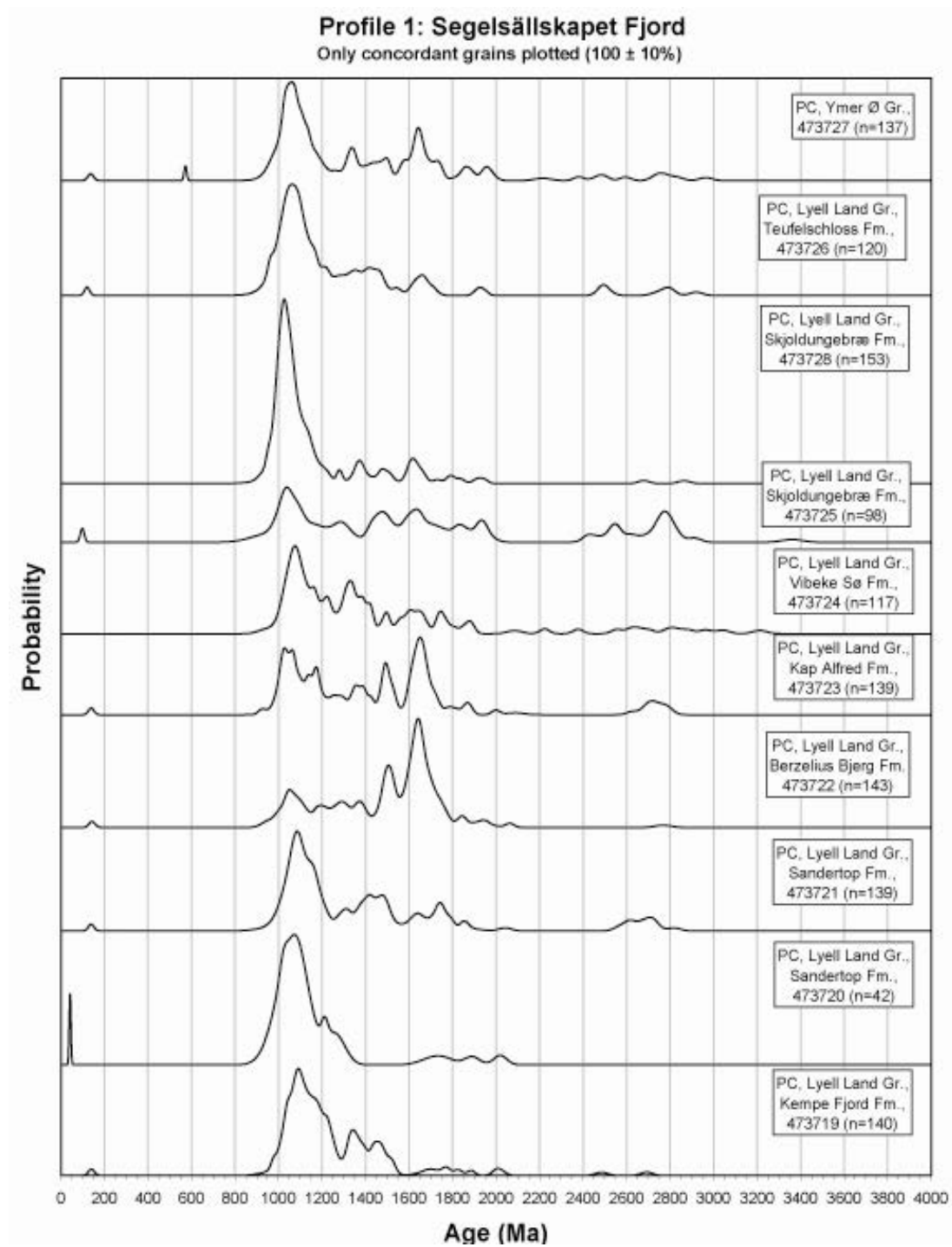


Figure 25. Stacked probability density plots of detrital zircon ages from Profile 1.

Profile 2: Ella Ø

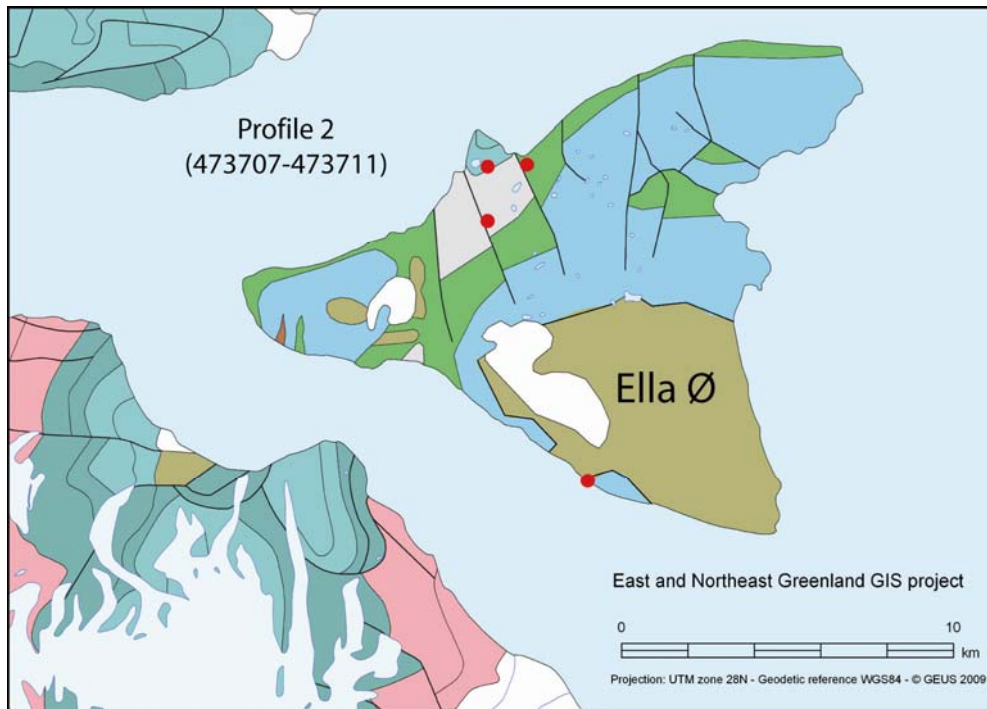


Figure 26. Locations of the sampling points of Profile 2.

This profile consists of five Late Neoproterozoic to Cambrian and Devonian samples. The two lowermost Precambrian samples have an age distribution reminiscent of the Eleonore Bay sediments presented above (see Figs. 5 and 25). However, the youngest sample from the Tillite Group and the Cambrian Kong Oscar Fjord Group sample show a significant shift towards locally derived basement detritus, with a major peak at 2800 Ma and a minor peak at 1900 Ma. These are the two principal components of East Greenland Precambrian basement (e.g. Thrane 2002) (see Fig. 4). The Devonian sample has an age distribution indicating mixed sources, both from older metasedimentary rocks and local basement rocks.

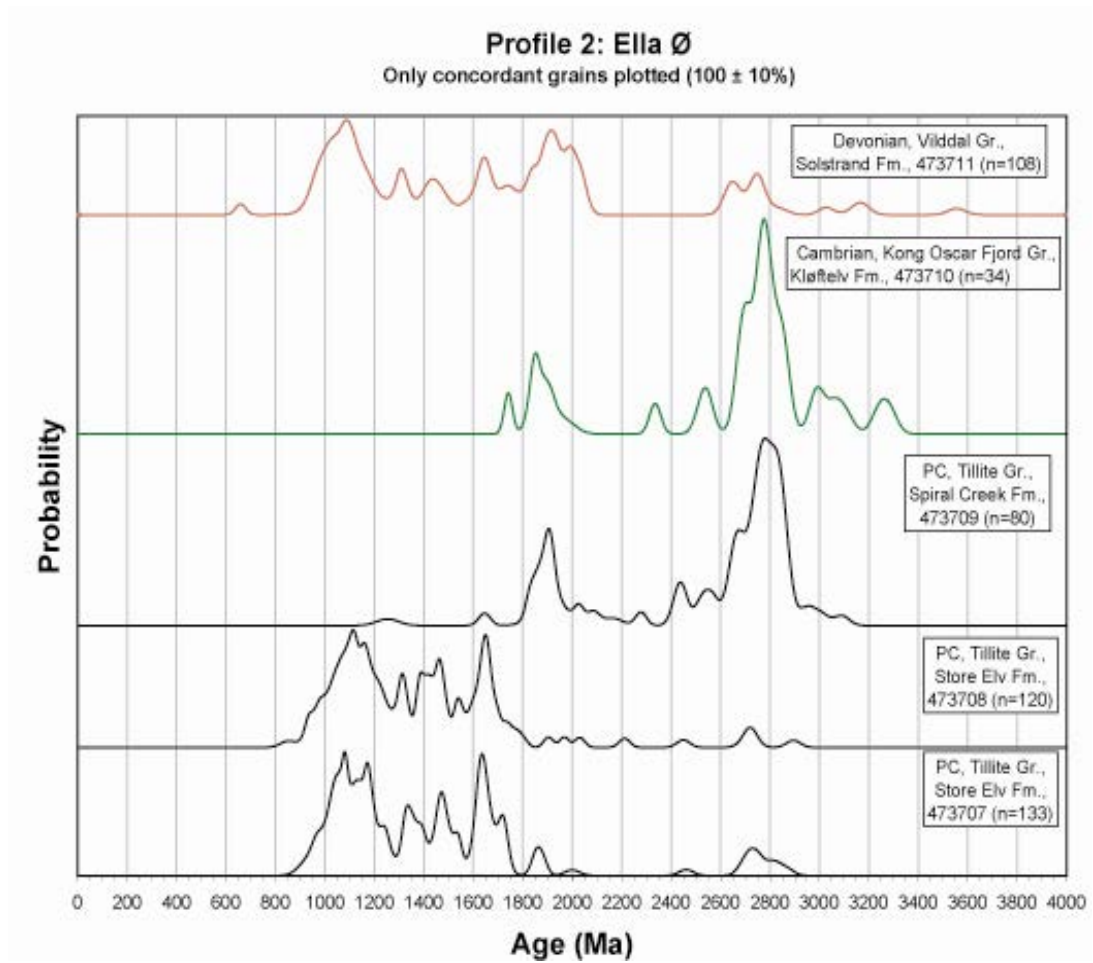


Figure 27. Stacked probability density plots of detrital zircon ages from Profile 2.

Profile 3: Mestersvig

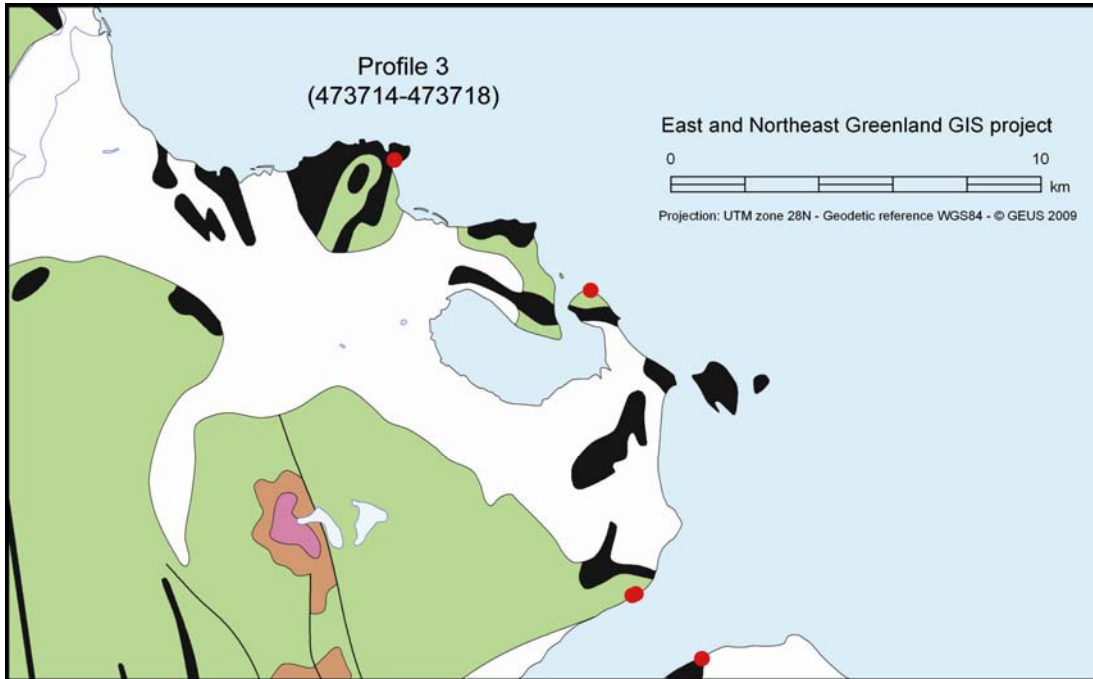


Figure 28. Locations of the sampling points of Profile 3.

This profile (Fig. 28) contains four Carboniferous samples and one Permian (Fig. 29). There is a persistent Archaean component, with some surprisingly old zircon grains at 3700-3500 Ma. Such old age are not present locally in East Greenland (e.g. Thrane 2002), but may have been derived from the west or the south. However, as the inland ice presently covers the internal parts of Greenland, it is not known how large the distances to these sources are. The main population covers the ages from about 2000 Ma to 950 Ma. The largest peaks are found between 1800 and 1600 Ma. In addition to the Precambrian ages, there is also a strong input of Caledonian zircon grains in the Carboniferous samples and a minor input in the Permian. The 1000-950 Ma possibly comes from Neoproterozoic intrusions, some of which can be found in the Stauning Alper area, to the southwest of Mestersvig. There are no major shifts in the age populations, and the age distribution pattern is consistent with derivation of the sediments from the west or southwest. They could be derived from the northwest as well, but this includes longer transport distances.

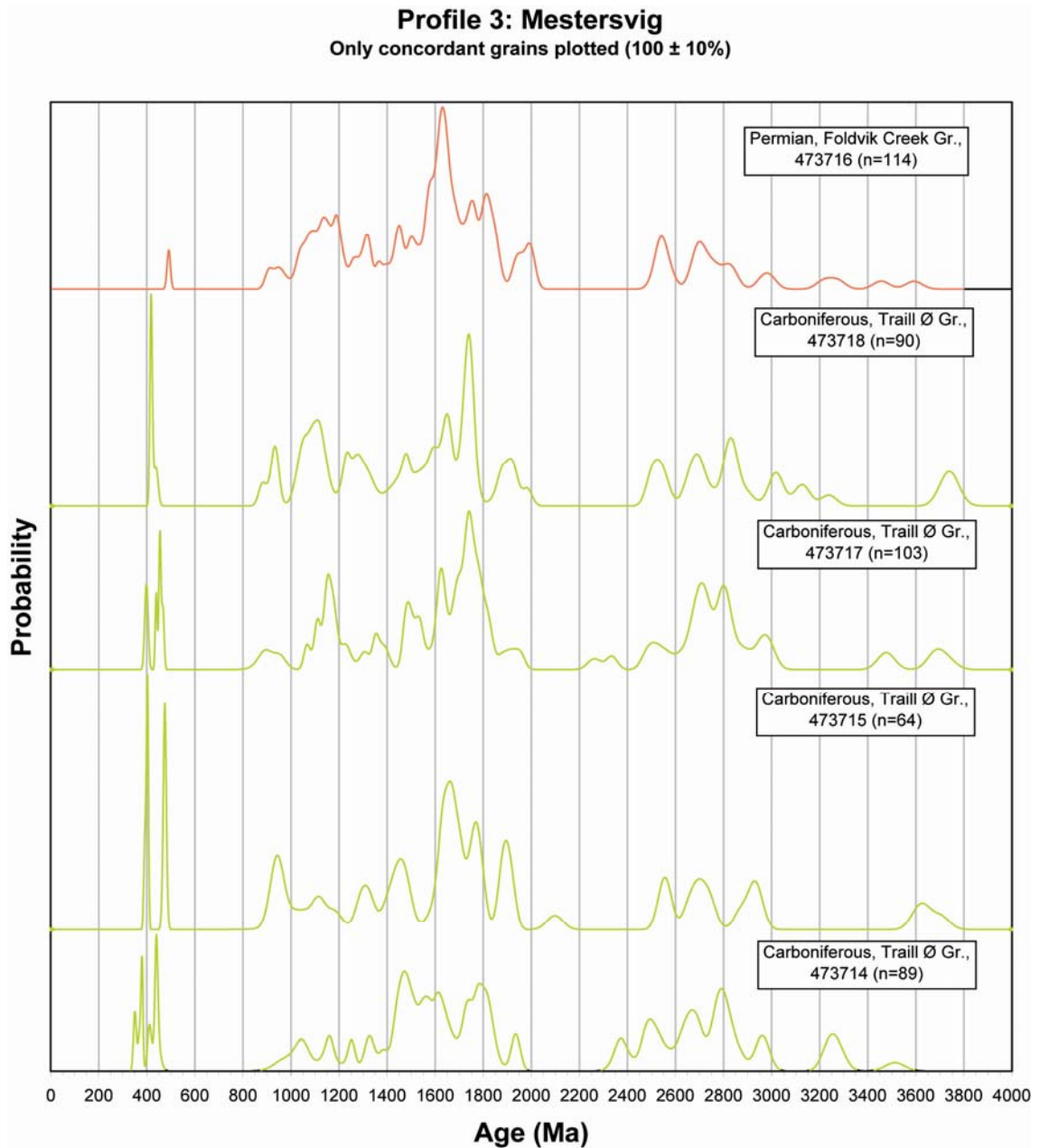


Figure 29. Stacked probability density plots of detrital zircon ages from Profile 3.

Profile 4: Gunnar Andersson Land

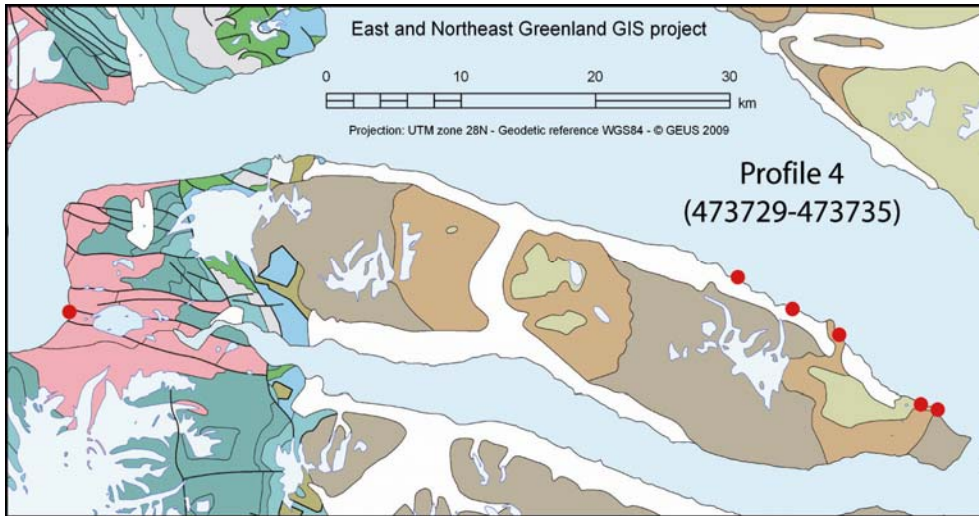


Figure 30. Locations of the sampling points of Profile 4.

This profile (Fig. 30) starts with a Precambrian sample and is followed by six Devonian samples (Fig. 31). The Precambrian sample has a typical Eleonore Bay signature, with varied both Archaean and Proterozoic populations (cf. Fig. 5). The two oldest samples in the profile have an insignificant Archaean population, a strong peak at 1950 Ma and minor contributions of detritus with variable ages down to 1000 Ma. There is no Caledonian population. This age distribution pattern is consistent with a strong contribution from Proterozoic basement areas and with minor contribution from metasediments. The following four Devonian samples have a variably frequent Archaean population, but all samples contain a 2700 Ma population. Zircon grains with ages between 2000 and 1000 Ma are more or less evenly distributed, with an increase between 1800 and 1600 Ma. All these characteristics are the same as the metasedimentary sequences in the thrust-sheets. In addition the samples have a Palaeozoic population. The two older samples have an Early Caledonian signature, whereas the two samples from the Celcius Bjerg Fm. have a mid-Caledonian signature. The Early Caledonian signature could indicate derivation from the southern part of the orogenic belt. The shift from basement dominated to metasediment dominated age pattern is significant and is most easily interpreted as a shift in transport direction from northerly to more southern source areas, since Palaeoproterozoic basement is not present south of ca. 73° N.

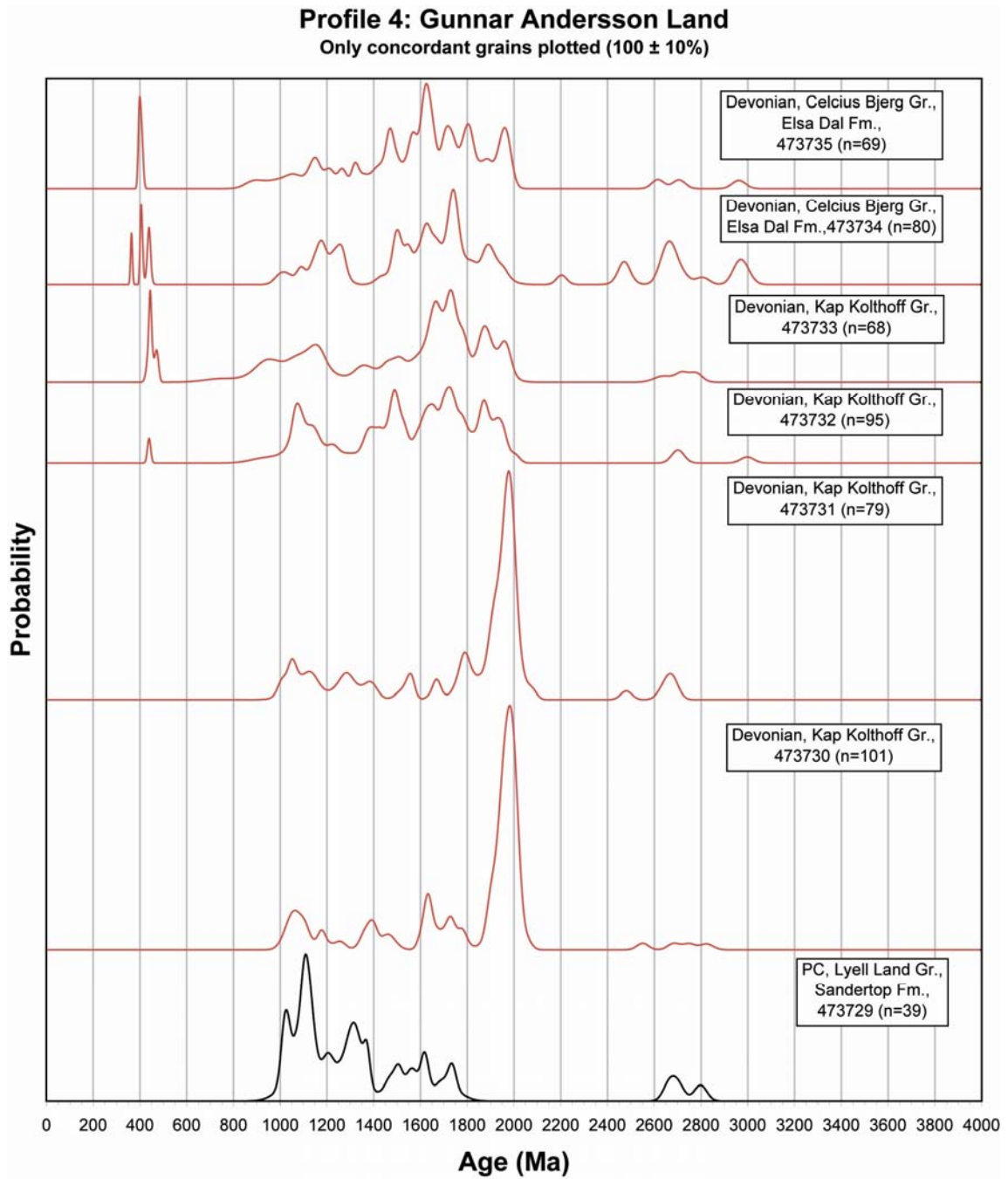


Figure 31. Stacked probability density plots of detrital zircon ages from Profile 4.

Profile 5: Harefjord

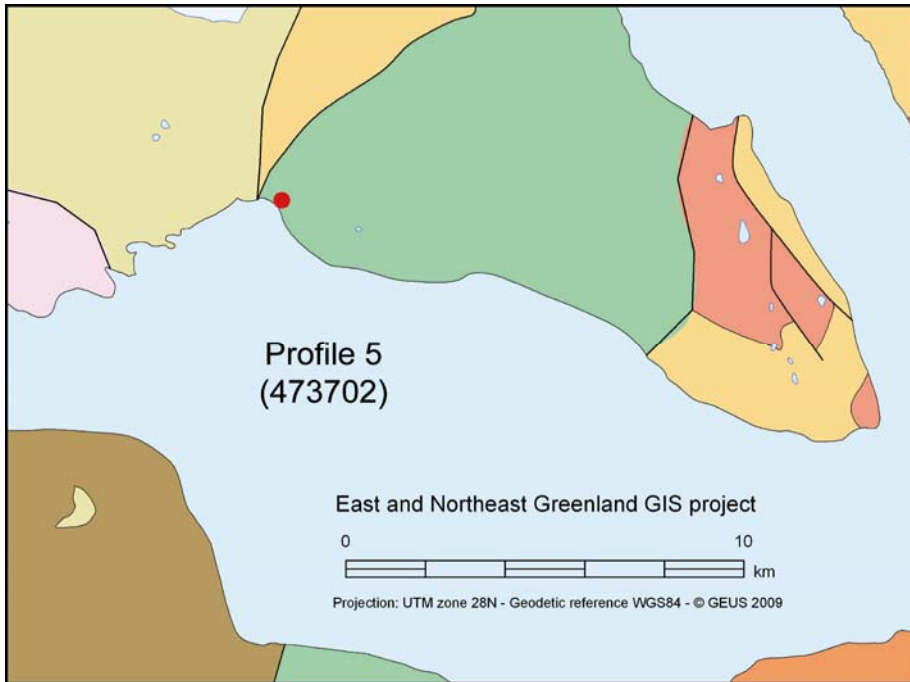


Figure 32. Locations of the sampling points of Profile 5.

This is a coarse-grained Permian conglomerate sample, deposited in a local intra-montane basin in the southern part of the study area (Fig. 32). It has a small Archaean component, variably frequent occurrences between 1900 and 1000 Ma (Fig. 33). There is prominent Palaeozoic population with multiple peaks. A few Neoproterozoic ages are noteworthy, but difficult to interpret.

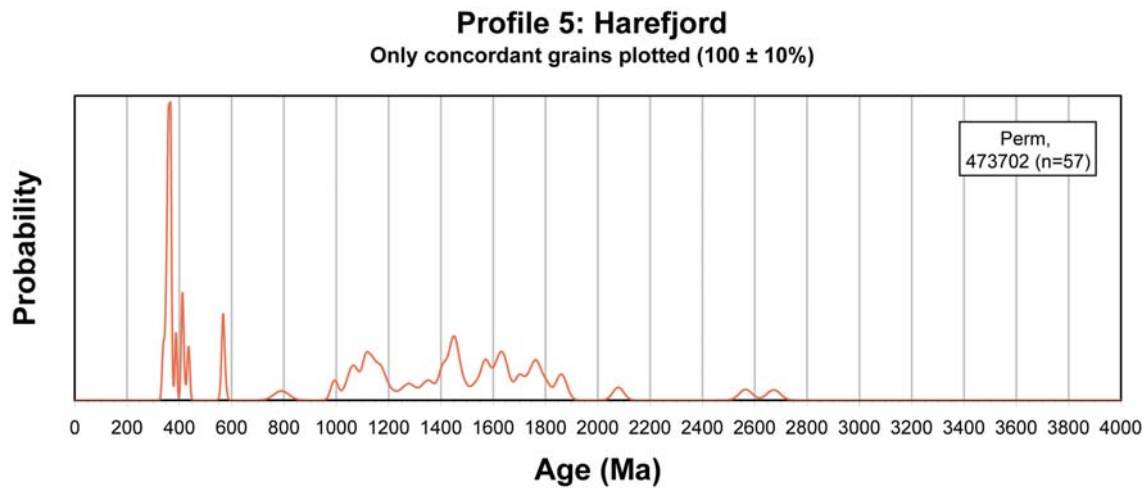


Figure 33. Stacked probability density plots of detrital zircon ages from Profile 5.

Post-Devonian profiles

South and East Jameson Land

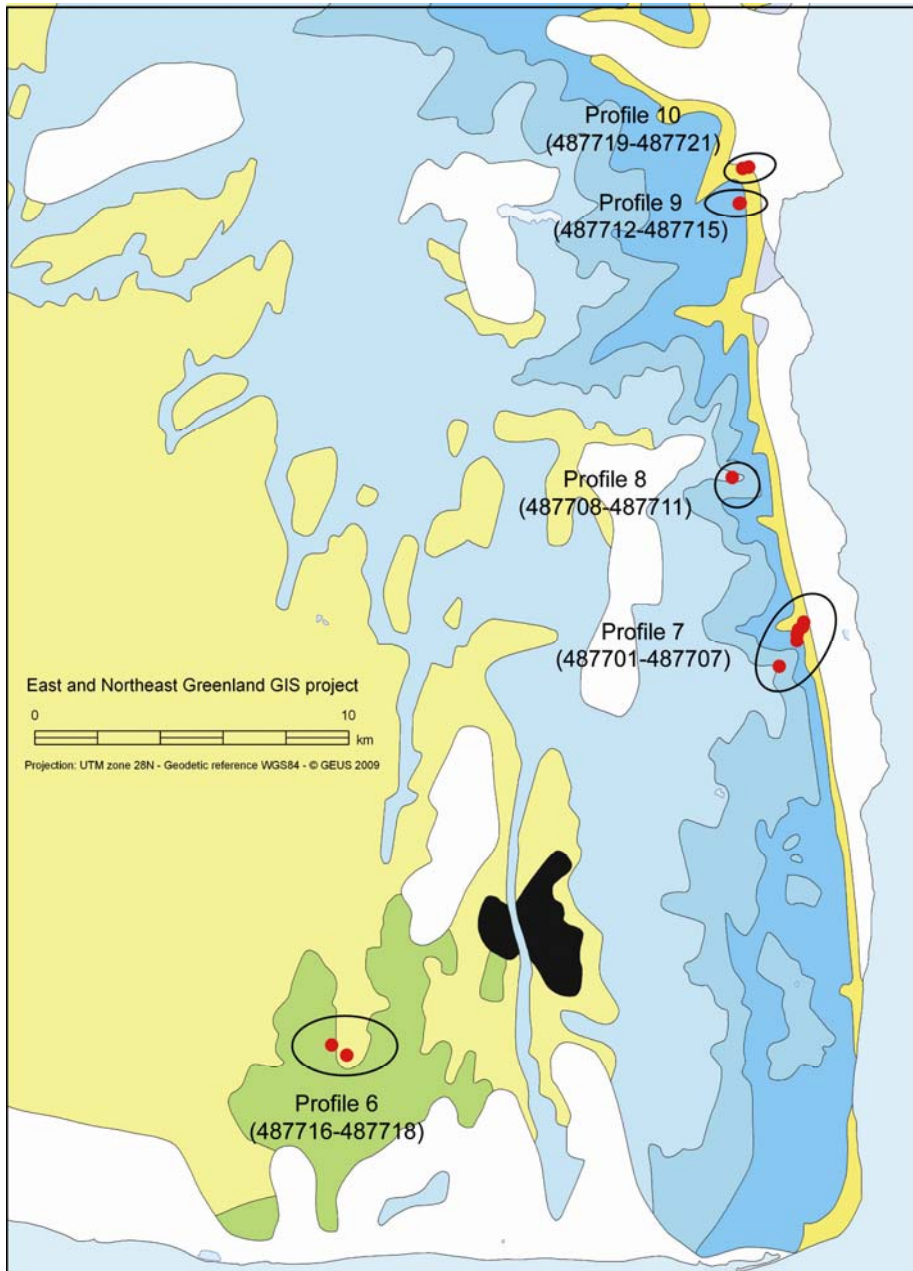


Figure 34. Locations of the sampling points of Profiles 6-10.

Profile 6: transect 4

This profile (Fig. 34) consists of one Jurassic samples from the Raukelv Fm. and two Cretaceous samples from the Hesteelv Fm. (Fig. 35). All samples are similar and have complex age patterns, with an Archaean population between 3400 and 2400 Ma and a Proterozoic population between 2000 and 800 Ma. Additionally there is a population with Palaeozoic ages. All the ages are consistent with a locally present sources in Liverpool Land, in the form of 1650 Ma gneisses, 420 Ma Caledonian intrusions and a varied metasedimentary source (see Figs. 5 and 7).

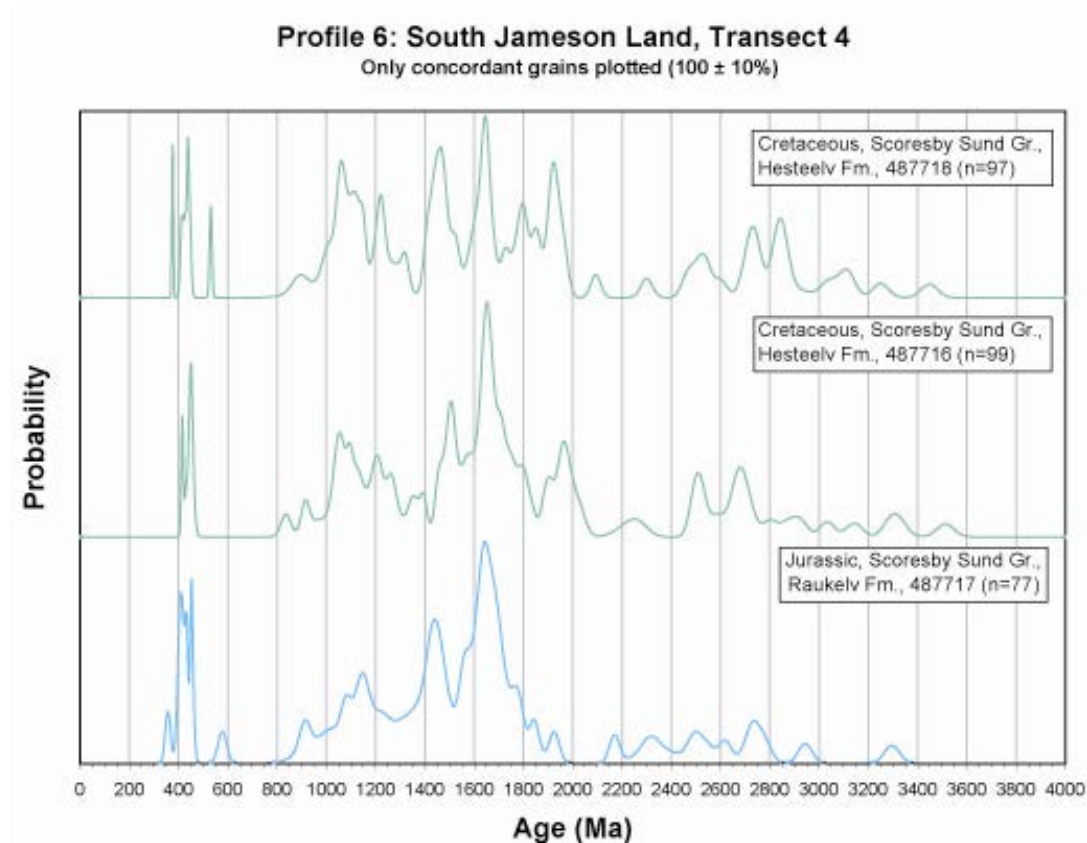


Figure 35. Stacked probability density plots of detrital zircon ages from Profile 6.

Profile 7: transect 3

This profile (Fig. 34) contains four Jurassic samples. The oldest sample is from the Rævekløft Fm., the next from the Gule Horn Fm. and the two youngest of unknown Fm., but belonging to the Neill Klintor Group as the two previous (Fig. 36). The three youngest samples are similar with a bimodal distribution of ages at 1650 and 450-400 Ma, but with some scattered minor ages. The oldest sample does not contain proportionally as much of the 1650 Ma component as the other samples and also have more of other scattered ages. The samples have an age distribution consistent with derivation from local sources, notably Liverpool Land, but with contribution from metasedimentary sources, especially in the oldest sample. There are metasediments present in Liverpool Land.

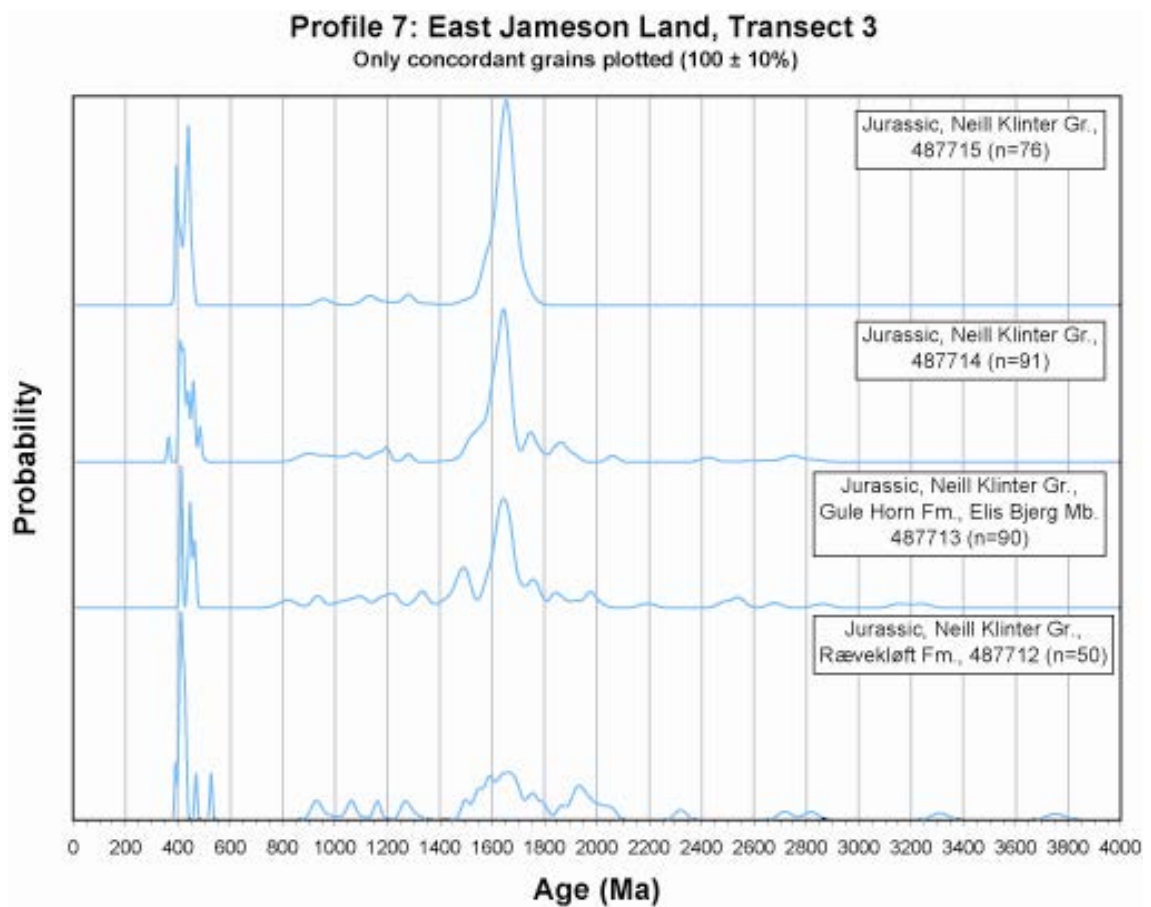


Figure 36. Stacked probability density plots of detrital zircon ages from Profile 7.

Profile 8: transect 2

This profile (Fig. 34) consists of four Jurassic samples from the Rætelv Fm., the Fossilbjerget Fm. and Hareelv Fm. (Fig. 37). The two youngest samples come from the Hareelv Fm. The oldest sample has a simple bimodal age distribution with a 1650 Ma and a 420 Ma peak. From the Fossilbjerget Fm. sample and upwards there is drastic increase in the input from a source with mixed contributions of Archaean and Proterozoic ages. This change could be attributed to a change in sediment transport direction or a palaeotopographic effect. All the ages can be interpreted as locally sourced (e.g. Johnston et al. 2010; Augland et al. 2010). The oldest sample could have a source in Liverpool Land and the younger samples would have a proportionally larger input from metasedimentary sources, possibly to the east.

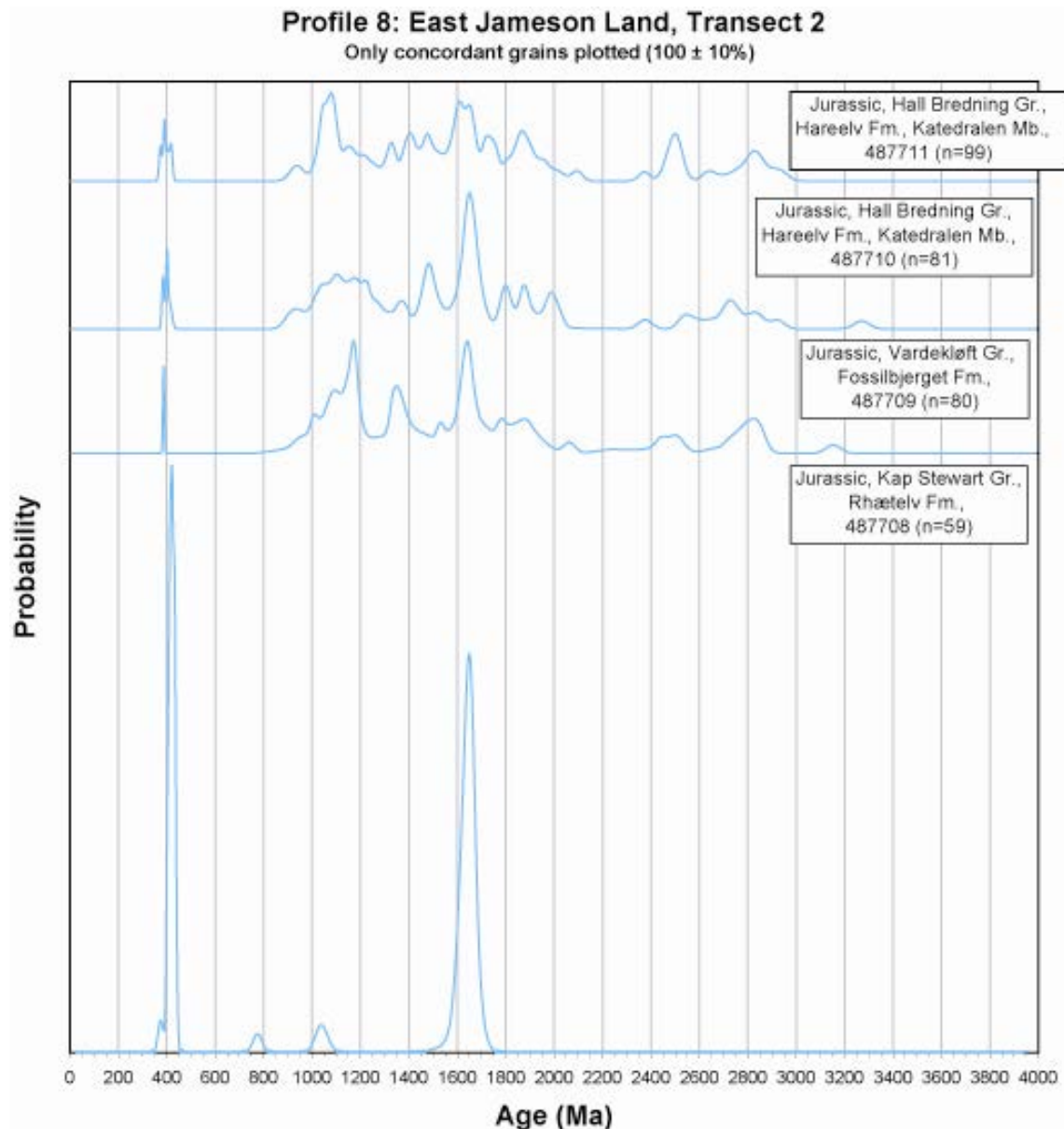


Figure 37. Stacked probability density plots of detrital zircon ages from Profile 8.

Profile 10: transect 6

This profile (Fig. 34) consists of three Upper Triassic-Lower Jurassic samples of the Innakajik Fm. (Fig. 38). They have a similar and simple bimodal age distribution. The samples contain two age peaks; one at 1650 Ma and one broader between 460 and 400 Ma. These ages are consistent with derivation from Liverpool Land, thus a transport from the east.

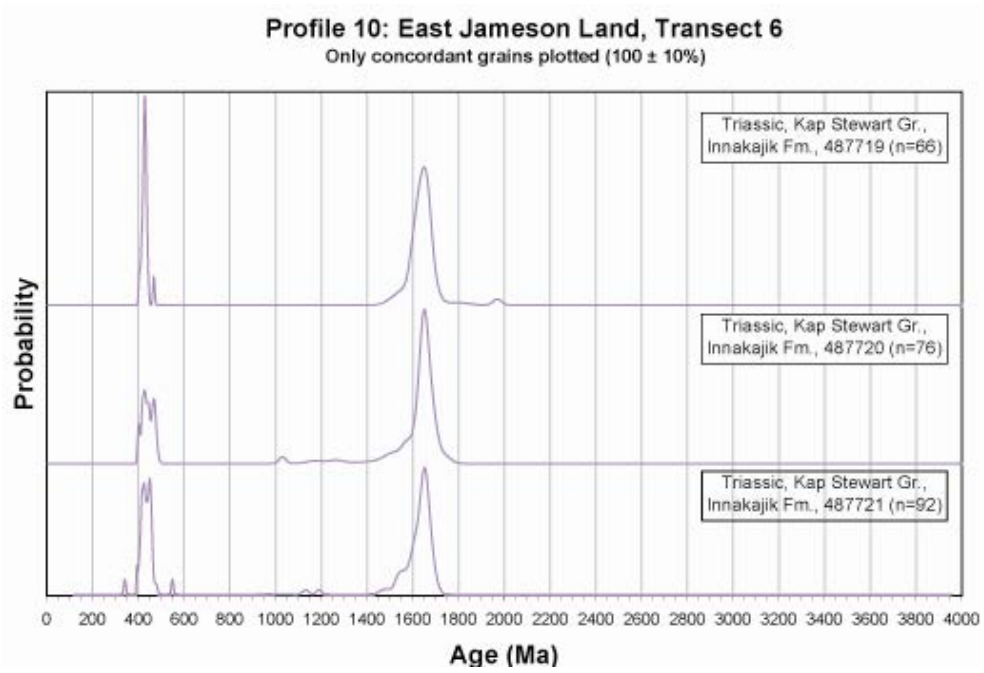


Figure 38. Stacked probability density plots of detrital zircon ages from Profile 10.

Profile 9: transect 1

The profile (Fig. 34) consists of seven Jurassic samples. The two oldest come from the Gule Horn Fm., the following four from the Ostreaelv Fm. and the youngest sample from the Hareelv Fm. (Fig. 39). The five oldest samples are similar and have a simple bimodal age distribution with one peak at 1650 Ma and one at ~420 Ma. Some of the Ostreaelv Fm. samples have a more diverse Phanerozoic age population, with both Carboniferous and Permian ages. The youngest Ostreaelv Fm. sample look like a transitional sample and in the Hareelv Fm. sample it is evident that there have been changes in the depositional system, with no signal from the 1650 ma and the 420 Ma sources, but a more spread out population with scattered peaks between 1800 and 900 ma, with additional minor input of Archaean detritus. All sources seem to be local, in the older samples from basement and Caledonian intrusions in Liverpool Land and in the youngest sample with input from a metasedimentary source. This change could be interpreted as a transgression, flooding the source areas of the older samples or a change in transport direction from easterly to westerly located sources.

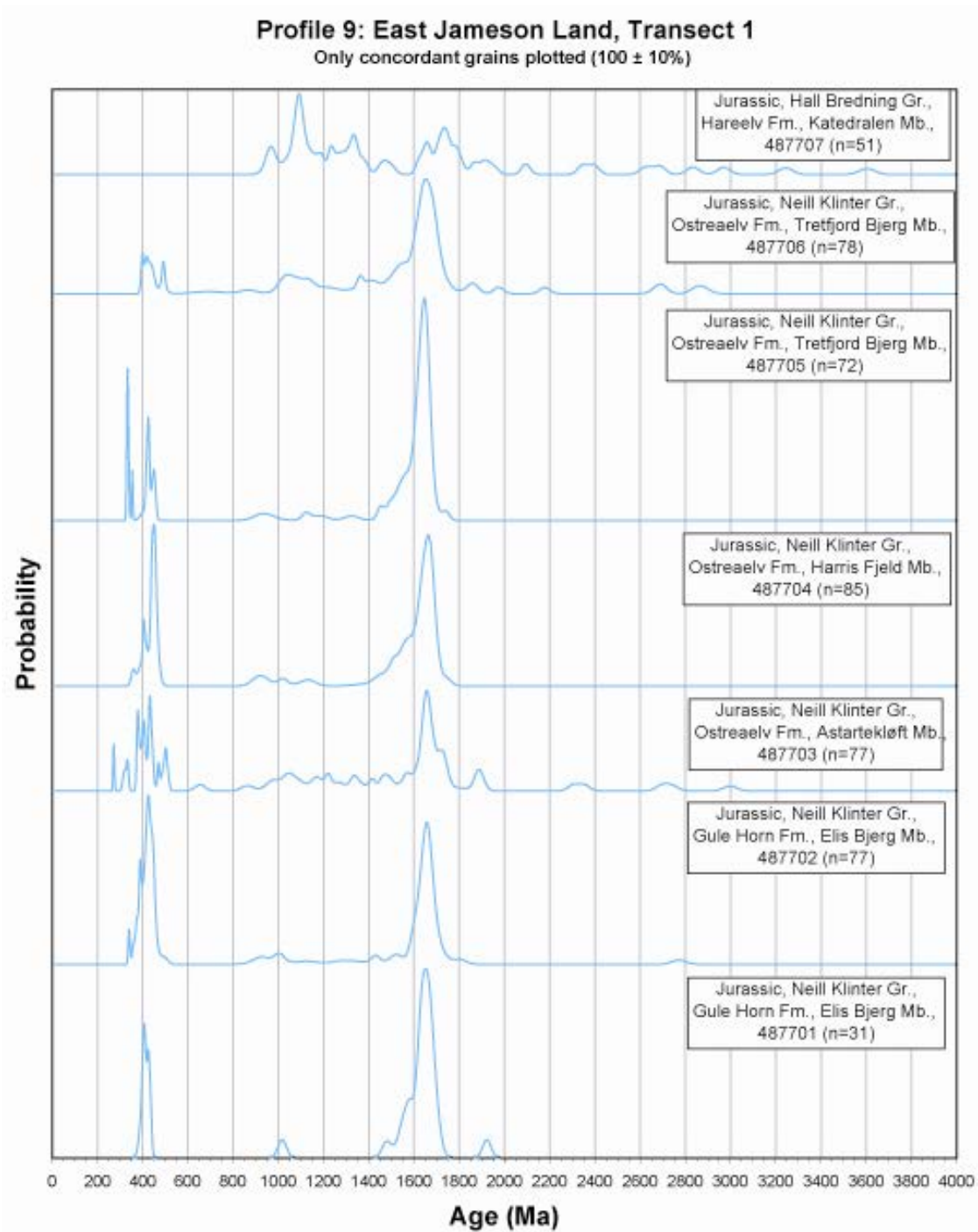


Figure 39. Stacked probability density plots of detrital zircon ages from Profile 9.

North-East Jameson Land

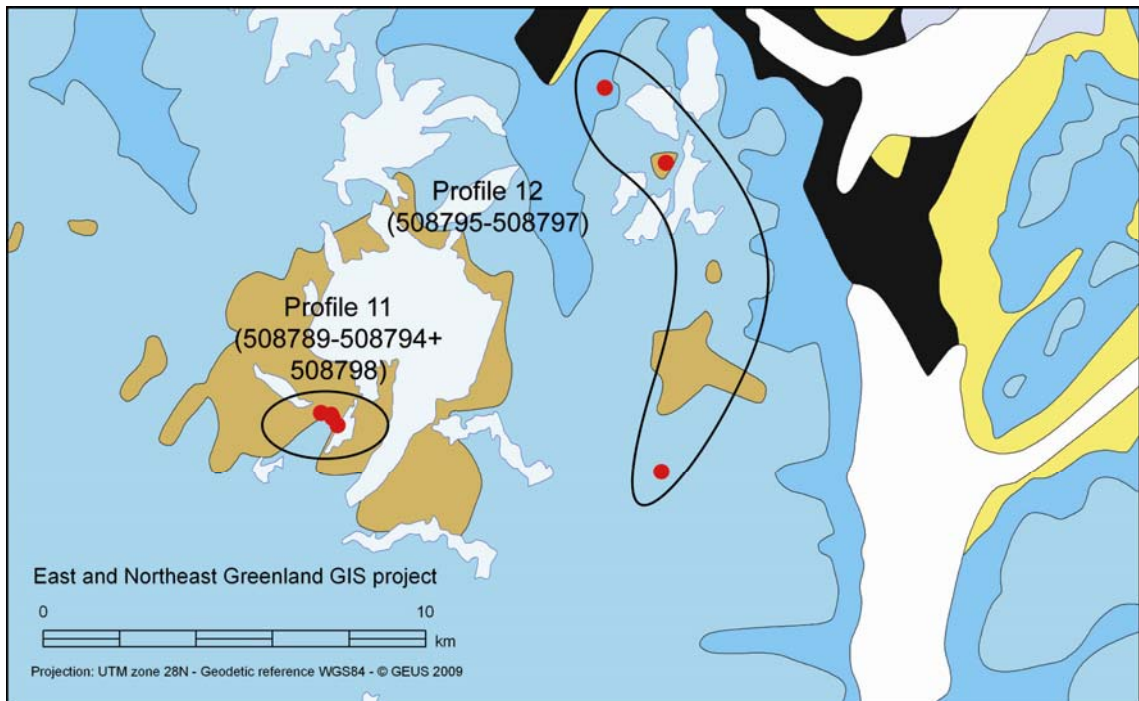


Figure 40. Locations of the sampling points of Profiles 11-12.

Profile 11: Pelion Mt., transect 17

This profile (Fig. 40) consists of three Jurassic samples from the Ostreaelv, Pelion and Olympen Fms. (Fig. 41). They have very similar zircon age distribution patterns. There is a persistent Archaean population centred on 2700 Ma, multi-component occurrences between 2000 and 1000 Ma, some 950 Ma zircon grains in the youngest sample and a Palaeozoic population. These samples seem to have local sources, possibly to the west judging from the abundance of recycled detritus and the 950 Ma zircons coming from Neoproterozoic intrusions.

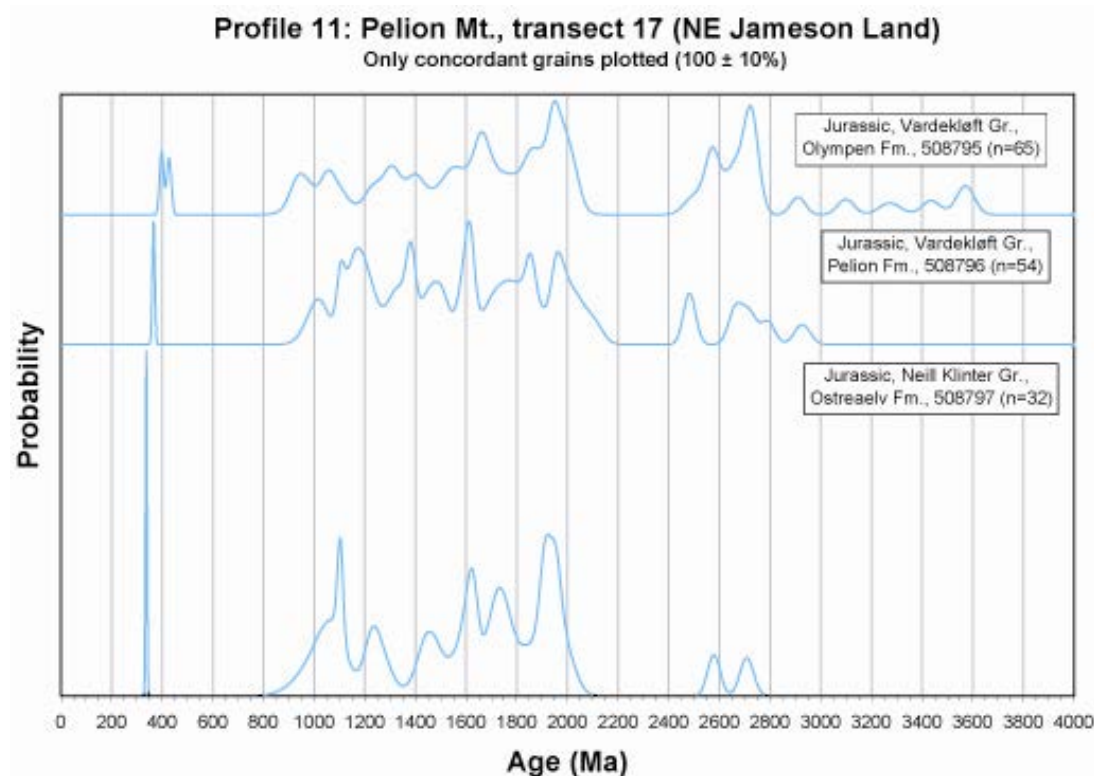


Figure 41. Stacked probability density plots of detrital zircon ages from Profile 11.

Profile 12: Olympen Mt., transect 16

This profile (Fig. 40) contains six samples of Jurassic age (Fig. 42), starting with a Fossilbjerget Fm. sample. The other five samples come from the Olympen Fm. The samples have a similar age distribution pattern and there are no significant shifts in the profile. There is a persistent Archaean population, primarily between 3200-2400 Ma, but with grains as old as 3700 Ma in one sample. There is a peak between 2000 and 1800 Ma in all samples and the relative proportion of this population seems to increase up-profile. There is an even distribution of ages between 1800 and 1000 Ma, with an elevated proportion of 1700-1600 Ma zircon grains in some samples. Most samples have 1000-900 Ma old zircon grains and almost all samples have a 430 Ma population and some samples have an additional population at 380 Ma. All the ages may be explained with derivation from local sources, except the ca. 3700 Ma grains. The sediments have a mixed signature from metasediments, basement components and Caledonian and Devonian igneous activity.

Profile 12: Olympen Mt., transect 16 (NE Jameson Land)
Only concordant grains plotted ($100 \pm 10\%$)

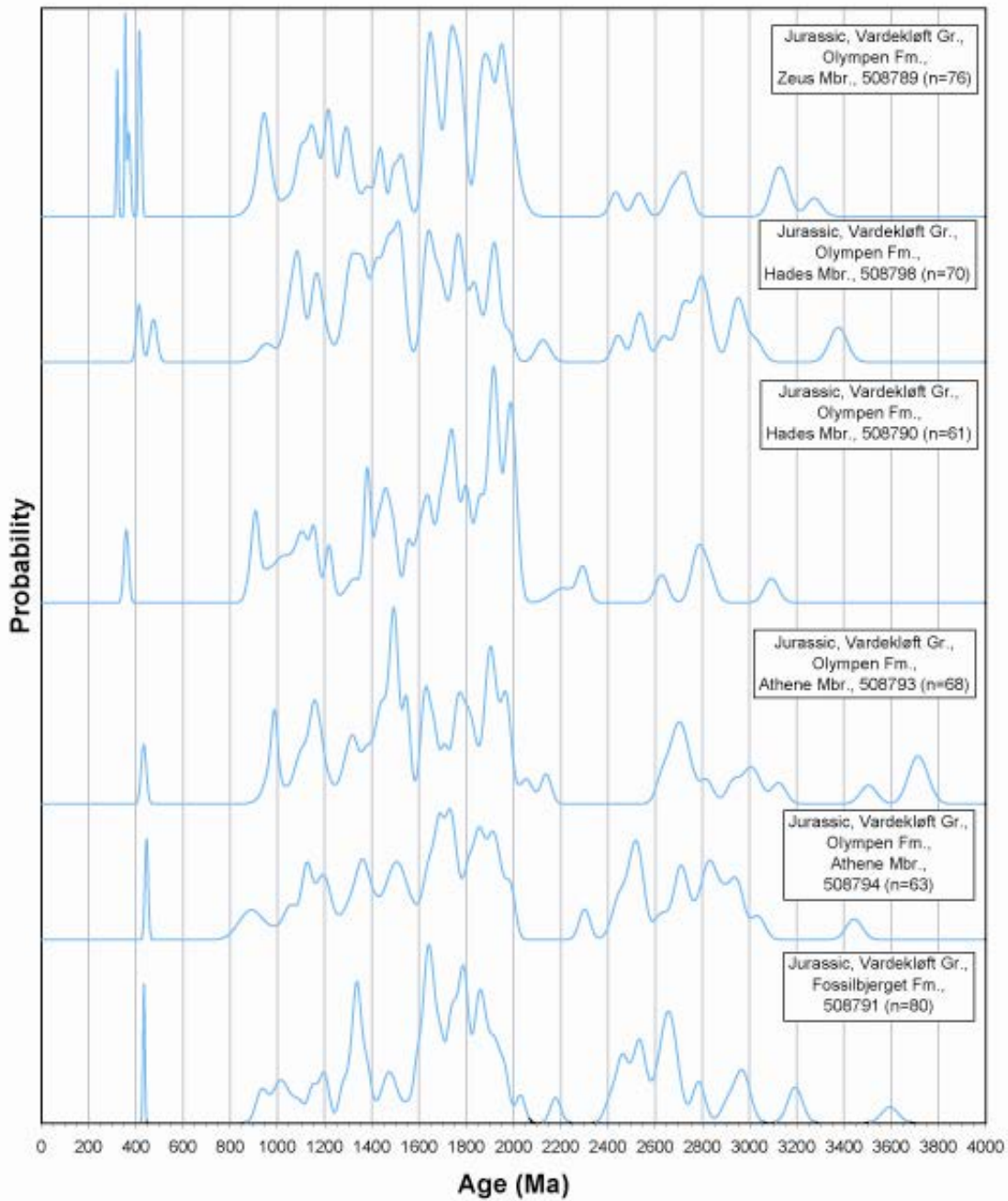


Figure 42. Stacked probability density plots of detrital zircon ages from Profile 12.

Trail Ø

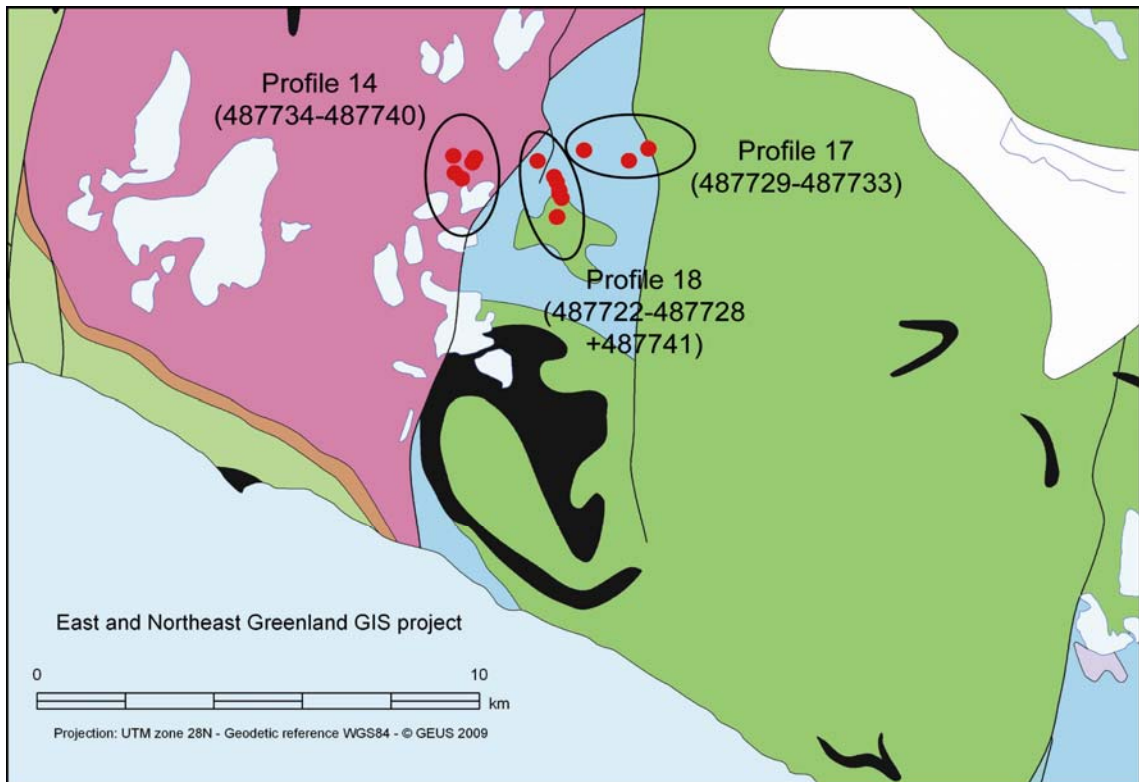


Figure 43. Locations of the sampling points of Profiles 14 and 17-18.

Profile 14: Svinhufvud Bjerger, transect 9

The profile (Fig. 43) consists of seven samples of Triassic age from the Wordie Creek Fm. (Fig. 44). All the samples have a similar and complex age distribution. They all contain a varied Archaean population together with a population varying between 2000 and 800 Ma. All samples have a significant peak at 1650 Ma and all samples contain zircon grains with ages between 450 and 400 Ma. All ages can be interpreted to have local sources, primarily from metasediments (see Fig. 5), perhaps with contribution from local gneisses in Liverpool Land with an age of 1650 Ma. There is also a large contribution from Caledonian intrusions. It is most likely with a transport direction from the south, due to the abundance of Caledonian zircons with a possible origin in Liverpool Land.

Profile 14: Traill Ø, Svinhufvud Bjerger, Transect 9

Only concordant grains plotted (100 ± 10%)

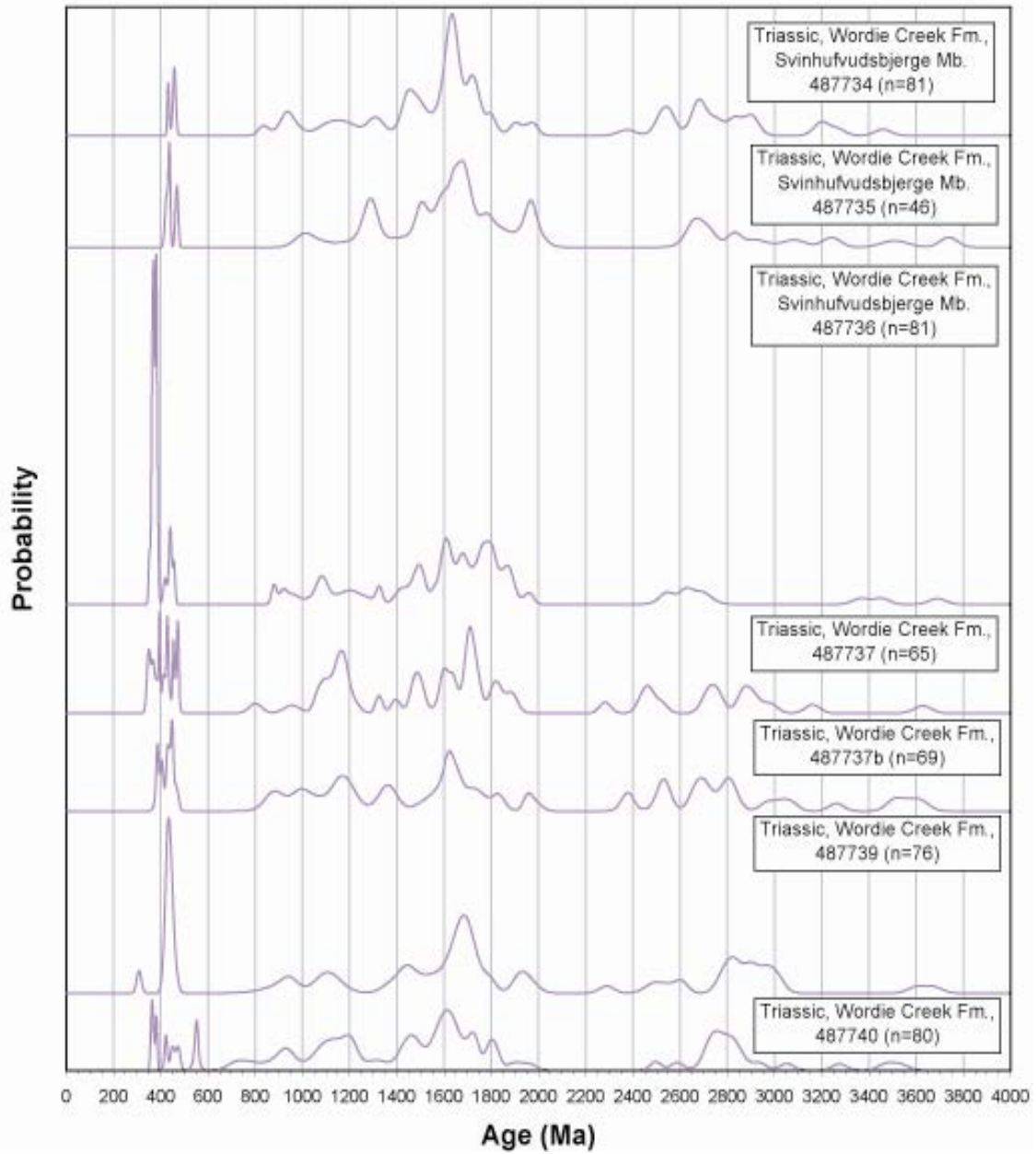


Figure 44. Stacked probability density plots of detrital zircon ages from Profile 14.

Profile 17: Svinhufvud Bjerge, transect 8

The profile (Fig. 43) consists of five samples of Mid Jurassic age (Fig. 45). The three lowermost samples come from the Bristol Elv Fm. and the topmost two from the Pelion Fm. All the samples have a similar age distribution and all samples contain an Archaean population together with a metasediment derived population varying between 2000 and 1000 Ma. All samples have a significant peak at 900 Ma and all samples contain zircon grains with ages between 450 and 400 Ma. One sample also contains 350 Ma grains. All ages can be interpreted to have local sources, primarily from metasediments, but also with contributions from Caledonian igneous activity and in one sample also Devonian. All the potential sources can be found in Liverpool Land and Canning Land and it is therefore most likely with a transport direction from the south.

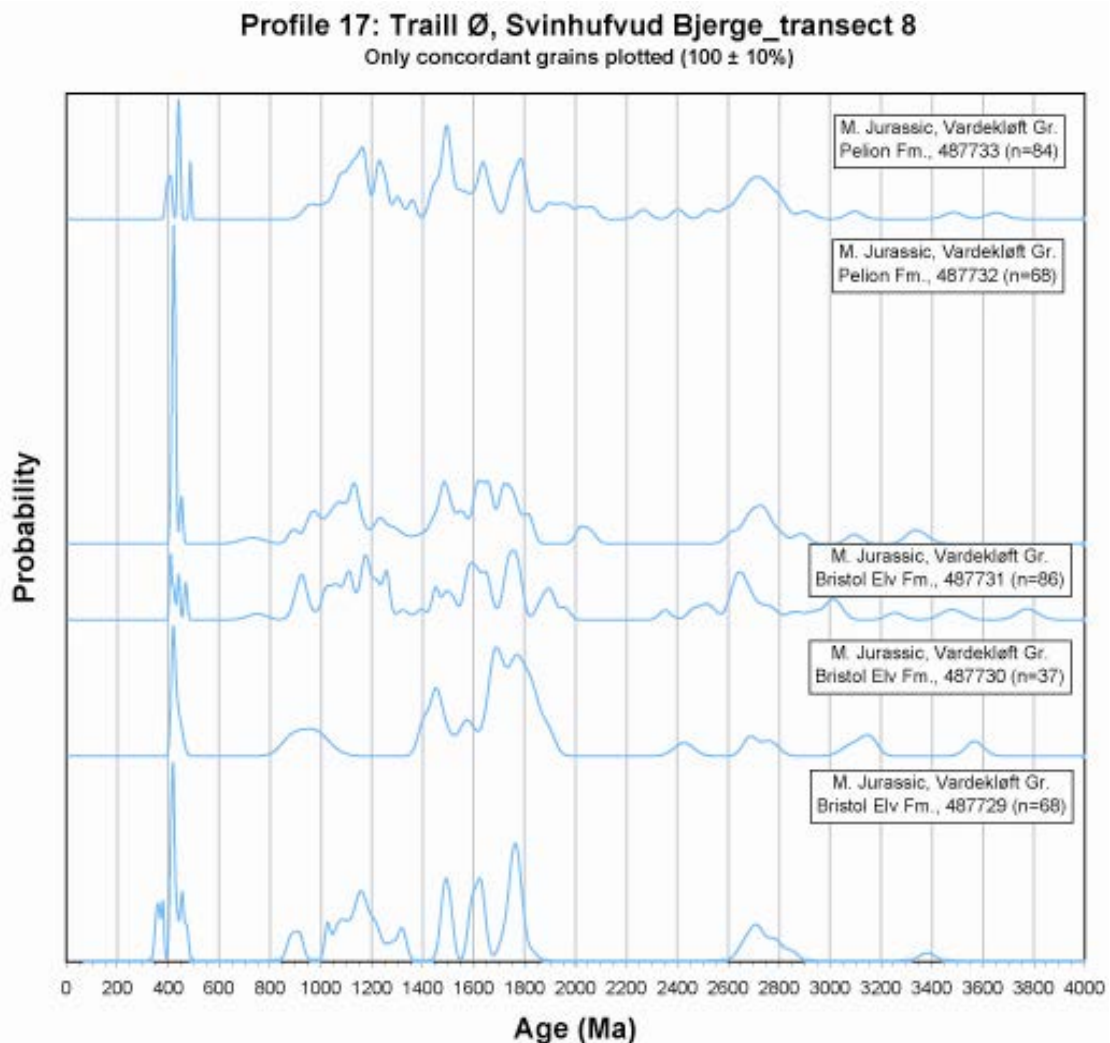


Figure 45. Stacked probability density plots of detrital zircon ages from Profile 17.

Profile 18: Svinhufvud Bjerger, transect 7

This profile (Fig. 43) contains six Jurassic samples from the Pelion Fm. and two Cretaceous samples from the Rold Bjerger Fm. (Fig. 46). The oldest sample is dominated by a Palaeozoic population with only minor Archaean and Proterozoic input. The second oldest sample has an important peak at 1950 Ma and otherwise variable, mostly Proterozoic input and a very minor Palaeozoic population. The remaining Jurassic samples have comparable age spectra, but differing in details. In common they have a persistent component at 1650 Ma and one smaller at 1950 Ma. The youngest Jurassic sample lacks a Palaeozoic population. The Cretaceous samples are similar to the Jurassic ones, with variable Archaean and Proterozoic populations and a two-peak Palaeozoic component. There is a generally larger input of the 1950 Ma component compared to the 1650 Ma component. There seems to be change after deposition of the oldest sample so that locally known basement gneisses, aged 1950 Ma and 1650 Ma, are exposed and subject to erosion. Through the whole profile there is an input from meta-sedimentary sources and there are contributions from Caledonian intrusions, especially in the oldest and the two youngest samples.

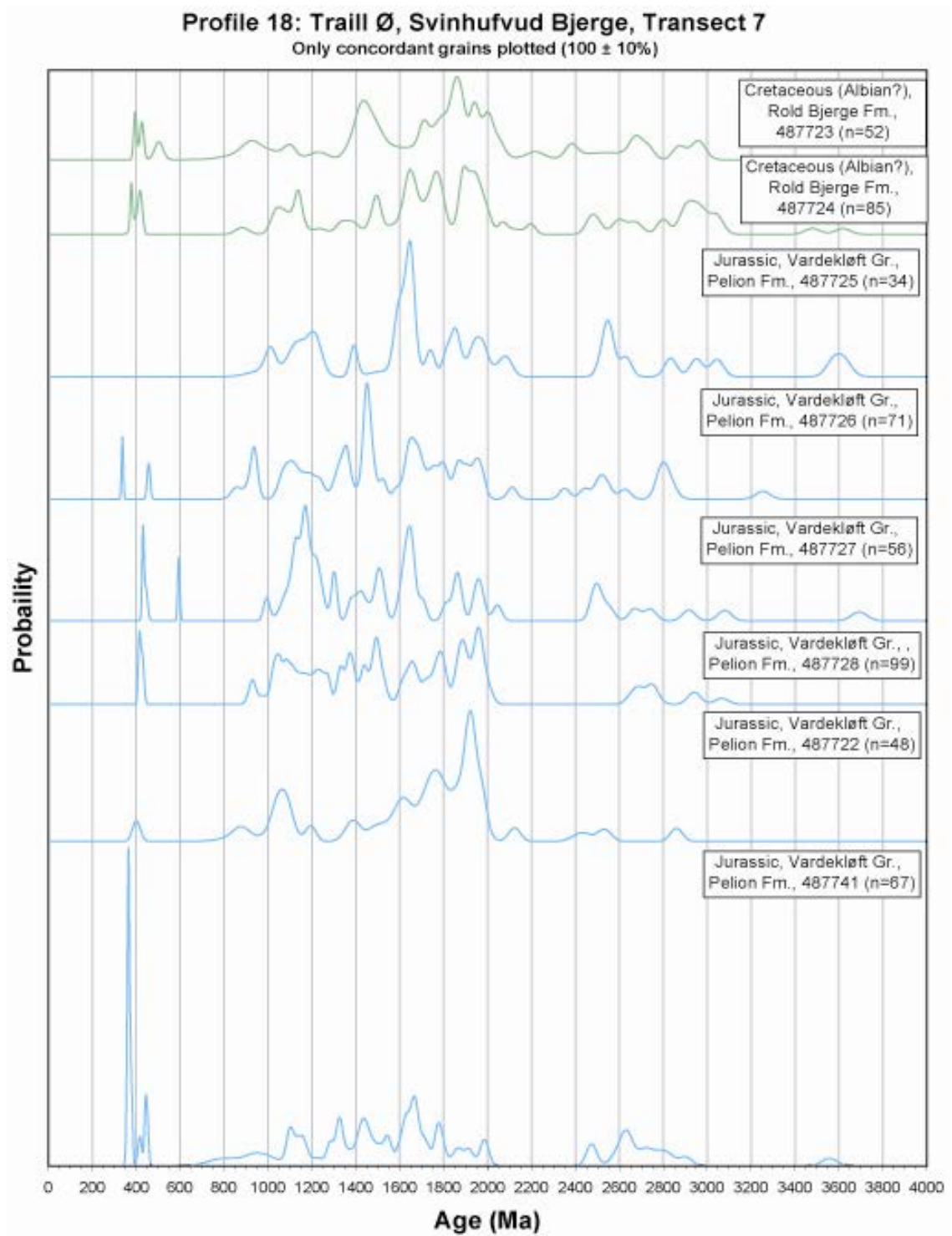


Figure 46. Stacked probability density plots of detrital zircon ages from Profile 18.

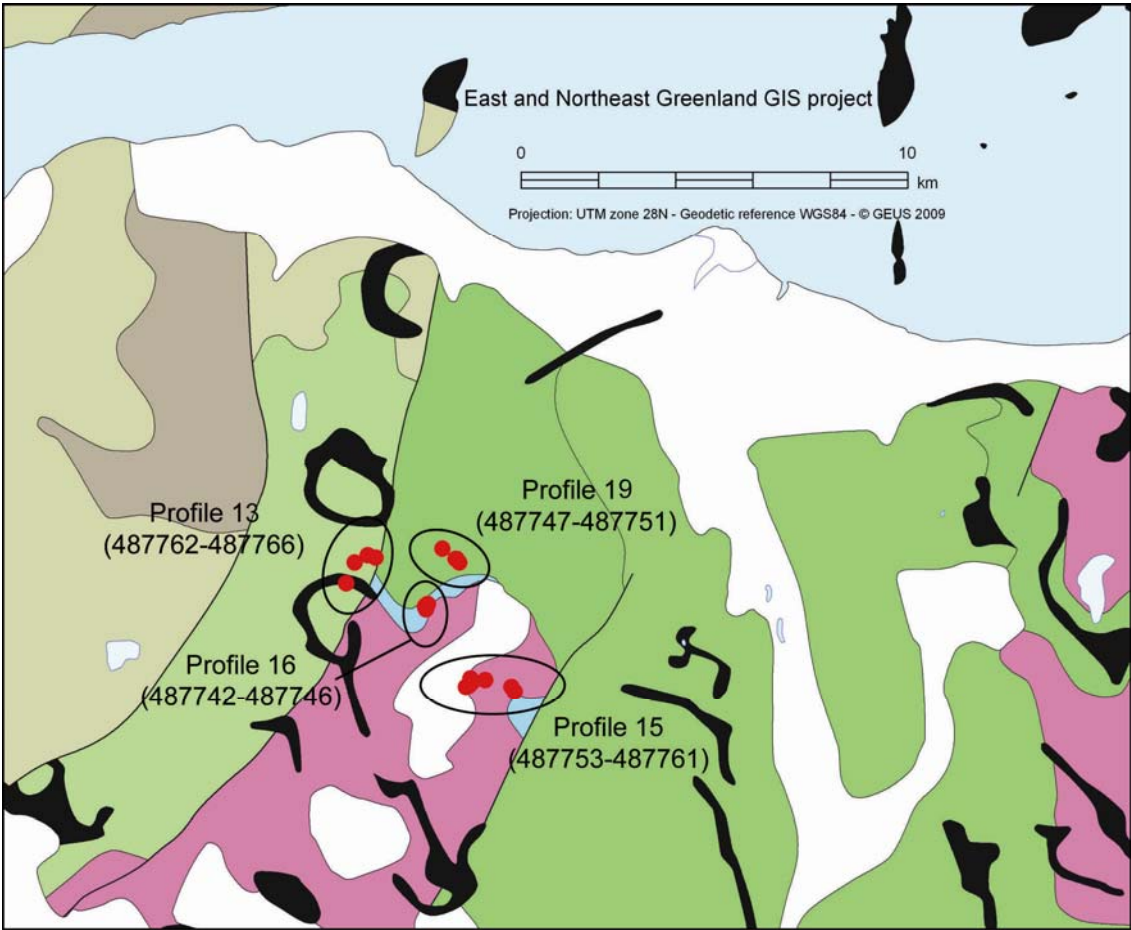


Figure 47. Locations of the sampling points of Profiles 13, 15-16 and 19.

Profile 13: Tørvestakken, transect 13

This profile (Fig. 47) contains five Carboniferous samples of the Traill Ø Group (Fig. 48). The age distribution patterns of the different samples are similar. They have an Archaean component, mainly in the age range of 3000-2400 Ma. There is a Proterozoic component with ages between 1800 and 900 Ma and lastly a Palaeozoic multipeak component. The Archaean and Proterozoic zircon ages indicate a metasedimentary source with minor input from known basement sources (see Fig. 4), whereas the Palaeozoic component probably comes from Caledonian intrusive rocks (see Fig. 7). There is no need to invoke exotic sources for these sediments.

Profile 13: Geographical Society Ø, Tørvestakken, Transect 13 Only concordant grains plotted (100 ± 10%)

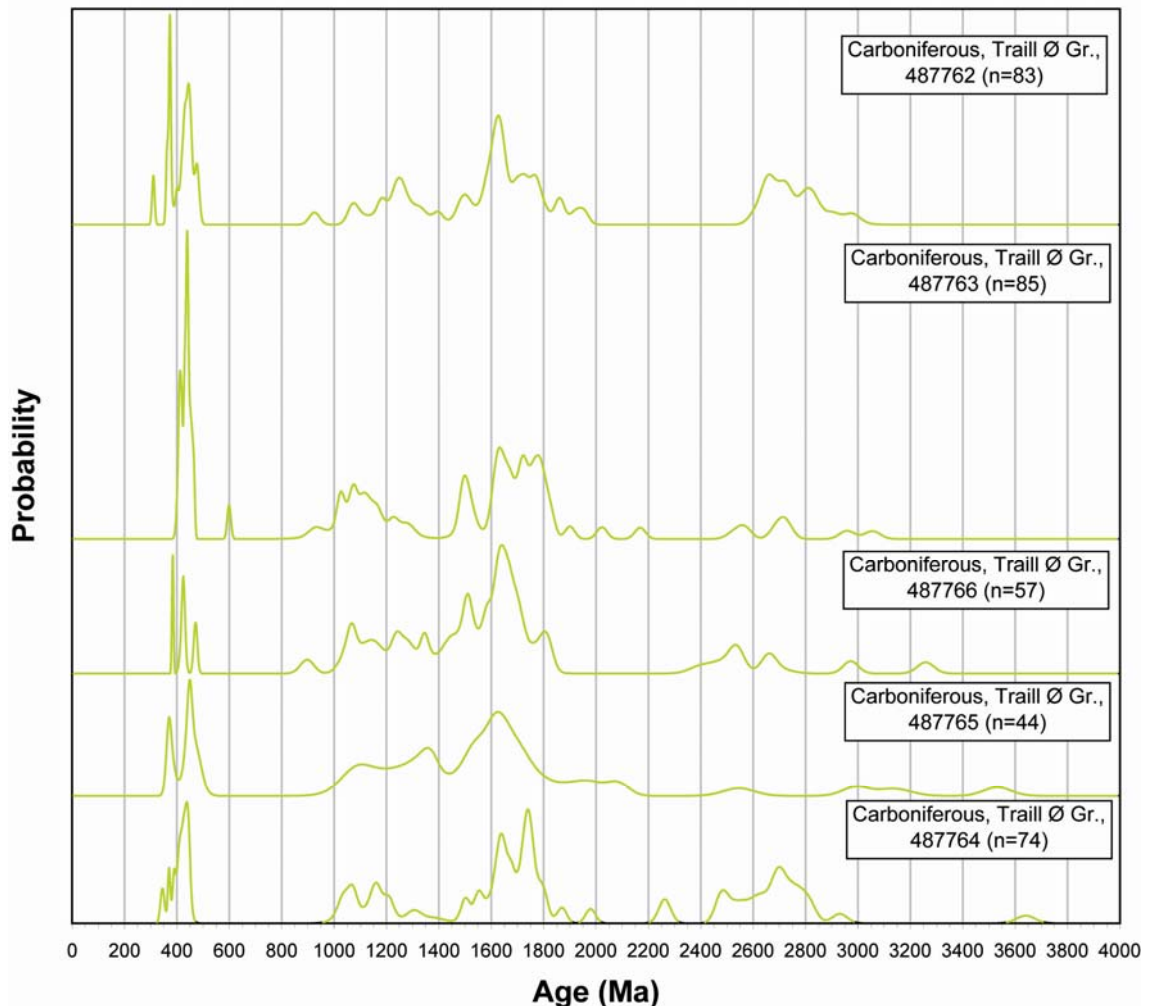


Figure 48. Stacked probability density plots of detrital zircon ages from Profile 13.

Profile 15: Tørvestakken, transect 12

This profile (Fig. 47) consists of nine Triassic samples from the Wordie Creek Fm. (Fig. 49). All samples are rather similar and have a complex age distribution pattern. There are minor variable Archaean ages, a Proterozoic component between 2000 and 900 Ma and a variable Palaeozoic input. The Palaeozoic input is waning upwards in the profile. All age groups are consistent with derivation from local sources, most importantly from Neoproterozoic metasedimentary rocks and Caledonian intrusions. There seems to be a negligible input from known basement sources. In the two oldest samples there are ~650 Ma zircon grains. The source of these is unknown, but zircon grains with similar ages in North Atlantic drill cores have been speculated to be sourced in the northern British Isles (Rehnström et al. 2007).

Profile 15: Geographical Society Ø, Tørvestakken, Trans. 12

Only concordant grains plotted (100 ± 10%)

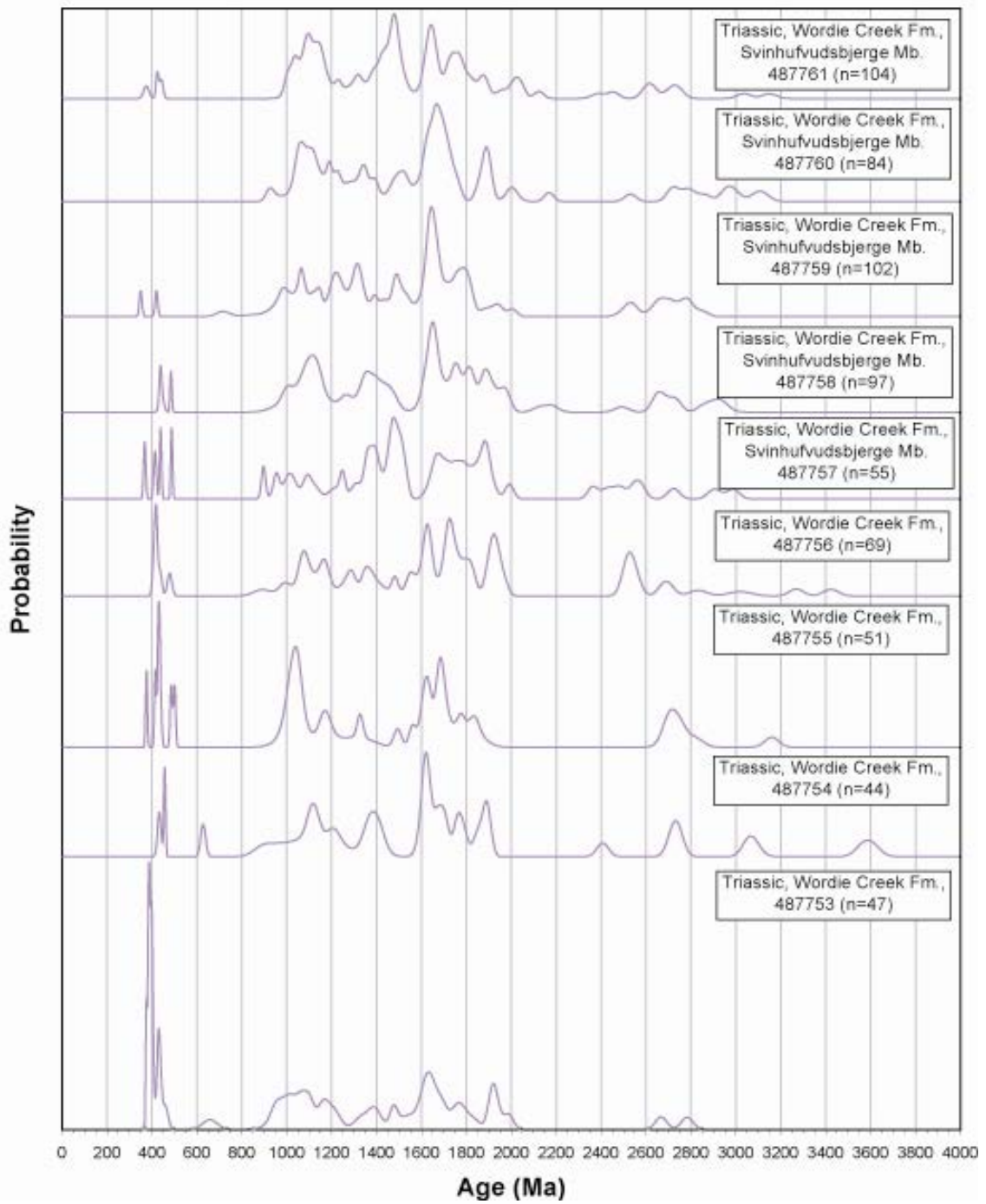


Figure 49. Stacked probability density plots of detrital zircon ages from Profile 15.

Profile 16: Tørvestakken, transect 10

This profile (Fig. 47) consists of one Triassic samples from the Wordie Creek Fm. and four Jurassic samples from the Pelion Fm. (Fig. 50). The Precambrian age distribution of all the samples is rather similar and complex. There is a minor and variable Archaean population, a Proterozoic component between 2000 and 900 Ma, notably with proportionally important peaks at 1650 and 1100 Ma. There is an increasing importance of a 1900 Ma population in the three youngest samples. The Jurassic samples have a variable Palaeozoic input, whereas the Triassic sample lacks Phanerozoic detritus. All age groups are consistent with derivation from local sources, most importantly from Neoproterozoic metasedimentary rocks and Caledonian intrusions. The input from known basement sources (~1900 Ma, see Fig. 4) seems to be increasing upwards in the profile and the source of Palaeozoic detritus was not available in the Triassic.

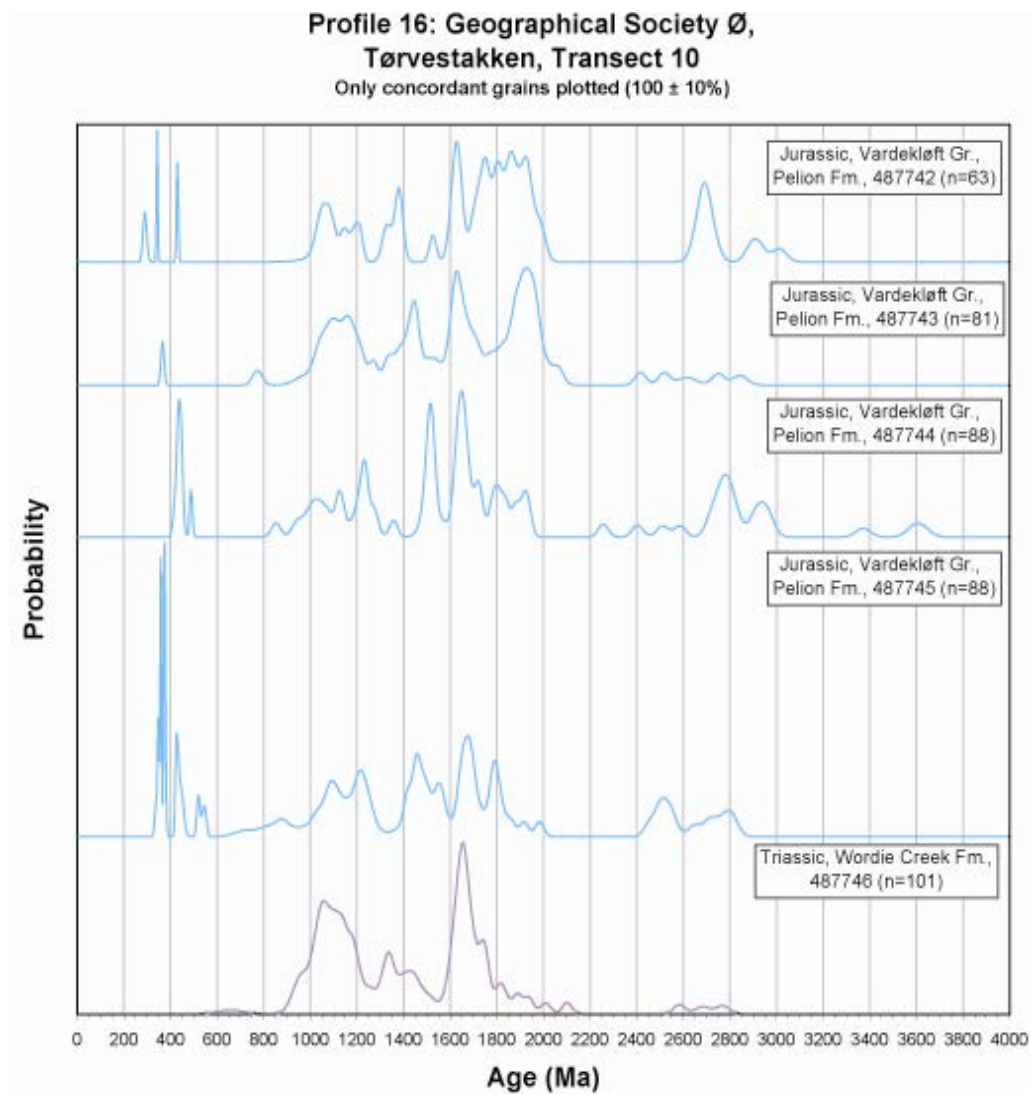


Figure 50. Stacked probability density plots of detrital zircon ages from Profile 16.

Profile 19: Tørvestakken, transect 11

The profile (Fig. 47) consists of five samples of Lower Cretaceous age, all from the Rold Bjerger Fm. (Fig. 51). The samples have a similar age distribution pattern and there are no indications for any major shift in source area in the profile. All the samples have an Archaean population, with a distinct peak at ca. 2700 Ma. In all samples there is discontinuous occurrence of grains with ages between 2500 and 600 Ma with a peak somewhere between 2000 and 1800 Ma. All the samples also have multiple peaks between 600 and 100 Ma. The oldest sample has significant peaks at 300 Ma and 125 Ma. The two youngest samples also have distinct peaks at 125 Ma. This age distribution pattern is unusual and cannot be explained entirely by contribution from local sources. The Archaean, Palaeoproterozoic and Mesoproterozoic ages can be explained from local sources in metasediments and basement, but the Neoproterozoic ages do not have any known equivalents in East Greenland. The Phanerozoic age distribution is not possible to explain by derivation from local sources. More distal sources have to be invoked and possibly also contribution from volcanic ash fall out. In offshore North Atlantic samples, such diverse ages have been interpreted as detritus sourced in the northern British Isles (Rehnström et al. 2007).

Profile 19: Geographical Society Ø, Tørvestakken-transect 11
Only concordant grains plotted ($100 \pm 10\%$)

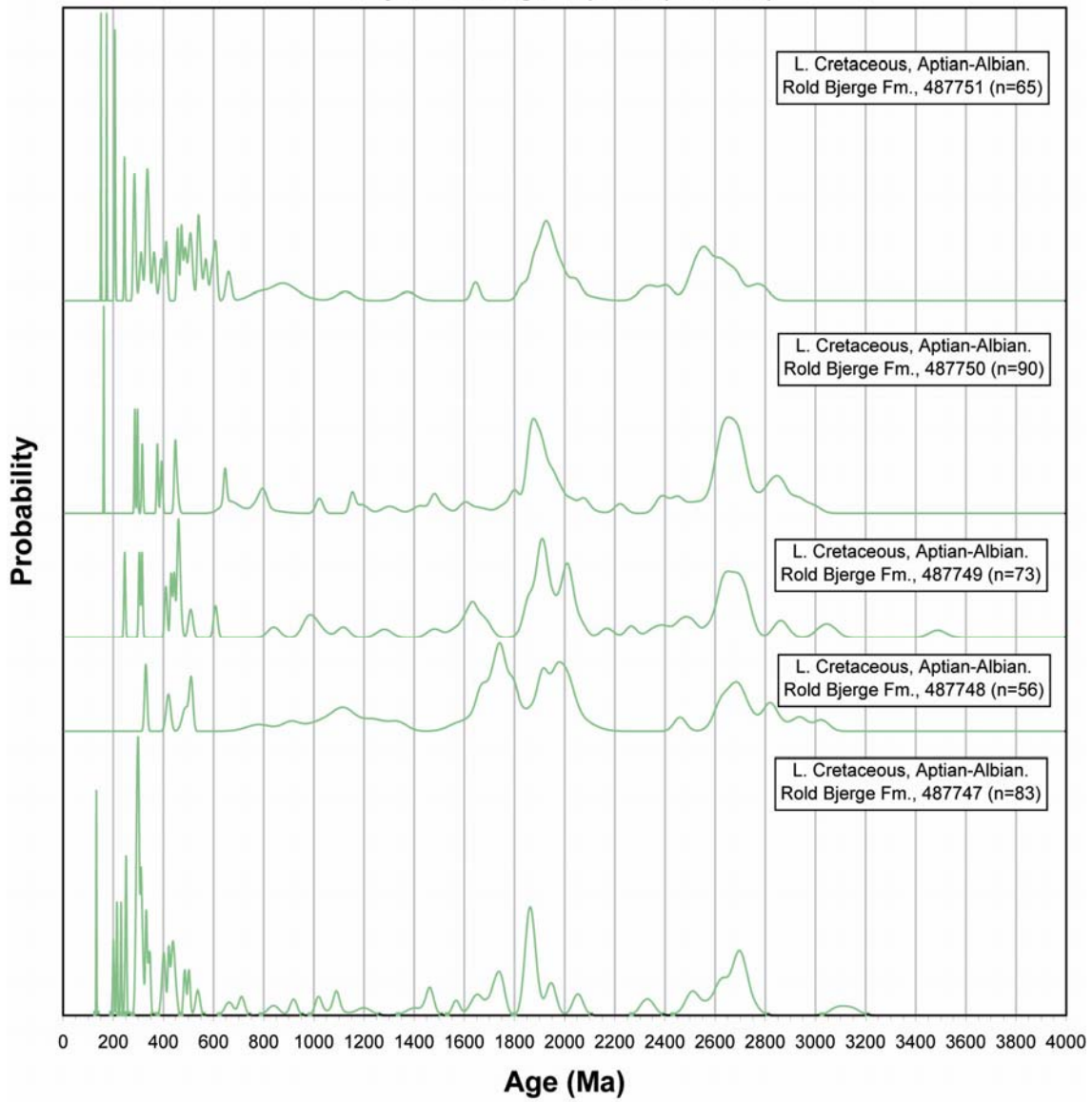


Figure 51. Stacked probability density plots of detrital zircon ages from Profile 19.

Hold with Hope

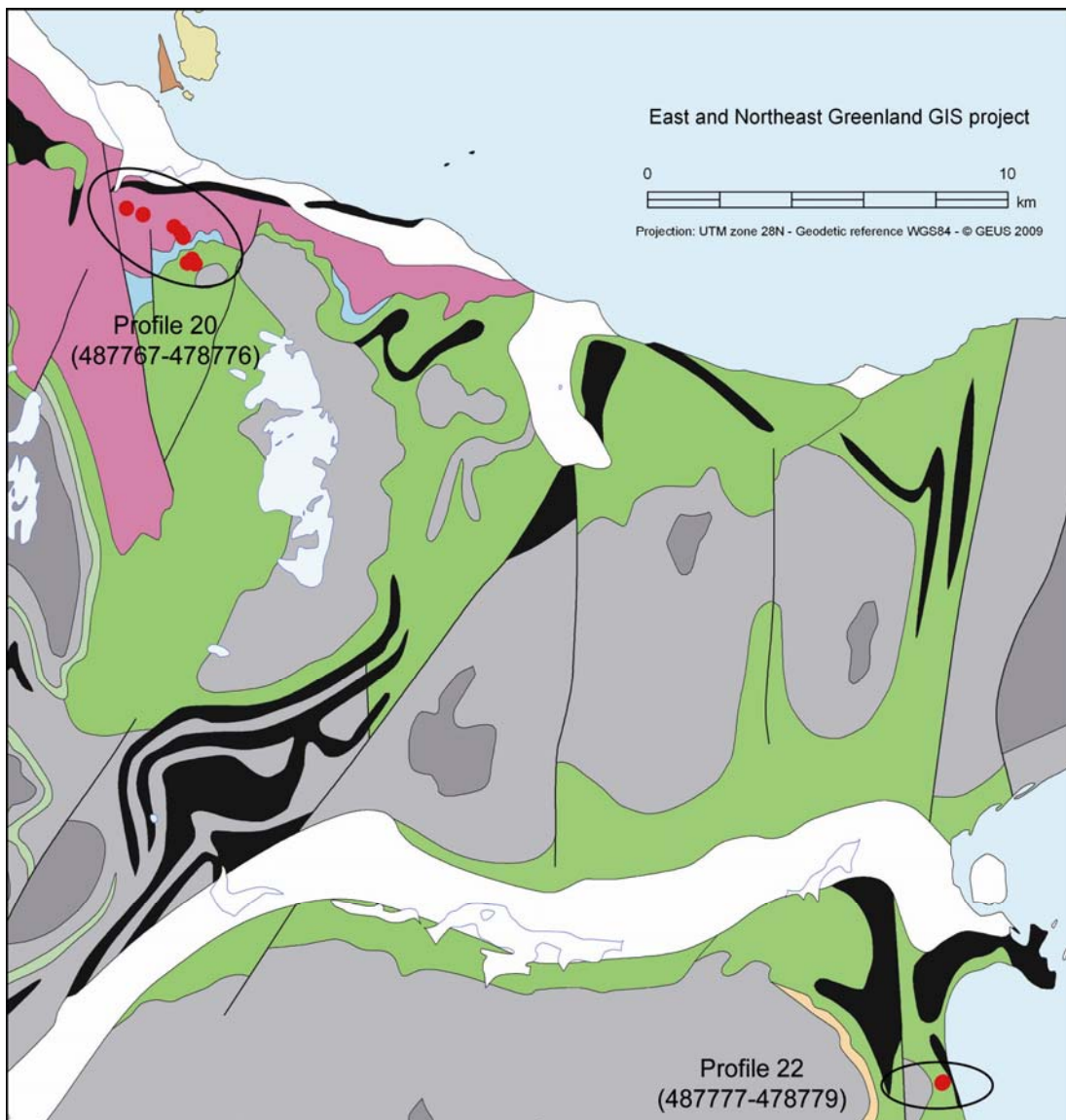


Figure 52. Locations of the sampling points of Profiles 20 and 22.

Profile 20: Gulelv, transect 14 and 15

This profile (Fig. 52) consists of four Triassic samples of the Wordie Creek Fm., three Jurassic samples of the Vardekløft Group and three Lower Cretaceous samples of the Hold with Hope Group (Fig. 53). The Triassic samples have a variable Proterozoic population with ages between 2000 and 900 Ma and a few Archaean grains. There is a significant input from a 1950 Ma source and all the Triassic samples contain Palaeozoic zircon grains, although a very minor population in the oldest sample. In the Jurassic samples there are again scattered Proterozoic zircon grains, with more prominent peaks at 1650 Ma and 1150 Ma. There is a smaller population at 1950 Ma and a Palaeozoic population, which however is lacking in the youngest Jurassic sample. The Cretaceous samples have a minor Archaean population a more significant population at 1950 Ma and at 1750 Ma. Few and scattered occurrences from other Proterozoic sources and a persistent Palaeozoic component. There are some evident changes upward in the profile. There is a metasedimentary source that is decreasing in importance upwards. The importance of the 1950 Ma basement source is diminishing in the Jurassic, but returning in the Cretaceous. The 1750 Ma basement source is only present in the Cretaceous and the 1650 Ma basement source is mainly important in the Jurassic. An unusual 1450 Ma peak in the youngest sample has an unknown source. The Palaeozoic component is of variable importance, but in a non-systematic way.

Profile 20: Hold with Hope north, Gulelv, Transects 14 & 15
 Only concordant grains plotted ($100 \pm 10\%$)

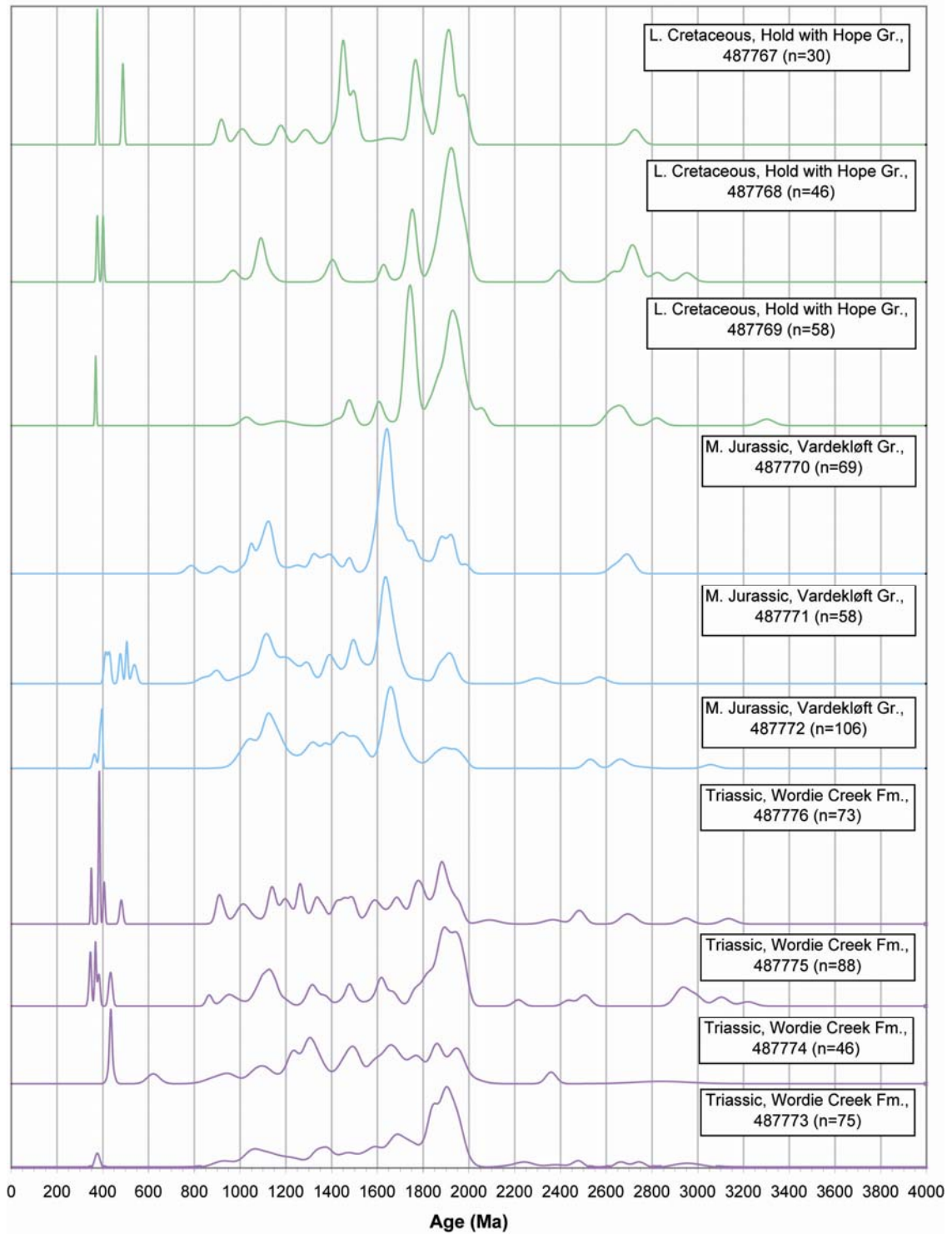


Figure 53. Stacked probability density plots of detrital zircon ages from Profile 20.

Profile 22: Knudshoved, transect 16, type locality by CASP: 3137

This profile (Fig. 52) consists of two Upper Cretaceous samples of the Home Foreland Fm. (Fig. 54). The samples have a similar Precambrian age distribution and the younger sample has an additional Palaeozoic peak that is missing in the older sample. They both have a broad age peak around 2700 Ma, another at ca. 1900 Ma and prominent peak at 1650 Ma. There are scattered peaks down to 900 Ma. These characteristics may be explained by a mixed derivation from local basement and metasedimentary sources, with some input from younger intrusions. Considering the 1650 Ma-peak in conjunction with the rest of the Precambrian signature it is possible to invoke a meta-sedimentary source for those zircon grains (see Fig. 5).

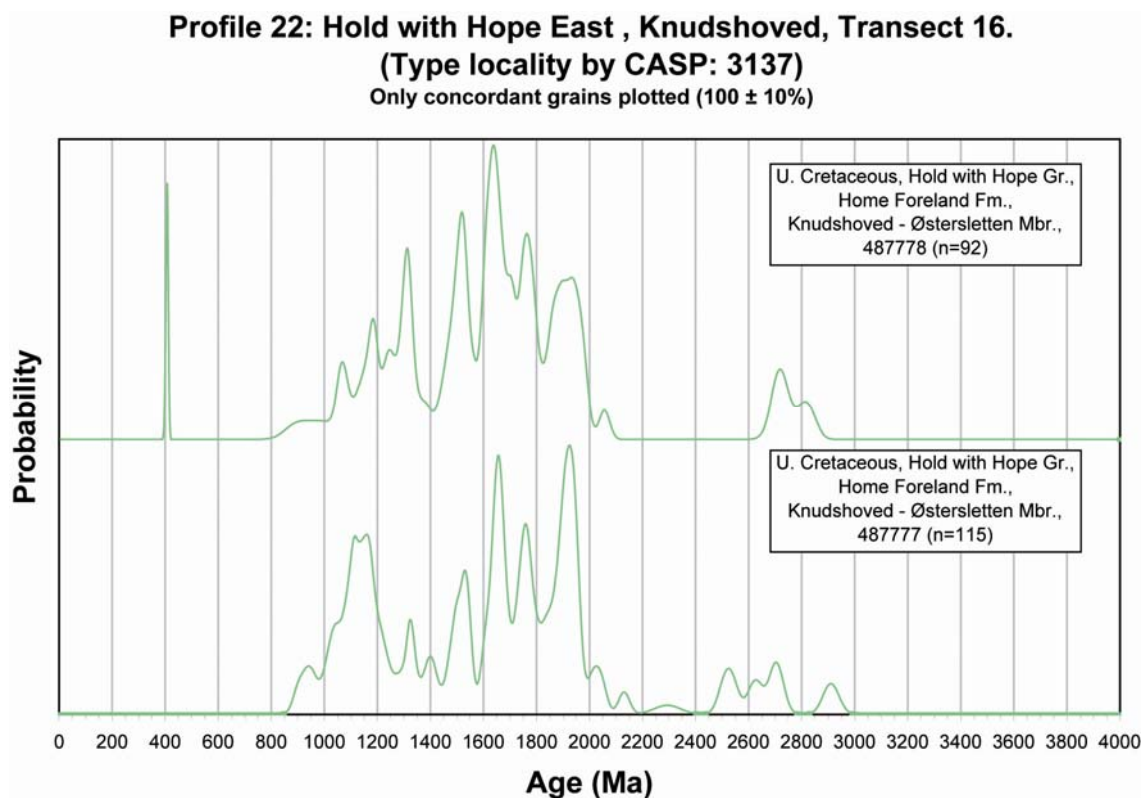


Figure 54. Stacked probability density plots of detrital zircon ages from Profile 22.

Wollaston Forland

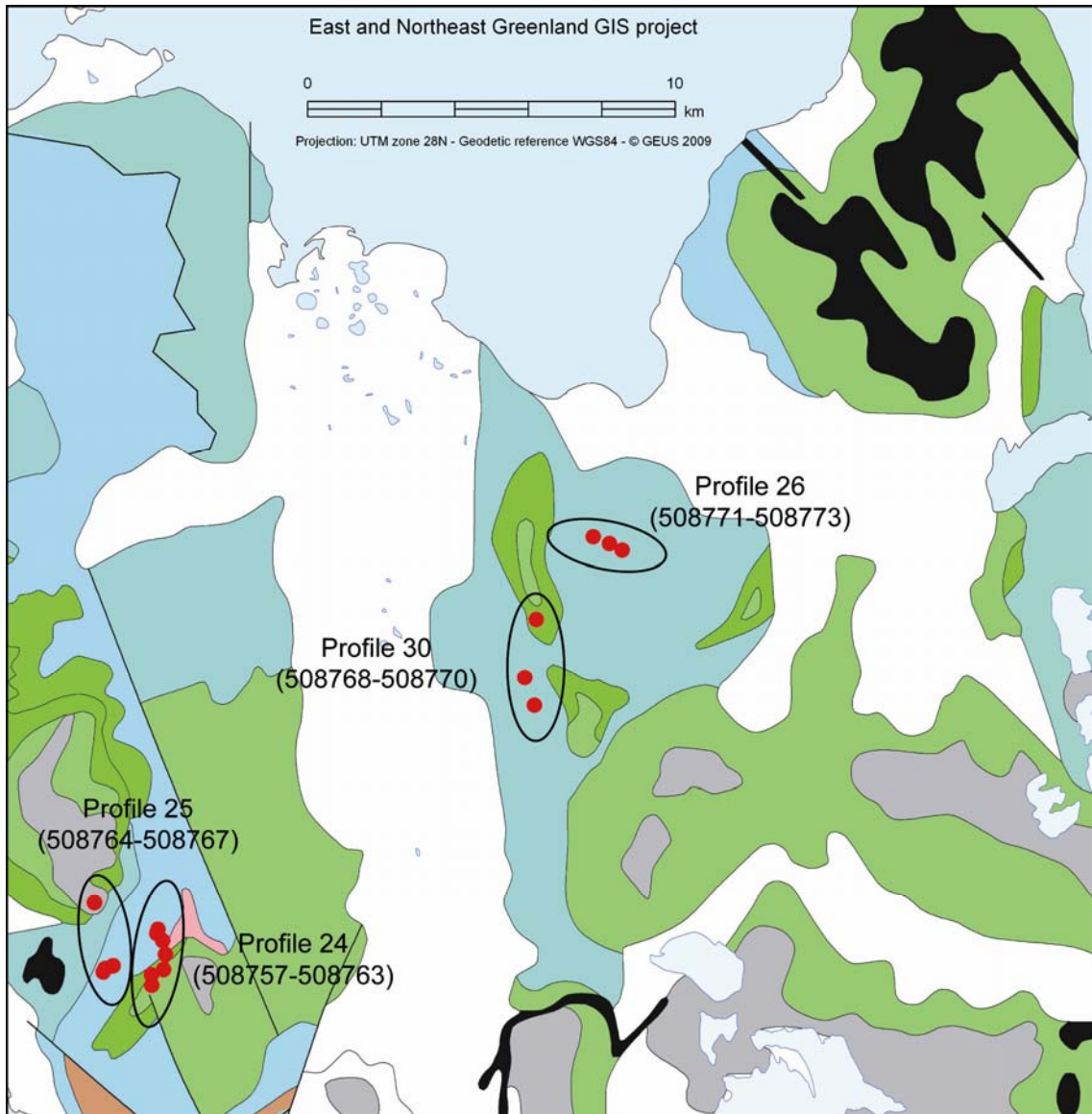


Figure 55. Locations of the sampling points of Profiles 24-26 and 30.

Profile 24: Cardiocerasdal, transect 10

The profile (Fig. 55) consists of four Jurassic and three Cretaceous samples. The oldest sample comes from the Pelion Fm, the next two from the Upper Jakobsstigen Fm., the next from the Bernbjerg and the top three samples from the Cretaceous Palnatokes Bjerg Fm. (Fig. 56). There is some interprofile variation in age distribution, especially there are some differences in the Bernbjerg Fm. sample and the lowest Palnatokes Bjerg Fm sample compared to the others. All samples contain a variable Archaean population and a consistent and important peak between 2000 and 1800 Ma. The three

lowest samples have a peak between 1700 and 1600 Ma. All samples have grains with ages down to 1000 Ma and the two above mentioned samples have a significant peak at 900 Ma. The two samples from the Upper Jakobsstigen Fm. have a Caledonian population which is not present in the other samples. There are some Palaeozoic zircon grains in the Bernbjerg Fm. sample, but there are no Phanerozoic grains in the Palnatokes Bjerg Fm. All age populations can be explained with derivation from local sources.

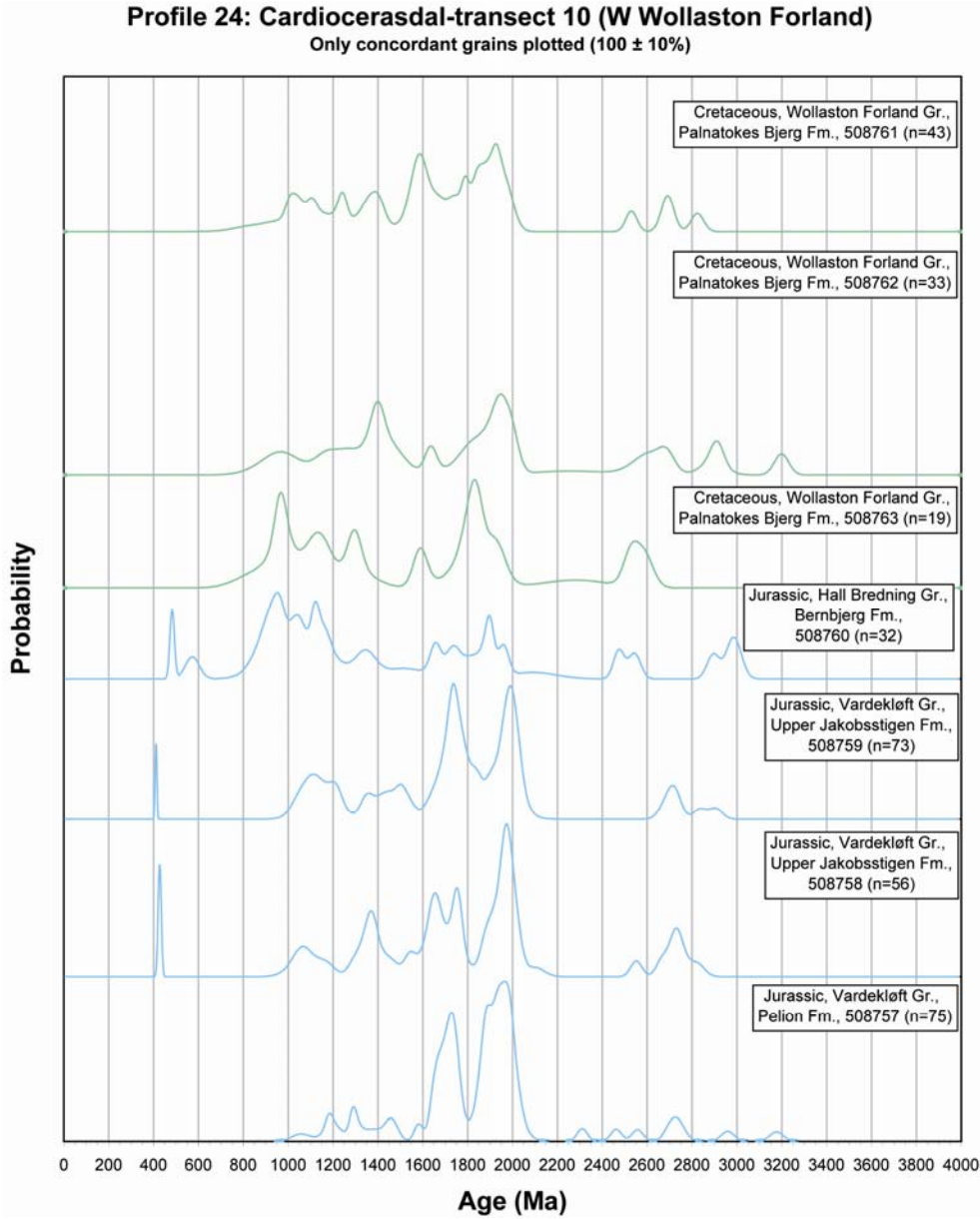


Figure 56. Stacked probability density plots of detrital zircon ages from Profile 24.

Profile 25: Cardiocerasdal, transect 11

This profile (Fig. 55) consists of four Jurassic samples from the Pelion Fm., the Lower Jakobstigen Fm. and two from the Bernbjerg Fm. (Fig. 57). All samples have a similar distribution of Precambrian ages; scattered Archaean grains and significant multiple peaks between 2000 and 1600 Ma. The two lowermost samples contain Devonian grains and the lower Bernbjerg Fm. sample Silurian grains, but the top samples do not contain any Phanerozoic ages. All the age populations can be explained with derivation from local sources, predominantly basement, but with some contribution from Palaeozoic igneous activity.

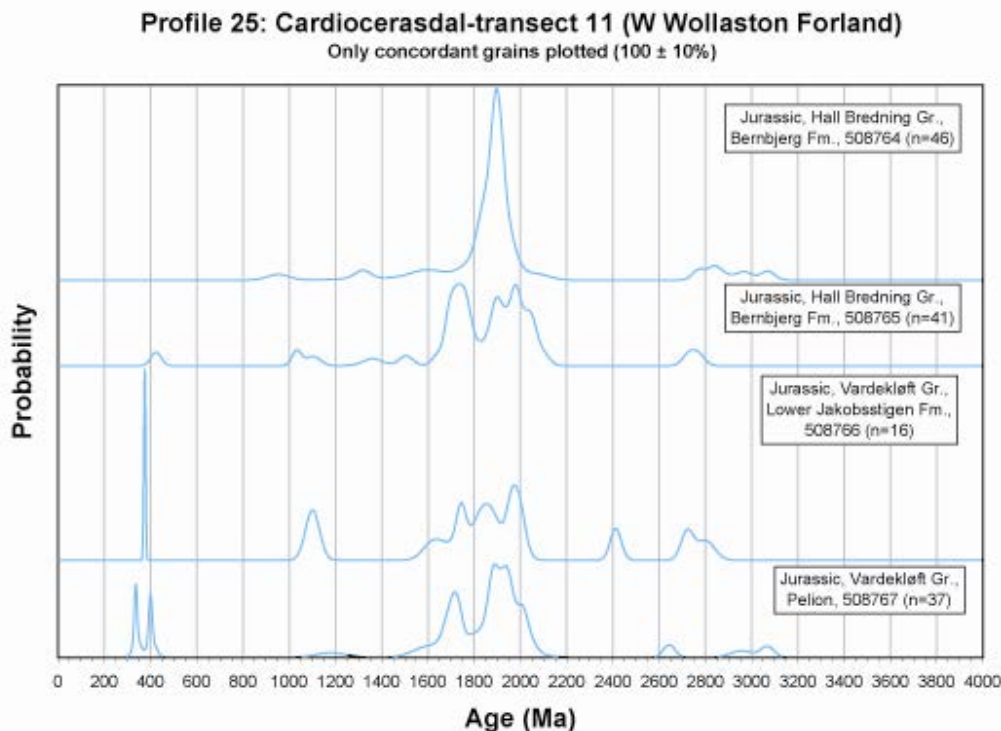


Figure 57. Stacked probability density plots of detrital zircon ages from Profile 25.

Profile 26: Rødryggen East, transect 13

This profile (Fig. 55) consists of three Jurassic samples of the Bernbjerg Fm. (Fig. 58). The samples have a similar distribution of ages and there are no major discrepancies between samples, except that the two youngest samples do not contain Phanerozoic zircon grains. They contain populations at ca. 2700, 2000, 1650 and 1200-1100 Ma. There are also scattered ages in between. The oldest sample contains both Silurian and Devonian zircon grains. The ages can be explained with derivation from local sources, both from basement and metasediments, with input from Phanerozoic igneous activity in the oldest sample.

Profile 30: Rødryggen, south, transect 12

This profile (Fig. 55) contains only one sample, which is mid-Cretaceous in age (Fig. 58). It has a broad age peak at 2800 Ma, another at ca. 1900 Ma and prominent peak at 1650 Ma. There are scattered peaks down to 900 Ma and a peak at 430 Ma. These characteristics may be explained by a mixed derivation from local basement and meta-sedimentary sources, with some input from younger intrusions. The 1650 Ma peak could potentially be from some undiscovered basement occurrence, however considering the 1650 Ma-peak in conjunction with the rest of the Precambrian signature it is not possible to exclude a metasedimentary source for those zircon grains.

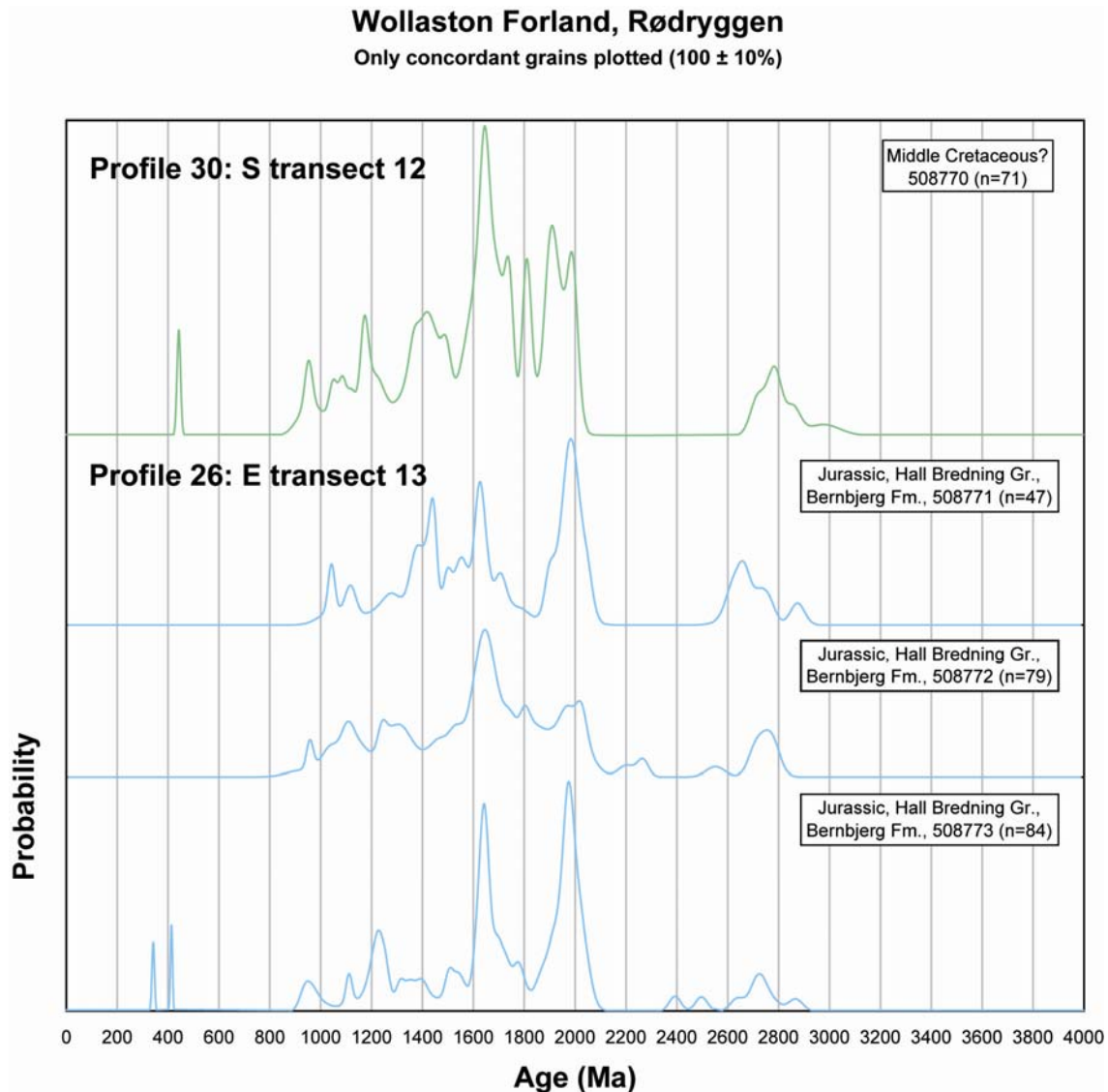


Figure 58. Stacked probability density plots of detrital zircon ages from Profiles 26 and 30.

NW Wollaston Forland: Niesen

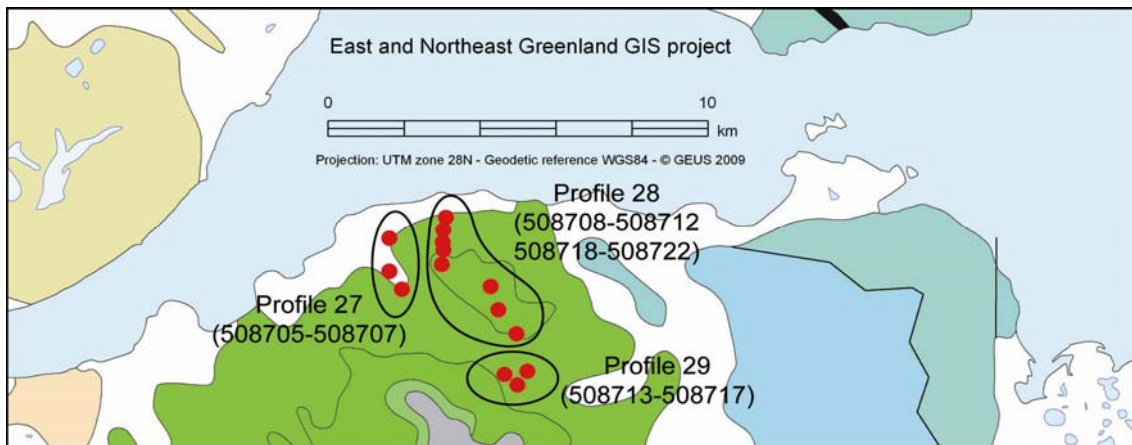


Figure 59. Locations of the sampling points of Profiles 27-29.

Profile 27: Niesen, transect 1

The profile (Fig. 59) consists of three Cretaceous samples from the Lindemans Bugt Fm. (Fig. 60). The oldest and youngest have a variable Archaean population between 3000 and 2500 Ma. The middle sample only contains a few Archaean grains. All three samples contain a peak at ca. 1900 Ma and scattered ages down to 900 Ma. The oldest sample contains Silurian zircons and the middle sample contains Devonian zircons. All ages present in these samples could have been derived from local sources with variable input from basement and metasedimentary sources, with some input from younger igneous activity.

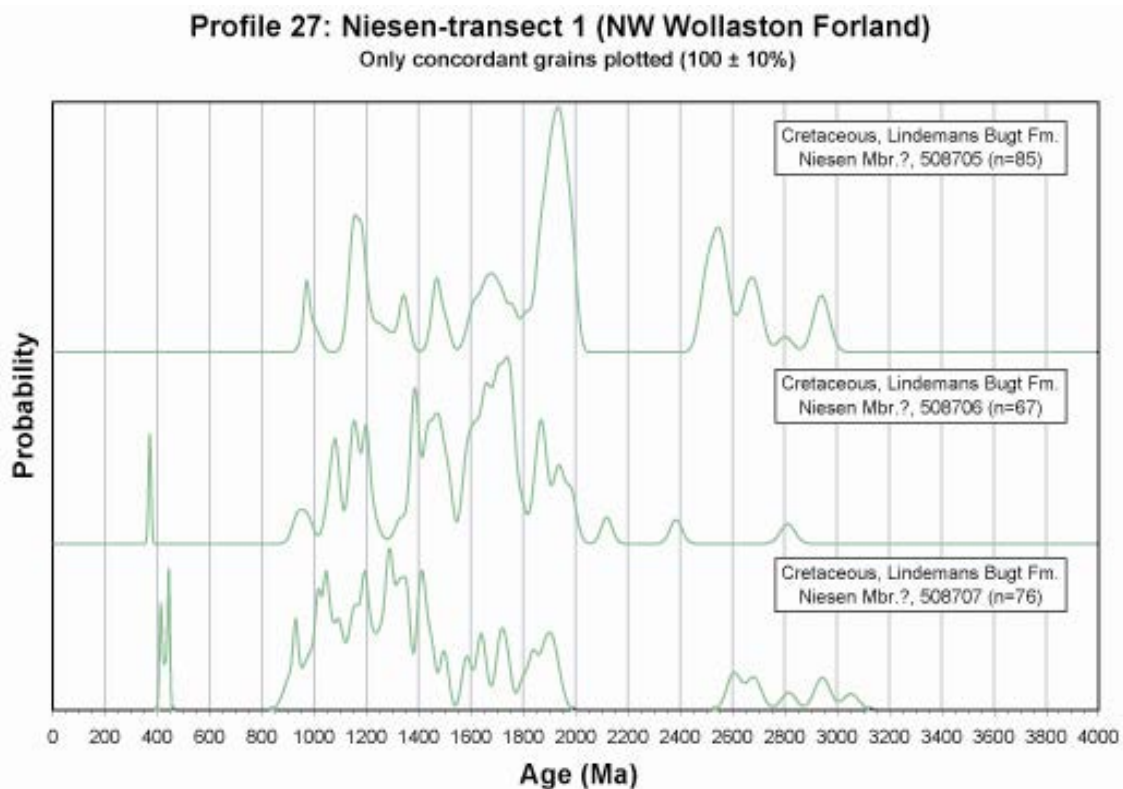


Figure 60. Stacked probability density plots of detrital zircon ages from Profile 27.

Profile 28: Niesen, transect 2

The profile (Fig. 59) consists of ten Cretaceous samples. The lowest six samples are from the Lindemans Bugt Fm. and the upper five samples from the Palnatokes Bjerg Fm. (Fig. 61). There is a significant change in the age distribution pattern between sample three and four. All samples contain Archaean grains, in different amounts and with different peaks in different samples. The three oldest samples have mixed ages between 1800 and 1000 Ma, in the two oldest samples there are also both Silurian and Devonian ages. The younger seven samples have an additional large peak at 1900 Ma. Only one of the younger samples has Palaeozoic zircon grains. Apart from these differences the younger samples have the same characteristics as the older. All the age populations maybe derived from local sources and there seems to be a shift towards a larger input from the northern basement province in the younger samples, as evident from the proportionally increasing importance of the ~1900 Ma peak. This is consistent with a waning input of Caledonian aged zircon grains.

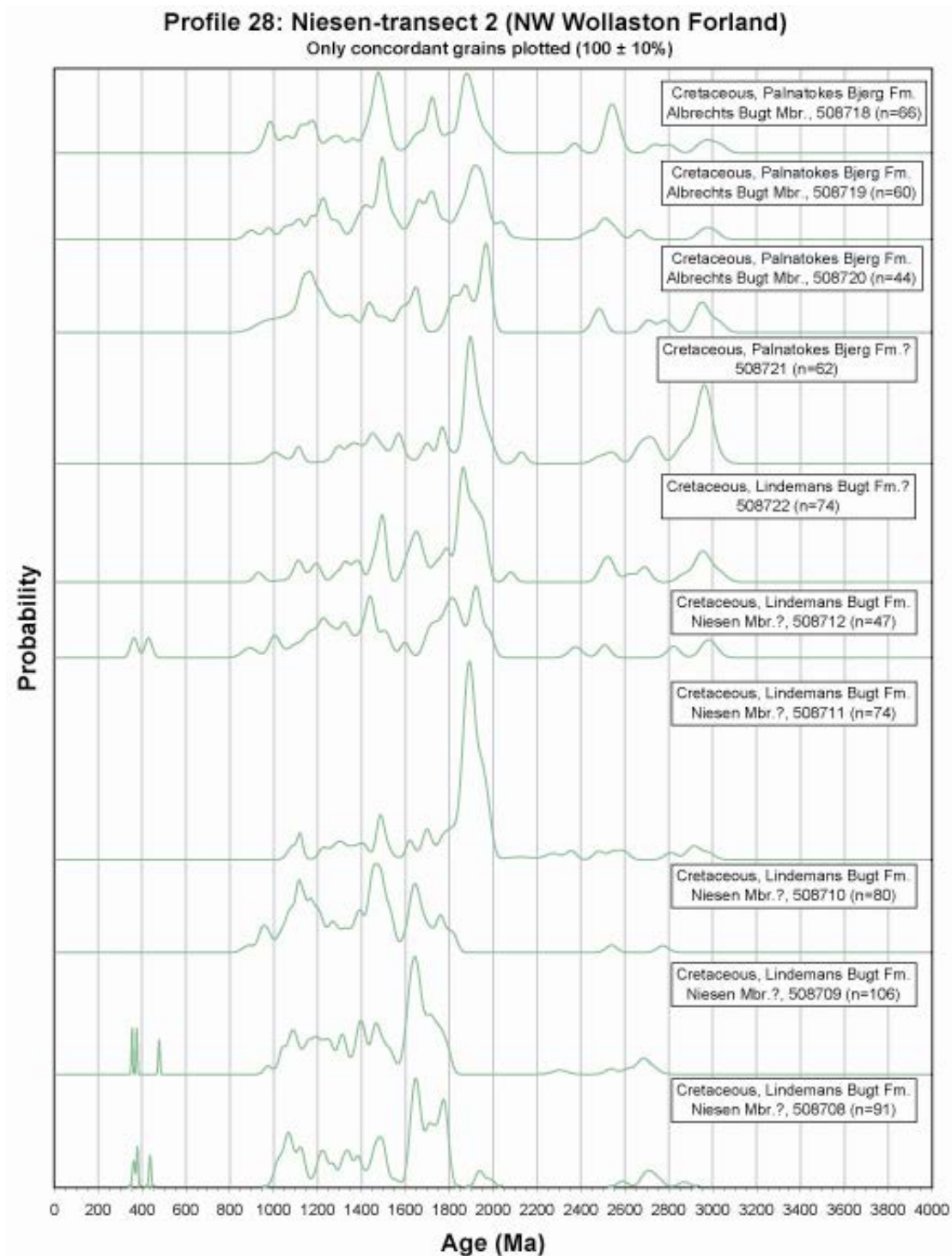


Figure 61. Stacked probability density plots of detrital zircon ages from Profile 28.

Profile 29: Niesen, transect 3

The profile (Fig. 59) consists of five Cretaceous samples, the oldest three from the Lindemans Bugt Fm. and the two youngest are Mid-Cretaceous but not assigned a formation name (Fig. 62). All samples contains a persistent Archean population from 3100 to 2400 Ma, a significant 1900 Ma-peak and scattered peaks from 1800 to 900 Ma. The oldest sample contain both Silurian and Devonian ages, the two other Lindemans Bugt Fm. samples contain a Silurian peak, whereas the Mid-Cretaceous samples do not contain any Palaeozoic zircon. All the ages present in the samples are probably derived from local sources and they are consistent with derivation from both basement and metasedimentary sources, with some input from younger igneous rocks in the lower part of the profile.

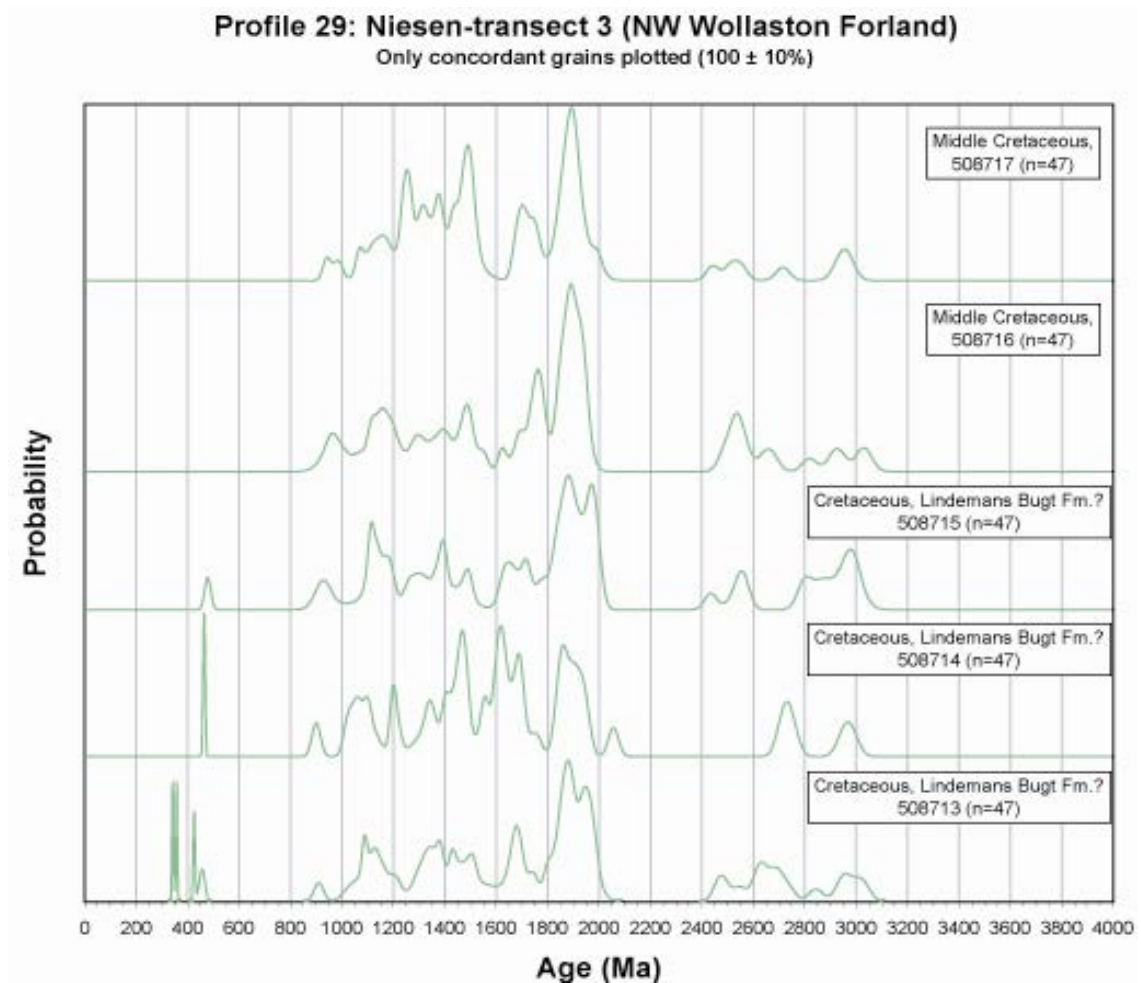


Figure 62. Stacked probability density plots of detrital zircon ages from Profile 29.

E Wollaston Forland

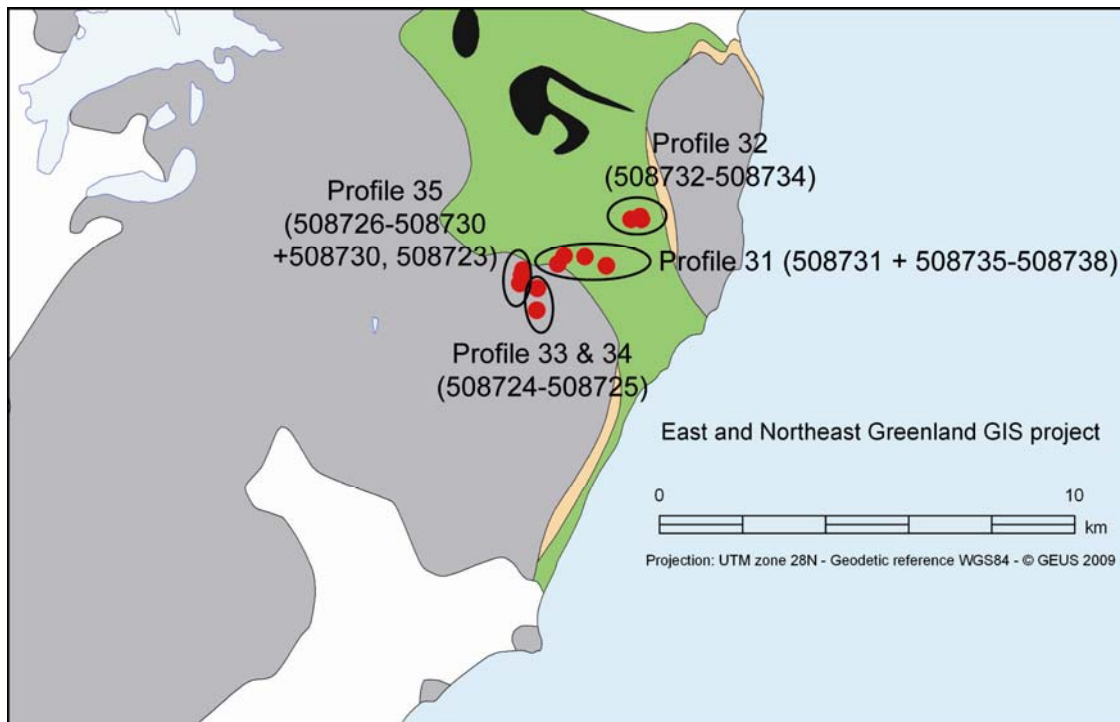


Figure 63. Locations of the sampling points of Profiles 31-35.

Profile 31: Haredal, transect 7

This profile (Fig. 63) consists of five samples, where the oldest sample is Early Cretaceous and the other ones are Palaeocene in age (Fig. 64). All samples have a similar age distribution pattern and there are no distinct breaks in the source material with time. All samples have Archaean zircons, but they are very scattered and of very variable ages. All samples also have peaks at ~1900 and 1800-1600 Ma, but in variable proportions. There are also scattered occurrences of grains with Mesoproterozoic and Early Neoproterozoic ages. The oldest and the two youngest samples have Devonian grains. These characteristics are in agreement with mixed basement and metasedimentary sources, perhaps with a relatively strong input from Palaeoproterozoic basement rocks. The 1800-1600 Ma peaks could potentially be from some undiscovered basement occurrence, however these peaks in conjunction with the rest of the Precambrian signature it is not possible to exclude a metasedimentary source for those zircon grains.

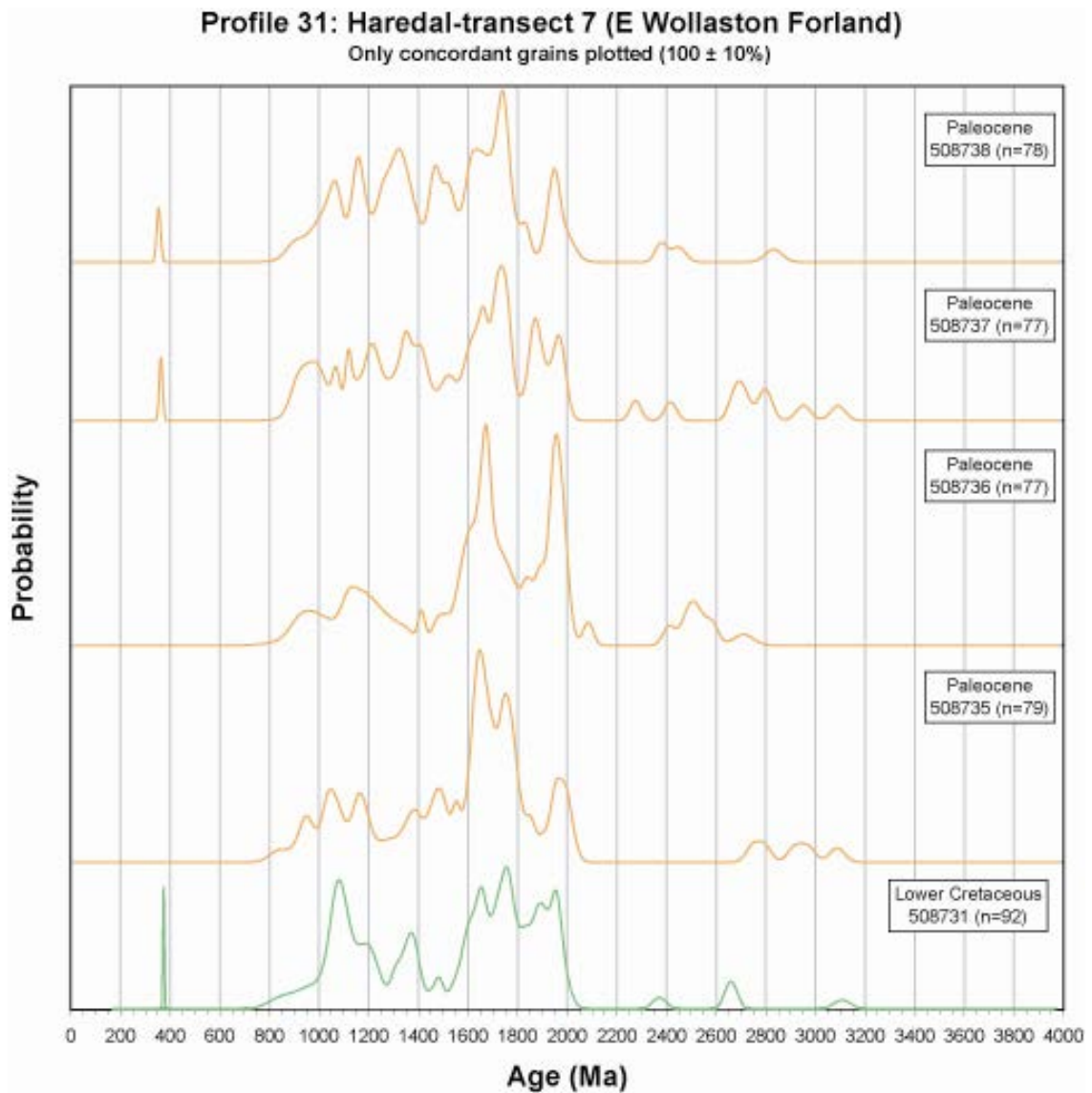


Figure 64. Stacked probability density plots of detrital zircon ages from Profile 31.

Profile 32: Haredal, transect 8

The profile (Fig. 63) consists of three Palaeocene samples (Fig. 65). All samples contain a persistent Archaean population from 3100 to 2400 Ma, a significant 1900 Ma-peak and scattered small peaks from 1800 to 900 Ma. The oldest sample does not contain any Phanerozoic zircon grains, whereas the younger samples contain a Devonian and a Permian peak respectively. All the ages present in the samples are probably derived from local sources and they are consistent with derivation from both basement and metasedimentary sources, with a proportionally more important contribution from the basement. There is also some input from younger igneous rocks in the upper part of the profile. The Permian source may represent material exotic to Greenland- no Permian igneous activity is known from this part of Greenland.

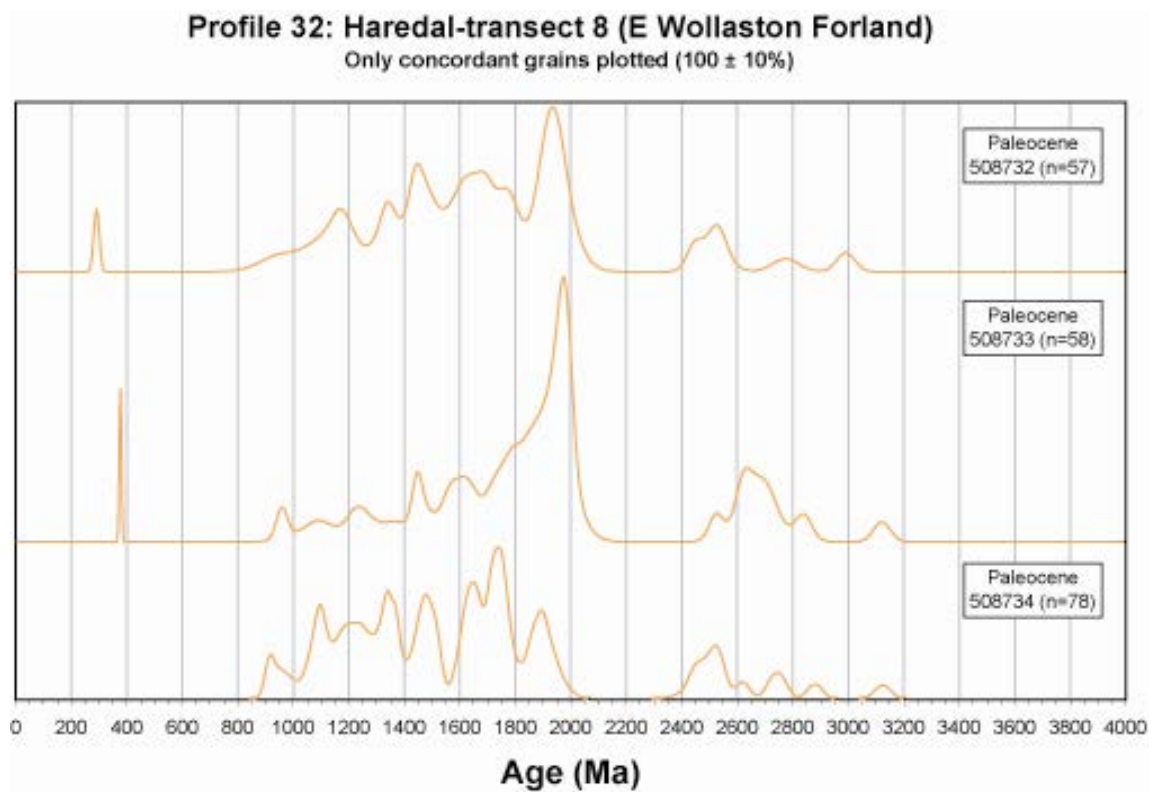


Figure 65. Stacked probability density plots of detrital zircon ages from Profile 32.

Profile 33: Haredal, transect 6

This profile (fig. 63) consists of one Palaeocene sample (Fig. 66). This sample contains an Archaean population between 3100-2400 Ma, a significant 1900 Ma-peak and scattered small peaks from 1800 to 1000 Ma. The sample contains a Devonian peak. All the ages present in the samples are probably derived from local sources and they are consistent with derivation from both basement and metasedimentary sources, with a proportionally more important contribution from the basement. There is also some input from younger igneous rocks.

Profile 34: Haredal, transect 5

This profile (Fig. 63) consists of only one sample of Palaeocene age (Fig. 66). The sample has Archaean zircons of variable ages. The sample also has peaks at ~1900, 1650, 1500, 1300 and 1100 Ma. There are no Phanerozoic grains in this rock. These characteristics are in agreement with mixed basement and metasedimentary sources, perhaps with a relatively strong input from Palaeoproterozoic basement rocks. The lack of Caledonian aged zircon is consistent with derivation from the northern basement gneiss area.

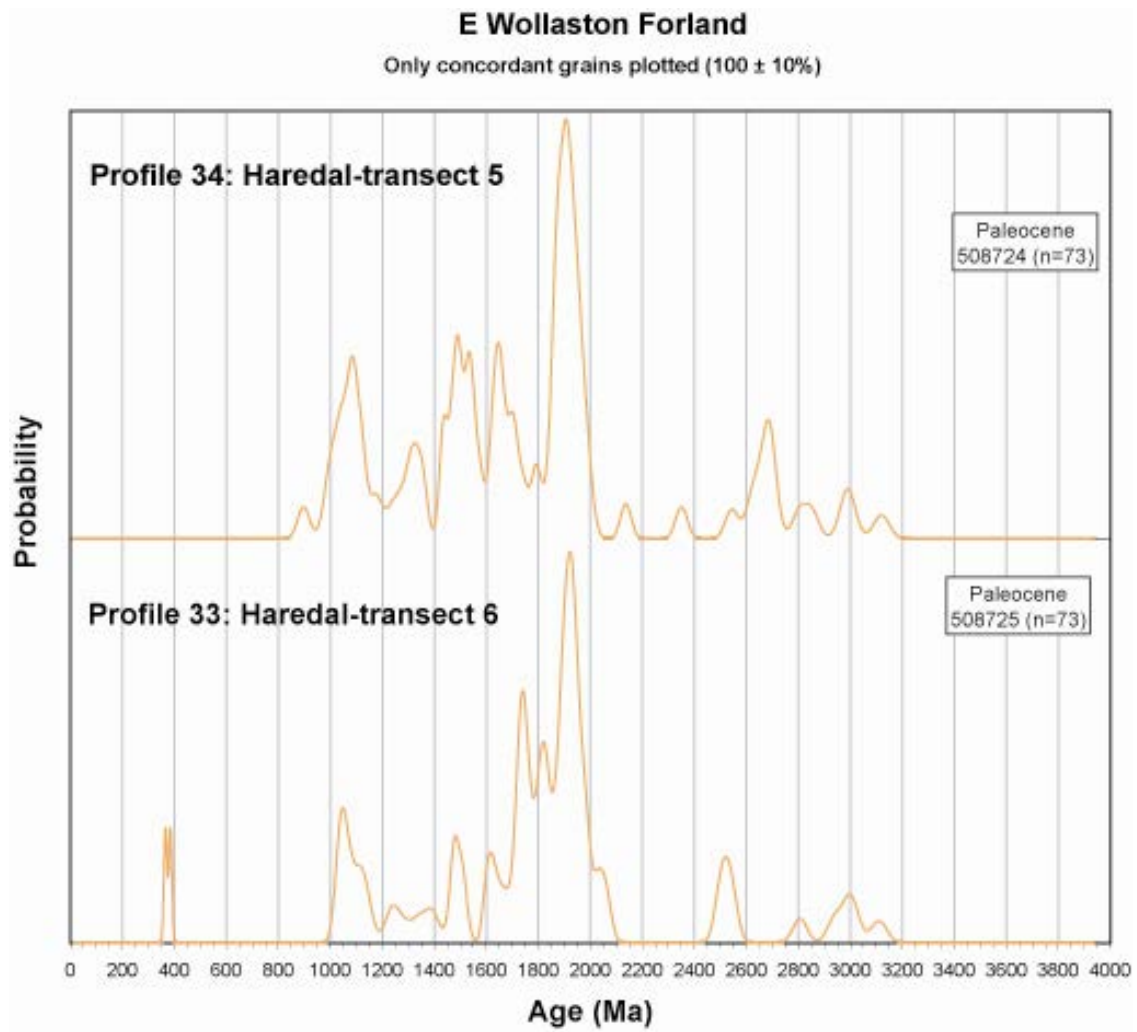


Figure 66. Stacked probability density plots of detrital zircon ages from Profiles 33 and 34.

Profile 35: Haredal, transect 4

This profile (Fig. 63) consists of five Palaeocene samples with roughly similar age distribution patterns (Fig. 67), but with a change in the proportions of different populations between sample 508727 and 508726. The two oldest samples are very similar, with a broad peak at ~2600 Ma, a smaller peak at 1900 Ma, a double peak between 1800 and 1600 Ma, a peak at 1150 Ma and scattered peaks in between. The oldest sample also contains a small Silurian peak. The third sample has a wider range of Archaean aged grains, a large 1650 Ma and scattered Proterozoic ages down to 800 Ma and a significant Siluro-Devonian peak. The two youngest samples are very similar with an Archaean double-peak at 2700 and 2500 Ma, a large 1900, a significant 1750 and scattered Proterozoic peaks down to 900 Ma. Only the older of the two samples have a Palaeozoic peak. The patterns seen here are consistent with derivation from local basement and metasedimentary sources. It is possible that there are signs of input from the more northern metasedimentary sources as well as basement in the northern gneiss region.

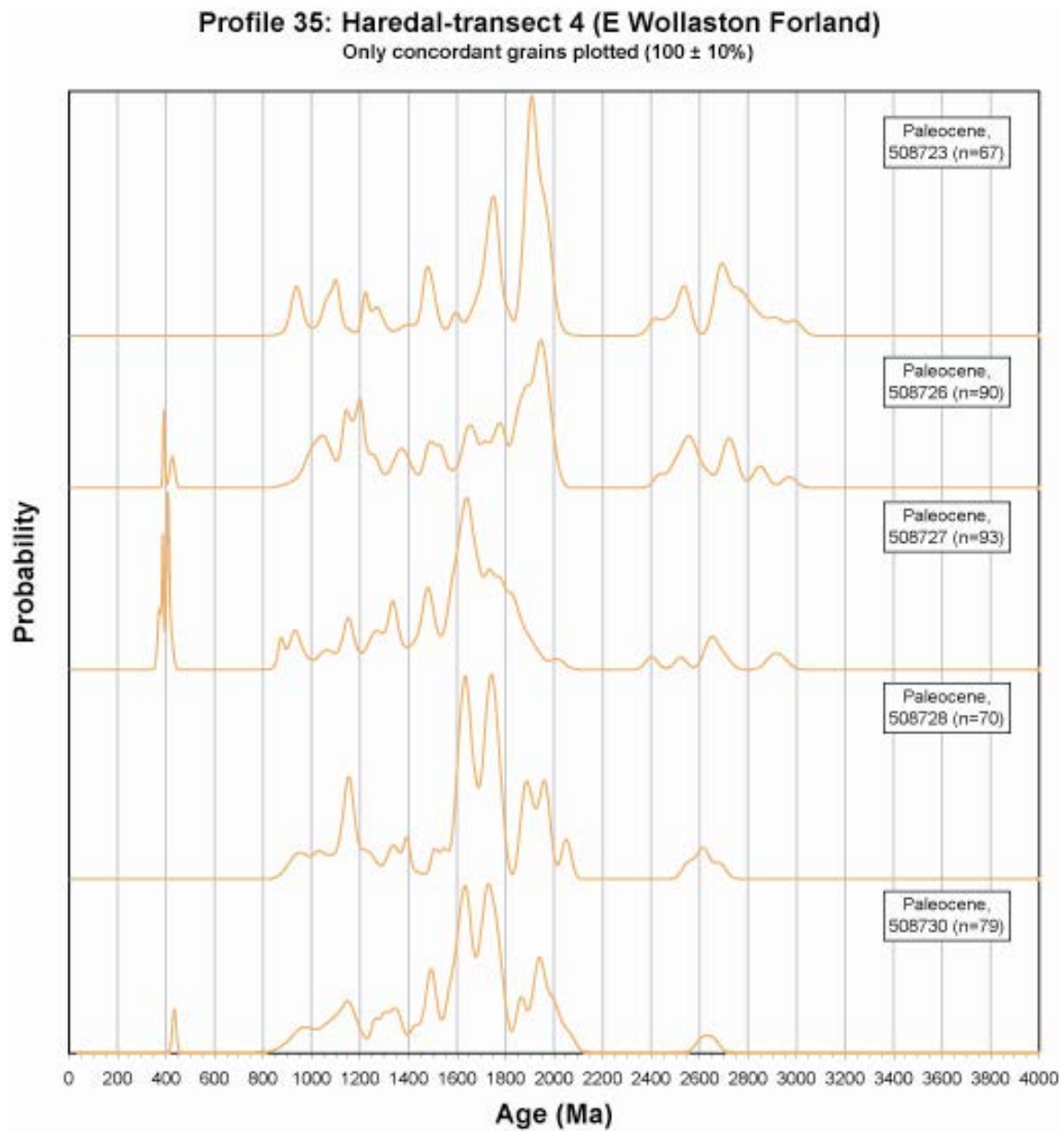


Figure 67. Stacked probability density plots of detrital zircon ages from Profile 35.

Kuhn Ø

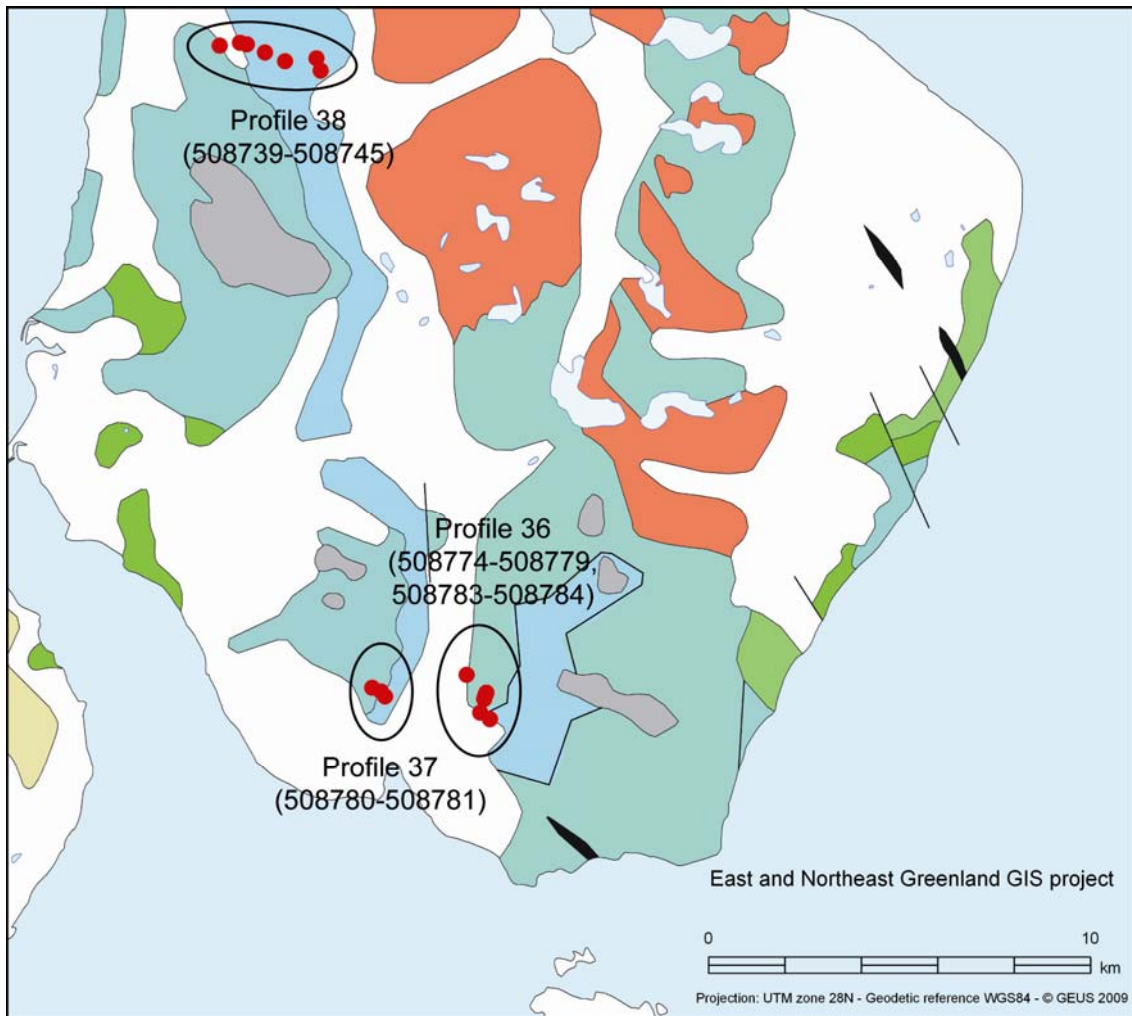


Figure 68. Locations of the sampling points of Profiles 36-38.

Profile 36: Payer Dal east, transect 14

This profile (Fig. 68) consist of eight Jurassic samples, with the oldest sample from the Muslingebjerg Fm., the next two from the Pelion Fm., one from the Uppermost Pelion Fm., two from the lower Payer Dal Fm. and the topmost two samples from the Upper Payer Dal Fm. (Fig. 69). The samples have similar age distribution patterns with no major changes in age populations. All samples have scattered, but rather variable Archaean aged grains. All samples have peaks at ~1950 and 1750 Ma of variable size. All the samples have scattered peaks down to 900 Ma. All samples except the Muslingebjerg and the Uppermost Pelion samples have Palaeozoic zircon grains. These

characteristics can all be explained by derivation from local sources, in this case mainly basement, with minor contributions from metasediments and Caledonian rocks.

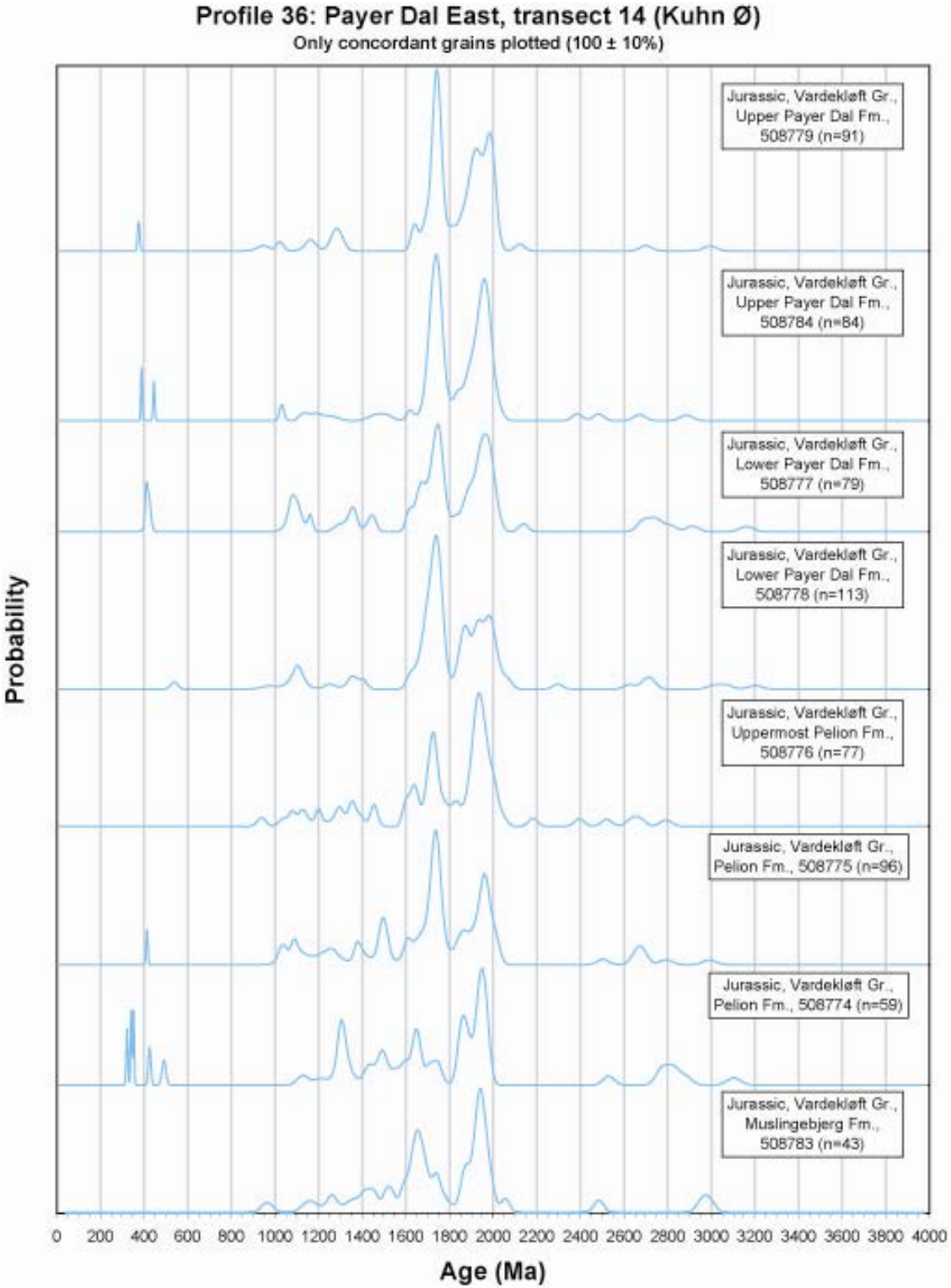


Figure 69. Stacked probability density plots of detrital zircon ages from Profile 36.

Profile 37: Payer Dal West, transect 15

The profile (Fig. 68) consists of three Jurassic samples from the Lower Payer Dal Fm., the Upper Payer Dal Fm. and the Bernbjerg Fm. (Fig. 70). All samples have a similar age distribution pattern and there are no major breaks in the source material with time. All samples have a small and varied, but persistent Archaean population. They have a strong 1950 Ma peak and a 1750 Ma peak that is dominating the oldest sample, but has more insignificant proportions in the youngest. All three samples contain scattered Mesoproterozoic ages and Palaeozoic zircon grains. The age pattern is compatible with derivation from local basement and metasedimentary sources. Especially the oldest sample has a very strong basement signature, with a dominating source, probably from the 1750 Ma granites in the area (Kalsbeek et al. 1993).

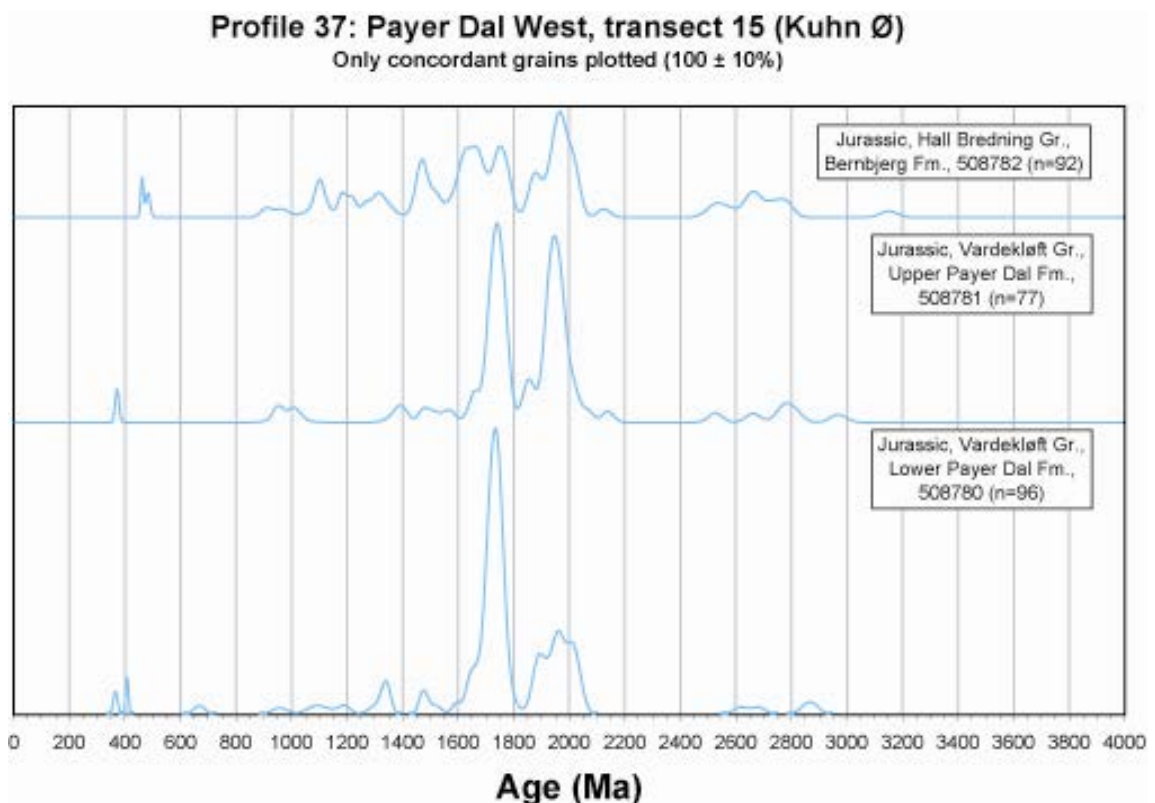


Figure 70. Stacked probability density plots of detrital zircon ages from Profile 37.

Profile 38: Bastian Dal, transect 9

The profile (Fig. 68) consists of seven Jurassic samples, one sample from the Bastians Dal Fm., one from the Muslingeberg Fm., one from the Lower Payer Dal Fm., two from the Payer Dal Fm., one from the Upper Payer Dal Fm. and one from the Bernbjerg Fm. (Fig. 71). There are some differences between samples. All samples contain a small Archaean population, but it rather insignificant and variable in the four oldest samples, whereas the two topmost samples contain an increasing peak at 2700 Ma. All samples

have a 1950 Ma peak, but it is not of proportionally significant size in the three oldest samples. One or two peaks are present in the age interval between 1800 and 1600 Ma in all samples, but the 1750 Ma peak is not present at all in the oldest sample. There are scattered grains of ages down to 900 Ma in all samples and a small Caledonian population in all samples. The two Payer Dal Fm. samples form a group together with the Upper Payer Dal sample with a generally stronger basement character in the age distribution, whereas the rest of the samples show a stronger metasedimentary input, especially the three oldest samples, where the influence from 1950 Ma basement is very insignificant.

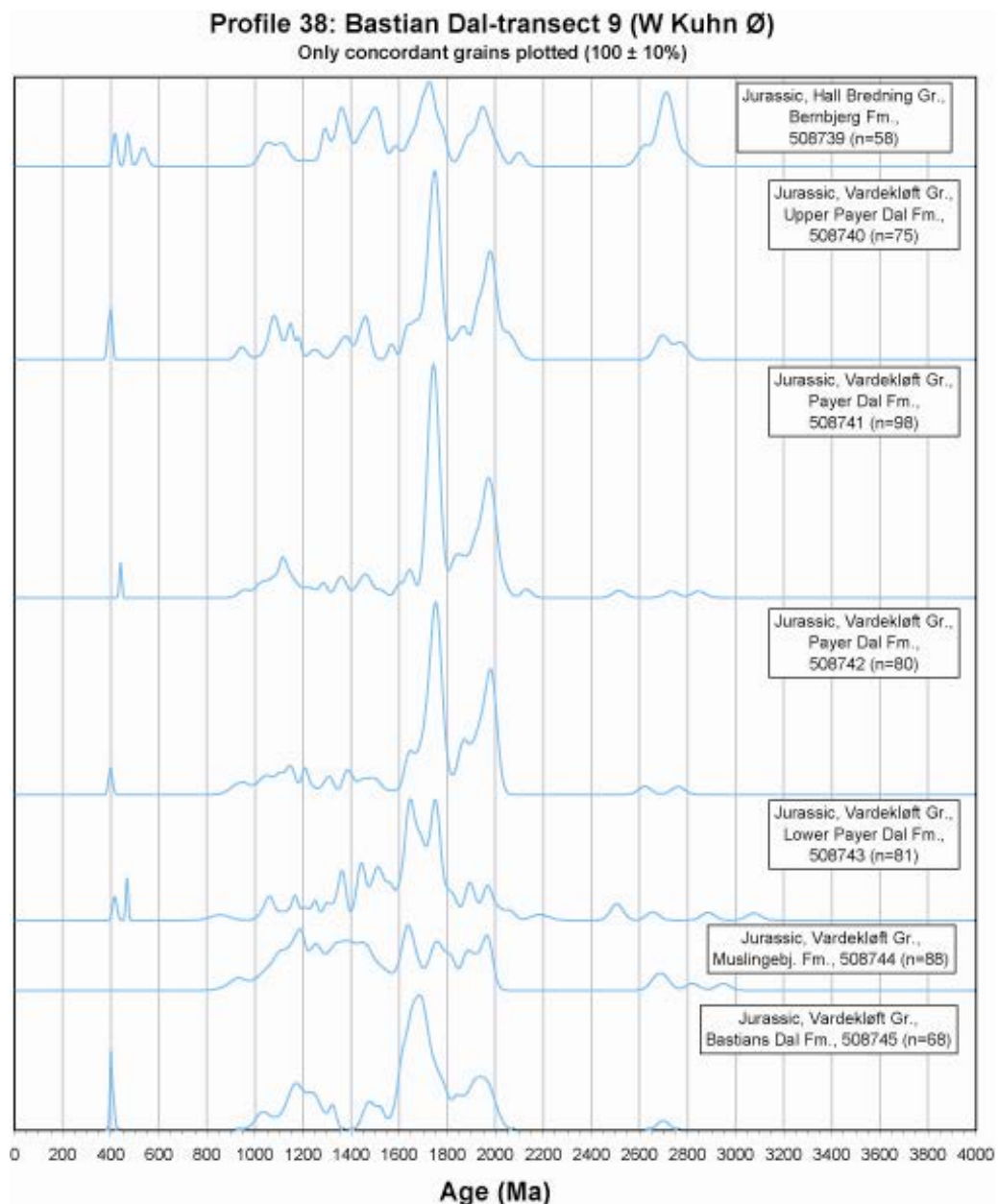


Figure 71. Stacked probability density plots of detrital zircon ages from Profile 38.

Kim Fjelde, Peary Land

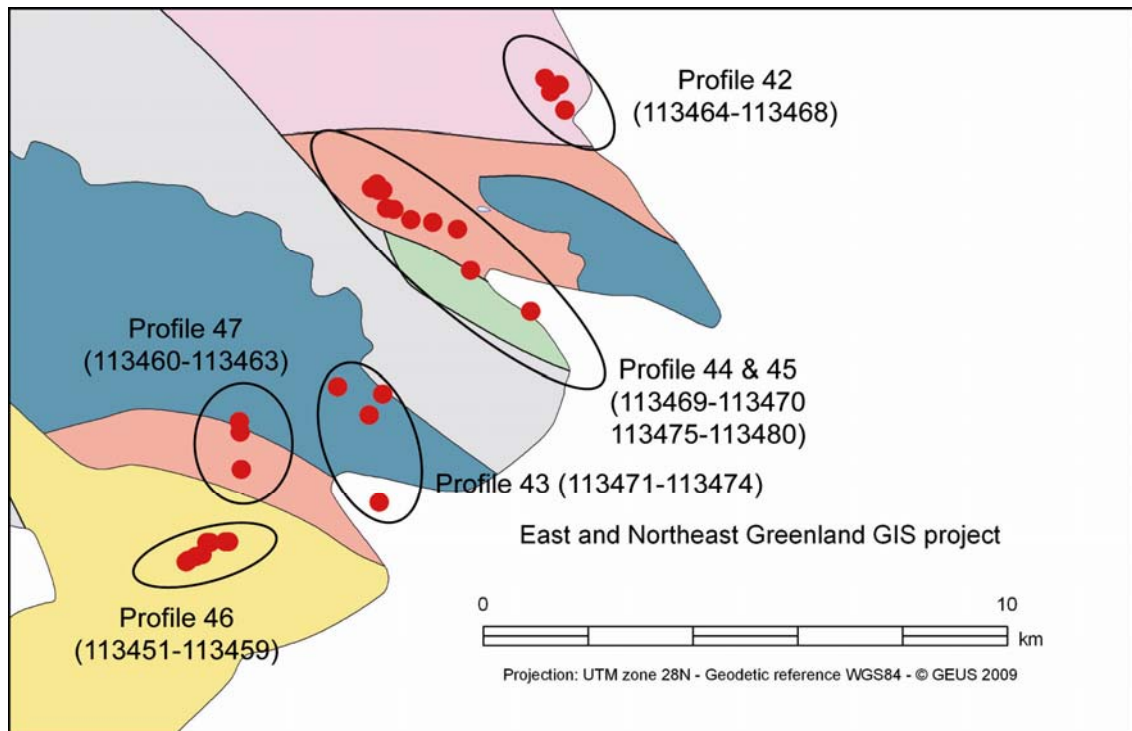


Figure 72. Locations of the sampling points of Profiles 42-47.

Profile 42: Dunken

This profile (Fig. 72) consists of five Triassic samples of the Dunken Fm. (Fig. 73). All the samples have some differences in the detrital zircon populations. All samples have a varied Archaean population, mainly with ages between 3000 and 2500 Ma. A 1950 Ma peak is the dominating peak in the oldest sample, but a peak between 1800 and 1600 Ma is dominant in most samples. All the samples have a peak in the abundance around 1100 Ma. All samples have scattered Proterozoic ages down to 900 Ma. Three of the samples have a small Palaeozoic age population. All age populations in the sample can be explained by derivation from local sources, with mixed basement and metasedimentary sources. It is evident from e.g. the 1100 Ma peak that there is large input from the northern sedimentary units (see Fig. 6 and Røhr et al. 2008).

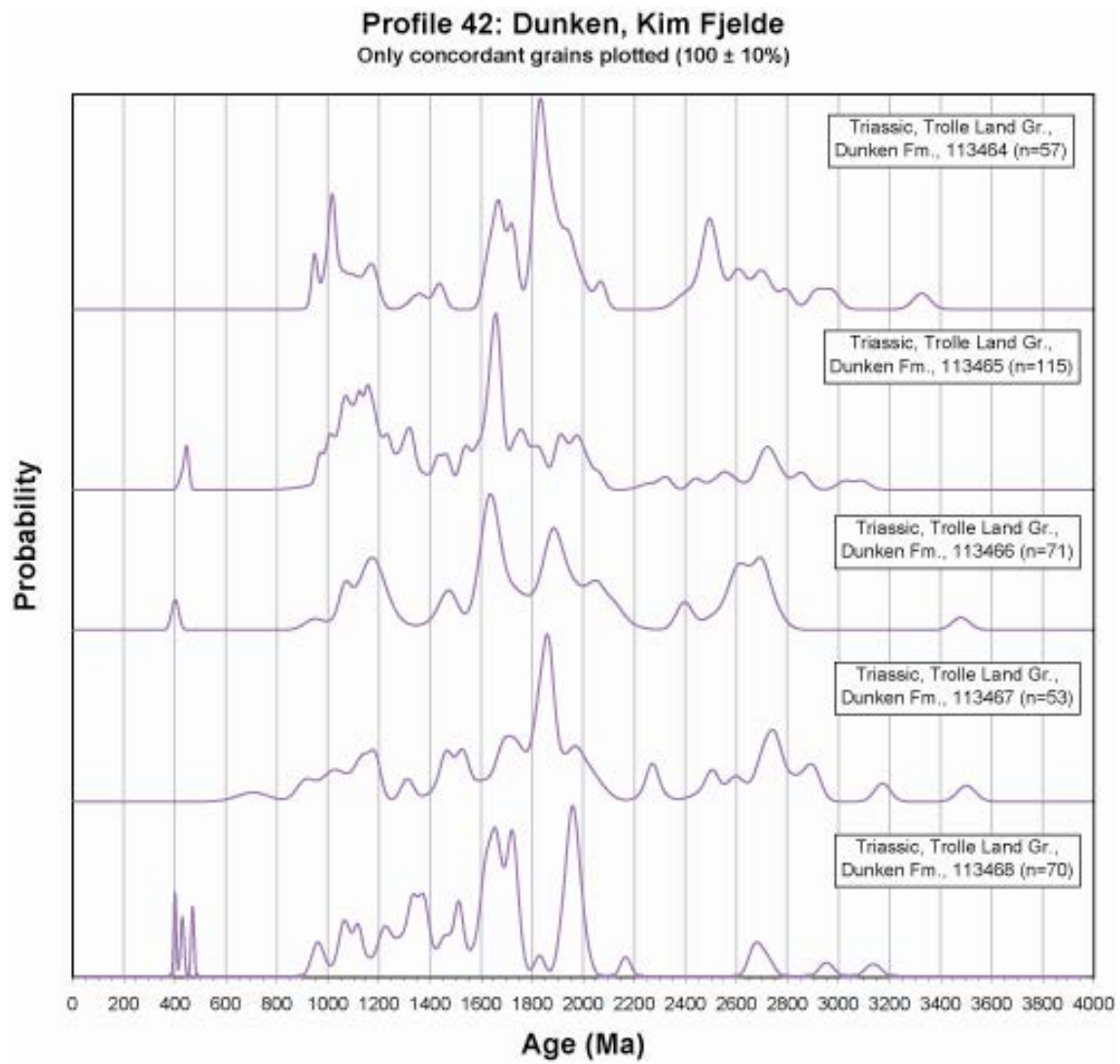


Figure 73. Stacked probability density plots of detrital zircon ages from Profile 42.

Profile 43: Ved Sletten

This profile (Fig. 72) consists of four Triassic samples from the Parish Bjerg Fm. (Fig. 74). They all have roughly similar age patterns. All samples have an Archaean population, present as a broad peak centred on 2700 Ma. There is a minor influence of 1950 Ma ages, but a strong influence of a 1650 Ma source. There are scattered occurrences between 2000 and 900 Ma. All samples have a distinct peak at 950 Ma. The three top samples have scattered and varied occurrences of few Neoproterozoic to Palaeozoic grains, between 800 and 400 Ma. This signal is most probably picked up from the northern sedimentary sequences (see Fig. 6). The overall age distribution pattern is consistent with derivation from northern sedimentary sources.

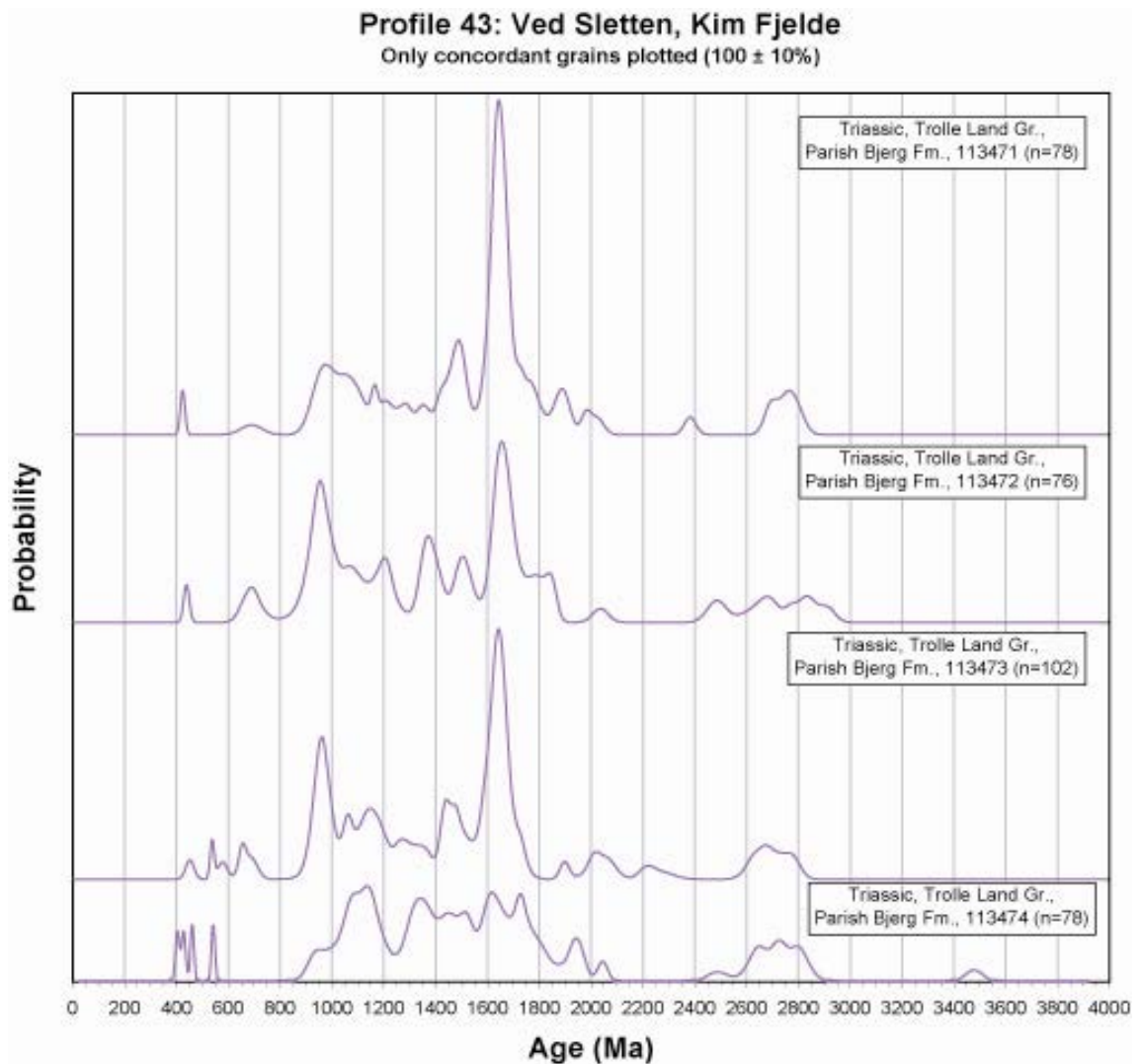


Figure 74. Stacked probability density plots of detrital zircon ages from Profile 43.

Profile 44: Falkefjeld

The profile (Fig. 72) consists of seven Triassic samples of the Parish Bjerg Fm. (Fig. 75). All the samples have similar age distribution pattern, but do display some internal variations in the proportions of different populations. All samples have a small Archaean population, primarily between 2800 and 2600 Ma. They all have a broad multi-peak component with ages between 2000 and 900 Ma, with distinct peaks at 1950, 1650, 1450 and 1000 Ma. The size of these peaks varies between the samples and there seems to be a growing influence of the 1950 Ma source upwards in the section, whereas there is a slight decrease in the proportion of 1650 Ma material. All the samples have scattered Neoproterozoic grains and multiple Caledonian and slightly older peaks. There does not seem to be any need to invoke non-local sources for these sediments, they all have mixed sources of local basement and metasedimentary origin together with some Caledonian input.

Profile 44: Falkefjeld, Kim Fjelde
Only concordant grains plotted ($100 \pm 10\%$)

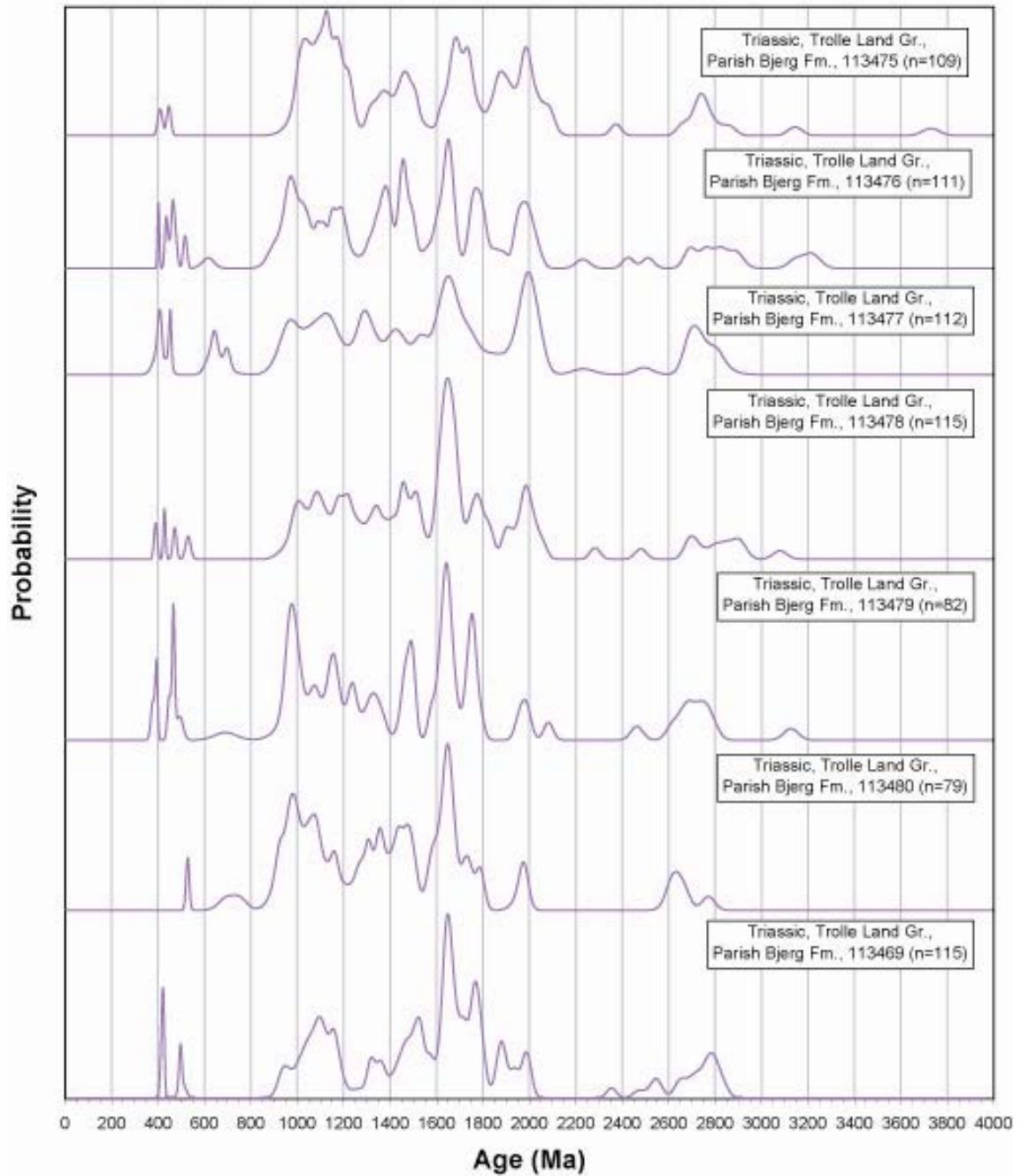


Figure 75. Stacked probability density plots of detrital zircon ages from Profile 44.

Profile 45: Falkedal

This profile (Fig. 72) is a single Triassic sample of the Parish Bjerg Fm. (Fig. 76). It has a broad Archaean peak, centred on 2700 Ma. There are distinct peaks at 1650, 1100 and 950 Ma and smaller occurrences in between 2100 and 900 Ma, but also with some occurrences in the rare age group between 800 and 600 Ma. The origin of these grains is unknown There are no Caledonian zircon grains.

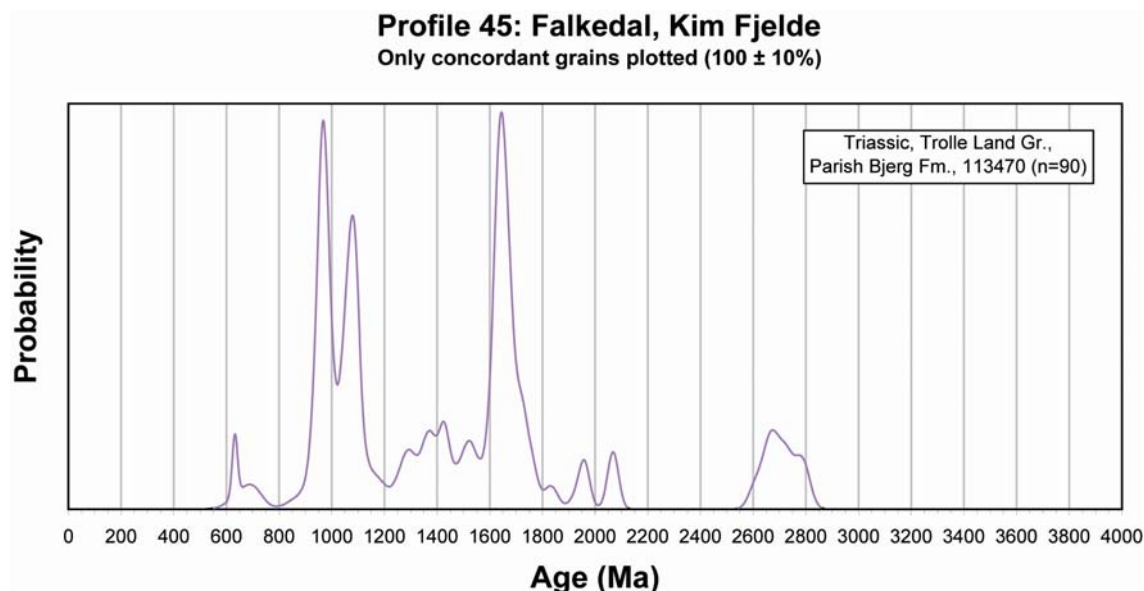


Figure 76. Stacked probability density plots of detrital zircon ages from Profile 451.

Profile 46: Søjlerne

This profile (Fig. 72) consists of eight samples of Oxfordian-Valanginian (Jurassic-Cretaceous) age of the Ladegårdsåen Fm. (Fig. 77). All samples contain an Archaean component and although it looks slightly different between the samples there is a concentration of ages around 2800-2700 Ma. The four oldest samples have a convex age pattern between 2100 and 900 Ma, with more pronounced peaks at 1650, 1500 and 1150 Ma. The younger samples have a flatter profile with distinct peaks at 1850, 1400 and 1100 Ma. This is slightly different than the older samples and suggests a rather radical shift in sediment source. All samples have Caledonian ages. The age patterns displayed here can all be explained with derivation from local sedimentary sources (see Fig. 6), but there is a significant change in populations seen in the profile.

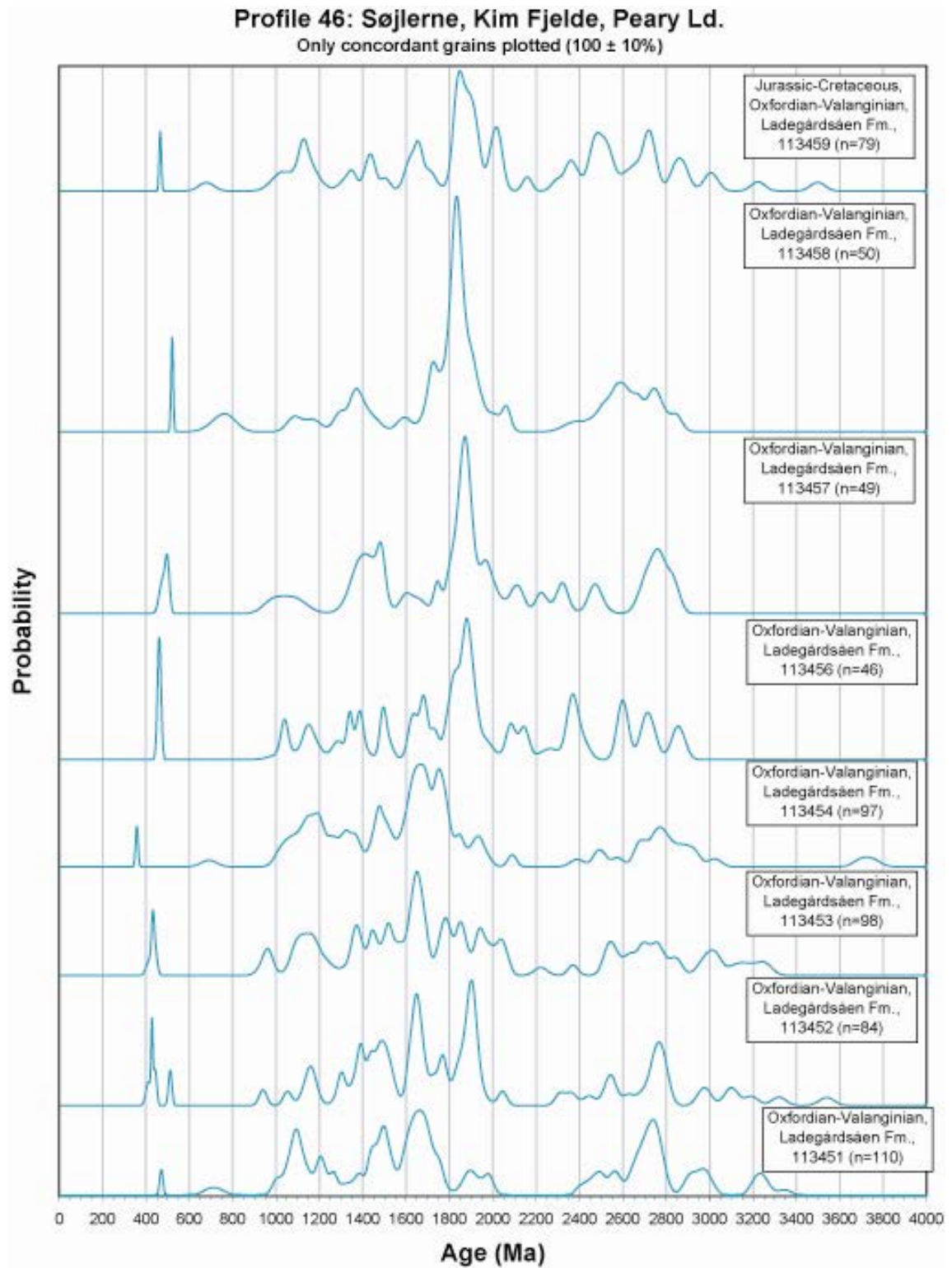


Figure 77. Stacked probability density plots of detrital zircon ages from Profile 46.

Profile 47: Ladegårdså sletten

This profile (Fig. 72) consists of four samples of Oxfordian-Valanginian age from the Ladegårdsåen Fm. (Fig. 78). The samples have very similar age groups and there are no changes in the sources through the profile. All samples have an Archaean peak centred on 2700 Ma. Further, all samples have variable amounts of ages between 2100 and 900 Ma, with distinct peaks at 1650 and 1500 Ma and a broad lower peak at ca. 1000 Ma. Some of the samples have a few grains with Neoproterozoic ages and all samples have Caledonian ages. The oldest sample also carries Devonian zircons. The samples have an age distribution with characteristics from both basement, metasediments and Palaeozoic igneous activity, but with a proportionally strong input from metasediments.

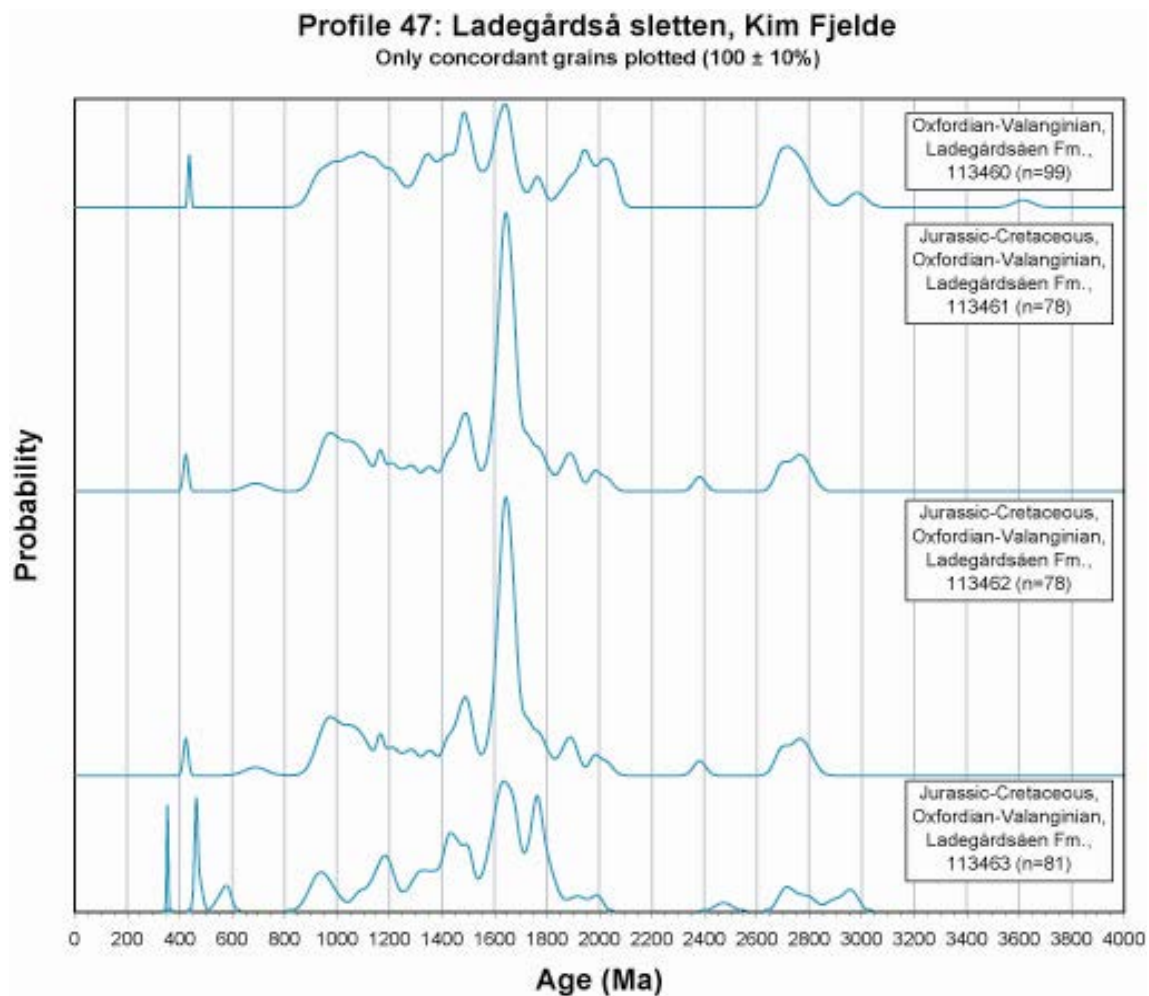


Figure 78. Stacked probability density plots of detrital zircon ages from Profile 47.

Discussion and Summary

Stream sediments

The stream sediments faithfully reflect the geology exposed in the catchment area of the sampled streams (Steenfelt & Kunzendorf 1979). Therefore, they offer a valuable tool for interpretation of detrital zircon age spectra from older sediments (Fig. 79).

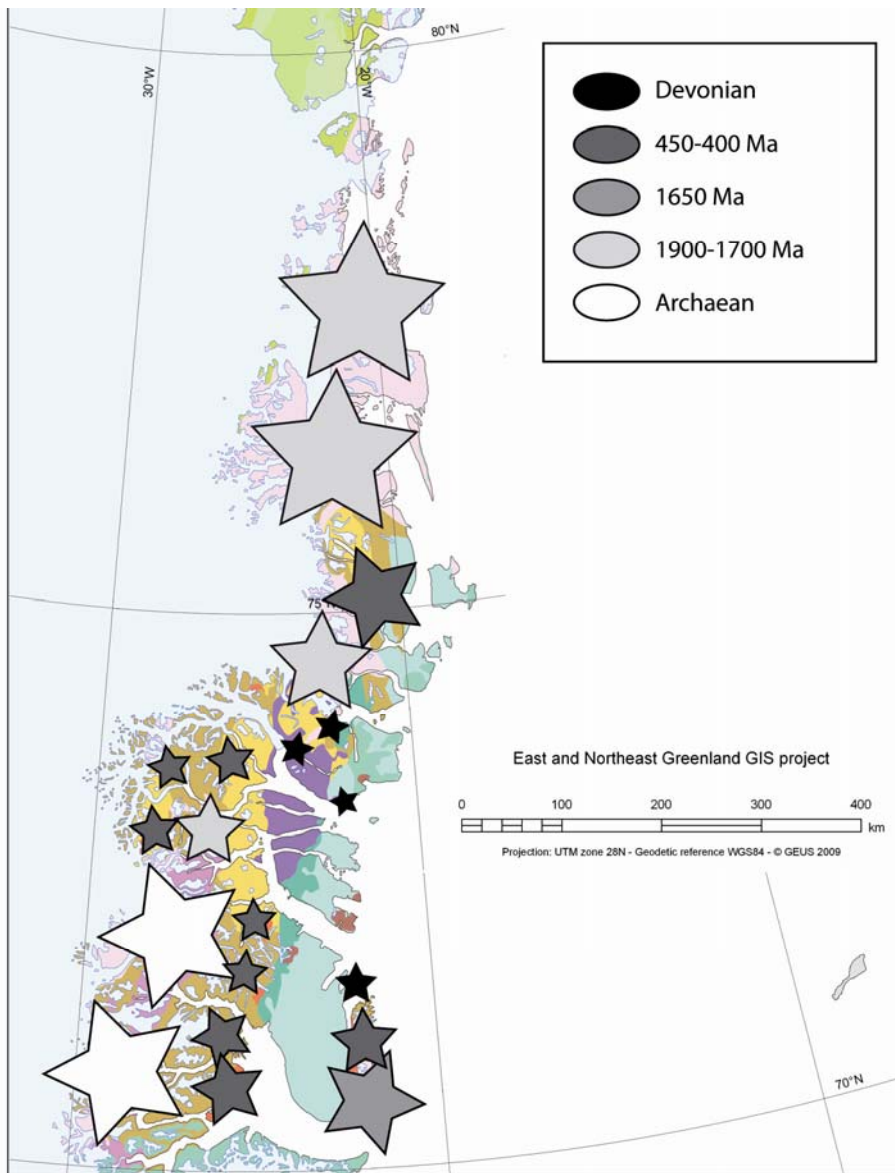


Figure 79. Overview of regions with orthogneisses and magmatic rocks that yield relatively simple ages.

The southernmost part (Fig. 79) is dominated by Caledonian aged zircon grains, which is expected given the large number of calc-alkaline intrusions with large amounts of core-free Palaeozoic zircons. The intrusions are primarily located in eastern Milne Land, eastern Renland and Liverpool Land. Minor contributions come from the Krummedal Sequence. The stream sediment group D display the characteristics of this part, with Caledonian, Devonian and a high proportion of 1650 Ma zircon grains in some samples, typical of Liverpool Land and Canning Land. The catchment areas of stream sediment groups E, F, G and H contain metasedimentary units and this is reflected in complex age spectra, with varying proportions of the different populations (see Fig. 5). Some populations are very common in some samples and this seem to reflect original differences in the stratigraphy of the metasedimentary sequences, e.g. an increasingly important 1100 Ma peak, which probably stems from erosion of the Eleonore Bay Supergroup (see sandstone profile 1). The northern stream sediment sample groups I, J and K reflect the increasing influence of basement rocks primarily with ages of ca. 1950 Ma and 1750 Ma. In the northernmost group there is a mixed signal from 1950 Ma basement and sedimentary detritus, probably from the Neoproterozoic Rivieradal Group and the Palaeo- to Mesoproterozoic Independence Fjord Group. From the zircon age data set there is no need to invoke exotic or unknown sources for the recent stream sediments encountered in northeast Greenland.

Neoproterozoic to Palaeocene sandstones - some general comments

The Neoproterozoic sandstones have an allochthonous character, they have been interpreted to have been deposited in Pannotian intra-cratonic rift-basins (Sønderholm et al. 2008). They retain a zircon memory from their initial source areas that were positively not Greenland, but has been interpreted to have been located in North America (e.g. Kalsbeek et al. 2000). The large volumes of the Precambrian metasedimentary and sedimentary rocks in the area make them large contributors of detrital zircon material. This may hamper the interpretations of source regions for the younger sediments because the signal is rather uniform over large areas and other relevant, but smaller populations may become obscured. Proportionally large peaks usually point towards basement sources, but in this case they may indicate an inherited population from older, scavenged sediment. Therefore the interpretations regarding basement populations are very conservative and based only on published data, that is, only known basement populations are considered.

The other over-all factor to influence the age distribution in a specific sediment is of course what kinds of rock were available for erosion at the time of deposition. This may for example explain the lack of Devonian aged zircon grains in the Post-Devonian sediments, because most of the time the locations of these intrusions and volcanic rocks were flooded.

Palaeogeographic reconstructions and depositional pathways

In this section, samples with the same age will be presented in a palaeogeographic framework. Interpretations can be made regarding different or similar sources for sediments in different areas. Sediments of all ages are not present in all areas and therefore not all areas can be compared in every time-slice presented. Some areas have at some points in time even acted as contributors of detritus instead of being basins. Only the Post-Devonian sections will be discussed in a time-slice perspective since the Pre-Devonian sediments sampled in this study are situated in allochthonous thrust-sheets and originally not deposited in Greenland. The southern and the northern part of the region will be discussed separately. Black arrows on the reconstructions indicate probable or possible source areas and hence transport directions. The probability density plots are in black with grey lines that divide for every 1000 million years. The scale for all the age plots is 0-4000 million years. It is important to remember that rocks that acted as source material for a sediment at a specific time may not be present today and the distribution of different lithological units may have been different than today.

Southern part of the study area

Late Devonian

The late Devonian samples have a signal of mixed basement and metasediments (Fig. 80, see also figs. 4 and 5). There seems to be a larger involvement of Palaeoproterozoic basement than Archaean basement and therefore a derivation from north of 73°N. The metasediments are indistinguishable Krummedal or Eleonore Bay successions (see Fig. 5). The Devonian sediments were probably sourced in highland areas to the west or northwest of where they were deposited.

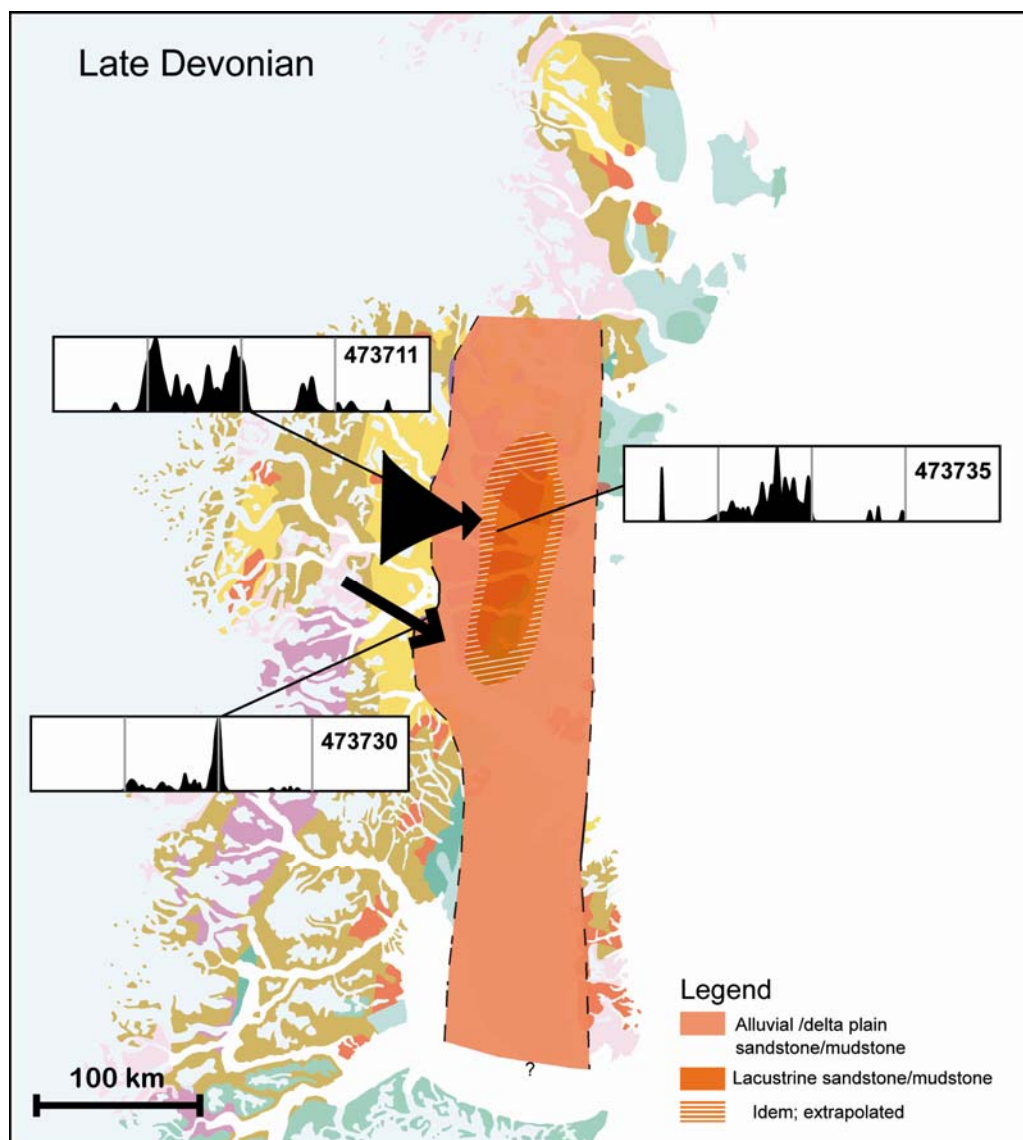


Figure 80. Palaeogeographic reconstruction of sedimentary facies in the Late Devonian

Late Carboniferous to Late Permian

The Late Carboniferous samples yield age spectra indicative of derivation from meta-sedimentary units (Fig. 81). The northernmost sample also contains Devonian zircon grains and therefore the specific transport path is drawn from an area where there possibly were Devonian intrusions exposed at the time. The Permian samples also have a primary derivation from metasediments. The southernmost sample also has a strong Caledonian input, which would be consistent with derivation from the east, since there are no Caledonian intrusives to the west of the sample location.

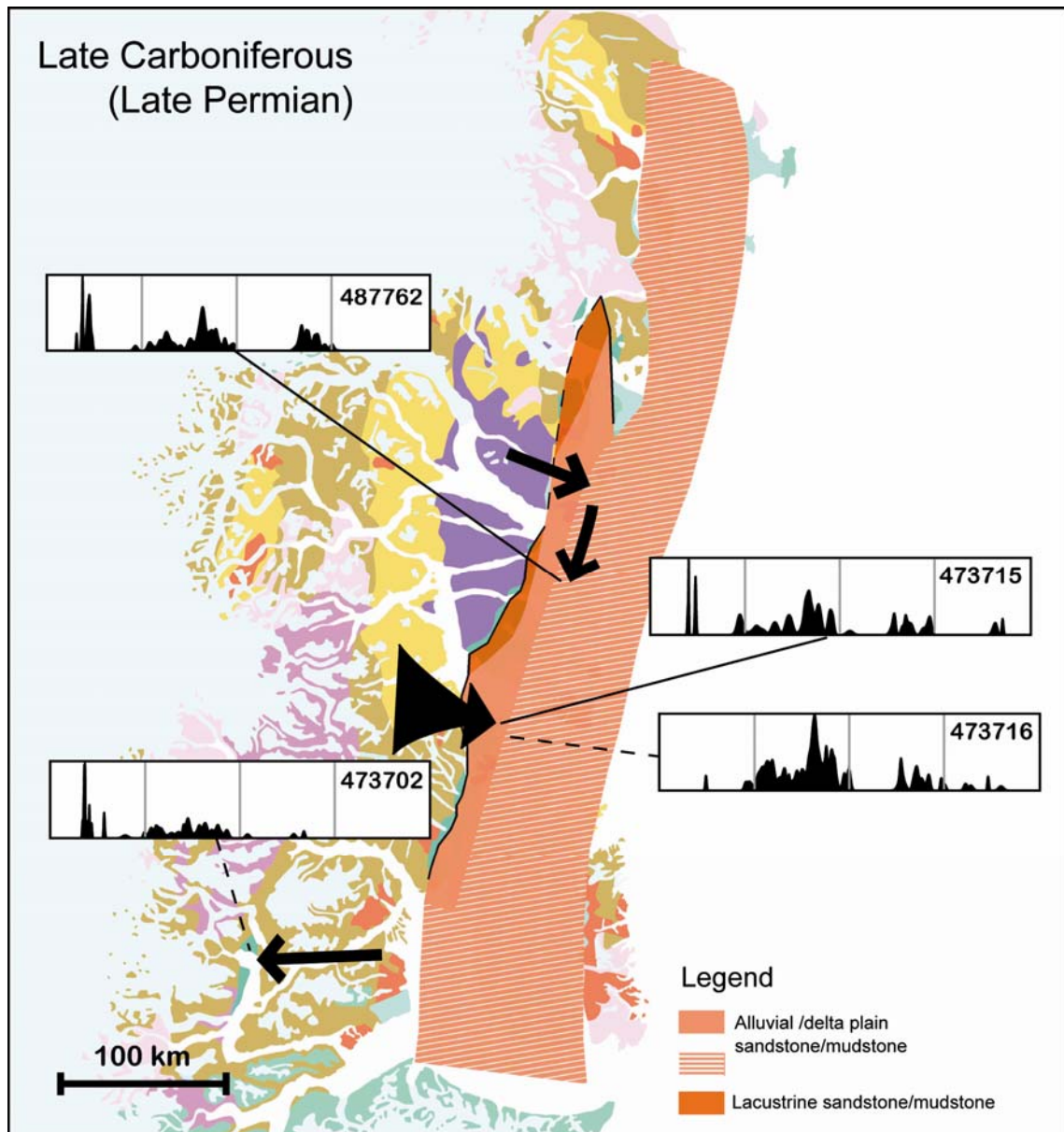


Figure 81. Palaeogeographic reconstruction of sedimentary environments in the Late Carboniferous- Late Permian. The locations of the Late Carboniferous samples are indicated with solid lines and the Late Permian samples with dashed lines.

Early Triassic

The two northern Early Triassic samples have a detrital age distribution pattern consistent with derivation from metasediments, basement and Caledonian intrusives (Fig. 82). There is a higher proportion of basement influence in the northernmost sample, based on the presence of a 1950 Ma peak (see Fig. 4), which is consistent with a location closer to the basement areas to the north. The southernmost sample has an age pattern that could be explained by derivation from Liverpool Land alone, including metasedimentary signals, a 1650 Ma basement peak and Caledonian zircons.

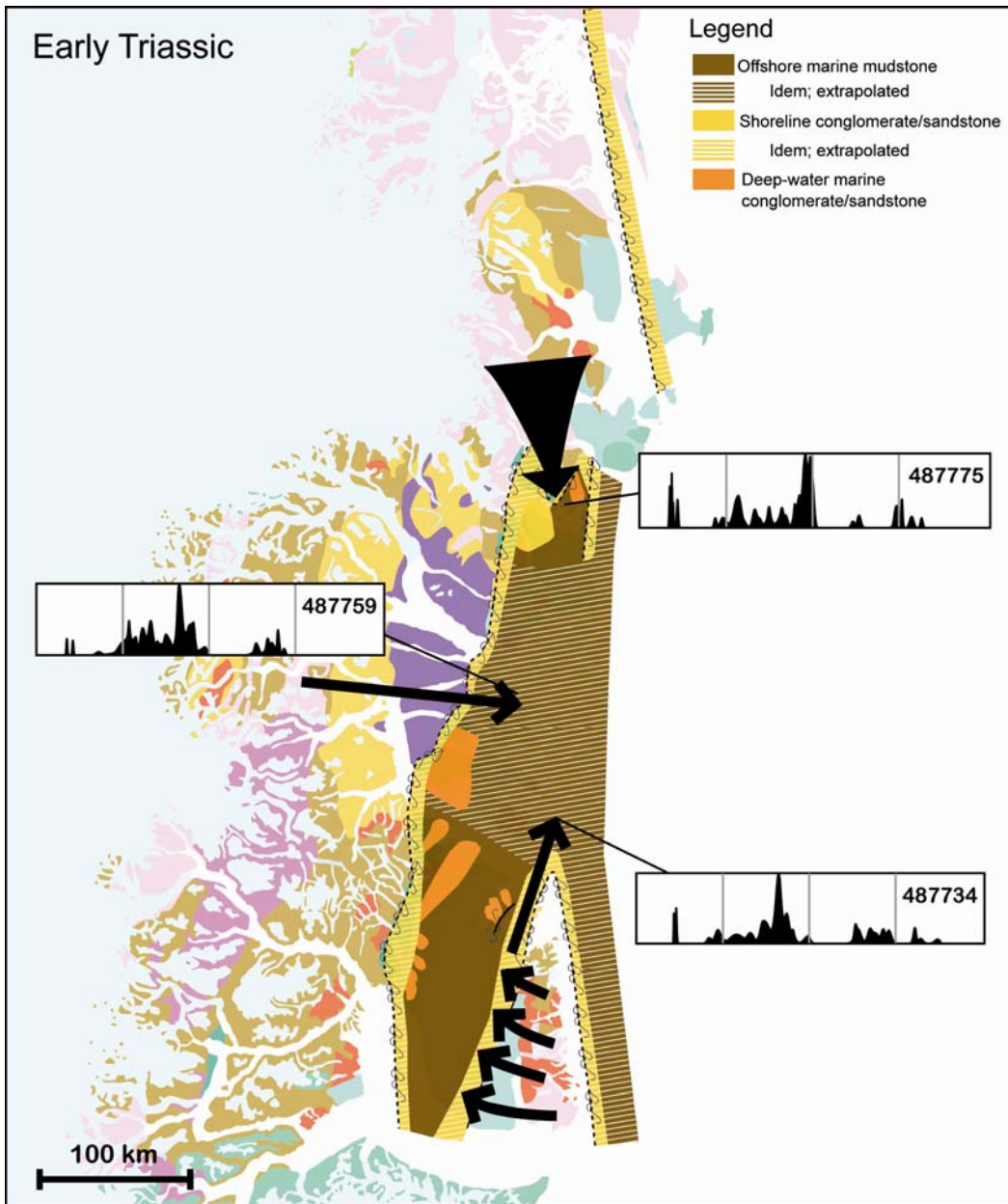


Figure 82. Early Triassic palaeogeographic map.

Triassic-Jurassic boundary

The latest Triassic- Middle Jurassic samples are locally derived (Fig. 83). The two southern samples are derived from the southern part of Liverpool Land, based on the occurrence of a 1650 Ma basement peak (occurs only in southern Liverpool Land) and a Caledonian peak. The northern sample lacks the 1650 peak and has various other Proterozoic and Archaean ages instead, which indicate derivation from metasediments. In conjunction with the Caledonian grains this indicates a derivation from the northern part of Liverpool Land.

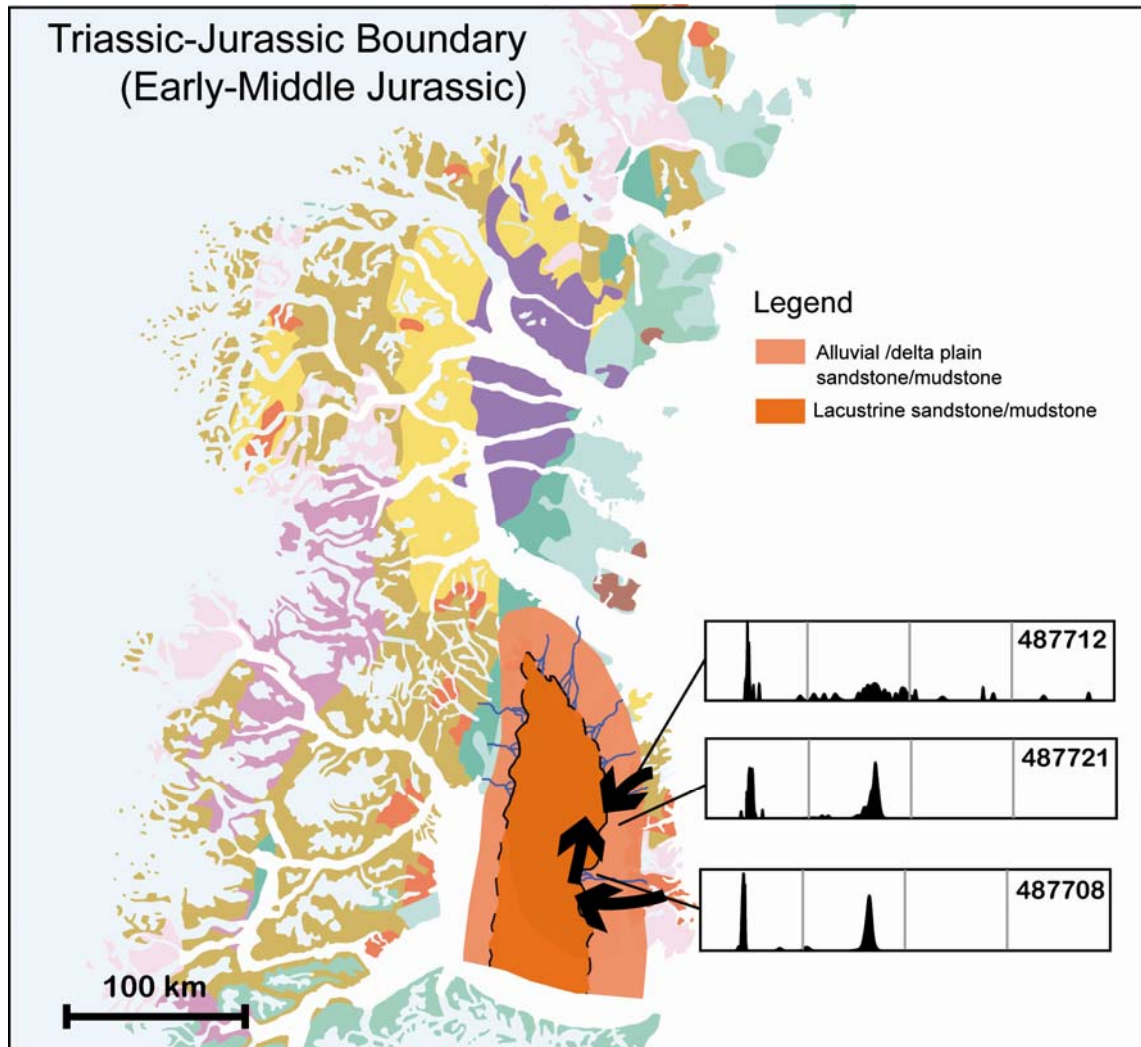


Figure 83. Palaeogeographic map Latest Triassic-Early Middle Jurassic depositional environments.

Middle Jurassic (Late Bajocian)

The Middle Jurassic sediments have zircon age characteristics of Krummedal Sequence and the Eleonore Bay Supergroup, but also with influence from both Archaean and Proterozoic basement (Fig. 84). They also contain Caledonian zircons, except one sample. The age distribution found in these samples is so non-distinctive that it is difficult to suggest specific transport directions except generally eastwards.

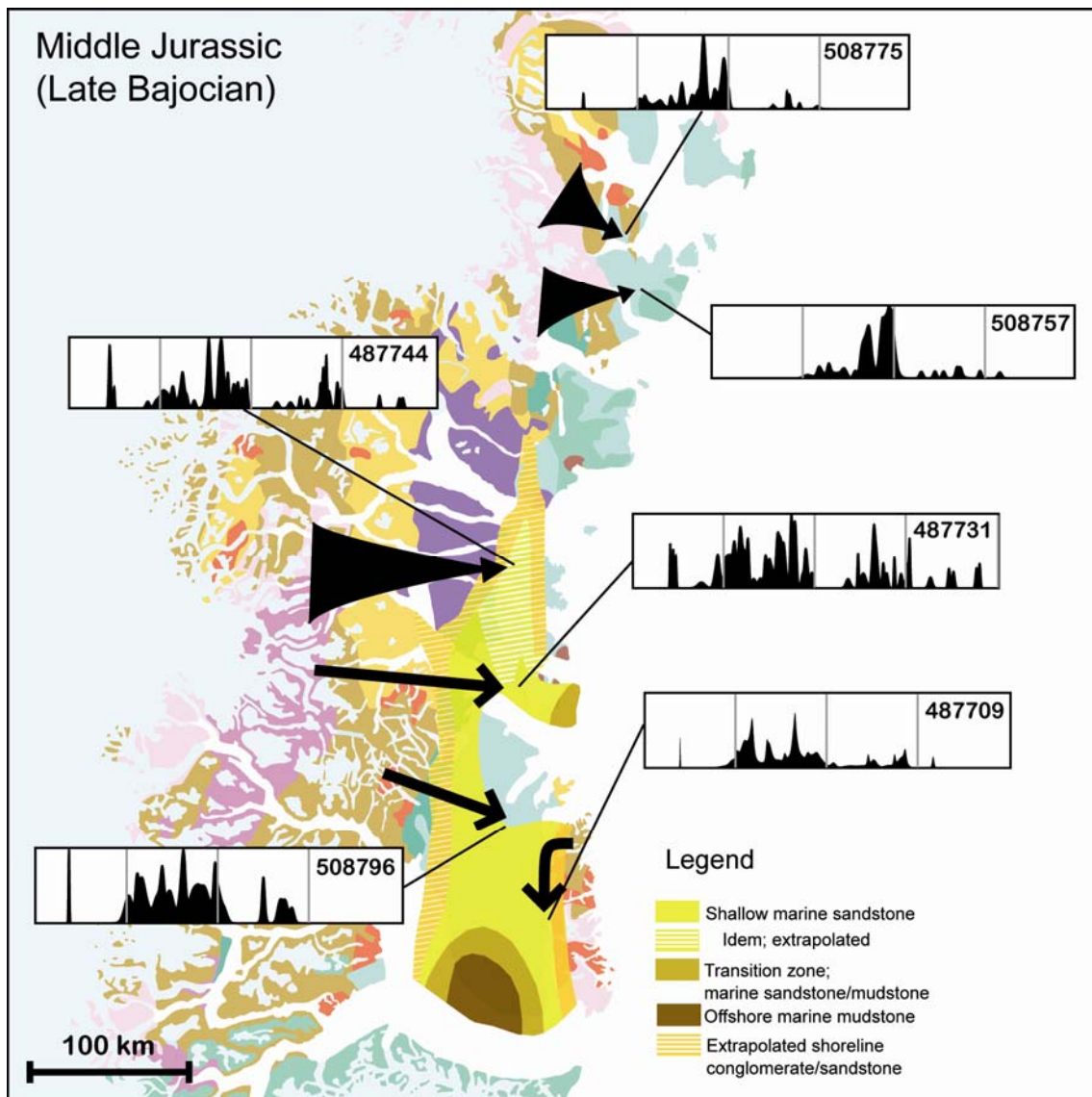


Figure 84. Palaeogeographic map of Middle Jurassic depositional environments.

Middle Jurassic (Late Bathonian)

The three northern samples have non-distinctive age profiles with influences from Krummedal, Eleonore Bay, Caledonian granites and Palaeoproterozoic basement (Fig. 85). They probably have a large catchment and consist of thoroughly mixed sediments. The same is true for sample 508791, but it also has an Archaean basement component, together with Krummedal and Caledonian ages.

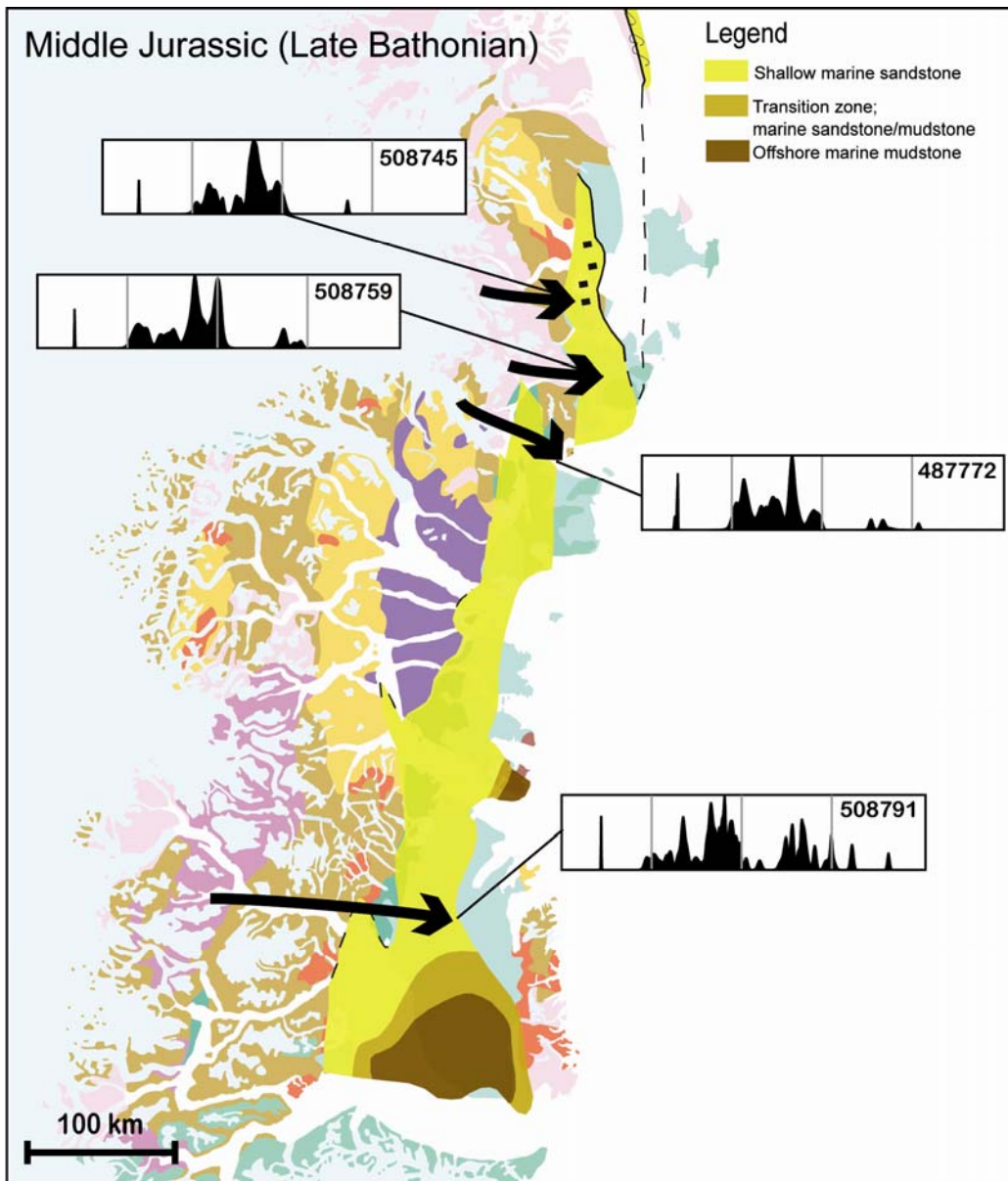


Figure 85. Palaeogeographic map of Middle Jurassic depositional environments.

Late Jurassic

These samples fall in two groups; a northern group dominated by basement ages (see Fig. 4) of ca. 1950 and 1750 Ma (Fig. 86). In sample 508771 there is larger component derived from metasediments, but the other three are almost exclusively sourced in basement areas. The southern group also has a large basement component, but with Archaean ages. The diverse Proterozoic populations are consistent with derivation from Krummedal metasediments (see Fig. 5) or reworked Krummedal.

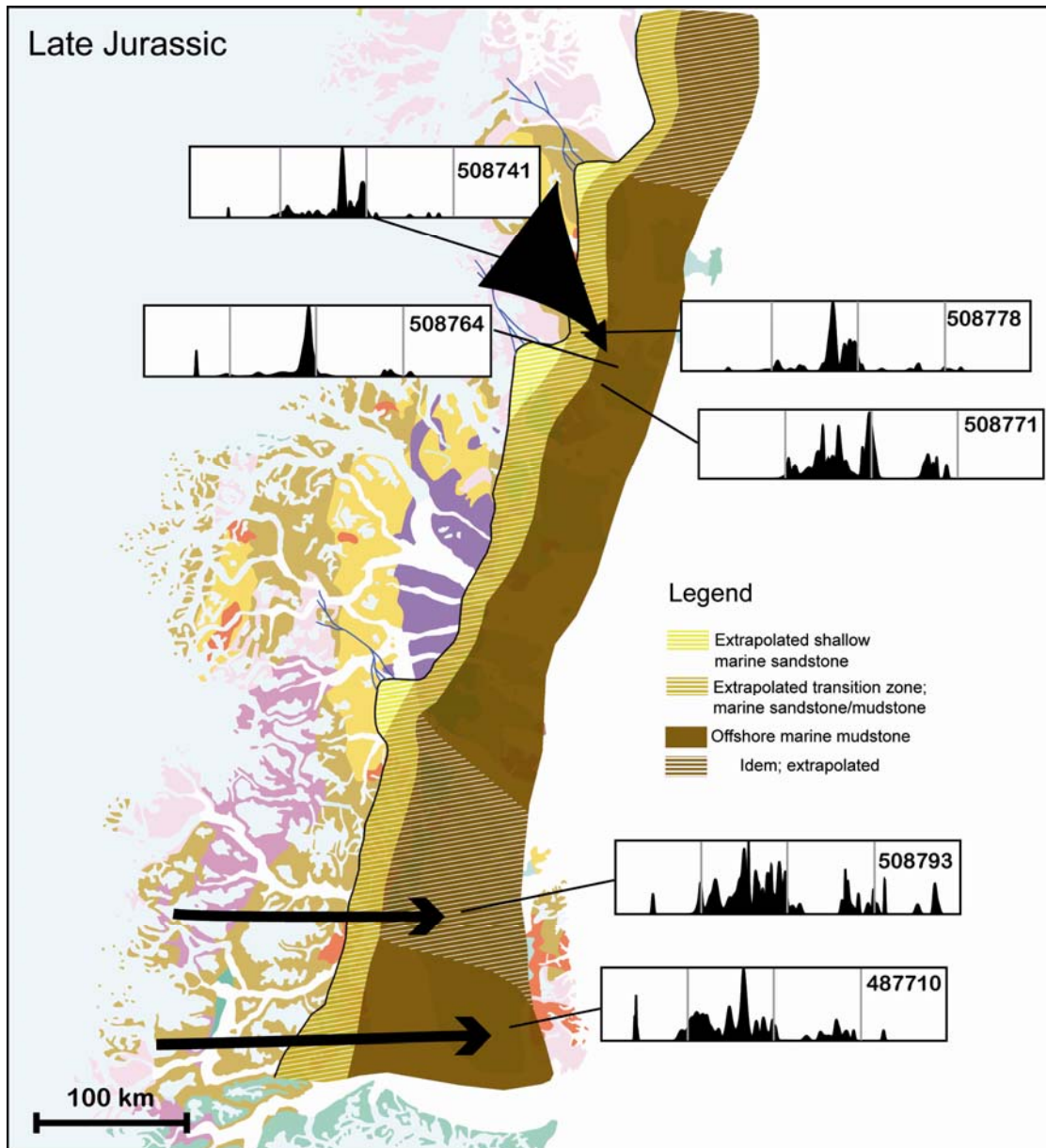


Figure 86. Palaeogeographic map of Late Jurassic depositional environments.

Jurassic-Cretaceous boundary

The northern samples have age spectra indicative of derivation from metasediments (see Fig. 5), probably Krummedal (Fig. 87). In sample 508722 there is a larger population of 1950 Ma basement and in sample 508761 there is an additional Caledonian population. This indicates derivation from the north. It could have been derived from the west also, but this area lacks Caledonian intrusions. The sample from Jameson Land has Archaean basement components, Krummedal components and a Caledonian population, consistent with derivation from the west.

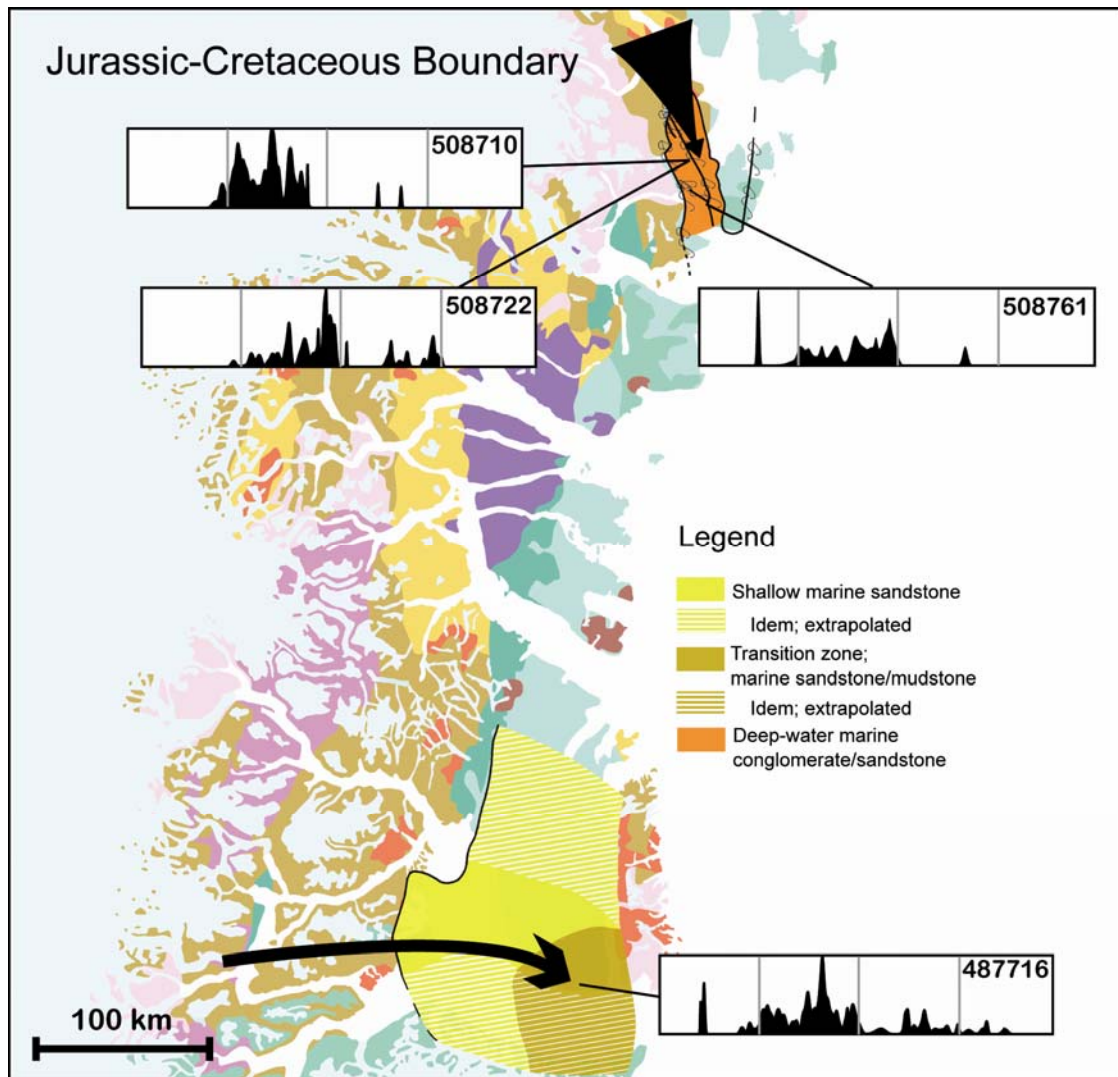


Figure 87. Palaeogeographic map of depositional environments at the Jurassic-Cretaceous boundary.

Mid Cretaceous

The Mid-Cretaceous samples have overall rather non-distinctive age patterns (Fig. 88). There are metasediment derived zircon grains of different ages in different proportions, with or without additional populations, such as basement derived or Caledonian. The exception is sample 487750, which has an unusual age composition consisting of distinct peaks at 2700 and 1900 and a varied and exceptionally young Phanerozoic population. The Precambrian ages could be derived from the basement, the Caledonian and Devonian zircons could also be accounted for locally, but the youngest zircons are Jurassic and there is no known source for Jurassic zircons in East Greenland. This detritus has to come from somewhere else.

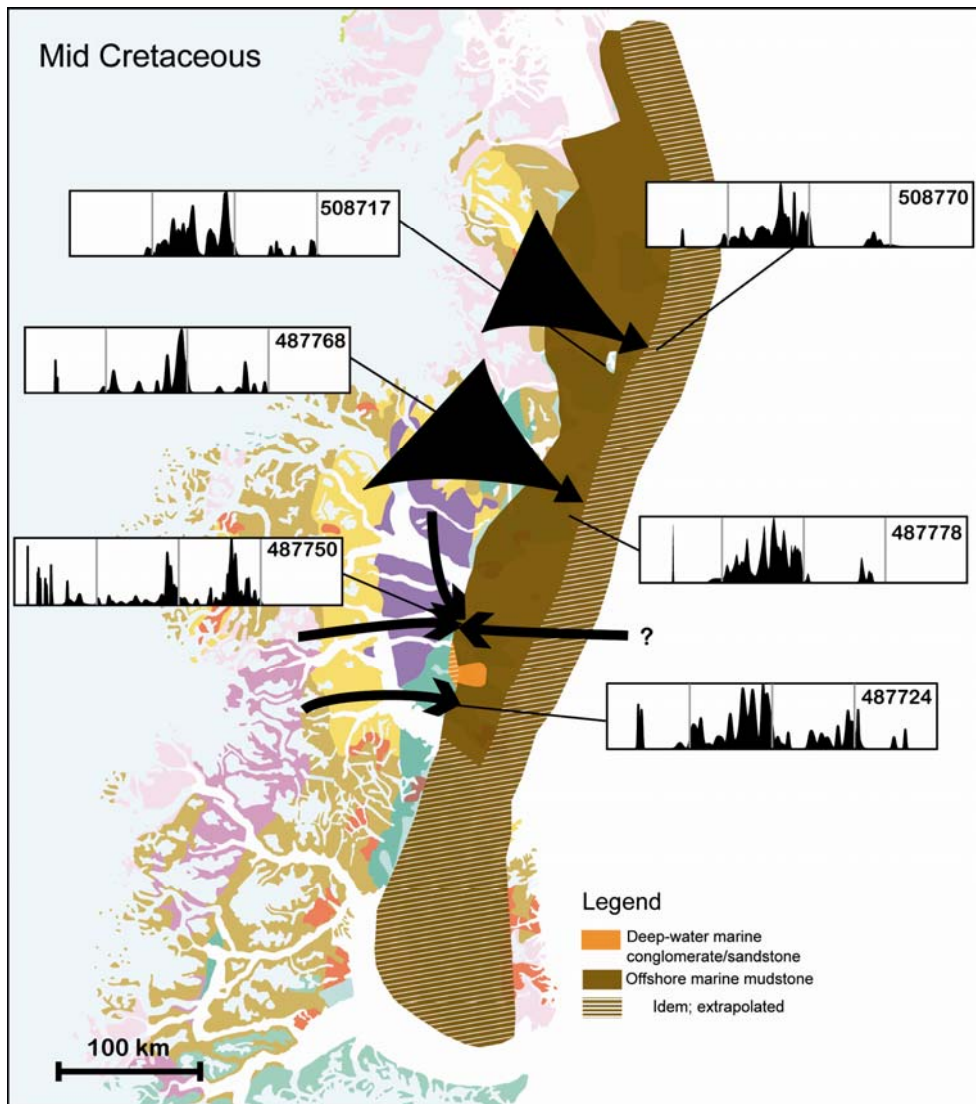


Figure 88. Palaeogeographic map of depositional environments in Mid-Cretaceous time.

Palaeocene

The Palaeocene samples have overall rather non-distinctive age patterns (Fig. 89). There are metasediment derived zircon grains of different ages in different proportions, with or without an additional basement population. None of the samples contain Caledonian zircon grains (but it should be noted that other samples from Palaeocene profiles in this area do contain some Caledonian grains). The sediments were probably derived from the west or northwest.

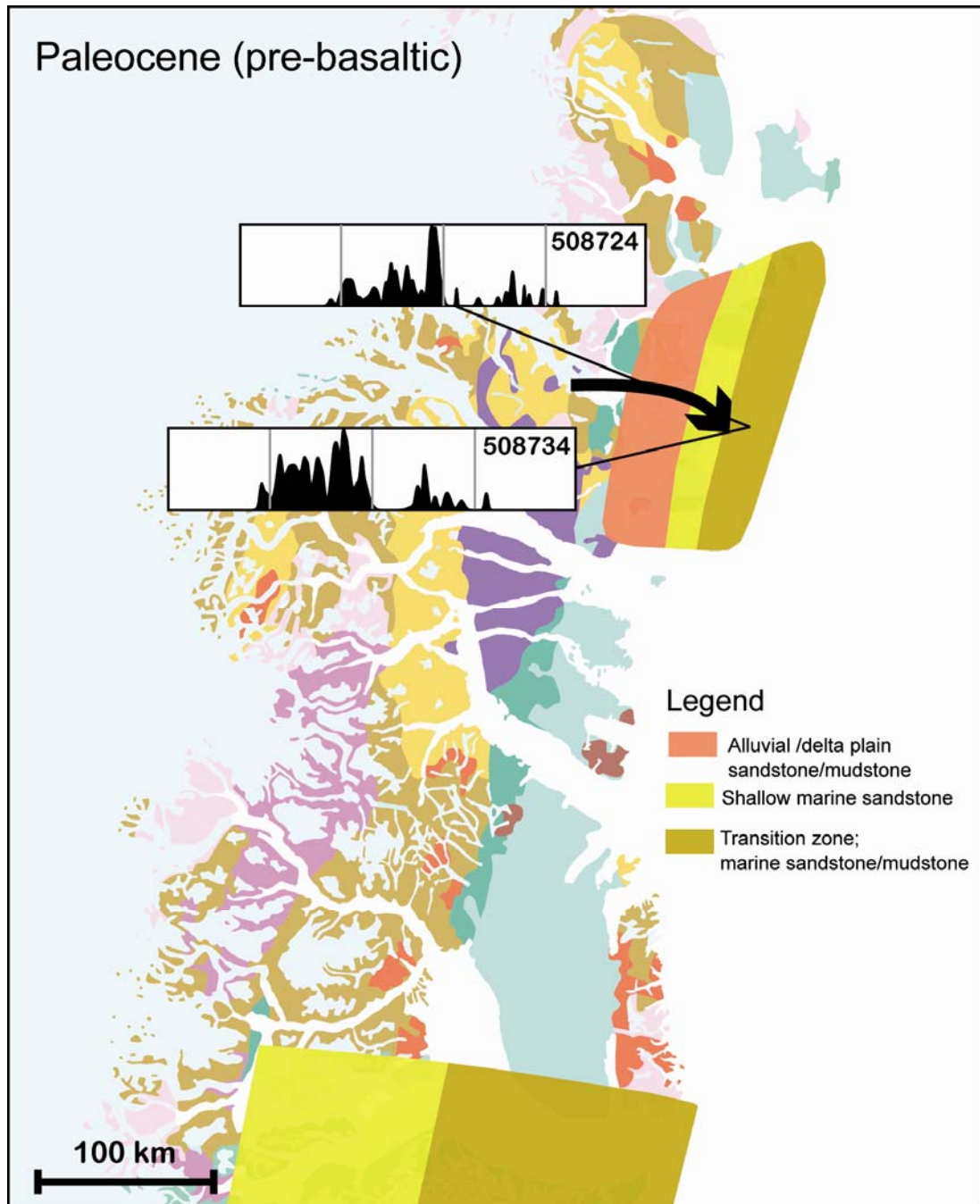


Figure 89. Palaeogeographic map of depositional environments in Palaeocene time.

Northern part of the study area

Early Triassic

The Triassic samples from Kim Fjelde in Peary Land have an age composition that reflects reworking from an older metasediment (Fig. 90). The age distribution is strongly reminiscent of that determined from sediments of these parts by Røhr et al. (2008). Additionally there are some Palaeozoic zircon grains. Their origin is uncertain.

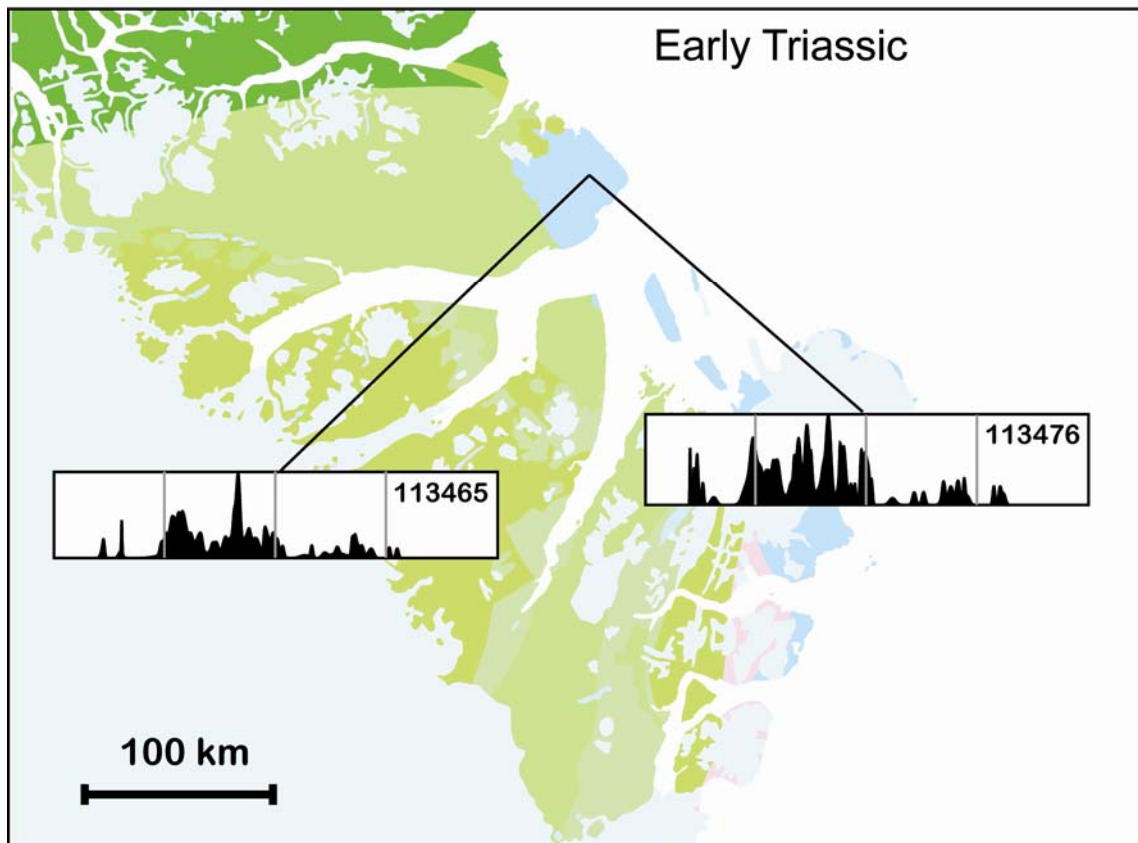


Figure 90. Palaeogeographic map of depositional environments in Early Triassic time in northernmost East Greenland.

Jurassic-Cretaceous boundary

The samples from the Jurassic-Cretaceous boundary in Peary Land have an age composition that reflects reworking from an older metasediment, with some addition from basement (Fig. 91). The age distribution is strongly reminiscent of that determined from sediments from these parts by Røhr et al. (2008). Additionally there are some Palaeozoic zircon grains. Their origin is uncertain.

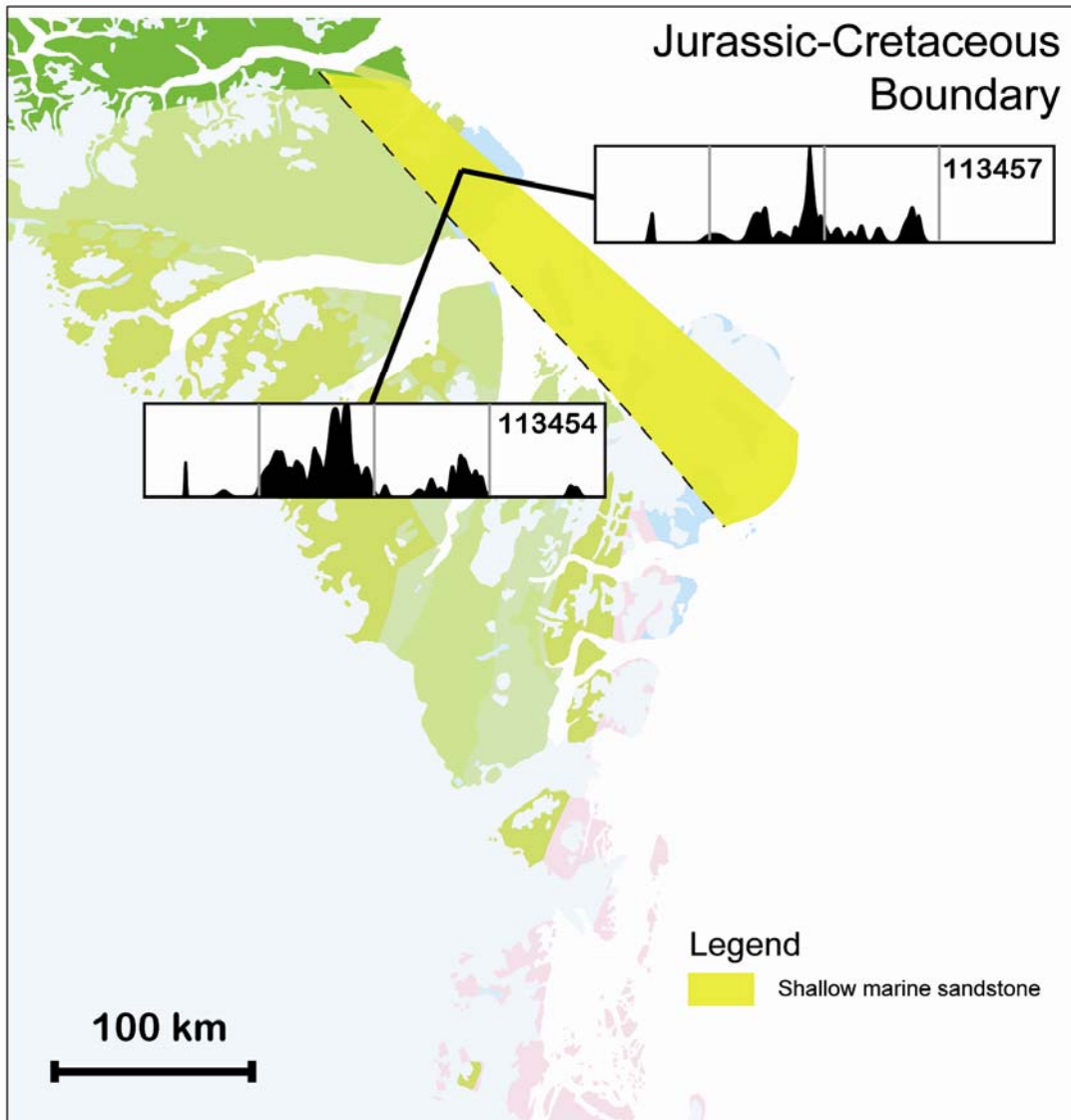


Figure 91. Palaeogeographic map of depositional environments from the Jurassic-Cretaceous boundary in northernmost East Greenland.

Acknowledgement

This report would not have been written without the help and support of a large number of people, which we would like to name and cordially thank here. The samples analysed for this study of Precambrian – Paleocene sandstone samples were collected by Dirk Frei, Matilde Rink Jørgensen, Christian Knudsen, Mette Olivarius, Christian Prinds, and Claus Heinberg. Stream sediments south of 75°N were collected by Nordic Mining Company, those north of 75°N were collected during several GEUS expeditions and were processed under supervision of Agnete Steenfelt.

Sample preparation (crushing, sieving, splitting, acid treatment, heavy liquid treatment, epoxy mounting, polishing) was performed by Fiorella Fabra Aguilera, Mojagan Alaei, Michael Nielsen, Karen Henriksen, Carsten Guvad, Jørgen Kystol, and circa 15 students from Copenhagen University. Fiorella Fabra Aguilera and Jørgen Kystol measured several of the zircon samples in the ICP-MS laboratory.

Frands Schjøth included all the data in the Provenance layers of the GIS product and Susanne Rømer helped with figure preparations.

Lotte M. Larsen kindly corrected the text. Nynke Keulen posed an invaluable help and sparring partner during manuscript preparation.

References

- Aftalion, M., Bowes, D.R. & Vrana, S. 1989: Early Carboniferous U-Pb zircon ages for garnetiferous perpotassic granulites, Blansky les massif, Czechoslovakia. *Neues Jahrbuch für Mineralogie, Monatshefte* **4**, 145-152.
- Andresen, A., Rehnström, E.F. & Holte, M.K., 2007: Evidence for simultaneous contraction and extension at different crustal levels during the Caledonian orogeny in NE Greenland. *Journal of the Geological Society* **164**, 869-880.
- Augland, L.E., Andresen, A., & Corfu, F. 2010: Age, structural setting, and exhumation of the Liverpool Land eclogite terrane, East Greenland Caledonides. *Lithosphere* **2**, 267-286.
- Brueckner, H.K., Gilotti, J.A. & Nutman, A. 1998: Caledonian eclogite facies metamorphism of early Proterozoic protoliths from the North-East Greenland eclogite province. *Contributions to Mineralogy and Petrology* **130**, 103-120.
- Condie, K.C. 1998: Episodic continental growth and supercontinents: a mantle avalanche connection? *Earth and Planetary Science Letters* **163**, 97-108.
- Christoffersen, M. & Jepsen, H. (compilers) 2007: Geological maps of North and North-East Greenland, 1:250 000. Copenhagen: Geological Survey of Denmark and Greenland.
- Dodson, M.H., Compton, W., Williams, I.S. & Wilson, J.F. 1988: A search for ancient detrital zircons in Zimbabwean sediments. *Journal of the Geological Society of London* **145**, 977-983.
- Dhuime, B., Boscha, D., Bruguier, O., Caby, R. & Pourtales, S. 2007: Age, provenance and post-deposition metamorphic overprint of detrital zircons from the Nathorst Land group (NE Greenland) — A LA-ICP-MS and SIMS study. *Precambrian Research* **155**, 24-106
- Escher, J.C. & Pulvertaft, T.C.R. 1995: Geological map of Greenland, scale 1:2 500 000. Copenhagen, Geological Survey of Greenland.
- Fedo, C.M., Sircombe, K.N. & Rainbird, R. H. 2003: Detrital zircon analysis of the sedimentary record. In: Hanchar, J.M., Hoskin, P.W.O. (eds.), *Zircon. Reviews in Mineralogy and Geochemistry* **53**, 277-303.
- Frei, D. & Gerdes, A. 2009: Precise and accurate in-situ zircon U-Pb dating with high sample throughput by automated La-SF-ICP-MS. *Chemical Geology* **261**, 261-270.
- Frei D., Hollis J.A., Gerdes A., Harlov D., Karlsson C., Vasquez P., Franz G., Johansson L., & Knudsen C. 2006: Advanced in-situ trace element and geochronological microanalysis of geomaterials by laser ablation techniques. *Geological Survey of Denmark and Greenland Bulletin* **10**, 25-28.
- Gilotti, J.A. 1995: Discovery of a medium-temperature eclogite province in the Caledonides of North-East Greenland. *Geology* **21**, 523-526.
- Gilotti, J.A., Jones, K.A. & Elvevold, S. 2008: Caledonian metamorphic patterns in Greenland. In Higgins, A. K.; Gilotti, J. A. & Smith, M.P., (eds.) *The Greenland Caledonides: Evolution of the Northeast Margin of Laurentia*. Geological Society of America Memoir **202**, 201-225.
- Haller, J. 1976: *Geology of the East Greenland Caledonides*. Interscience, London, 413 p.
- Hartz, E., Andresen, A., Martin, M.W. & Hodges, K.V. 2000: U-Pb and ⁴⁰Ar/³⁹Ar constraints on the Fjord Region Detachment Zone; a long-lived extensional fault in the central East Greenland Caledonides. *Journal of the Geological Society, London* **157**, 795-809.
- Hartz, E., Andresen, A., Hodges, K.V. & Martin, M. 2001. Syn-contractional extension and exhumation of deep crustal rocks in the East Greenland Caledonides. *Tectonics* **20**, 58-77.
- Hartz, E.H., Condon, D., Austrheim, H. & Erambert, M. 2005: Rediscovery of the Liverpool Land eclogites (Central East Greenland): a post- and supra-subduction UHP province. *Mitteilungen des Österreichischen Mineralogische Gesellschaft* **150**, 50.
- Henriksen, N. 1986: Descriptive text to 1:500 00 sheet 12 Scoresby Sund, 27 pp. Copenhagen: Grønlands Geologiske Undersøgelse.
- Henriksen, N. 2003: Caledonian Orogen, East Greenland 70°-82° N. Geological map 1: 1 000 000. Copenhagen, Geological Survey of Denmark and Greenland.
- Henriksen, N. & Higgins, A.K. 1970: Preliminary results of mapping in the crystalline complex of Renland, the southern Stauning Alper and south-west Liverpool Land, Scoresby Sund, east Greenland. *Grønlands Geologiske Undersøgelse Report* **30**, 5-16.

- Higgins, A.K. & Leslie, A.G. 2000: Restoring thrusting in the East Greenland Caledonides. *Geology* **27**, 1019-1022.
- Higgins, A.K. & Leslie, A.G. 2008: Architecture and evolution of the East Greenland Caledonides—an introduction. In: Higgins, A. K.; Gilotti, J. A. & Smith, M.P., eds. *The Greenland Caledonides: Evolution of the Northeast Margin of Laurentia*. Geological Society of America Memoir **202**, 29-53.
- Higgins, A.K., Henriksen, N.H., Jepsen, H.F., Kalsbeek, F., Thrane, K., Elvevold, S., Esher, J.C., Frederiksen, K.S., Gilotti, J.A., Jones, K., Leslie, A.G., Smith, M.P., Kinny, P.D. & Watt, G.R. 2004: The foreland-propagating architecture of the East Greenland Caledonides 720-750 N. *Journal of the Geological Society* **161**, 1009-1026.
- Horie, K., Nutman, A.P., Friend, C.R.L. & Hidaka, H. 2010: The complex age of orthogneiss protoliths exemplified by the Eoarchaeon Itsaq Gneiss Complex (Greenland) SHRIMP and old rocks. *Precambrian Research* **183**, 25-43.
- Horstwood, M., Foster, G.L., Parrish, R.R. & Nobel, S.R. 2003: Common-Pb corrected in situ U-Pb accessory mineral geochronology by LA-MC-ICP-MS. *Journal of Analytical Atomic Spectrometry* **18**, 837-846.
- Jackson, S., Pearson, N.J., Griffin, W.L. & Belousova, E.A. 2004: The application of laser ablation – inductively coupled plasma – mass spectrometry to in situ U-Pb zircon geochronology. *Chemical Geology* **211**, 47-69.
- Johnston, S.M., Hartz, E.H., Brueckner, H.K. & Gehrels, G.E. 2010: U–Pb zircon geochronology and tectonostratigraphy of southern Liverpool Land, East Greenland: Implications for deformation in the overriding plates of continental collisions. *Earth and Planetary Science Letters* **297**, 512–524.
- Kalsbeek, F., Nutman, A.P. & Taylor, P.N. 1993: Palaeoproterozoic basement province in the Caledonian fold belt of North-East Greenland. *Precambrian Research* **63**, 163-178.
- Kalsbeek, F., Thrane, K., Nutman, A.P. & Jepsen, H.F. 2000: Late Mesoproterozoic to early Neoproterozoic history of the East Greenland Caledonides: evidence for Grevillian orogenesis? *Journal of the Geological Society* **157**, 1215-1225.
- Kalsbeek, F., Jepsen, H.F. & Nutman, A.P., 2001: From source migmatites to plutons; tracking the origin of ca. 435 Ma S-type granites in the East Greenland Caledonian Orogen. *Lithos* **57**, 1-21.
- Kalsbeek, F., Higgins, A.K., Jepsen, H.F., Frei, R. & Nutman, A.P. 2008: Granites and granites in East Greenland Caledonides. In Higgins, A.K., Gilotti, J.A. & Smith, M.P. (eds.) *The Greenland Caledonides: Evolution of the Northeast Margin of Laurentia*. Geological Society of America Memoir **202**, 227-249.
- Keulen, N. 2010. Modal heavy mineral distribution and garnet composition patterns in sandstones and stream sediments from East Greenland north of 70°N- A contribution to the project: Provenance study of possible reservoir sandstone units in East and North-East Greenland. Danmark og Grønlands Geologiske Undersøgelse Rapport. **2010/131**. Pp. 111 + appendices.
- Knudsen, C. & Steenfelt, A. 2010. Major and trace element composition of sandstones and stream sediments from East Greenland north of 70°N- A contribution to the project: Provenance study of possible reservoir sandstone units in East and North-East Greenland. Danmark og Grønlands Geologiske Undersøgelse Rapport. **2010/132**. Pp. 90 + appendices.
- Kosler, J. & Sylvester, P.J. 2003: Present trends and the future of zircon in geochronology: Laser ablation ICP-MS. In: Hanchar, J.M. & Hoskin, P.W.O. (eds.) *Zircon. Reviews in Mineralogy and Geochemistry* **53**, Mineralogical Society of America, Washington, DC, 243-275.
- Larsen, P.-H. & Bengaard, H.-J. 1991: The Devonian basin initiation in East Greenland: a result of sinistral wrench faulting and Caledonian extensional collapse. *Journal of the Geological Society* **148**, 355-368.
- Larsen, P.-H., Olsen, H. & Clack, J.A. 2008: The Devonian basin in East Greenland—review of basin evolution and vertebrate assemblages. In: Higgins, A.K., Gilotti, J.A. & Smith, M.P. (eds.) *The Greenland Caledonides: Evolution of the Northeast Margin of Laurentia*. Geological Society of America Memoir **202**, 273-292.
- Leslie, A.G. & Nutman, A.P. 2003. Evidence for Neoproterozoic orogenesis and early high temperature Scandian deformation events in the southern East Greenland Caledonides. *Geological Magazine* **140**, 309-333.

- Ludwig, K.R., 1999: Isoplot/Ex version 2.00 – A geochronological toolkit for Microsoft Excel. Berkeley Geochronology Center, Special Publication No. 2
- Rehnström, E.F., 2010: Prolonged Palaeozoic calc-alkaline magmatism in the Central E Greenland Caledonides: implications for tectonic setting constrained by U-Pb ages and Hf isotopes. *Journal of Geology* **118**, 447-465.
- Rehnström, E.F., Andresen, A. & Graham, S. 2007: Zircon ages, Hf-isotopes and provenance of Upper Cretaceous sediments from drill cores of the North Sea: an LA-ICP-MS pilot study. *Abstracts and Proceedings of the Geological Society of Norway 1:2007*, p. 80.
- Røhr, T.S., Andersen, T. & Dypvik, H. 2008: Provenance of lower cretaceous sediments in the Wandel Sea Basin, North Greenland. *Journal of the Geological Society* **165**, 755-767.
- Sircombe, K.N. 2004: AgeDisplay: an Excel workbook to evaluate and display univariant geochronological data using binned frequency histograms and probability density distributions. *Computer and Geosciences* **30**, 21-31.
- Stacey, J.S. & Kramers, J.D. 1975: Approximation of terrestrial lead isotope evolution by a two-stage model. *Earth and Planetary Science Letters* **26**, 297-221.
- Strachan, R.A., Nutman, A.P. & Friderichsen, J.D. 1995: SHRIMP U-Pb geochronology and metamorphic history of the Smallefjord sequence, NE Greenland Caledonides. *Journal of the Geological Society* **152**, 779-784
- Strachan, R.A., Martin, M.W. & Friderichsen J.D. 2001: Evidence for contemporaneous yet contrasting styles of granite magmatism during extensional collapse of the northeast Greenland Caledonides. *Tectonics* **20**, 458-473.
- Steenfelt, A. & Kunzendorf, H. 1979: Geochemical methods in uranium exploration in northern East Greenland. In: Watterson, J.R. & Theobald, P.K. (eds): *Geochemical exploration 1978*. Association of Exploration Geochemists, Special Volume **7**, 429-442.
- Sylvester, P.J. & Ghaderi, M. 1997: Trace element analysis of scheelite by excimer laser ablation inductively coupled plasma mass spectrometry (ELA-ICP-MS) using a synthetic glass standard. *Chemical Geology* **141**, 49-65.
- Sønderholm, M., Frederiksen, K.S., Smith, P.M. & Tirsgaard, H. 2008: Neoproterozoic sedimentary basins with glaciogenic deposits of the East Greenland Caledonides. In: Higgins, A.K., Gilotti, J.A. & Smith, M. P. (eds.) *The Greenland Caledonides: Evolution of the Northeast Margin of Laurentia*. Geological Society of America Memoir **202**, 99-136.
- Thrane, K. 2002: Relationships between Archaean and Palaeoproterozoic crystalline basement complexes in the southern part of the East Greenland Caledonides; an ion microprobe study. *Precambrian Research* **113**, 19-42.
- Tucker, R.D., Dallmeyer, R.D. & Strachan, R.A. 1993: Age and tectonothermal record of Laurentian basement, Caledonides of NE Greenland. *Journal of the Geological Society* **150**, 371-379.
- Vermeesch, P. 2004: How many grains are needed for a provenance study? *Earth and Planetary Science Letters* **224**, 351-441.
- Watt, G.R., Kinny, P.D. & Friderichsen, J.D. 2000: U-Pb geochronology of Neoproterozoic and Caledonian tectonothermal events in the East Greenland Caledonides. *Journal of the Geological Society of London* **157**, 1031-1048
- Watt, G.R. & Thrane, K. 2001: Early Neoproterozoic events in East Greenland. *Precambrian Research* **110**, 165-184.
- Williams, I.S. & Claesson, S. 1987: Isotopic evidence for the Precambrian provenance and Caledonian metamorphism of high grade paragneisses from the Seve Nappes, Scandinavian Caledonides: II. Ion microprobe zircon U-Th-Pb. *Contribution to Mineralogy and Petrology* **97**, 205-217.
- White, A.P., Hodges, K.V., Martin, M.W. & Andresen, A. 2002: Geological constraints on middle-crustal behaviour during broadly synorogenic extension in the central East Greenland Caledonides. *International Journal of Earth Science* **91**, 187-208.
- Whitehouse, M.J., Kamber Balz, S. & Moorbath, S. 1999: Age significance of U-Th-Pb zircon data from early Archaean rocks of West Greenland; a reassessment based on combined ion-microprobe and imaging studies. *Chemical Geology* **160**, 201-224.

Appendix A

Sample information table

Locality name	Area	sample_nr	Longitude	Latitude	Altitude	type	System/series	Stage	Group	Formation	Member	Palaeogeography
STREAM SEDIMENT SAMPLES												
Gåseland E	A	7203612	-26,558139	70,30902		stream sediment						17
Gåseland W	A	7111116A	-28,397351	70,03244		stream sediment						17
Jameson Land E	A	7502851	-22,978474	71,75169		stream sediment						17
Jameson Land S	A	7502852	-22,744796	70,86855		stream sediment						17
Liverpool Land N	A	7502881	-22,383427	71,1703		stream sediment						17
Liverpool Land N	A	7502885	-22,384801	71,24798		stream sediment						17
Milne Land S	A	71111109	-25,932382	70,66707		stream sediment						17
Milne Land S	A	71111148	-25,85315	70,6187		stream sediment						17
Rødefjord	A	7203613	-28,327598	70,67063		stream sediment						17
Nathorst Land N	B	7910694	-25,813336	72,39567		stream sediment						17
Nathorst Land N	B	7910695	-25,714064	72,38741		stream sediment						17
Nathorst Land N	B	7910696	-25,683719	72,38774		stream sediment						17
Stauning Alps N	B	7907651	-24,387753	72,11326		stream sediment						17
Stauning Alps N	B	7907659	-24,367043	72,16216		stream sediment						17
Stauning Alps N	B	7907661	-24,36749	72,16732		stream sediment						17
Stauning Alps N	B	7907666	-24,344137	72,20454		stream sediment						17
Stauning Alps S	C	8004072_08	-24,793955	71,35951		stream sediment						17
Stauning Alps S	C	8004078_06	-24,841155	71,4153		stream sediment						17
Canning Land	D	8101189_11	-22,245033	71,6167		stream sediment						17
Canning Land	D	8101191/3	-22,262086	71,60442		stream sediment						17
Canning Land	D	8101194_1	-22,420831	71,61733		stream sediment						17
Canning Land	D	8101194_2	-22,259936	71,60593		stream sediment						17
Scoresby Land	D	7111129/A	-24,291506	71,95863		stream sediment						17
Scoresby Land	D	7111131/A	-24,281978	71,95762		stream sediment						17
Wegener Halvø	D	8101197_1	-22,415099	71,77745		stream sediment						17
Wegener Halvø	D	8101197_2	-22,419407	71,77746		stream sediment						17
Lyell Land	E	7910690	-25,73343	72,45493		stream sediment						17
Lyell Land	E	7910691	-25,864713	72,4332		stream sediment						17
Lyell Land	E	7910693	-25,844275	72,43412		stream sediment						17
Lyell Land	E	8106242	-25,22587	72,69537		stream sediment						17
Lyell Land	E	8106246	-25,141726	72,71681		stream sediment						17
Suess Land	E	8105181	-25,000038	73,02026		stream sediment						17
Traill Ø W	E	7510257_5N	-23,485561	72,66546		stream sediment						17
Traill Ø W	E	7510257_5S	-23,485561	72,66546		stream sediment						17
Ymer Ø E	F	8105161	-23,142313	73,09844		stream sediment						17
Ymer Ø E	F	8105162	-23,075164	73,09908		stream sediment						17
Ymer Ø E	F	8105164	-23,10422	73,16948		stream sediment						17
Ymer Ø W	F	8105150	-25,122938	73,15014		stream sediment						17
Ymer Ø W	F	8105153	-25,105922	73,14098		stream sediment						17
Ymer Ø W	F	8105185	-25,146566	73,16006		stream sediment						17
Ymer Ø W	F	8307750	-25,028877	73,29462		stream sediment						17
Ymer Ø W	F	8307751	-25,036053	73,2946		stream sediment						17
Hudson Land E	G	8106248	-22,516684	73,70752		stream sediment						17
Hudson Land E	G	8106451	-22,468381	73,70239		stream sediment						17
Hudson Land E	G	8106463	-22,507032	73,70285		stream sediment						17
Hudson Land E	G	8106466	-22,421692	73,70506		stream sediment						17
Hudson Land E	G	8101198_6	-22,708093	74,06334		stream sediment						17
Hudson Land E	G	8101198_6	-22,708093	74,06334		stream sediment						17
Hudson Land W	G	8101198_2	-23,552758	74,02794		stream sediment						17
Hudson Land W	G	8101198_2_4	-22,974909	74,06842		stream sediment						17

Locality name	Area	sample_nr	Longitude	Latitude	Altitude	type	System/series	Stage	Group	Formation	Member	Palaeogeography
STREAM SEDIMENT SAMPLES												
Andrée Land E	H	8106478	-25,832315	73,4063		stream sediment						17
Andrée Land E	H	8106498	-25,439403	73,77069		stream sediment						17
Andrée Land E	H	8106499	-25,48721	73,79246		stream sediment						17
Strindberg Land	H	8106611	-24,991157	73,66598		stream sediment						17
Strindberg Land	H	8106620	-24,954066	73,62009		stream sediment						17
Strindberg Land	H	8106621	-24,898673	73,59687		stream sediment						17
Clavering Ø	I	8101199_10	-20,795795	74,33485		stream sediment						17
Clavering Ø	I	8101199_3	-21,292343	74,13058		stream sediment						17
Clavering Ø	I	8101199_4	-21,28177	74,12876		stream sediment						17
Steno Land	I	8101198_3	-23,335874	74,0842		stream sediment						17
Zackenber	I	473739	-20,603	74,460		stream sediment						16
Dr. Margrethe II Land	J	367513	-20,84693	75,91786		stream sediment						17
Jensen Land	J	367425	-20,289829	76,10096		stream sediment						17
Jensen Land	J	367428	-20,91659	76,29434		stream sediment						17
H.C.Andersen Fjelde	J	367459	-24,11215	76,3348		stream sediment						17
Dove bugt	J	367413	-22,55867	76,42006		stream sediment						17
Dove bugt	J	367444	-21,42135	76,56533		stream sediment						17
Dr. Louise Land	J	367491	-23,13682	76,67278		stream sediment						17
Dr. Louise Land	J	367462	-25,06731	76,70294		stream sediment						17
Germania Land	J	367535	-18,89823	76,8531		stream sediment						17
Germania Land	J	367528	-20,74432	76,95236		stream sediment						17
Germania Land	J	367524	-21,812531	76,98496		stream sediment						17
Germania Land	J	367517	-21,0445	77,15101		stream sediment						17
Germania Land	J	342523	-18,951691	77,16562		stream sediment						17
Germania Land	J	342549	-21,488359	77,28386		stream sediment						17
Penthièvre Fjord	K	342516	-19,15457	77,5478		stream sediment						17
Penthièvre Fjord	K	342503	-19,672779	77,61847		stream sediment						17
Nordmarken	K	348221	-20,354031	77,83583		stream sediment						17
Hertugen af Orléans Land	K	342558	-22,03105	77,91211		stream sediment						17
Danske Øer	K	348202	-19,633829	78,26245		stream sediment						17
Lambert Land	K	382899	-19,717979	79,17462		stream sediment						17
Lambert Land	K	381159	-19,545601	79,27405		stream sediment						17
Lambert Land	L	382931	-21,094179	79,29213		stream sediment						17
Skallingen	L	381356	-21,905661	79,31807		stream sediment						17
Hovgaard Ø	L	381276	-20,222191	79,93854		stream sediment						17
Centrum Sø	L	381236	-22,873289	80,1446		stream sediment						17
Holm Land	L	382722	-17,14167	80,16834		stream sediment						17
Holm Land	L	382715	-17,955509	80,30837		stream sediment						17
Keglen	L	381241	-21,3603	80,43789		stream sediment						17
Pr. Elisabeth Alper	L	382682	-18,773451	80,61736		stream sediment						17
Amdrup Land	L	382696	-15,82225	80,79049		stream sediment						17
Amdrup Land	L	382708	-17,361589	80,80656		stream sediment						17
Romer Sø	L	382946	-19,209009	81,05812		stream sediment						17

Locality name	Profile	sample_nr	Longitude	Latitude	Altitude	type	System/series	Stage	Group	Formation	Member	Palaeogeography
SANDSTONE SAMPLES												
PRE-CARBONIFEROUS												
Harefjord	5	473702	-28,021	70,968	100	sandstone	Permian					2
Gunnar Andersson Land	4	473730	-23,845	73,365	1	sandstone			Kap Kolthoff	Devonian		2
Gunnar Andersson Land	4	473731	-23,735	73,348	1	sandstone	Devonian		Kap Kolthoff			2
Gunnar Andersson Land	4	473732	-23,610	73,326	1	sandstone	Devonian		Kap Kolthoff			2
Gunnar Andersson Land	4	473733	-23,504	73,309	1	sandstone	Devonian		Kap Kolthoff			2
Gunnar Andersson Land	4	473734	-23,319	73,262	1	sandstone	Devonian		Celcius Bjerg	Elsa Dal		2
Gunnar Andersson Land	4	473735	-23,280	73,258	1	sandstone	Devonian		Celcius Bjerg	Elsa Dal		2
Blomsterbugten	4	473729	-25,287	73,330	1	sandstone	Precambrian		Lyell Land	Sandertop		0
Mestersvig	3	473716	-23,693	72,144	50	sandstone	Permian		Foldvik Creek			4
Mestersvig	3	473718	-23,744	72,160	50	sandstone	Carboniferous		Trail Ø			3
Mestersvig	3	473717	-23,747	72,160	50	sandstone	Carboniferous		Trail Ø			3
Mestersvig	3	473715	-23,774	72,236	1	sandstone	Carboniferous		Trail Ø			3
Mestersvig	3	473714	-23,927	72,270	1	sandstone	Carboniferous		Trail Ø			3
Ella Ø	2	473711	-25,036	72,789	1	sandstone	Devonian		Viiddal	Solstrand		2
Ella Ø	2	473710	-25,091	72,875	130	sandstone	Cambrian		Kong Oscar Fjord	Kløftelv		0
Ella Ø	2	473709	-25,127	72,874	120	sandstone	Precambrian		Tillite	Spiral Creek		0
Ella Ø	2	473708	-25,127	72,860	170	sandstone	Precambrian		Tillite	Storelv		0
Ella Ø	2	473707	-25,127	72,860	170	sandstone	Precambrian		Tillite	Storelv		0
Segelsällskapet Fjord	1	473727	-24,845	72,475	1	sandstone	Precambrian		Ymer Ø			0
Segelsällskapet Fjord	1	473726	-24,927	72,460	1	sandstone	Precambrian		Lyell Land	Teufelsschloss		0
Segelsällskapet Fjord	1	473728	-24,708	72,469	1	sandstone	Precambrian		Lyell Land	Skjoldungebræ		0
Segelsällskapet Fjord	1	473725	-24,996	72,458	1	sandstone	Precambrian		Lyell Land	Skjoldungebræ		0
Segelsällskapet Fjord	1	473724	-25,097	72,444	1	sandstone	Precambrian		Lyell Land	Vibeke Sø		0
Segelsällskapet Fjord	1	473723	-25,189	72,435	1	sandstone	Precambrian		Lyell Land	Kap Alfred		0
Segelsällskapet Fjord	1	473722	-25,230	72,434	1	sandstone	Precambrian		Lyell Land	Berzelius Bjerg		0
Segelsällskapet Fjord	1	473721	-25,279	72,435	1	sandstone	Precambrian		Lyell Land	Sandertop		0
Segelsällskapet Fjord	1	473720	-25,320	72,441	1	sandstone	Precambrian		Lyell Land	Sandertop		0
Segelsällskapet Fjord	1	473719	-25,352	72,443	1	sandstone	Precambrian		Lyell Land	Kempe Fjord		0
POST-DEVONIAN												
S and E Jameson Land												
South Jameson Land_Transect 4	6	487718	-23,049	70,499	250	sandstone	Cretaceous	Valanginian	Scoresby Sund Gr.	Hesteelv		12
South Jameson Land_Transect 4	6	487716	-23,062	70,502	250	sandstone	Cretaceous	Valanginian	Scoresby Sund Gr.	Hesteelv		12
South Jameson Land_Transect 4	6	487717	-23,049	70,499	95	sandstone	Jurassic	Volgian	Scoresby Sund Gr.	Raukelv		12
East Jameson Land_Transect 1	9	487707	-22,666	70,604	645	sandstone	Jurassic	Oxfordian/Kimmerigian	Hall Bredning	Hareelv	Katedralen	11
East Jameson Land_Transect 1	9	487706	-22,650	70,611	440	sandstone	Jurassic	Toarcian	Neill Klinter	Ostreaelv	Tretfjord Bjerg	7
East Jameson Land_Transect 1	9	487705	-22,649	70,613	405	sandstone	Jurassic	Toarcian	Neill Klinter	Ostreaelv	Tretfjord Bjerg	7
East Jameson Land_Transect 1	9	487704	-22,648	70,614	340	sandstone	Jurassic	Toarcian	Neill Klinter	Ostreaelv	Harris Fjeld	7
East Jameson Land_Transect 1	9	487703	-22,644	70,615	288	sandstone	Jurassic	Pliensbachian	Neill Klinter	Ostreaelv	Astartekløft	7
East Jameson Land_Transect 1	9	487702	-22,643	70,616	225	sandstone	Jurassic	Pliensbachian	Neill Klinter	Gule Horn	Ells Bjerg	7
East Jameson Land_Transect 1	9	487701	-22,643	70,616	220	sandstone	Jurassic	Pliensbachian	Neill Klinter	Gule Horn	Elis Bjerg	7
East Jameson Land_Transect 2	8	487711	-22,661	70,719	718	sandstone	Jurassic	Oxfordian/Kimmerigian	Hall Bredning	Hareelv	Katedralen	11
East Jameson Land_Transect 2	8	487710	-22,699	70,658	717	sandstone	Jurassic	Oxfordian/Kimmerigian	Hall Bredning	Hareelv	Katedralen	11
East Jameson Land_Transect 2	8	487709	-22,699	70,658	715	sandstone	Jurassic	Bathonian	Vardekløft	Fossilbjerget		9
East Jameson Land_Transect 2	8	487708	-22,699	70,658	110	sandstone	Jurassic	Sinemurian	Kap Stewart	Rætelv		7
East Jameson Land_Transect 3	7	487715	-22,678	70,735	440	sandstone	Jurassic		Neill Klinter			7
East Jameson Land_Transect 3	7	487714	-22,680	70,735	410	sandstone	Jurassic		Neill Klinter			7
East Jameson Land_Transect 3	7	487713	-22,683	70,735	320	sandstone	Jurassic	Pliensbachian	Neill Klinter	Gule Horn	Elis Bjerg	7
East Jameson Land_Transect 3	7	487712	-22,683	70,735	290	sandstone	Jurassic	Pliensbachian	Neill Klinter	Rævekløft		7
East Jameson Land_Transect 6	10	487719	-22,674	70,745	60	sandstone	Triassic	Rhaetian-Sinemurian	Kap Stewart	Innakajik		7
East Jameson Land_Transect 6	10	487720	-22,674	70,745	40	sandstone	Triassic	Rhaetian-Sinemurian	Kap Stewart	Innakajik		7
East Jameson Land_Transect 6	10	487721	-22,679	70,745	25	sandstone	Triassic	Rhaetian-Sinemurian	Kap Stewart	Innakajik		7

Locality name	Profile	sample_nr	Longitude	Latitude	Altitude	type	System/series	Stage	Group	Formation	Member	Palaeogeography
NE Jameson Land												
Olympen mt., transect 16 (NE Jameson Land)	12	508789	-23,587	71,407	913	sandstone	Jurassic		Vardekløft	Olympen	Zeus	11
Olympen mt., transect 16 (NE Jameson Land)	12	508798	-23,580	71,406	845	sandstone	Jurassic		Vardekløft	Olympen	Hades	11
Olympen mt., transect 16 (NE Jameson Land)	12	508790	-23,580	71,406	845	sandstone	Jurassic		Vardekløft	Olympen	Hades	11
Olympen mt., transect 16 (NE Jameson Land)	12	508793	-23,579	71,406	789	sandstone	Jurassic		Vardekløft	Olympen	Athene	11
Olympen mt., transect 16 (NE Jameson Land)	12	508794	-23,579	71,406	789	sandstone	Jurassic		Vardekløft	Olympen	Athene	11
Olympen mt., transect 16 (NE Jameson Land)	12	508791	-23,576	71,404	692	sandstone	Jurassic		Vardekløft	Fossilbjerget		10
Olympen mt., transect 16 (NE Jameson Land)	12	508792	-23,576	71,404	692	sandstone	Jurassic		Vardekløft	Fossilbjerget		10
Pelion mt., transect 17 (NE Jameson Land)	11	508795	-23,328	71,463	1217	sandstone	Jurassic		Vardekløft	Olympen		11
Pelion mt., transect 17 (NE Jameson Land)	11	508796	-23,339	71,391	857	sandstone	Jurassic		Vardekløft	Pelion		9
Pelion mt., transect 17 (NE Jameson Land)	11	508797	-23,372	71,481	469	sandstone	Jurassic		Neill Klinter	Ostreaelv		7
Trail Ø + Geographical Society Ø												
Geographical Society Ø, Tørvestakken-tr 11	19	487751	-23,075	72,967	650	sandstone	L. Cretaceous	Aptian-Albian		Rold Bjerge		14
Geographical Society Ø, Tørvestakken-tr 11	19	487750	-23,066	72,966	565	sandstone	L. Cretaceous	Aptian-Albian		Rold Bjerge		14
Geographical Society Ø, Tørvestakken-tr 11	19	487749	-23,056	72,964	510	sandstone	L. Cretaceous	Aptian-Albian		Rold Bjerge		14
Geographical Society Ø, Tørvestakken-tr 11	19	487748	-23,055	72,964	460	sandstone	L. Cretaceous	Aptian-Albian		Rold Bjerge		14
Geographical Society Ø, Tørvestakken-tr 11	19	487747	-23,053	72,963	415	sandstone	L. Cretaceous	Aptian-Albian		Rold Bjerge		14
Trail Ø, Svinhufvud Bjerge_transect 7	18	487723	-23,298	72,446	1075	sandstone	Cretaceous	Albian		Rold Bjerge		14
Trail Ø, Svinhufvud Bjerge_transect 7	18	487724	-23,294	72,450	1065	sandstone	Cretaceous	Albian		Rold Bjerge		14
Trail Ø, Svinhufvud Bjerge_transect 7	18	487725	-23,296	72,451	960	sandstone	Jurassic	Bathonian	Vardekløft	Pelion		9
Trail Ø, Svinhufvud Bjerge_transect 7	18	487726	-23,296	72,451	900	sandstone	Jurassic	Bathonian	Vardekløft	Pelion		9
Trail Ø, Svinhufvud Bjerge_transect 7	18	487727	-23,297	72,453	865	sandstone	Jurassic	Bathonian	Vardekløft	Pelion		9
Trail Ø, Svinhufvud Bjerge_transect 7	18	487728	-23,299	72,454	800	sandstone	Jurassic	Bathonian	Vardekløft	Pelion		9
Trail Ø, Svinhufvud Bjerge_transect 7	18	487722	-23,298	72,446	730	sandstone	Jurassic	Bathonian	Vardekløft	Pelion		9
Trail Ø, Svinhufvud Bjerge_transect 7	18	487741	-23,353	72,458	610	sandstone	Jurassic	Bajocian	Vardekløft	Pelion		9
Trail Ø, Svinhufvud Bjerge_transect 8	17	487733	-23,235	72,460	460	sandstone	M. Jurassic	Bajocian	Vardekløft	Pelion		9
Trail Ø, Svinhufvud Bjerge_transect 8	17	487732	-23,248	72,457	460	sandstone	M. Jurassic	Bajocian	Vardekløft	Pelion		9
Trail Ø, Svinhufvud Bjerge_transect 8	17	487731	-23,278	72,460	425	sandstone	M. Jurassic	Bajocian	Vardekløft	Bristol Elv		9
Trail Ø, Svinhufvud Bjerge_transect 8	17	487730	-23,278	72,460	323	sandstone	M. Jurassic	Bajocian	Vardekløft	Bristol Elv		9
Trail Ø, Svinhufvud Bjerge_transect 8	17	487729	-23,310	72,458	320	sandstone	M. Jurassic	Bajocian	Vardekløft	Bristol Elv		9
Geographical Society Ø, Tørvestakken-tr 10	16	487742	-23,079	72,954	380	sandstone	Jurassic	Bajocian/Bathonian	Vardekløft	Pelion		9
Geographical Society Ø, Tørvestakken-tr 10	16	487743	-23,079	72,954	355	sandstone	Jurassic	Bajocian/Bathonian	Vardekløft	Pelion		9
Geographical Society Ø, Tørvestakken-tr 10	16	487744	-23,081	72,953	335	sandstone	Jurassic	Bajocian/Bathonian	Vardekløft	Pelion		9
Geographical Society Ø, Tørvestakken-tr 10	16	487745	-23,081	72,953	320	sandstone	Jurassic	Bajocian/Bathonian	Vardekløft	Pelion		9
Geographical Society Ø, Tørvestakken-tr 10	16	487746	-23,081	72,952	300	sandstone	Triassic	Griesbachian		Wordie Creek		5
Geographical Society Ø, Tørvestakken-tr 12	15	487761	-23,013	72,933	850	sandstone	Triassic	Griesbachian		Wordie Creek	Svinhufvud Bjerge	5
Geographical Society Ø, Tørvestakken-tr 12	15	487760	-23,015	72,934	800	sandstone	Triassic	Griesbachian		Wordie Creek	Svinhufvud Bjerge	5
Geographical Society Ø, Tørvestakken-tr 12	15	487759	-23,047	72,936	670	sandstone	Triassic	Griesbachian		Wordie Creek	Svinhufvud Bjerge	5
Geographical Society Ø, Tørvestakken-tr 12	15	487758	-23,036	72,936	570	sandstone	Triassic	Griesbachian		Wordie Creek	Svinhufvud Bjerge	5
Geographical Society Ø, Tørvestakken-tr 12	15	487757	-23,046	72,935	470	sandstone	Triassic	Griesbachian		Wordie Creek	Svinhufvud Bjerge	5
Geographical Society Ø, Tørvestakken-tr 12	15	487756	-23,049	72,935	435	sandstone	Triassic	Griesbachian		Wordie Creek		5
Geographical Society Ø, Tørvestakken-tr 12	15	487755	-23,049	72,935	435	sandstone	Triassic	Griesbachian		Wordie Creek		5
Geographical Society Ø, Tørvestakken-tr 12	15	487754	-23,049	72,934	420	sandstone	Triassic	Griesbachian		Wordie Creek		5
Geographical Society Ø, Tørvestakken-tr 12	15	487753	-23,051	72,934	400	sandstone	Triassic	Griesbachian		Wordie Creek		5
Geographical Society Ø, Tørvestakken-tr 12	15	487752	-23,057	72,934	370	sandstone	Triassic	Griesbachian		Wordie Creek?		5
Trail Ø, Svinhufvud Bjerge_transect 9	14	487734	-23,235	72,460	1180	sandstone	Triassic	Griesbachian		Wordie Creek	Svinhufvud Bjerge	5
Trail Ø, Svinhufvud Bjerge_transect 9	14	487735	-23,361	72,454	1180	sandstone	Triassic	Griesbachian		Wordie Creek	Svinhufvud Bjerge	5
Trail Ø, Svinhufvud Bjerge_transect 9	14	487736	-23,361	72,454	1150	sandstone	Triassic	Griesbachian		Wordie Creek	Svinhufvud Bjerge	5
Trail Ø, Svinhufvud Bjerge_transect 9	14	487737	-23,366	72,456	1125	sandstone	Triassic	Griesbachian		Wordie Creek		5
Trail Ø, Svinhufvud Bjerge_transect 9	14	487737b	-23,353	72,458	1075	sandstone	Triassic	Griesbachian		Wordie Creek		5
Trail Ø, Svinhufvud Bjerge_transect 9	14	487739	-23,352	72,459	1045	sandstone	Triassic	Griesbachian		Wordie Creek		5
Trail Ø, Svinhufvud Bjerge_transect 9	14	487740	-23,366	72,459	970	sandstone	Triassic	Griesbachian		Wordie Creek		5
Geographical Society Ø, Tørvestakken-tr 13	13	487762	-23,143	72,959	980	sandstone	Carboniferous	Viséan-Westphalian	Trail Ø			3
Geographical Society Ø, Tørvestakken-tr 13	13	487763	-23,143	72,959	980	sandstone	Carboniferous	Viséan-Westphalian	Trail Ø			3
Geographical Society Ø, Tørvestakken-tr 13	13	487766	-23,136	72,964	615	sandstone	Carboniferous	Viséan-Westphalian	Trail Ø			3
Geographical Society Ø, Tørvestakken-tr 13	13	487765	-23,125	72,965	484	sandstone	Carboniferous	Viséan-Westphalian	Trail Ø			3
Geographical Society Ø, Tørvestakken-tr 13	13	487764	-23,119	72,965	455	sandstone	Carboniferous	Viséan-Westphalian	Trail Ø			3

Locality name	Profile	sample_nr	Longitude	Latitude	Altitude	type	System/series	Stage	Group	Formation	Member	Palaeogeography
Hold with Hope												
Hold with Hope East , Knudshoved -Transect 16	22	487778	-20,543	73,707	21	sandstone	Upper Cretaceous		Hold with Hope	Home Forland	Knudshoved - Østersletten	14
Hold with Hope East , Knudshoved -Transect 16	22	487777	-20,542	73,707	21	sandstone	Upper Cretaceous		Hold with Hope	Home Forland	Knudshoved - Østersletten	14
Hold with Hope North, Gulelv-transect 14	21	487767	-21,164	73,919	557	sandstone	L. Cretaceous		Hold with Hope	Steensby Bjerg		14
Hold with Hope North, Gulelv-transect 14	21	487768	-21,166	73,925	488	sandstone	L. Cretaceous		Hold with Hope	Steensby Bjerg		14
Hold with Hope North, Gulelv-transect 14	21	487769	-21,167	73,926	452+7	sandstone	L. Cretaceous		Hold with Hope	Steensby Bjerg		14
Hold with Hope North, Gulelv-transect 14	21	487770	-21,167	73,926	452+5	sandstone	M. Jurrassic			Vardekløft		10
Hold with Hope North, Gulelv-transect 14	21	487771	-21,168	73,927	420	sandstone	M. Jurrassic			Vardekløft		10
Hold with Hope North, Gulelv-transect 14	21	487772	-21,174	73,928	381	sandstone	M. Jurrassic			Vardekløft		10
Hold with Hope North, Gulelv-transect 15	20	487776	-21,157	73,919	761	sandstone	Triassic			Wordie Creek		5
Hold with Hope North, Gulelv-transect 15	20	487775	-21,160	73,920	751	sandstone	Triassic			Wordie Creek		5
Hold with Hope North, Gulelv-transect 15	20	487774	-21,215	73,933	150	sandstone	Triassic			Wordie Creek		5
Hold with Hope North, Gulelv-transect 15	20	487773	-21,201	73,932	217	sandstone	Triassic			Wordie Creek		5
Wollaston Forland												
Haredal-transect 4 (E Wollaston Forland)	35	508723	-19,361	74,344	428	sandstone	Paleocene					15
Haredal-transect 4 (E Wollaston Forland)	35	508726	-19,360	74,344	423	sandstone	Paleocene					15
Haredal-transect 4 (E Wollaston Forland)	35	508727	-19,360	74,344	420	sandstone	Paleocene					15
Haredal-transect 4 (E Wollaston Forland)	35	508728	-19,359	74,346	372	sandstone	Paleocene					15
Haredal-transect 4 (E Wollaston Forland)	35	508729	-19,359	74,346	372	sandstone	Paleocene					15
Haredal-transect 4 (E Wollaston Forland)	35	508730	-19,357	74,347	332	sandstone	Paleocene					15
Haredal-transect 5 (E Wollaston Forland)	34	508724	-19,349	74,338	505	sandstone	Paleocene					15
Haredal-transect 6 (E Wollaston Forland)	33	508725	-19,347	74,343	417	sandstone	Paleocene					15
Haredal-transect 8 (E Wollaston Forland)	32	508732	-19,259	74,356	170	sandstone	Paleocene					15
Haredal-transect 8 (E Wollaston Forland)	32	508733	-19,260	74,356	164	sandstone	Paleocene					15
Haredal-transect 8 (E Wollaston Forland)	32	508734	-19,268	74,356	96	sandstone	Paleocene					15
Haredal-transect 7 (E Wollaston Forland)	31	508738	-19,324	74,349	235	sandstone	Paleocene					15
Haredal-transect 7 (E Wollaston Forland)	31	508737	-19,307	74,349	178	sandstone	Paleocene					15
Haredal-transect 7 (E Wollaston Forland)	31	508736	-19,291	74,346	130	sandstone	Paleocene					15
Haredal-transect 7 (E Wollaston Forland)	31	508735	-19,291	74,346	130	sandstone	Paleocene					15
Haredal-transect 7 (E Wollaston Forland)	31	508731	-19,329	74,348	58	sandstone	Lower Cretaceous					14
Rødryggen, South-transect 12	30	508770	-19,842	74,513	169	sandstone	middle Cretaceous					14
Niesen-transect 3 (NW Wollaston Forland)	29	508717	-20,484	74,627	558	sandstone	middle Cretaceous					14
Niesen-transect 3 (NW Wollaston Forland)	29	508716	-20,484	74,627	558	sandstone	middle Cretaceous					14
Niesen-transect 3 (NW Wollaston Forland)	29	508715	-20,495	74,630	325	sandstone	Cretaceous		Wollaston Forland	Lindemans Bugt		12
Niesen-transect 3 (NW Wollaston Forland)	29	508714	-20,475	74,630	297	sandstone	Cretaceous		Wollaston Forland	Lindemans Bugt		12
Niesen-transect 3 (NW Wollaston Forland)	29	508713	-20,475	74,630	297	sandstone	Cretaceous		Wollaston Forland	Lindemans Bugt		12
Niesen-transect 2 (NW Wollaston Forland)	28	508718	-20,501	74,652	660	sandstone	Cretaceous		Wollaston Forland	Palnatokes Bjerg	Albrechts Bugt	13
Niesen-transect 2 (NW Wollaston Forland)	28	508719	-20,501	74,652	660	sandstone	Cretaceous		Wollaston Forland	Palnatokes Bjerg	Albrechts Bugt	13
Niesen-transect 2 (NW Wollaston Forland)	28	508720	-20,501	74,652	660	sandstone	Cretaceous		Wollaston Forland	Palnatokes Bjerg	Albrechts Bugt	13
Niesen-transect 2 (NW Wollaston Forland)	28	508721	-20,496	74,646	617	sandstone	Cretaceous		Wollaston Forland	Palnatokes Bjerg		13
Niesen-transect 2 (NW Wollaston Forland)	28	508722	-20,482	74,640	484	sandstone	Cretaceous		Wollaston Forland	Lindemans Bugt		12
Niesen-transect 2 (NW Wollaston Forland)	28	508712	-20,543	74,658	459	sandstone	Cretaceous		Wollaston Forland	Lindemans Bugt	Niesen	12
Niesen-transect 2 (NW Wollaston Forland)	28	508711	-20,541	74,661	375	sandstone	Cretaceous		Wollaston Forland	Lindemans Bugt	Niesen	12
Niesen-transect 2 (NW Wollaston Forland)	28	508710	-20,541	74,663	312	sandstone	Cretaceous		Wollaston Forland	Lindemans Bugt	Niesen	12
Niesen-transect 2 (NW Wollaston Forland)	28	508709	-20,539	74,666	159	sandstone	Cretaceous		Wollaston Forland	Lindemans Bugt	Niesen	12
Niesen-transect 2 (NW Wollaston Forland)	28	508708	-20,536	74,669	92	sandstone	Cretaceous		Wollaston Forland	Lindemans Bugt	Niesen	12
Niesen-transect 1 (NW Wollaston Forland)	27	508705	-20,580	74,652	134	sandstone	Cretaceous		Wollaston Forland	Lindemans Bugt	Niesen	12
Niesen-transect 1 (NW Wollaston Forland)	27	508706	-20,590	74,657	115	sandstone	Cretaceous		Wollaston Forland	Lindemans Bugt	Niesen	12
Niesen-transect 1 (NW Wollaston Forland)	27	508707	-20,588	74,665	67	sandstone	Cretaceous		Wollaston Forland	Lindemans Bugt	Niesen	12

Locality name	Profile	sample_nr	Longitude	Latitude	Altitude	type	System/series	Stage	Group	Palaeogeography		
Wollaston Forland												
Rødryggen, East-transect 13	26	508771	-19,743	74,542	188	sandstone	Jurassic		Hall Bredning	Bernbjerg	11	
Rødryggen, East-transect 13	26	508772	-19,754	74,544	150	sandstone	Jurassic		Hall Bredning	Bernbjerg	11	
Rødryggen, East-transect 13	26	508773	-19,768	74,546	38	sandstone	Jurassic		Hall Bredning	Bernbjerg	11	
Cardiocerasdal-transect 11 (W Wollaston F)	25	508764	-20,250	74,467	428	sandstone	Jurassic		Hall Bredning	Bernbjerg	11	
Cardiocerasdal-transect 11 (W Wollaston F)	25	508765	-20,245	74,450	231	sandstone	Jurassic		Hall Bredning	Bernbjerg	Ugpik Ravine	11
Cardiocerasdal-transect 11 (W Wollaston F)	25	508766	-20,247	74,450	168	sandstone	Jurassic		Vardekløft	Lower Jakobsstigen	10	
Cardiocerasdal-transect 11 (W Wollaston F)	25	508767	-20,238	74,451	128	sandstone	Jurassic		Vardekløft	Pelion	9	
Cardiocerasdal-transect 10 (W Wollaston F)	24	508761	-20,192	74,449	413	sandstone	Cretaceous		Wollaston Forland	Palnatokes Bjerg	12	
Cardiocerasdal-transect 10 (W Wollaston F)	24	508762	-20,204	74,446	426	sandstone	Cretaceous		Wollaston Forland	Palnatokes Bjerg	12	
Cardiocerasdal-transect 10 (W Wollaston F)	24	508763	-20,204	74,448	449	sandstone	Cretaceous		Wollaston Forland	Palnatokes Bjerg	12	
Cardiocerasdal-transect 10 (W Wollaston F)	24	508760	-20,190	74,453	478	sandstone	Jurassic		Hall Bredning	Bernbjerg	11	
Cardiocerasdal-transect 10 (W Wollaston F)	24	508759	-20,191	74,456	433	sandstone	Jurassic		Vardekløft	Upper Jakobsstigen	10	
Cardiocerasdal-transect 10 (W Wollaston F)	24	508758	-20,196	74,458	343	sandstone	Jurassic		Vardekløft	Upper Jakobsstigen	10	
Cardiocerasdal-transect 10 (W Wollaston F)	24	508757	-20,194	74,459	314	sandstone	Jurassic		Vardekløft	Pelion	9	
Kuhn Ø												
Bastian Dal-transect 9 (W Kuhn Ø)	38	508739	-20,443	74,905	50	sandstone	Jurassic		Hall Bredning	Bernbjerg	11	
Bastian Dal-transect 9 (W Kuhn Ø)	38	508740	-20,424	74,906	70	sandstone	Jurassic		Vardekløft	Upper Payer Dal	11	
Bastian Dal-transect 9 (W Kuhn Ø)	38	508741	-20,418	74,905	84	sandstone	Jurassic		Vardekløft	Payer Dal	11	
Bastian Dal-transect 9 (W Kuhn Ø)	38	508742	-20,402	74,903	153	sandstone	Jurassic		Vardekløft	Payer Dal	11	
Bastian Dal-transect 9 (W Kuhn Ø)	38	508743	-20,385	74,900	217	sandstone	Jurassic		Vardekløft	Lower Payer Dal	11	
Bastian Dal-transect 9 (W Kuhn Ø)	38	508744	-20,357	74,901	232	sandstone	Jurassic		Vardekløft	Muslingebjerg	10	
Bastian Dal-transect 9 (W Kuhn Ø)	38	508745	-20,354	74,898	168	sandstone	Jurassic		Vardekløft	Bastians Dal	10	
Payer Dal West, transect 15 (Kuhn Ø)	37	508782	-20,352	74,752	190	sandstone	Jurassic		Hall Bredning	Bernbjerg	Ugpik Ravine	11
Payer Dal West, transect 15 (Kuhn Ø)	37	508781	-20,344	74,751	136	sandstone	Jurassic		Vardekløft	Upper Payer Dal	11	
Payer Dal West, transect 15 (Kuhn Ø)	38	508780	-20,341	74,750	106	sandstone	Jurassic		Vardekløft	Lower Payer Dal	11	
Payer Dal East, transect 14 (Kuhn Ø)	36	508779	-20,249	74,743	460	sandstone	Jurassic		Vardekløft	Upper Payer Dal	11	
Payer Dal East, transect 14 (Kuhn Ø)	36	508784	-20,258	74,744	415	sandstone	Jurassic		Vardekløft	Upper Payer Dal	11	
Payer Dal East, transect 14 (Kuhn Ø)	36	508777	-20,253	74,748	355	sandstone	Jurassic		Vardekløft	Lower Payer Dal	11	
Payer Dal East, transect 14 (Kuhn Ø)	36	508778	-20,253	74,748	355	sandstone	Jurassic		Vardekløft	Lower Payer Dal	11	
Payer Dal East, transect 14 (Kuhn Ø)	36	508776	-20,252	74,748	308	sandstone	Jurassic		Vardekløft	uppermost Pelion	9	
Payer Dal East, transect 14 (Kuhn Ø)	36	508775	-20,252	74,748	293	sandstone	Jurassic		Vardekløft	Pelion	9	
Payer Dal East, transect 14 (Kuhn Ø)	36	508774	-20,251	74,749	248	sandstone	Jurassic		Vardekløft	Pelion	9	
Payer Dal East, transect 14 (Kuhn Ø)	36	508783	-20,267	74,754	163	sandstone	Jurassic		Vardekløft	Muslingebjerg	10	
Kronprins Christian Land & Peary Land												
Ladegårdsåen, Kim Fjelde	47	113460	-21,499	82,572	153	sandstone	Jurassic-Cretaceous	Oxfordian-Valanginian		Ladegårdsåen	12	
Ladegårdsåen, Kim Fjelde	47	113461	-21,487	82,727	156	sandstone	Jurassic-Cretaceous	Oxfordian-Valanginian		Ladegårdsåen	12	
Ladegårdsåen, Kim Fjelde	47	113462	-21,498	82,578	163	sandstone	Jurassic-Cretaceous	Oxfordian-Valanginian		Ladegårdsåen	12	
Ladegårdsåen, Kim Fjelde	47	113463	-21,498	82,580	157	sandstone	Jurassic-Cretaceous	Oxfordian-Valanginian		Ladegårdsåen	12	
Søjljerne, Kim Fjelde, Peary Land	46	113459	-21,579	82,556	217	sandstone	Jurassic-Cretaceous	Oxfordian-Valanginian		Ladegårdsåen	12	
Søjljerne, Kim Fjelde, Peary Land	46	113458	-21,576	82,557	210	sandstone	Jurassic-Cretaceous	Oxfordian-Valanginian		Ladegårdsåen	12	
Søjljerne, Kim Fjelde, Peary Land	46	113457	-21,566	82,557	183	sandstone	Jurassic-Cretaceous	Oxfordian-Valanginian		Ladegårdsåen	12	
Søjljerne, Kim Fjelde, Peary Land	46	113456	-21,557	82,557	173	sandstone	Jurassic-Cretaceous	Oxfordian-Valanginian		Ladegårdsåen	12	
Søjljerne, Kim Fjelde, Peary Land	46	113454	-21,550	82,559	152	sandstone	Jurassic-Cretaceous	Oxfordian-Valanginian		Ladegårdsåen	12	
Søjljerne, Kim Fjelde, Peary Land	46	113453	-21,546	82,559	143	sandstone	Jurassic-Cretaceous	Oxfordian-Valanginian		Ladegårdsåen	12	
Søjljerne, Kim Fjelde, Peary Land	46	113452	-21,526	82,559	144	sandstone	Jurassic-Cretaceous	Oxfordian-Valanginian		Ladegårdsåen	12	
Søjljerne, Kim Fjelde, Peary Land	46	113451	-21,521	82,559	152	sandstone	Jurassic-Cretaceous	Oxfordian-Valanginian		Ladegårdsåen	12	
Dunken, Kim Fjelde	42	113464	-21,065	82,636	507	sandstone	Triassic/?Jurassic		Trolle Land	Dunken	5	
Dunken, Kim Fjelde	42	113465	-21,059	82,634	511	sandstone	Triassic		Trolle Land	Dunken	5	
Dunken, Kim Fjelde	42	113466	-21,047	82,635	487	sandstone	Triassic		Trolle Land	Dunken	5	
Dunken, Kim Fjelde	42	113467	-21,041	82,630	399	sandstone	Triassic		Trolle Land	Dunken	5	
Dunken, Kim Fjelde	42	113468	-21,042	82,630	386	sandstone	Triassic		Trolle Land	Dunken	5	

Locality name	Profile	sample_nr	Longitude	Latitude	Altitude	type	System/series	Stage	Group	Formation	Member	Palaeogeography
Kronprins Christian Land & Peary Land												
Falkefjeld, Kim Fjelde	44	113475	-21,297	82,620	344	sandstone	Triassic		Trolle Land	Parish Bjerg		5
Falkefjeld, Kim Fjelde	44	113476	-21,305	82,619	315	sandstone	Triassic		Trolle Land	Parish Bjerg		5
Falkefjeld, Kim Fjelde	44	113477	-21,295	82,619	304	sandstone	Triassic		Trolle Land	Parish Bjerg		5
Falkefjeld, Kim Fjelde	44	113478	-21,290	82,619	277	sandstone	Triassic		Trolle Land	Parish Bjerg		5
Falkefjeld, Kim Fjelde	44	113479	-21,286	82,616	185	sandstone	Triassic		Trolle Land	Parish Bjerg		5
Falkefjeld, Kim Fjelde	44	113480	-21,277	82,615	199	sandstone	Triassic		Trolle Land	Parish Bjerg		5
Dunken, Kim Fjelde	44	113469	-21,104	82,596	131	sandstone	Triassic		Trolle Land	Parish Bjerg		5
Ved Sletten, Kim Fjelde	43	113471	-21,366	82,585	174	sandstone	Triassic		Trolle Land	Parish Bjerg		5
Ved Sletten, Kim Fjelde	43	113472	-21,326	82,580	230	sandstone	Triassic		Trolle Land	Parish Bjerg		5
Ved Sletten, Kim Fjelde	43	113473	-21,320	82,565	205	sandstone	Triassic		Trolle Land	Parish Bjerg		5
Ved Sletten, Kim Fjelde	43	113474	-21,307	82,583	199	sandstone	Triassic		Trolle Land	Parish Bjerg		5